Oxidation-dependent regulation of the selective autophagy receptor SQSTM1/p62

Diego Manni

Doctor of Philosophy

Campus for Ageing and Vitality

Institute for Cell and Molecular Biosciences

Newcastle University

January 2017

Abstract

Oxidative stress and impairment of autophagy can lead to the accumulation and aggregation of damaged proteins, a common feature of most age-related neurodegenerative disorders such as Alzheimer's disease and Parkinson's disease. SQSTM1/p62, a receptor and a substrate of selective autophagy, is implicated in the degradation of damaged and polyubiquitinated substrates. Importantly, p62 has been detected in many types of protein inclusions found in neurodegenerative diseases, together with other disease-related proteins. However, the mechanisms allowing p62 to selectively recruit and degrade autophagic substrates in conditions of oxidative stress remain unknown. The aim of this thesis work is to understand the mechanisms underlying the oligomerisation and the aggregation of p62 during oxidation, looking at post-translational modifications that can lead to the formation of protein aggregates.

We found that p62 senses and is regulated by oxidative stress. In response to oxidation, two cysteine (Cys) residues C105 and C113 of p62 mediate the formation of disulphide-linked conjugates (DLC). The formation of p62 DLC was reduced upon antioxidants addition, while inhibitors of the antioxidant system enhanced their development. This feature was critical for the function of p62 as an autophagy receptor as well as for the accumulation of polyubiquitinated aggregates. Indeed, the accumulation and degradation of p62 and its substrates was impaired following mutation of the Cys residues implicated in DLC formation, while the interaction between p62 and polyubiquitinated substrates was not affected. Oxidation of p62 was also required for cell survival in conditions of oxidative stress, indicating the physiological importance of the correct function of p62 in selective autophagy. In addition, formation of p62 DLC was increased in ageing and age-related neurodegenerative diseases, possibly as a compensatory mechanism to protect cells in increased oxidative conditions.

In conclusion, we reveal a new mechanism of p62 oligomerisation aiding the selective autophagy of dysfunctional proteins under oxidative stress conditions.

Acknowledgments

I would like to thank the NIHR Newcastle Biomedical Research Centre for funding this project, as well as for providing me with my first taste of economic independence (it did not last long though!).

I would like to express my sincere gratitude to my main supervisor Dr Viktor I. Korolchuk for his guidance and continuous support throughout this project. He certainly gave me the motivation to keep going during tough times, and pushed me to achieve my full potential (sounds classic but it is true, I swear). Also, I would like to thank my second supervisor Prof Johannes Attems for his positive criticisms.

I would also like to thank Dr Gabriele Saretzki and Dr Christopher Morris for fairly evaluating my progresses during the year reports (and for not failing me along the path). I take this opportunity to also thank Dr Alberto Sanz Montero and Prof Robert Layfield for making my viva examination a much more bearable experience, turning a much-dreaded day into a memorable moment (four hours long actually).

A big thank you to Gisela Otten (otherwise known as Elsje G.) for contributing to this project with her insightful ideas and hard work (as well as her artistic proficiency with Illustrator). I would also like to thank Dr Bernadette Carroll, Dr Alison Howard, Dr Yoana Rabanal Ruiz, Dr Graeme Hewitt, Alvaro Martinez Guimera and Lucy Sedlackova for their suggestions and help over these (long) years.

Thanks to Joseph Sheppard and Hanna Salmonowicz for teaching me how to supervise students (or rather pretend to), and for giving me the possibility to grow both as a person as well as a scientist (saying it still frightens me).

Many thanks also to Dr Diana Jurk, Dr Graham Smith and Dr Fiona Menzies for their contributions to the project (and for saving precious days of my life worth of time).

I would like to seize the opportunity to thank all the other colleagues and friends that have helped, talked, listened, criticised or simply spent their time with me, you are too many to mention in these two mere pages (or maybe I am just being lazy). You all contributed to make me who I am, and I am grateful for that (seriously).

I would like to thank Yasamin Pishvaei for her(/our) love and patience during these years. Her presence and encouragements have been vital throughout this experience, which I will be eternally grateful for.

Finally, the greatest thanks go to my parents Mario and Cettina and my brother Fabio for their unconditional love and support since I acquired consciousness, to whom I dedicate this thesis (although they will most probably not read a page of it, for which I will surely not blame them!).

Table of Contents

List of Figures

List of Tables

Abbreviation List

$^{\bullet}$HO:	hydroxyl radical
8-OHdG:	8-hydroxy-2'-deoxyguanosine
a.a.:	amino acid
AAA^{+}:	ATPase associated with diverse cellular activities
AD:	Alzheimer's disease
ADP:	adenosine diphosphate
AHA:	L-azidohomoalanine
Ala (A):	alanine residue
Alfy:	autophagy-linked FYVE protein
ALS:	amyotrophic lateral sclerosis
AMPA:	α-amino-3-hydroxy-5-methyl-4-isoxazolepropionic acid
AMPK:	adenosine monophosphate-activated protein kinase
Ams1:	α-mannosidase
AP-1:	activator protein 1
Ape1:	aminopeptidase 1
APF1:	ATP-dependent proteolysis factor 1
Apg:	autophagy genes
aPKC:	atypical protein kinase C
ARE:	antioxidant response element
Arg (R):	arginine residue
Asp (D):	aspartate residue
ATF6:	activating transcription factor 6
Atg:	autophagy-related genes
ATP:	adenosine triphosphate
Aut:	autophagy genes
AV:	autophagic vacuoles
Baf:	bafilomycin A1
BAG1/3	Bcl-2-associated athanogene 1/3
Bcl-2:	B-cell lymphoma 2

BDNF:	brain-derived neurotrophic factor
BH3:	Bcl-2 homology 3
BRCA1:	breast cancer-associated 1
BSA:	bovine serum albumin
BTB:	broad complex, tramtrack and bric-a-brac
BUZ:	binding-of-ubiquitin zinc
bZIP:	basic leucine zipper
CCD:	coiled-coil domain
CHIP:	C-terminus of Hsp70-interacting protein
CHX:	cycloheximide
CK2:	casein kinase 2
CMA:	chaperone-mediated autophagy
CNC:	cap'n'collar
CO_2:	carbon dioxide
Co^{2+}:	cobalt ion
CP:	core particle
C_p:	peroxidatic cysteine
CQ:	chloroquine
C_r:	resolving cysteine
Cvt:	cytoplasm-to-vacuole-targeting
CYLD:	cylindromatosis tumor suppressor protein
Cys (C):	cysteine residue
DHR:	dihydrorhodamine
DLB:	dementia with Lewy bodies
DLC:	disulphide-linked conjugates
DLG:	aspartate-leucine-glycine
DMSO:	dimethyl sulfoxide
DNA	deoxyribonucleic acid
DUB:	deubiquitinating enzyme
E. coli:	*Escherichia coli*
E1:	ubiquitin-activating enzyme
E2:	ubiquitin-conjugating enzyme

E3:	ubiquitin ligase
E6-AP:	E6-associated protein
EBI:	European Bioinformatic Institute
ECACC:	European Collection of Cell Cultures
EDTA:	ethylene-diamine-tetraacetic acid
ER:	endoplasmic reticulum
ERAD:	ER-associated degradation
ERK:	extracellular signal-activated kinase
ETGE:	glutamate-threonine-glycine-glutamate
FACS:	fluorescence-activated cell sorting
FAK:	focal adhesion kinase
FBS:	fetal bovine serum
FIP200:	FAK family-interacting protein of 200 kDa
FOXO:	forkhead box protein O
FTD:	frontotemporal dementia
FTLD:	frontotemporal lobar degeneration
GABARAP:	gamma-aminobutyric acid receptor-associated protein
GAP:	GTPase-activating protein
GAPDH:	glyceraldehyde 3-phosphate dehydrogenase
GATE-16:	Golgi-associated ATPase enhancer of 16 kDa
GDP:	guanosine diphosphate
GFP:	green fluorescent protein
Gln (Q):	glutamine residue
Glu (E):	glutamate residue
Gly (G):	glycine residue
Gpx:	glutathione peroxidase
GSH:	glutathione
GSSG:	glutathione disulphide
GTP:	guanosine triphosphate
H_2O:	water
H_2O_2:	hydrogen peroxide
HD:	Huntington’s disease

HDAC6:	histone deacetylase 6
HECT:	homologous to E6-AP carboxy-terminus
HEK293:	human embryonic kidney 293 cells
HeLa:	Henrietta Lacks cells
Hip:	Hsc70-interacting protein
His (H):	histidine residue
Hop:	Hsp70-Hsp90 organising protein
HRP:	horseradish peroxidase
Hsc70:	heat shock cognate of 70 kDa
Hsp:	heat shock protein
Hsp70/90:	heat shock protein of 70/90 kDa
HSR:	heat shock response
IKK:	IκB kinase
IL1:	interleukin 1
IP:	immunoprecipitation
IRE1:	inositol-requiring protein 1
IVR:	intervening region
IκB:	inhibitor of κB
kDa:	kilo (10^3) Dalton
Keap1:	Kelch-like ECH-associated protein 1
KFERQ:	lysine-phenylalanine-glutamate-arginine-glutamine pentapeptide
KIR:	Keap1-interacting region
Lamp2a:	lysosome-associated membrane protein type 2a
LC3:	MAP light chain 3
LIR:	LC3-interacting region
LRS:	LC3 recognition sequence
LTP:	long term potentiation
ly-Hsc70:	lysosomal Hsc70
Lys (K):	lysine residue
mA:	milli (10^{-3}) Ampere
Maf:	muscoloaponeuretic fibrosarcoma
MAP:	microtubule-associated protein

MAPK:	mitogen-activated protein kinase
MDa:	mega (10^6) Dalton
MEFs:	mouse embryonic fibroblasts
Mfn1/2:	mitofusin 1/2
MG132:	carbobenzoxy-Leu-Leu-leucinal
mM:	milli (10^{-3}) Molar
MTOC:	microtubule organising centre
mTOR:	mechanistic/mammalian target of rapamycin
mTORC1/2:	mTOR complex 1/2
MW:	molecular weight
NAC:	N-acetylcysteine
NADPH:	nicotinamide adenine dinucleotide phosphate
NBR1:	neighbour of BRCA1 gene 1
NCBI:	National Center for Biotechnology Information
ND:	neurodegenerative disease
NDP52:	nuclear domain 10 protein of 52 kDa
Neh:	Nrf2-ECH homology
NEM:	N-ethylmaleimide
NEMO:	NF-κB essential modulator
NES:	nuclear export signal
NF-κB:	nuclear factor-kappa B
NGF:	nerve growth factor
NLS1/2:	nuclear localisation signals 1/2
nM:	nano (10^{-9}) Molar
Nrf2:	nuclear factor erythroid 2-related factor 2
NSM:	non-selective microautophagy
Ntn:	N-terminal nucleophile
O_2:	oxygen
$O_2^{\bullet-}$:	superoxide anion radical
OPCA:	OPR/PC/AID motif
OPR/PC/AID:	octicosapeptide repeat/Phox and Cdc/aPKC-interacting domain
OPTN:	optineurin

$p56^{lck}$:	lymphocyte-specific protein tyrosine
$p62^{-/-}$:	p62 knock-out cells
PAS:	pre-autophagosomal structure
PB1:	Phox and Bem1p
PBS:	phosphate-buffered saline
PCD:	programmed cell death
PCR:	polymerase chain reaction
PD:	Parkinson's disease
PDB:	Paget's disease of bone
PE:	phosphatidylethanolamine
Pep4:	proteinase 4
PERK:	PKR-like ER kinase
PEST:	proline-glutamate-serine-threonine rich sequence
PI:	phosphatidylinositol
PI3K:	PI 3-kinase
PI3P:	phosphatidylinositol 3-phosphate
PIKK:	PI3K-related kinase
PINK1:	PTEN-induced putative kinase 1
pK_a:	acid dissociation constant
PM:	*post-mortem*
PN:	proteostasis network
PPi:	pyrophosphate
PQ:	paraquat
PR-619:	2,6-diaminopyridine-3,5-bis(thiocyanate)
prApe1:	precursor of Ape1
PRK:	protein kinase RNA-activated
prp73:	peptide recognition protein of 73 kDa
Prx:	peroxiredoxin
PTEN:	phosphatase and tensin homolog
PTP:	protein Tyr phosphatases
PVDF:	polyvinylidene difluoride
RANK:	receptor activator of NF-kB

RANKL:	receptor activator of NF-kB ligand
Raptor:	regulatory-associated protein of mTOR
Ras:	rat sarcoma
Rheb:	Ras homolog enriched in brain
Rictor:	rapamycin-insensitive companion of mTOR
RING:	really interesting new gene
RIP1:	receptor-interacting protein 1
RIPA:	radioimmunoprecipitation assay
RNA:	ribonucleic acid
ROS:	reactive oxygen species
RP:	regulatory particle
Rpn:	regulatory particle non-ATPase
Rpt:	regulatory particle triple-A protein
S:	Svedberg
S^-:	thiolate ion
S5a:	subunit 5a
SDS:	sodium dodecyl sulphate
SDS-PAGE:	SDS polyacrylamide gel electrophoresis
Sec:	selenocysteine
s.e.m.:	standard error of the mean
Ser (S):	serine residue
SH:	thiol group
siRNA:	small interfering RNA
SO_2H:	sulphinic acid
SO_3H:	sulphonic acid
SOD1:	superoxide dismutase 1
SOH:	sulphenic acid
SQSTM1:	sequestosome 1
Srx:	sulphiredoxin
S-S:	disulphide bond
Sti1:	stress inducible protein 1
TANK:	TRAF family member-associated NF-κB activator

TAR:	transactive response
TBK1:	TANK binding kinase 1
TBS:	TRAF6 binding site
TDP-43:	TAR DNA-binding protein of 43 kDa
TNF:	tumor necrosis factor
TRAF6:	TNF receptor-associated factor 6
Tris:	Tris(hydroxymethyl)aminomethane
Trx:	thioredoxin
TrxR:	thioredoxin reductase
TSC1/2:	tuberous sclerosis complex 1 (hamartin) and 2 (tuberin)
Tyr (Y):	tyrosine residue
UBA:	ubiquitin-associated
UBD:	ubiquitin-binding domain
UBL:	ubiquitin-like
ULK1:	Unc-51-like kinases 1
UPR:	unfolded protein response
UPS:	ubiquitin-proteasome system
UVRAG:	UV irradiation resistance-associated gene
VCP:	valosin-containing protein
VDAC1:	voltage-dependent anion channel 1
Vps:	vacuolar protein sorting
VSV-G:	vesicular stomatitis virus G glycoprotein
WD:	tryptophan-aspartate dipeptide
Zn^{2+}:	zinc ion
Z-VAD-FMK:	carbobenzoxy-valyl-alanyl-aspartyl-[O-methyl]fluoromethylketone
ZZ:	zinc-zinc finger domain
β-ME:	beta-mercaptoethanol
µM:	micro (10^{-6}) Molar

Chapter 1. Introduction

1.1 Oxidative Stress and Redox Homeostasis

The term “oxidative stress” relates to the imbalance between pro-oxidants and reducing agents (antioxidants) in a biological system. The mechanisms of oxygen toxicity began to be investigated over 70 years ago, when it was suggested that oxygen poisoning and ionising radiation (e.g. X-rays) both shared the formation of chemically-reactive free radicals (molecules containing at least one unpaired electron) (Gerschman *et al.*, 1954). Soon after, endogenously-formed free radicals were proposed to be the cause of the ageing process in living organisms, leading to increased interest in the free radical area (Harman, 1956). The discovery of the superoxide dismutase (SOD) also suggested that the living systems had developed protective mechanisms against free radicals, such as the superoxide anion (McCord and Fridovich, 1969).

The free radical theory of ageing was then modified by the same author, which proposed that mitochondria had a central role in ageing, where the genetically-determined rate of oxygen consumption and formation of free radicals could have had a direct impact on the life span (Harman, 1972). The theory was then supported by further evidence that oxidative damage increases during the ageing process (Van Remmen and Richardson, 2001), although there is still a lack of direct evidence that oxidative stress might limit the life span of different organisms (Bokov *et al.*, 2004; Muller *et al.*, 2007). The term oxidative stress, however, does not solely refer to the cellular damage caused by free radicals, but also by non-free radical species (Hybertson *et al.*, 2011).

1.1.1 Reactive oxygen species (ROS)

Reactive oxygen species (ROS) are radical and non-radical molecules that arise from oxygen (O_2) during normal metabolism reactions as well as following certain types of damage (e.g. irradiation) (Ray *et al.*, 2012). Common examples of ROS are the superoxide anion radical ($O_2^{\bullet-}$), hydrogen peroxide (H_2O_2) and the hydroxyl radical ($^{\bullet}HO$). Although commonly believed as highly reactive, some ROS can be less reactive than others (e.g. $^{\bullet}HO$ is more reactive than $O_2^{\bullet-}$), and their reactivity is also dependant on their local concentration (Sanz, 2016). An uncontrolled accumulation of ROS can determine oxidative stress towards a wide range of biological molecules, such as proteins, lipids and DNA (deoxyribonucleic acid), and has been connected to various diseases such as diabetes, cancer and neurodegeneration (Waris and Ahsan, 2006). However, there is growing evidence that ROS can serve as signalling mediators by interacting with a wide variety of proteins, thus regulating various signalling pathways among which are cellular growth, antioxidant defences and degradation pathways (Ray *et al.*, 2012). Additionally, recent evidence suggests a possible role of mitochondrial ROS-mediated signalling in actually increasing the life span of lower organisms (e.g. *Caenorhabditis elegans* and *Drosophila melanogaster*) (Sanz, 2016).

It is widely accepted that mitochondria are the principal source of ROS through the respiratory chain, which takes place in the mitochondrial inner membrane and matrix (Murphy, 2009). During oxidative phosphorylation, the oxygen (O_2) is reduced into H_2O (water) to produce ATP (adenosine triphosphate), the nucleotide used as the general energy currency as well as a coenzyme in every cell (Maruyama, 1991). However, the reduction of oxygen can be incomplete following the leak of electrons from mitochondrial complexes (complex I and III mainly), leading to the generation of the superoxide anion (Lenaz, 2001). The superoxide can be reduced to H_2O_2 by the action of SOD, which in turn can be further decomposed through the Fenton reaction (an iron- and copper-catalysed process) to form the highly reactive hydroxyl radical (Fridovich, 1995; Luehrs *et al.*, 2007). Hence, the superoxide can be considered as

the “primary” ROS, from which the “secondary” ROS, such as H_2O_2 and the hydroxyl radical, can be generated (Valko *et al.*, 2007).

Although mitochondrial respiration (together with SOD) accounts for the majority of H_2O_2 production in the cell, other important sources are organelles (e.g. peroxisomes and endoplasmic reticulum) and enzymatic systems (e.g. nicotinamide adenine dinucleotide phosphate - NADPH - oxidase, xanthine oxidase) (Giorgio *et al.*, 2007). Among the previously mentioned ROS, H_2O_2 is the less reactive, most stable and most concentrated ROS in the cell (10^{-7} M), it can be quickly produced intracellularly and degraded by the cellular antioxidant system (Giorgio *et al.*, 2007). Due to its controlled turnover and unique chemical features, as well as its high propensity to diffuse, H_2O_2 appears to be suitable as a second messenger for signal transduction (Forman *et al.*, 2010; Paulsen and Carroll, 2010).

1.1.2 Redox signalling and regulation

The term redox (contraction for reduction-oxidation) refers to chemical reactions where electrons and/or hydrogen atoms are gained (reduction) or lost (oxidation) by different species. Due to their chemical nature, ROS can efficiently function as redox signalling molecules. As mentioned earlier, ROS can interact with target proteins which can “sense” oxidation levels through reversible modification of their sulphur-containing cysteine and methionine residues (Jones, 2008; Paulsen and Carroll, 2010). The thiol (SH) side chain of the cysteine (Cys) residue is particularly sensitive towards oxidation, and at physiological pH, its thiolate ion (S^-) acts as a nucleophile (a molecule that donates an electron pair) in reaction with H_2O_2 (Winterbourn and Metodiewa, 1999). The equilibrium between thiol and thiolate ion is determined by the acid dissociation constant (pK_a), where a high pK_a reflects an equilibrium shifted towards the protonated thiol at physiological pH (~7), while a low p*K*a shifts the equilibrium towards the thiolate ion (Roos *et al.*, 2013). Although free Cys residues have rather high pK_a (8.6) and are protonated at physiological pH, such value can decrease to as low as 3.4 when Cys residues are incorporated into proteins (Grauschopf *et al.*, 1995). Notably, Cys reactivity can be modulated by other polar

amino acids in their proximity that can stabilise the thiolate form (Salsbury *et al.*, 2008), as well as by other structural features like reactive sites related to the protein tertiary structure (Peskin *et al.*, 2007).

Upon reaction with H_2O_2, the Cys thiol group undergoes oxidation and produces its sulphenic acid (SOH), a reversible moiety involved in numerous biochemical reactions (**Figure 1.1**) (Paulsen and Carroll, 2010; Roos and Messens, 2011). This sulphenic derivative is fairly unstable, and usually tends to interact with a thiol group from another Cys to form a disulphide bond (S-S) (Poole *et al.*, 2004). Disulphide bonds are much more stable than sulphenic acid derivatives, forming either intra- or inter-molecular bonds depending on whether the two Cys residues belong to the same or to another protein, respectively. Both the sulphenic acid and the disulphide bond are reversible modifications, and their reduction is tightly regulated by redox buffering systems, highlighting the importance of thiols dynamisms in redox signalling. Following extreme oxidative stress, the further oxidation of the Cys thiol group can also lead to the formation of additional derivatives such as sulphinic (SO_2H) and sulphonic (SO_3H) acids (**Figure 1.1**) (Roos and Messens, 2011). These oxidative states tend to alter the conformation and function of proteins, often leading to their inactivation or degradation (Reddie and Carroll, 2008). The sulphinic and sulphonic states are usually considered irreversible, although it has been discovered that the sulphinic acid can be reduced by the ATP-dependent enzyme sulphiredoxin (Srx) (Biteau *et al.*, 2003).

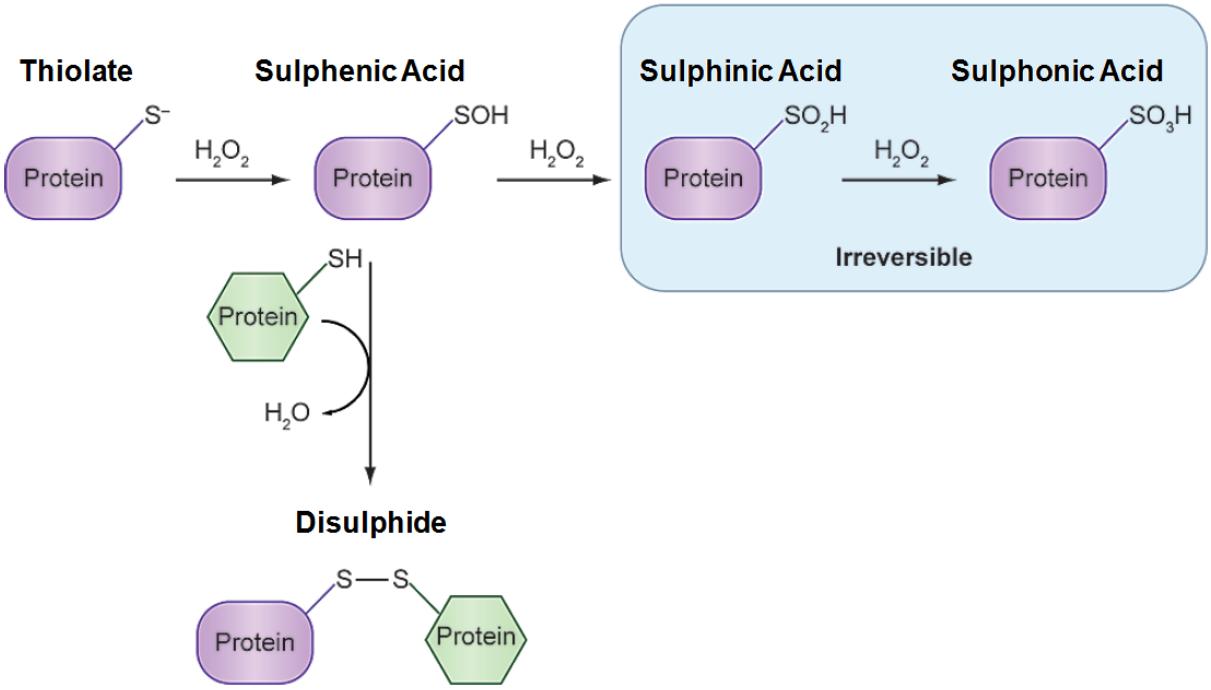

Figure 1.1 | The thiol group of cysteine residues can sense intracellular oxidation levels. Following the reaction with H_2O_2, the thiolate ion (S^-) of a cysteine residue (Cys) becomes oxidised and forms its sulphenic acid (SOH), which can be further oxidised to sulphinic (SO_2H) and sulphonic (SO_3H) acids, or react with another thiol group from a different Cys to form a disulphide bond (S-S). Adapted from (Paulsen and Carroll, 2010).

The formation of disulphide bonds can lead to conformational changes in the proteins and thereby alter their function, interactions and localization (Paulsen and Carroll, 2010; Holmstrom and Finkel, 2014). One example of ROS-mediated regulation is the increase of tyrosine (Tyr) phosphorylation following stimulation with growth factors (Bae *et al.*, 1997). Such increase is mediated by ROS action on protein Tyr phosphatases (PTPs), where the oxidation of a conserved Cys residue in the active site of the PTPs causes their inactivation (Denu and Tanner, 1998; Holmstrom and Finkel, 2014). In a similar manner, deubiquitinating enzymes (DUBs) can be reversibly inactivated by ROS, which oxidise the catalytic Cys residue in the DUBs active site (Cotto-Rios *et al.*, 2012; Lee *et al.*, 2013). Another example of ROS regulation is the activation of autophagy during starvation. Here, starvation induces an increase in mitochondrial ROS production which, in turn, leads to the inactivation

of Atg4 (through Cys oxidation), a protease that regulates the formation of autophagosomes (Scherz-Shouval and Elazar, 2007; Scherz-Shouval *et al.*, 2007).

Furthermore, ROS play a pivotal role in cell proliferation by activating the MAPK (mitogen-activated protein kinase) pathway, specifically acting on p38 MAPK upon palmitic acid-mediated signalling (Wang *et al.*, 2011). Importantly, ROS can also regulate the activity of specific transcription factors, such as AP-1 (activator protein 1) and FOXO (forkhead box protein O), by oxidation of specific Cys residues (Abate *et al.*, 1990; Putker *et al.*, 2013). For instance, the formation of a disulphide bond between FOXO4 and the nuclear import receptor transportin-1 determines the nuclear localisation and activation of the transcriptional factor, which leads to the expression of ROS-scavenging enzymes (Putker *et al.*, 2013). In this way, ROS can directly influence the response of the cell to different stimuli and activate different pathways, such as growth, proliferation and survival (Trachootham *et al.*, 2008).

Considering how ROS appear to be important in regulating a vast array of cellular pathways, their production as well as their scavenging must be tightly regulated, and cells have developed several ways to protect their intracellular environment from harmful oxidative levels.

1.1.3 Antioxidant responses

Since high levels of ROS may produce irreversible modifications in protein thiols and affect their functions, it is fundamentally important for the cell to promptly activate effective antioxidant defences and alleviate the intracellular oxidising burden. In physiological conditions, the redox buffering is mainly mediated by glutathione (GSH), a highly abundant low-molecular-weight tripeptide (glutamate-cysteine-glycine) containing a thiol group (Filomeni *et al.*, 2002). Essentially, GSH provides a pool of thiols which buffers oxidation generated by ROS, thus providing a more reduced environment. Thus, GSH becomes oxidised and generates a disulphide

bond with another molecule of GSH, forming the glutathione disulphide GSSG (Meister and Anderson, 1983). The enzyme glutathione reductase (GR) then reduces GSSG back to GSH using the reducing equivalents (i.e. electrons) provided by NADPH, which in turn becomes oxidised ($NADP^+$) (Deponte, 2013). This GSH-GSSG-GSH cycle provides a balanced intracellular environment which protects proteins from harmful ROS levels. Additionally, the selenoprotein glutathione peroxidase (Gpx), which bears a selenocysteine (Sec) in its catalytic site, directly catalyses the reduction of H_2O_2 using GSH as a reductant (Brigelius-Flohe and Maiorino, 2013).

Another important family of proteins involved in the endogenous antioxidant buffering is the thioredoxin (Trx) (**Figure 1.2**). The ubiquitous Trx family is composed of small 12 kDa (kilo Dalton) dithiol protein reductases which, together with the homodimeric selenoprotein thioredoxin reductase (TrxR), reduce target proteins by thiol-disulphide exchange (Lu and Holmgren, 2014). TrxR is the only known enzyme that reduces Trx by using the reducing equivalents from NADPH (Argyrou and Blanchard, 2004). The TrxR homodimers are head-to-tail oriented, with the N-terminus of one molecule facing the C-terminus of the other molecule, forming a redox-active centre (Sandalova *et al.*, 2001). The N-terminus bears a double Cys dithiol active site, while the C-terminal region contains a Cys-Sec pair (homologous to Gpx) (Zhong *et al.*, 1998). The disulphide bond in the N-terminus of TrxR becomes reduced by NADPH, then the N-terminal dithiol reduces the selenylsulphide bond in the C-terminus of the homodimeric subunit, which in turn reduces the disulphide bond in the active site of Trx (Lu and Holmgren, 2009). There seem to be clear redundancies between the GSH and Trx/TrxR systems, in order to maintain redox homeostasis when either of the systems is compromised (Schmidt, 2015; Tebay *et al.*, 2015).

The reducing power supplied by GSH and Trx/TrxR is promptly employed by a multitude of proteins, of which the peroxiredoxin (Prx) family of peroxidases is the most known example (**Figure 1.2**) (Hofmann *et al.*, 2002). Prxs are a ubiquitous family of antioxidant proteins which reduce peroxides such as H_2O_2, thus having important implications in H_2O_2-mediated signalling (Wood *et al.*, 2003a). Prxs were originally characterised into two categories, the 1-Cys and 2-Cys Prxs, based on the

number of Cys residues catalytically active, although subsequently the 2-Cys Prxs were further divided into two classes called the 'typical' and 'atypical' 2-Cys Prxs (Wood *et al.*, 2003b).

The largest class of Prxs are the typical 2-Cys Prxs, obligated homodimers, each containing a peroxidatic Cys (C_p) and a resolving Cys (C_r) (Hall *et al.*, 2009). The C_p thiol of one subunit reduces the peroxide substrate and becomes oxidised by forming a sulphenic acid (SOH), then reacts with the C_r of the second subunit to form a disulphide bond which, in turn, is reduced by Trx or another reductase (Wood *et al.*, 2003b; Rhee *et al.*, 2012). The atypical 2-Cys Prxs, instead, are functionally monomeric but share the same mechanism as the typical 2-Cys Prxs (Seo *et al.*, 2000). Here, both the C_p and its corresponding C_r are contained within the same subunit, thus forming an intramolecular disulphide bond (Rhee *et al.*, 2012). The 1-Cys Prxs, as the name suggests, only contain the C_p while missing the correspondent C_r (Choi *et al.*, 1998). This last class of Prxs only forms the C_p sulphenic acid after reacting with the peroxide substrate (Rhee *et al.*, 2012).

Eukaryotic Prxs, compared to prokaryotic Prxs, are more susceptible to hyperoxidation due to their conformation, which restricts the access of the oxidised C_p to the C_r (Wood *et al.*, 2003a). Thus, especially in the presence of higher levels of H_2O_2, the C_p thiol tends to form the sulphenic and sulphonic acids, losing its peroxidatic activity (**Figure 1.2**) (Yang *et al.*, 2002; Hall *et al.*, 2011). The "Floodgate" model proposes that such inactivation of Prxs might increase the signalling functions of H_2O_2 in eukaryotic cells (Wood *et al.*, 2003a). The only enzyme that can revert the sulphinic state of the Prxs C_p is the ATP-dependent Srx, thus reactivating the peroxidatic function and blocking H_2O_2 signalling (Hall *et al.*, 2011; Jeong *et al.*, 2012). Interestingly, the hyperoxidation of Prxs can also facilitate the formation of higher molecular weight (MW) complexes with chaperone activity, important in protecting the cell from high levels of ROS (Jang *et al.*, 2004; Lim *et al.*, 2008).

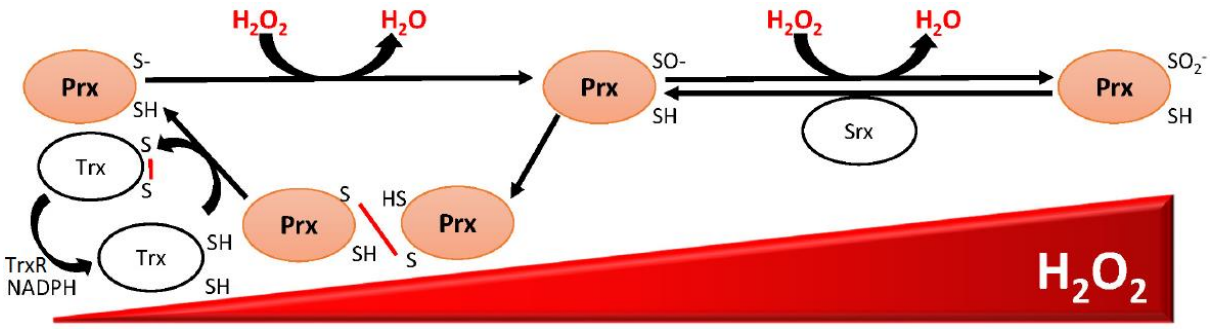

Figure 1.2 | Schematic representation of H_2O_2 scavenging by the peroxiredoxin/thioredoxin system. The cysteine (Cys) residue of a peroxiredoxin (Prx) reacts with H_2O_2 to form a sulphenic acid derivative (SO^-). This is followed by the formation of a disulphide bond between such Cys and the resolving Cys of a neighbouring Prx. The resulting Prx disulphides are reduced by thioredoxin family proteins (Trx) by thioredoxin reductase (TrxR) using electrons from NADPH. At high concentrations of H_2O_2, the Cys of Prx can become hyperoxidised to a sulphinic acid (SO_2^-), which can be reduced by sulphiredoxin (Srx) back to the SO^- form. Adapted from (Latimer and Veal, 2016).

During oxidative stress, very high levels of ROS can overwhelm the redox buffering system. Hence, the cell has developed mechanisms which can assist the antioxidant response and increase cell survival. The Nrf2 (nuclear factor erythroid 2-related factor 2) pathway controls the expression of a spectrum of genes involved in cellular defence against oxidative stress and toxic compounds (Vomhof-Dekrey and Picklo, 2012). Nrf2 is the most studied stress-activated, cap'n'collar (CNC)-family basic leucine zipper (CNC-bZIP) transcription factor (Sykiotis and Bohmann, 2010). Nrf2 contains six conserved Neh (Nrf2-ECH homology) domains in its sequence, allowing the binding with molecular partners and regulators, as well as with components of the transcriptional apparatus (Jaramillo and Zhang, 2013). The transcription of genes in mediated primarily by a dimer of Nrf2 (mediated by Neh1 domain) and a member of the small Maf (muscoloaponeuretic fibrosarcoma) oncogene family proteins (Itoh *et al.*, 1997). An increase in cellular oxidative conditions leads to the translocation of the Nrf2-Maf dimer from the cytoplasm to the nucleus to bind the antioxidant response element (ARE) sequence in the promoter of different genes, leading to their transcription (Nioi *et al.*, 2003).

The main regulator of the Nrf2 pathway is Keap1 (Kelch-like ECH-associated protein 1), a Cullin3-based E3 ubiquitin ligase. In normal cellular conditions Keap1 homodimerizes, acting as an adaptor for the Cullin3-dependent ubiquitination and subsequent proteasomal degradation of Nrf2 (Kobayashi *et al.*, 2004). The dimerisation of Keap1 in mediated by the BTB (broad complex, tramtrack and bric-a-brac) domain, while the Kelch repeats (which form a four-stranded β-sheet motif) ensure the interaction with the ETGE (glutamate-threonine-glycine-glutamate) and DLG (aspartate-leucine-glycine) motifs in the Nhe2 domain of Nrf2 (Itoh *et al.*, 1999; Lo *et al.*, 2006; Tong *et al.*, 2006). An oxidative or chemical stimulus induces a conformational change in three reactive cysteines within the IVR (intervening region) domain of Keap1, which disrupts the interaction with the DLG motif of Nrf2 (Dinkova-Kostova *et al.*, 2002). The lost interaction with Keap1 disturbs the ubiquitination process and leads to the stabilization of Nrf2, its accumulation in the cytosol and translocation into the nucleus (Bryan *et al.*, 2013). Target genes that respond to Nrf2 include enzymes responsible for the biosynthesis of GSH and its utilisation, Trx production and regeneration, NAPDH generation and expression of various other cytoprotective proteins (Gorrini *et al.*, 2013).

Failure in keeping the intracellular environment in the correct redox state may cause irreversible changes in protein structure and function, lead to protein aggregation and inclusions formation and ultimately to cell death. Thus, cells have developed numerous molecular pathways to control the folding state of proteins, their function and degradation, in order to maintain a normal intracellular environment.

1.2 Control of Proteostasis

The entirety of proteins within a cell, termed proteome, determines the cell functions and fate. Indeed, proteins are vital molecules that provide regulatory, structural and catalytic functions. It has been estimated that the proteins copy number in a single cell is of 2 to 4 million per cubic micron (Milo, 2013), a huge amount of molecules that needs to be monitored and coordinated in the different subcellular compartments. As the proteome faces countless changes during cellular development and ageing, cells must have developed highly responsive mechanisms in order to regulate the trafficking and folding state of the proteins. In fact, newly synthesised proteins need to be correctly folded to achieve their functional state. This is a remarkably dynamic process, by which the cell can change the folding state and therefore the function of selected proteins following environmental challenges to ensure cell survival (Gidalevitz *et al.*, 2011).

Through the proteostasis (i.e. protein homeostasis), cells can tightly regulate the production and degradation of the proteins as well as their correct folding, in order to maintain an appropriate intracellular environment. Hence, proteostasis is the key mechanism that cells adopt to face changes in their surroundings, maintain the proteome integrity and prevent the onset of different diseases (Balch *et al.*, 2008). Loss of proteostasis often leads to the formation of misfolded and aggregated proteins, with catastrophic consequences for the cell (Hartl *et al.*, 2011).

The term proteostasis network (PN) has been given to the complex regulatory system that operates in order to control the proteome stability, avoiding the occurrence of protein misfolding and aggregation (Balch *et al.*, 2008). The main function of the PN is to coordinate the synthesis, assembly, trafficking, disassembly and degradation of the proteins (Balch *et al.*, 2008). The PN consists of: a translational machinery for the synthesis of proteins, molecular chaperones involved in the correct folding of proteins, degradative pathways like the proteasome and the autophagy pathway, plus essential PN modifiers such as cellular stress responses and post-translational modifications (Balch *et al.*, 2008; Labbadia and Morimoto,

2015). Thus, it has been proposed that proteins have (beyond their primary, secondary, tertiary and quaternary structural states) a quinary physiological state given by the PN, which regulates their folding state and function in relation to the surrounding environment, enhancing the survival and the evolvability of the cell (Powers and Balch, 2013).

Defects in any of the molecular machineries involved in the control of proteostasis may lead to the disruption of the PN functionality, leading to various diseases (Labbadia and Morimoto, 2015). This could lead to the conformational change of proteins towards misfolded states, leading to protein aggregation and/or degradation. Environmental stresses such as oxidation as well as ageing appear to be the major risk factors in the loss of PN functionality (Taylor and Dillin, 2011; Di Domenico *et al.*, 2014; Labbadia and Morimoto, 2014).

1.2.1 The unfolded protein response (UPR)

As protein misfolding and aggregation can represent a serious threat for the cytosolic environment, cells have developed several measures to counteract these menaces. An important reaction to the increase in the protein misfolding levels is through the activation of stress responses. Here, different transcription factors are activated in response to non-native protein conformations, ensuring the cellular adaptation to stress and survival (Labbadia and Morimoto, 2015). This is particularly important at the endoplasmic reticulum (ER) level, where the newly synthesised proteins must be correctly folded to be subsequently secreted. In fact, the ER is a highly dynamic organelle involved in the biosynthesis of lipid and proteins, particularly important in specialized secretory cells. Protein maturation and folding in the ER can be extremely demanding, surpassing the capacity of the folding machinery. This can generate a source of stress which is managed through the unfolded protein response (UPR) (Walter and Ron, 2011; Hetz, 2012). The UPR is an adaptive and complex mechanism that senses the misfolding in the ER, exerting its function through three different stress transducers to preserve the ER function (Ron and Walter, 2007).

The first branch of the UPR consists of the activation of IRE1 (inositol-requiring protein 1), an ER-transmembrane protein with serine/threonine kinase and endoribonuclease (RNase – ribonucleic acid hydrolase) activity that senses the unfolded proteins levels (Cox *et al.*, 1993; Walter and Ron, 2011). The genes activated by IRE1 signalling are involved in the upregulation of the ER membrane biogenesis and folding machinery, as well as the ERAD (ER-associated degradation), a pathway which links the ER with the protein degradation machinery in the cytosol (Wang and Kaufman, 2012). The second branch of the UPR is mediated by PERK (protein kinase RNA-activated – PKR –like ER kinase), another transmembrane kinase (Ron and Walter, 2007). The PERK signalling can have a dual role: to protect the cell from protein accumulation or, in case of high levels of stress, to drive the cell to death. The third branch of the UPR is mediated by ATF6 (activating transcription factor 6), which represents a group of transmembrane proteins involved in transducing the ER stress and in encoding transcription factors (Hetz, 2012).

As it appears, different signalling pathways tightly control the misfolding in the ER. However, the cell has developed additional pathways to better regulate the stress associated with misfolded proteins, by allowing their correct folding or, when the folding capacity is exceeded, their degradation.

1.2.2 Molecular chaperones

During translation, proteins are synthesised as linear sequences of amino acids, however their functionality only arises from a correct folding process. Although a minor number of small proteins can fold autonomously, the majority of the bigger-sized, multi-domain proteins need folding assistance. Molecular chaperones are a complex network of catalytic enzymes with the pivotal role of ensuring the correct folding of proteins (Kim *et al.*, 2013). Chaperones are also known as heat shock proteins (Hsps), due to the fact that their expression is induced in conditions of stress such as heat shock or oxidation, which usually cause destabilisation of the native structure of proteins (Morano *et al.*, 2012). Chaperones are classified according to

their MW, where Hsp70s and Hsp90s (Hsps of 70 and 90 kDa, respectively) are the most characterised as well as the most abundant families, constituting 1-2% of the total amount of proteins in many cells (Labbadia and Morimoto, 2015). The heat shock response (HSR) is a stress response which upregulates the chaperone activity following an increase in the misfolding and aggregation of proteins, usually in response to increased temperature as well as other sources of stress (Richter *et al.*, 2010).

Activity of chaperones depends on their ability to bind and hydrolyse ATP. In fact, chaperones undergo an ATP/ADP (adenosine diphosphate) exchange cycle where the affinity for their substrates (known as clients) is highly influenced by the nucleotide binding (Kampinga and Craig, 2010). The hydrolysis of ATP to ADP leads to the conformational change of chaperones and increases their affinity for hydrophobic sequences of unfolded proteins, thus preventing protein aggregation (Hartl *et al.*, 2011; Kim *et al.*, 2013). The Hsp70s family of chaperones comprises the constitutively expressed Hsc70 (heat shock cognate of 70 kDa) and the stress-inducible Hsp70 (Liu *et al.*, 2012). The two chaperones share a high degree of homology, yet Hsp70 association with substrates and changes in the secondary structure upon oxidative stress are more pronounced than Hsc70 (Callahan *et al.*, 2002). Hsp90s are a highly conserved family of chaperones which, like Hsp70s, use ATP to exert their function in protein folding (Taipale *et al.*, 2010).

The activities of Hsp70s and Hsp90s are aided by the action of non-client binding partners known as co-chaperones, which assist the activity of chaperones (Caplan, 2003; Hartl *et al.*, 2011). The main functions of co-chaperones are the regulation of the ATPase cycle, the facilitation of client binding and the shuttling of chaperones to different subcellular locations. Thus, the complex made by chaperones/co-chaperones forms the functional machinery that regulates the folding of proteins in the cell. Interestingly, the co-chaperone Hop (Hsp70-Hsp90 organising protein, also known as Sti1 - stress inducible protein 1), can bind both Hsp70s and Hsp90s, thus connecting the two chaperone systems and allowing the concerted folding of clients (Carrigan *et al.*, 2006). Another co-chaperone, known as Hip (Hsc70-interacting

protein), binds instead to Hsc70 and activates its ATPase activity, stabilising the ADP state and enhancing the affinity for its clients (Hohfeld *et al.*, 1995).

Other co-chaperones are instead involved in the degradation of misfolded proteins that fail the refolding process and can lead to aggregation, as well as short-lived regulatory proteins that need to be degraded (Arndt *et al.*, 2007). An important player in the chaperone-mediated protein degradation is the C-terminus of Hsp70-interacting protein (CHIP), an E3 ubiquitin ligase and co-chaperone of both Hsp70s and Hsp90s which creates a bridge between the chaperones and the proteasome degradative machinery, facilitating the degradation of the protein substrates (Connell *et al.*, 2001; Demand *et al.*, 2001). Another co-chaperone important for chaperone-mediated protein folding and degradation is BAG1 (B-cell lymphoma 2 – Bcl-2 – associated athanogene 1), initially known as a biding partner of the apoptosis-inhibiting regulator Bcl-2. BAG1 bears a BAG domain which binds to Hsp70s and connects the chaperone network to the proteasome (Luders *et al.*, 2000; Arndt *et al.*, 2007). Furthermore, BAG1 can facilitate the CHIP-mediated degradation of chaperone substrates by facilitating their interactions with the proteasome (Demand *et al.*, 2001). The BAG-family component BAG3, instead, mediates the recognition of misfolded proteins by binding to Hsp70s and drives their degradation through macroautophagy (Gamerdinger *et al.*, 2009; Behl, 2011).

Since molecular chaperones have an important role in promoting the correct folding of protein as well as targeting misfolded proteins for degradation, they are considered valuable therapeutic targets especially in neurons, where proteostasis is paramount for their survival (Smith *et al.*, 2015).

1.2.3 Protein misfolding and aggregation

Protein misfolding can have deleterious effects for the cellular environment, since the exposure of otherwise hidden hydrophobic regions of the proteins could lead to their irreversible, non-native interaction and formation of insoluble aggregates (**Figure 1.3**) (Hartl *et al.*, 2011; Kim *et al.*, 2013). Therefore, it is fundamental for the cell to

implement several strategies to ensure the correct folding of proteins, especially under stress conditions. This is particularly important in neurons, since they are non-dividing cells and therefore more susceptible to stresses, especially to proteotoxicity caused by misfolded proteins (Morimoto, 2008; Douglas and Dillin, 2010). In fact, many different neurodegenerative diseases are characterised by the accumulation of misfolded proteins in aggregates and ultimately in insoluble inclusions (see **Chapter 1.7**) (Soto, 2003; Douglas and Dillin, 2010).

The aggregation process can be either chaotic, led by hydrophobic forces to form amorphous aggregates, or ordered, following the development of proteins into β-sheet conformation (**Figure 1.3**) (Moreno-Gonzalez and Soto, 2011). The β-sheet structure permits a more favourable interaction between proteins and leads to the formation of oligomers, proto-fibrils and fibrils, known to be toxic for the cell (Caughey and Lansbury, 2003; Moreno-Gonzalez and Soto, 2011). The toxicity elicited by soluble oligomers appears to be the highest, as they could induce apoptosis and impair the synaptic activity in neurons (Demuro *et al.*, 2005; Shankar *et al.*, 2008).

The larger proto-fibrils may also contribute to apoptosis by creating pore-like structures in the plasma membrane and destabilising the intracellular environment (Lin *et al.*, 2001). Fibrils are long and straight formations that are less toxic compared to oligomers and proto-fibrils, and tend to accumulate to form insoluble aggregates (**Figure 1.3**) (Caughey and Lansbury, 2003). Considering the high toxicity of soluble formation such as oligomers and proto-fibrils, it has been proposed that fibrils and ultimately insoluble inclusions could serve as a protective mechanism for the cell to sequester smaller, harmful species from causing damage, although this remains a controversial point (Ross and Poirier, 2005; Winklhofer *et al.*, 2008; Treusch *et al.*, 2009).

Aberrant conformation of proteins could arise from specific mutations (either sporadic or inherited) which destabilise the native state and alter the hydrophobicity, the charge and the secondary structure (Chiti *et al.*, 2003). These aggregation-prone proteins tend to hinder the folding and degradation machineries and lead normal, unrelated proteins to misfolding and accumulation, thus exacerbating the toxicity in

the cell (Bates, 2006). The term “conformational diseases” has been given to those conditions where certain proteins undergo a toxic gain-of-function, becoming aggregate-prone and leading to cellular degeneration (Gidalevitz *et al.*, 2010).

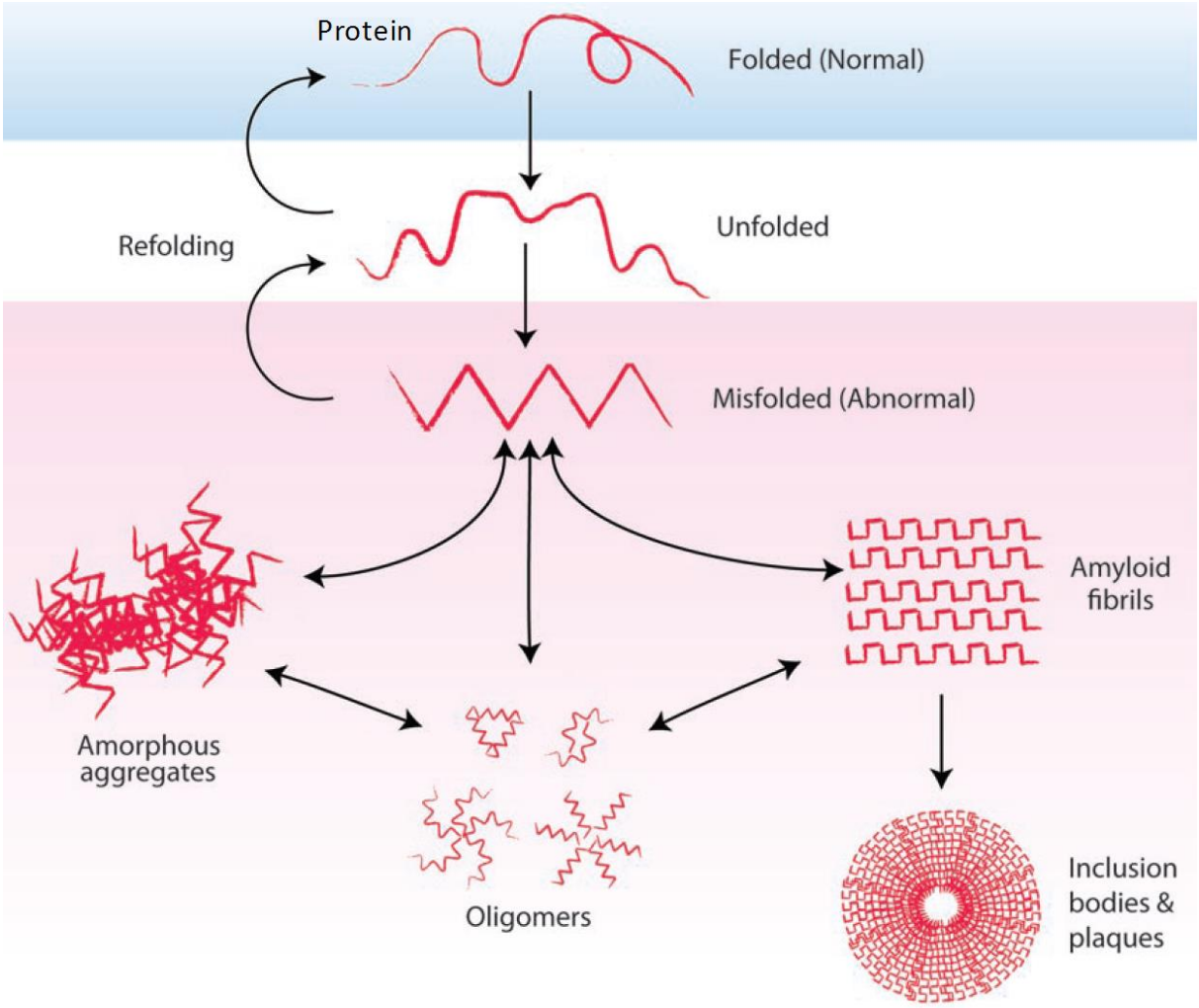

Figure 1.3 | Protein aggregate formation following misfolding. The loss of correct protein conformation (unfolding) can lead to misfolding, where the protein abnormal structure can oligomerise and form either amorphous aggregates or ordinate fibrils. The latter can in turn lead to inclusion bodies and extracellular plaques formation, a prominent feature of most neurodegenerative diseases. Adapted from (Treusch *et al.*, 2009).

1.3 Ubiquitin and Protein Degradation

Degradation pathways have a fundamental role in the control of proteostasis, since many regulatory as well as damaged proteins need to be turned over in order to protect the cell from abnormal protein accumulation. Proteolysis is not only involved in the protein quality control but also important for a wide array of cellular processes like cell division, signal transduction and apoptosis. Intracellular proteolysis has been studied for more than 70 years, and the discovery of the lysosome as a proteases-containing organelle led to the hypothesis that the degradation processes would have only been lysosome-mediated (Ciechanover, 2005).

It later became clear that some non-lysosomal machinery was also involved in the degradation of the majority of the soluble, short-lived proteins, which was dependent on energy expenditure in form of ATP (Ciechanover, 2005). An essential component of this intracellular catalytic pathway was therefore called APF1 (ATP-dependent proteolysis factor 1), which was found to be covalently attached to the target substrates (Ciechanover *et al.*, 1980; Hershko *et al.*, 2000). It soon became clear that APF1 was in reality a ubiquitous protein known long before, yet without a recognisable function, called ubiquitin (Wilkinson *et al.*, 1980).

1.3.1 Ubiquitination process

Ubiquitin is a small, heat-stable, highly conserved protein of 76 amino acids and 8.5 kDa which was originally found ubiquitously (from here the given name) in every living organism, including prokaryotes (Goldstein *et al.*, 1975). Subsequently, it became clear that ubiquitin was instead only present in eukaryotes, but its name has been kept for historical reasons (Ciechanover, 2005). Ubiquitin serves as a signalling molecule that tags damaged or unfolded proteins in a covalent way, leading to their degradation through cytosolic or lysosomal proteases (Glickman and Ciechanover, 2002; Callis, 2014). Therefore, it is considered a post-translational modification similar to, yet more complex than, phosphorylation (Komander, 2009). Ubiquitination can also serve to regulate different important processes in the cell beyond protein

degradation, such as endocytosis, DNA repair, signal transduction and protein trafficking (Mukhopadhyay and Riezman, 2007).

Three different enzymes enable the attachment of ubiquitin to a substrate in an ATP-dependent manner, called E1 (ubiquitin-activating enzyme), E2 (ubiquitin-conjugating enzyme) and E3 (ubiquitin ligase) (**Figure 1.4**) (Hershko *et al.*, 1983; Welchman *et al.*, 2005). The reaction is initiated by the activation of ubiquitin through ATP expenditure, which leads to the formation of a reactive thioester bond between a cysteine (Cys) residue of E1 and the C-terminal glycine (Gly) of ubiquitin (Gly76) (Hershko and Ciechanover, 1998). In the second step, the ubiquitin C-terminus is transferred to a E2 Cys residue thus forming another thioester bond; then, ubiquitin is transferred onto the substrate by an E3 enzyme, which mediates the formation of an isopeptide bond between the Gly76 of ubiquitin and the ε-NH_2 group of a Lys residue of the target protein (**Figure 1.4**) (Ciechanover, 1994; Pickart, 2001). Therefore, the enzymatic system for ubiquitin activation appears hierarchical: so far, two E1s have been identified to activate ubiquitin (Groettrup *et al.*, 2008), which is transferred to several dozens of E2s and finally binds to its substrates through hundreds of E3s, the substrate-recognition modules (Pickart and Eddins, 2004).

The E3s can be divided in two classes, depending on the type of domain present in their structure: HECT (homologous to E6-AP – E6-associated protein – carboxy-terminus) domains and RING (really interesting new gene) finger domains (Metzger *et al.*, 2012). The HECT domain E3s are large monomeric proteins that accept an ubiquitin moiety from E2s and form a thioester bond between their active-site cysteine and ubiquitin, prior to transferring it to their substrates (Rotin and Kumar, 2009). There are ~30 HECT domain E3s in mammals, compared to the RING finger domain-containing enzymes which are more than 600 (Li *et al.*, 2008). The RING finger domain E3s can be either monomeric or part of multimeric complexes, acting as scaffolds by facilitating the direct transfer of ubiquitin from the E2s to the substrates (Deshaies and Joazeiro, 2009). Ubiquitination is a reversible process, where DUB proteases cleave ubiquitin to either recycle it or reverse the modification of the target proteins (Reyes-Turcu *et al.*, 2009).

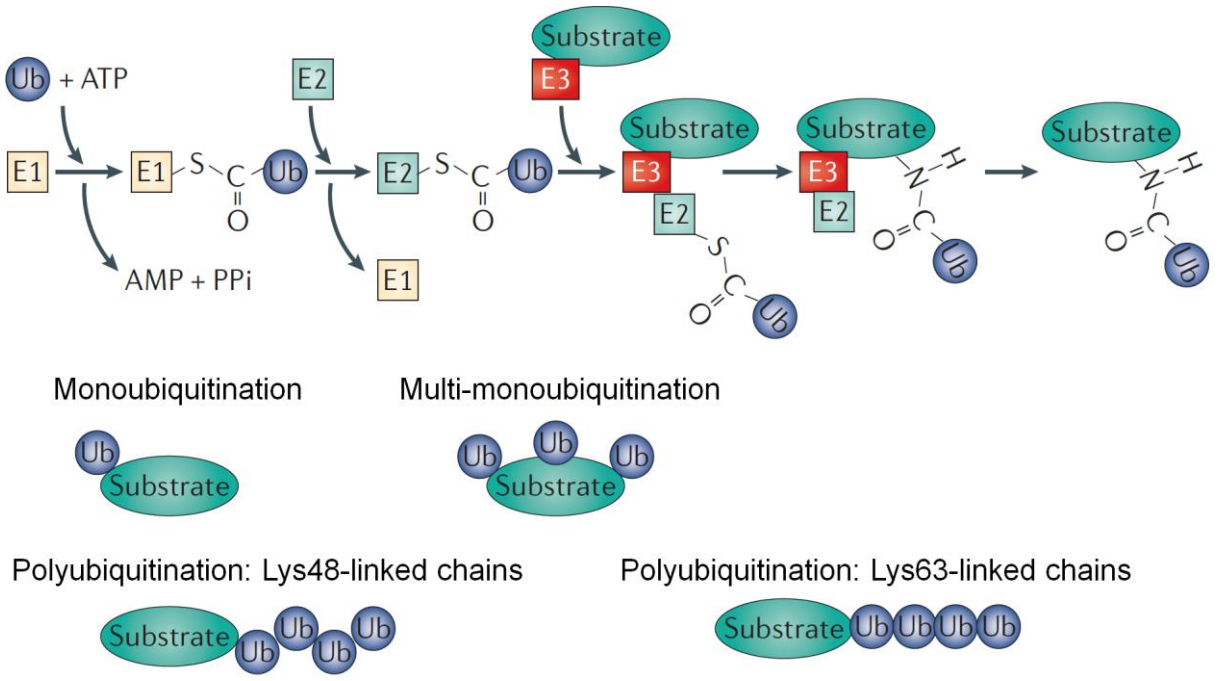

Figure 1.4 | Ubiquitin process and different types of ubiquitination. Ubiquitin (Ub) is first activated in an ATP-dependent manner and forms a thioester bond with the cysteine of an ubiquitin-activating enzyme (E1). Then, Ub is transferred to an ubiquitin-conjugating enzyme (E2), forming a second thioester bond with an E2 cysteine. Lastly, an ubiquitin ligase (E3) mediates the transfer of Ub from the E2 to the substrate protein by forming an isopeptide bond. Multiple cycles of ubiquitination can determine the formation of mono-, multi-mono- and polyubiquitinated proteins. Lys48-linked chains present a closed conformation compared to the linear Lys-63-linked chains. PPi: pyrophosphate. Adapted from (Lipkowitz and Weissman, 2011).

1.3.2 Types of ubiquitination

A single ubiquitin modification is known as monoubiquitination, whereas multiple ubiquitin molecules could give rise to multi-monoubiquitination or polyubiquitination (**Figure 1.4**) (Komander, 2009). In fact, the presence of other Lys residues (positions 6, 11, 27, 29, 33, 48 and 63) on itself allows ubiquitin to become an acceptor of other ubiquitin molecules, leading to the formation of different homotypic polyubiquitin chains (Komander, 2009; Behrends and Harper, 2011). In addition, the N-terminal methionine (Met1) can also contribute in the assembly of linear head-to-tail

polyubiquitin chains (Rieser *et al.*, 2013). Notably, there is increasing evidence for mixed polyubiquitin chains where two or more different Lys residues of one ubiquitin moiety become available for attachment to other ubiquitin molecules, thus forming branched or “forked” chains (Kim *et al.*, 2007; Komander, 2009).

While mono-ubiquitination has been found to be important in regulating the endocytosis of cell-surface receptors and in the DNA-damage response (Sigismund *et al.*, 2004), polyubiquitination appears fundamental in targeting damaged proteins for degradation and in regulating different signalling pathways, such as DNA repair and inflammation (Sun and Chen, 2004). Interestingly, the most abundant ubiquitin-ubiquitin linkage occurs through Lys (K) in position 48 (K48), which adopts a more closed conformation compared to other linkages and represents the signal for proteasomal degradation (Komander, 2009; Fushman and Walker, 2010). By contrast, K63-linked polyubiquitin chains adopt a more linear conformation and are associated with signal transduction, although they can also signal the lysosomal degradation of substrates (**Figure 1.4**) (Tan *et al.*, 2008; Behrends and Harper, 2011).

Ubiquitination is often regulated by numerous proteins containing at least 16 different ubiquitin-binding domains (UBDs), which recognise the ubiquitin moieties through non-covalent interactions and mediate most of their effects in the intracellular environment (Hurley *et al.*, 2006). Besides ubiquitin, nearly 20 ubiquitin-like (UBL) protein modifiers have been discovered, which bear the β-grasp fold (known as the ubiquitin-fold) and can be attached by their C-terminus onto protein substrates to regulate different cellular processes (van der Veen and Ploegh, 2012).

1.4 The Ubiquitin-Proteasome System (UPS)

Ubiquitinated proteins are often degraded through the proteasome, giving rise to the ubiquitin-proteasome system (UPS). The UPS is highly selective, degrading the majority of the soluble, short-lived proteins with regulatory functions as well as damaged proteins tagged for the degradation (Ciechanover, 2005). Proteasomes are enormous protein complexes that can be found in all eukaryotes and archaea as well as some bacteria, located both in the cytoplasm and in the nucleus (Peters *et al.*, 1994).

The proteasome is a giant protease of 2.5 MDa (mega Dalton) composed of a core particle (CP) known as the 20S complex (S for Svedberg, coefficient of sedimentation) and one or two regulatory particles (RP) known as the 19S complex (**Figure 1.5**) (Finley, 2009). Cells contain two different forms of proteasome depending on the number of regulatory subunits attached to the CP, as one (RP1CP) or two (RP2CP) regulatory subunits constitute the 26S and 30S proteasomes, respectively (Tanaka *et al.*, 2012). Because of some lack of accuracy, many refer to the proteasome as the 26S complex, although the physiological functioning unit in the cell seems to be the RP2CP (Tanaka *et al.*, 2012). For simplicity, we will refer to the 26S proteasome as the main and active form.

1.4.1 The 20S and 19S complexes

The 20S (CP) complex of ~730 kDa has a barrel-shaped structure composed by four rings of seven subunits each, up to a total of 28 subunits (Finley, 2009). The two outer α-rings are made up of α-subunits (α-α'_{1-7}), which surround the two inner β-rings of β-subunits (β-β'_{1-7}) (**Figure 1.5**) (Lowe *et al.*, 1995; Groll *et al.*, 1997). The α-rings structure is almost completely closed, thus preventing non-target proteins to enter inside the CP cavity formed by the β-rings, which contains the proteasome-proteolytic sites. The subunits β_1, β_2 and β_5 possess the catalytic sites exposed to the inner face of the chamber, bearing caspase-like, trypsin-like and chymotrypsin-like activities, respectively (Bochtler *et al.*, 1999). These proteolytic subunits belong to the

N-terminal nucleophile (Ntn) hydrolase family, which share an active N-terminal threonine residue for peptide-bond cleavage (Brannigan *et al.*, 1995).

To gain access to the proteolytic sites, the substrates have to pass through the α-rings located at the edges of the barrel. In the closed α-rings conformation, the N-termini of the α-subunits assemble centrally, creating a network that topologically occludes the barrel pore (Groll *et al.*, 2000). Importantly, at the interface between different α-subunits there are 7 α-pockets which face the external environment, permitting the interaction with the RP complex which, in turn, opens the channel, giving access to the proteolytic sites (Groll *et al.*, 1997; Smith *et al.*, 2007).

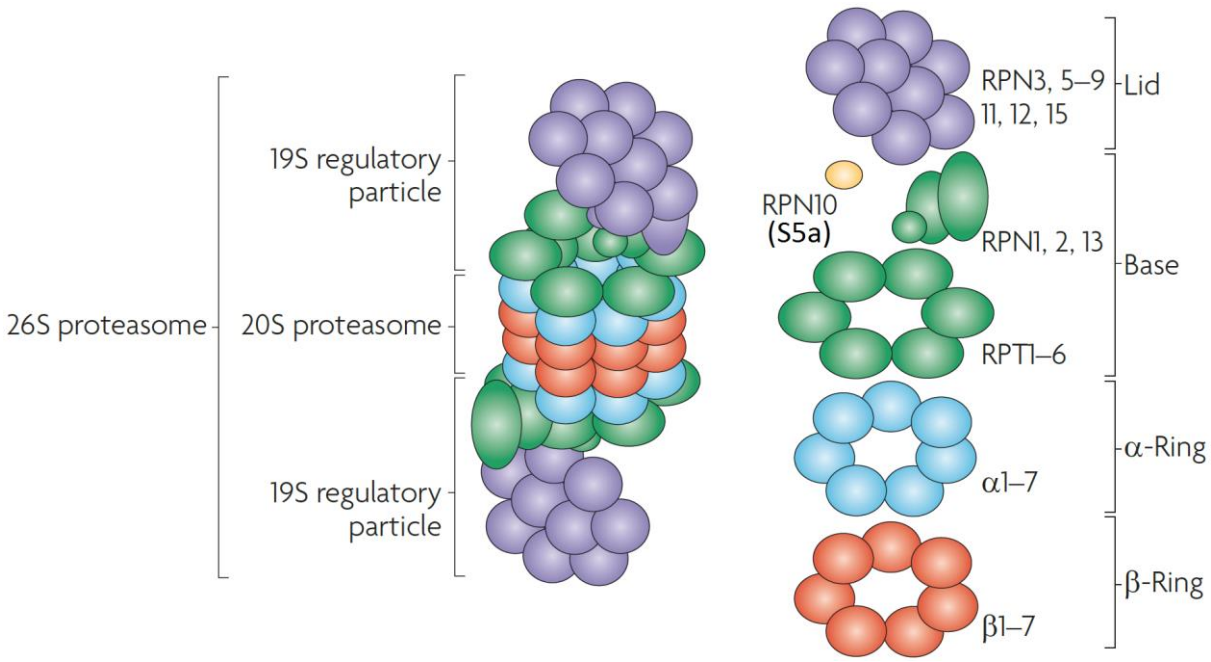

Figure 1.5 | Structure of the 26S proteasome. The 26S proteasome is composed of one core particle (20S) and two regulatory particles (19S). The core particle consists of two outer α-rings and two inner β-rings, each of them composed of 7 subunits. The regulatory particles consist of 6 regulatory triple-A subunits (Rpt) and 9 regulatory non-ATPase subunits (Rpn), which constitute the base and lid subcomplexes. The Rpn10 (S5a) subunit interacts with both the base and the lid. Adapted from (Murata *et al.*, 2009).

Two 19S (RP) complexes of ~900 kDa bind at both ends of the 20S barrel, thus forming the complete proteasome of 26S (**Figure 1.5**) (Finley, 2009). Each RP comprises 19 subunits, which can be further classified into two groups: triple-A or AAA^+ (ATPase associated with diverse cellular activities) subunits (also known as Rpt, regulatory particle triple-A protein) and non-ATPase (also known as Rpn, regulatory particle non-ATPase) subunits (Finley *et al.*, 1998; Tanaka *et al.*, 2012). These subsets of subunits are arranged to form two different subcomplexes: a base, which includes 6 ATPase (Rpt1-6) and 3 non-ATPase subunits (Rpn1, 2 and 13), and a lid, comprising the other 9 non-ATPase subunits (Rpn3, 5-9, 11, 12 and 15) (Glickman and Ciechanover, 2002; Murata *et al.*, 2009). The ATPase subunits of the base bind to the α-subunits of the 20S barrel, while the lid can attach and detach from the base through the interaction with Rpn10 (known as S5a – subunit 5a – in mammals) (Glickman *et al.*, 1998). The binding of the lid to the base is important for the recognition of the ubiquitinated substrates that need to be degraded.

1.4.2 Substrate recognition and degradation

The recognition of the substrates and their degradation is mediated by a multistep mechanism involving both the 19S and the 20S complexes (Pickart and Cohen, 2004). The signal for degradation through the proteasome is the ubiquitination, where at least 4 ubiquitin moieties are attached to the substrate through K48 linkage (Thrower *et al.*, 2000). The polyubiquitin chain is then recognised by the 19S subunits Rpn10/S5a and Rpt5 (an ATPase), driving the substrate towards the base subcomplex (Deveraux *et al.*, 1994; Lam *et al.*, 2002). The base of the 19S bears a chaperone-like activity, in fact the ATPase activity of the Rpt subunits determines the unfolding of the substrates (Braun *et al.*, 1999).

As only unfolded proteins can pass through the 19S complex and reach the proteolytic sites in the 20S complex (Glickman *et al.*, 1998), the polyubiquitin chain of the substrates must be detached prior the entry into the proteasome. The Rpn11 subunit is a zinc (Zn)-dependent DUB, which cleaves the polyubiquitin chain proximally to the substrate, and the released chain is further cleaved by additional

DUBs in order to recycle the ubiquitin moieties (Verma *et al.*, 2002; Yao and Cohen, 2002). Ubiquitin detachment is essential also because of its high stability, which would make its degradation too slow and therefore would reduce the flux of substrates through the proteasome (Pickart and Cohen, 2004). Once the substrate has been unfolded and its polyubiquitin chain detached, it can reach the proteolytic sites of the 20S complex and undergo degradation (Glickman and Ciechanover, 2002).

Due to the high selectivity in substrate recognition and elimination, the UPS cannot be employed in the degradation of insoluble protein aggregates, which instead can be efficiently degraded through autophagy.

1.5 The Autophagy Pathway

Autophagy (from the Greek *auto-phagein*, “self-eating”) is an evolutionary conserved cellular catabolic process involving the lysosomal system, implicated in the regulation of long-lived proteins as well as in the degradation and recycling of whole cytoplasmic organelles (Klionsky and Emr, 2000). The autophagy pathway was described almost contemporary with the discovery of the lysosomes (De Duve *et al.*, 1955; De Duve and Wattiaux, 1966), and it has been linked to diverse physiological and pathophysiological roles such as development, apoptosis, immunity, cancer, ageing and age-related neurodegeneration (Mizushima *et al.*, 2008). Initially thought to be a non-selective pathway for bulk degradation (in contrast with the UPS), it is now assured that autophagy is also involved in the selective elimination of specific targets, such as protein aggregates, lipid droplets, damaged organelles and invading pathogens (see **Chapter 1.5.4**) (Reggiori *et al.*, 2012; Fimia *et al.*, 2013). Before its selectivity was assessed, autophagy used to be distinguished into “baseline”, where cytosolic component are turned over for intracellular clearance, and “induced”, also known as non-selective or bulk autophagy, where the degradation is triggered by a lack of nutrients (Mizushima, 2005). During starvation, the cytoplasmic components are degraded through autophagy to produce free amino acids and fatty acids, which can be either used to synthesise new proteins or oxidised to produce ATP and ensure cell survival (Levine and Yuan, 2005). Signals including insulin, growth factors and amino acids converge and inhibit mTOR (mechanistic/mammalian target of rapamycin), an evolutionarily conserved serine/threonine, phosphatidylinositol (PI) 3-kinase (PI3K)-related kinase (PIKK) considered the master regulator of cell growth and metabolism (Hay and Sonenberg, 2004; Laplante and Sabatini, 2009).

The target of rapamycin TOR1 and TOR2 genes were first discovered in *Saccharomyces cerevisiae* after testing the inhibitory effects of the immunosuppressant, anti-fungal and anti-proliferative agent rapamycin (Heitman *et al.*, 1991), a macrolide found in *Streptomyces hygroscopicus* from an Easter Island’s soil sample (Vezina *et al.*, 1975). Rapamycin directly inhibits mTOR, thus leading to the cellular growth arrest and to the activation of the autophagy pathway (Dobashi *et*

al., 2011). Additionally, autophagy can also be stimulated in response to several stresses such as changes in the cellular volume, pathogen infection, oxidative stress and accumulation of damaged proteins (He and Klionsky, 2009). In fact, a key function of autophagy is to aid proteostasis by degrading misfolded and aggregate-prone proteins, especially when the activity of the proteasome is compromised (Wong and Cuervo, 2010; Lilienbaum, 2013). An excessive induction, however, can lead to autophagic cell death, a type II programmed cell death (PCD) distinct from apoptosis (type I PCD) and necrosis (Levine and Yuan, 2005; Chen and Klionsky, 2011). As mentioned above, it was in the late 1950s that autophagy was discovered and its associated vesicles described by electron microscopy (Eskelinen *et al.*, 2011). The first to coin the term “autophagy” as a process of cellular self-catabolism has been De Duve, after identifying membrane-limited bodies containing cytoplasmic material which he called “autophagic vacuoles” (De Duve, 1963). The study of the autophagic pathway continued based on morphological analysis until the late 1990s, when by means of molecular biology approaches it became possible to identify and manipulate the genes involved in the process (Yang and Klionsky, 2010).

Although it has been first described in mammals, most of the genetic characterisation of autophagy has arisen from studies on the yeast vacuolar system, similar to the mammalian lysosomal system (Takeshige *et al.*, 1992; Huang and Klionsky, 2002). Furthermore, a biosynthetic pathway involving the vacuolar trafficking called the cytoplasm-to-vacuole-targeting (Cvt) pathway in yeasts shares analogous mechanisms with the autophagic pathway (Yorimitsu and Klionsky, 2005). Genetic screenings using *Saccharomyces cerevisiae* led to the identification of the first autophagy-defective mutants, named Apg (autophagy), which were unable to accumulate autophagic bodies inside the vacuoles (Tsukada and Ohsumi, 1993). The identification of autophagocytosis mutants Aut (autophagy) was also described following colony screening procedures (Thumm *et al.*, 1994). Also, different mutants for the Cvt pathway were discovered (Harding *et al.*, 1995), several of which were overlapping with the autophagy-deficient Aut and Apg mutants, showing a tight relationship between the two pathways (Harding *et al.*, 1996; Scott *et al.*, 1996). Therefore, it has been proposed a unified nomenclature for the identified mutants,

which have been called Atg (autophagy-related) (Klionsky *et al.*, 2003). To date, more than 40 Atg proteins have been identified in yeast, many of them having their mammalian orthologues (Mochida *et al.*, 2015; Wesselborg and Stork, 2015).

Autophagy can be divided in three different sub-pathways with their distinct delivery modality, specificity and regulation: microautophagy, chaperone-mediated autophagy (CMA) and macroautophagy (**Figure 1.6**). The activation of one autophagic route instead of another plays an important role in the adaptation to environmental changes, guaranteeing a specific yet flexible substrate degradation through the lysosomal system (Cuervo, 2004).

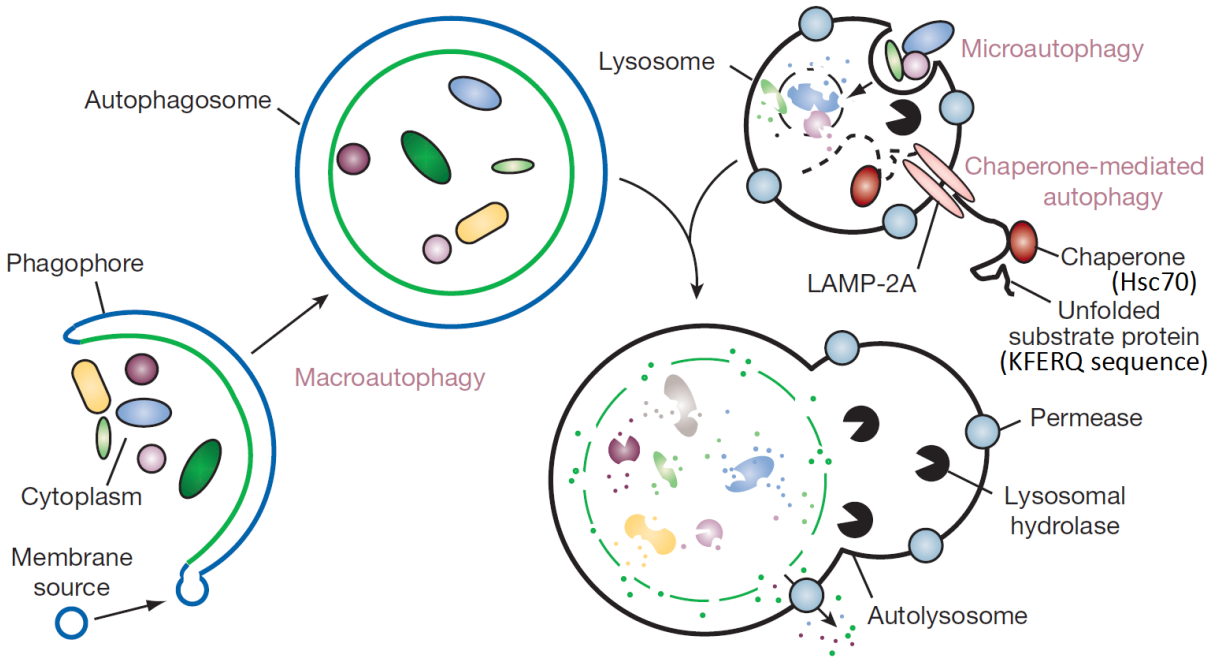

Figure 1.6 | The autophagy pathway. Autophagy is a catabolic pathway which can be distinguished into three different sub-pathways. Microautophagy is mediated by lysosomal engulfment of portions of the cytoplasm. Chaperone-mediated autophagy (CMA) consists in the recognition and unfolding of proteins bearing the KFERQ motif by the chaperone Hsc70, and the targeting to the lysosomal membrane receptor LAMP-2A. Macroautophagy is mediated by the formation of an isolation structure called the phagophore, which engulfs the cytoplasm and then expands to form the autophagosome, a double-membrane structure that fuses with lysosomes to form the autolysosome, where the cytoplasm is degraded. Adapted from (Mizushima *et al.*, 2008).

1.5.1 Microautophagy

Microautophagy consists in the engulfment of whole cytosolic regions directly by the lysosomal membrane, which are then subsequently degraded by the lysosomal hydrolases (**Figure 1.6**) (Li *et al.*, 2012b). Microautophagy has been first described in mammalian cells subjected to long- and short-term starvation, where the lysosomes appeared to be able to internalise their membranes (Ahlberg *et al.*, 1982; Mortimore *et al.*, 1988). Its main functions are to maintain the homeostasis of organelles and membranes in the cell, especially under nitrogen starvation (Li *et al.*, 2012b).

Microautophagy can be either non-selective or selective, depending on whether random cytoplasmic components or specific organelles are degraded through the lysosomes. In the non-selective microautophagy (NSM, also known as “basal autophagy”), small cytoplasmic constituents are engulfed by the lysosome through the tubular invaginations of its membrane (Mijaljica *et al.*, 2011). The process of tubular invagination requires the action of an ATPase to maintain the proton gradient and a GTPase (guanosine triphosphate hydrolase) to preserve the membrane potential (Sattler and Mayer, 2000). This “autophagic tube” presents a striking decrease in the density of transmembrane proteins at the top of the invagination, possibly through a lateral sorting mechanism of protein transportation (Muller *et al.*, 2000).

Following the invagination, a vesicle starts to form due to the imbalance between lipids and proteins in a phase-separation process, which enzymatically expands until it completely separates from the lysosomal membrane and becomes internalised (Li *et al.*, 2012b). To date, the degradation of mitochondria (micromitophagy), of the nucleus (micronucleophagy) and of the peroxisomes (micropexophagy) have been identified as selective processes of microautophagy. The selective microautophagy of these cellular components does not involve the formation of an autophagic tube, rather the lysosomal membrane protrudes to form arm-like structures that surrounds the organelles (Mijaljica *et al.*, 2011).

Most of the mechanisms of microautophagy have been described in yeasts, with little understanding of the pathway in mammalian cells (Mijaljica *et al.*, 2011). Further studies are needed to unveil the role of microautophagy in higher organisms and its possible connections with other degradative pathways.

1.5.2 Chaperone-mediated autophagy (CMA)

The main characteristic of CMA, compared to the micro- and macroautophagy, consists in the direct translocation of proteins through the lysosomal membrane, without the formation of intermediate vesicles (**Figure 1.6**) (Kaushik and Cuervo, 2012). Differently from the other forms of autophagy, CMA is exclusively selective towards its substrates. CMA was first described in human fibroblasts cultured under acute depletion of serum growth factors (Neff *et al.*, 1981; Backer and Dice, 1986), and further characterised as a selective degradation pathway involving the lysosomes by J. Fred Dice over 40 years of research (Dice, 2009; Cuervo, 2011). CMA is activated after more than 10 hours of starvation, reaching a plateau after ~36 hours and remaining active for up to 3 days, differently from other types of autophagy where the activation can start as early as 30 minutes after deprivation of nutrients (Cuervo *et al.*, 1995; Kaushik *et al.*, 2011). CMA can be also upregulated by oxidative stress, hypoxia or following protein denaturation and unfolding (Cuervo *et al.*, 1999; Kiffin *et al.*, 2004; Dohi *et al.*, 2012).

The signal for CMA degradation was found by comparing the half-life of RNase A and its related RNase S-protein (lacking the first 20 amino acids) (Cuervo, 2011). The turnover of the latter was not increased during serum withdrawal, yet it was restored upon reconstitution of the missing N-terminal sequence (S-peptide) (Backer *et al.*, 1983). The attachment of the S-peptide also enhanced the removal of other proteins upon to serum starvation (Backer and Dice, 1986). The sequence was subsequently narrowed down to the amino acids 7-11 of the S-peptide, the pentapeptide KFERQ (Lys-Phe-Glu-Arg-Gln) (Dice *et al.*, 1986). It later became clear that approximately 20-30% of the cytosolic soluble proteins possess a pentapeptide sequence related to

KFERQ, which are selectively degraded through CMA (Chiang and Dice, 1988; Dice, 1990).

The KFERQ sequence is recognised in the cytosol by the constitutively expressed Hsc70 (firstly characterised as Hsp73 or prp73 – peptide recognition protein of 73 kDa) of the Hsp70s chaperone family in an ATP-dependent manner (**Figure 1.6**) (Chiang *et al.*, 1989; Terlecky *et al.*, 1992). Therefore, the name chaperone-mediated autophagy was given to this selective lysosomal degradation pathway (Cuervo and Dice, 2000a). The recognition motif may be hidden by the protein folding state, the attachment of other subunits, the sub-compartmentalisation or by post-translational modifications, which make the KFERQ sequence not accessible to Hsc70 and thus regulate protein degradation (Cuervo, 2010). After the Hsc70 binding to the recognition motif, the client proteins are translocated to the lysosome for degradation in a saturable and vesicle-free process (Cuervo *et al.*, 1994).

The search for a lysosomal receptor ended up with the identification of Lamp2a (lysosome-associated membrane protein type 2a), a single-span membrane protein that mediates the recognition of the Hsc70-substrate complex at the lysosomal membrane (Cuervo and Dice, 1996). This binding to Lamp2a promotes its multimerisation into a ~700 kDa complex, a necessary step for the substrate unfolding and translocation inside the lysosome, while an Hsp90 in the lysosomal luminal side stabilises the complex (Bandyopadhyay *et al.*, 2008). The complete substrate translocation, which requires the complete protein unfolding prior to lysosomal internalisation, takes place through the aiding action of a lysosomal Hsc70 (ly-Hsc70) (Agarraberes *et al.*, 1997; Salvador *et al.*, 2000).

The translocation machinery undergoes continuous cycles of assembly/disassembly, both mediated by Hsc70 (Bandyopadhyay *et al.*, 2008). In fact, the expression levels of Lamp2a are tightly regulated, along with a controlled distribution of the receptor between the lysosomal membrane and matrix (Cuervo and Dice, 2000b). The presence of lipid micro-domains on the lysosomal membrane ensures the degradation of Lamp2a through the lysosomal protease cathepsin A, which mediates

the release of the receptor in the lysosomal matrix and its subsequent elimination by the resident hydrolases (Cuervo *et al.*, 2003; Kaushik *et al.*, 2006).

1.5.3 Macroautophagy

Macroautophagy (usually, and from here on, simply referred to as autophagy) is the principal and most characterised form of autophagy (Ravikumar *et al.*, 2009). Here, the cytoplasmic components (known as cargo) are sequestered in a newly synthesised double membrane structure, the autophagosome; this cargo is then delivered to the lysosome to fuse and form an autolysosome, where the degradation of the enclosed material occurs by means of the lysosomal hydrolyses (**Figure 1.6**) (Eskelinen, 2005). The source of membranes for the formation of autophagic vesicles is still on debate (Lamb *et al.*, 2013). It has been proposed that the membrane source can either derive from existing organelles (maturation model), or that different lipid molecules assemble *de novo* in a specific site (assembly model) (Juhasz and Neufeld, 2006; Tooze and Yoshimori, 2010). However, recent evidence have shown that the ER can work as a membrane platform, by interacting with other organelles such as mitochondria and Golgi apparatus, for the autophagosome formation (Shibutani and Yoshimori, 2014).

In mammals, the first step in the formation of autophagosomes is the sequestration of cytoplasmic components from a unique membrane called phagophore that expands to enclose the substrate (Mizushima, 2007). This “Initiation” step is controlled by mTOR activity (**Figure 1.7**). As previously discussed, mTOR is mainly sensitive to nutrient levels within the cell (see **Chapter 1.5**). During nutrient-rich conditions, mTOR is active and inhibits autophagy, whereas during starvation mTOR is inhibited, activating autophagy (Dobashi *et al.*, 2011). There are two different protein complexes formed by mTOR, known as mTOR complex 1 (mTORC1) and mTOR complex 2 (mTORC2), showing an opposite sensitivity to rapamycin (Loewith *et al.*, 2002). The two complexes are regulated by Raptor (regulatory-associated protein of mTOR) and Rictor (rapamycin-insensitive companion of mTOR), respectively (Hara *et al.*, 2002; Sarbassov *et al.*, 2004). The activity of mTORC1 is tightly regulated by

the master sensor of energy status AMPK (adenosine monophosphate-activated protein kinase), the heterodimer TSC (tuberous sclerosis complex) composed by TSC1 (or hamartin) and TSC2 (or tuberin) which functions as a GTPase-activating protein (GAP), and the small GTPase Rheb (Ras – rat sarcoma – homolog enriched in brain) which directly interacts and activates mTORC1 (Laplante and Sabatini, 2009). Following low energy levels, AMPK is activated and phosphorylates TSC2, which increases its GAP activity and converts Rheb into its inactive GDP-bound state, thus mediating the release and inactivation of mTORC1 (Inoki *et al.*, 2003a; Inoki *et al.*, 2003b).

The inhibition of mTOR releases the activity of another serine/threonine kinase known as ULK1 (Unc-51-like kinases 1 – Unc-51 is the *Caenorhabditis elegans* homologous of the yeast Atg1), which forms a complex with mAtg13 (orthologue of yeast Atg13), FIP200 (focal adhesion kinase – FAK – family-interacting protein of 200 kDa, a yeast Atg17 orthologous) and Atg101, a conserved eukaryotic protein not present in *S. cerevisiae* that has no homology with other Atg proteins and interacts directly with mAtg13 (**Figure 1.7**) (Hosokawa *et al.*, 2009b; Jung *et al.*, 2009; Mercer *et al.*, 2009). The ULK1-mAtg13-FIP200-Atg101 complex is constitutively expressed in the cytosol, and in the presence of nutrients it is phosphorylated and inhibited by mTORC1 (Ganley *et al.*, 2009). In the absence of nutrients, mTORC1 ceases to interact with ULK1, determining the dephosphorylation and the activation of ULK1, which then phosphorylates itself and its complex partners (except Atg101), leading to the initiation of autophagosome formation (Hosokawa *et al.*, 2009a; Mizushima, 2010; Wong *et al.*, 2013). In yeast, autophagosomes generate from a site next to the vacuolar membrane called PAS (pre-autophagosomal structure), not found in mammals, where many of the Atg proteins gather and assemble (Suzuki *et al.*, 2001). Among these, the multispanning membrane protein Atg9, present on cytoplasmic mobile vesicles derived from the Golgi under the action of Atg23 and Atg27, assembles at the PAS and is required for autophagosomal membrane formation (Yamamoto *et al.*, 2012).

Subsequently, a “Nucleation” event is driven by Vps34 (vacuolar protein sorting 34), a specific class III PI3K (**Figure 1.7**). This kinase phosphorylates the PI generating

the phosphatidylinositol 3-phosphate (PI3P), a lipid that promotes the formation of the autophagosome membrane (Obara and Ohsumi, 2008). The Vps34 forms a complex with Vps15/p150, Atg14 and Beclin-1 (mammalian orthologous of Vps30/Atg6 in yeast and BEC-1 in *C. elegans*), which initiate the nucleation event (Mizushima, 2007; Kang *et al.*, 2011). Beclin-1 is a key regulator of the autophagic pathway. It was originally identified as an interaction partner of Bcl-2, an anti-apoptotic factor (Liang *et al.*, 1998). The interaction between Beclin-1 and Bcl-2 is mediated by the BH3 (Bcl-2 homology 3) domain of Beclin-1 and exerts an inhibitory activity towards autophagy (Sinha and Levine, 2008). This interaction is reduced during nutrient deprivation, determining the release of Beclin-1 and the activation of autophagy (Pattingre *et al.*, 2005). Another Beclin-1 partner is UVRAG (UV irradiation resistance-associated gene), an oncosuppressor gene that interacts with his CCD (coiled-coil domain) with Beclin-1, positively regulating autophagy by enhancing the activity of the PI3K complex (Liang *et al.*, 2006).

The “Elongation” of the membrane is regulated by two UBL conjugation systems (**Figure 1.7**) (Ohsumi, 2001; Shpilka *et al.*, 2012). The first identified system is mediated by the UBL protein Atg12, which covalently attaches to Atg5 (Mizushima *et al.*, 1998; Nakatogawa, 2013). The attachment between Atg12 and Atg5 is mediated by two E1- and E2-like enzymes, Atg7 and Atg10, respectively (Shintani *et al.*, 1999; Tanida *et al.*, 1999). In yeasts, the Atg12-Atg5 complex interacts non-covalently with Atg16, a self-oligomerising coiled-coil protein, forming a complex of ~350 kDa dependent on Atg16 oligomerisation (Mizushima *et al.*, 1999; Kuma *et al.*, 2002). In mammals, the Atg12-Atg5 complex interacts with the orthologue Atg16L (Atg16-like), which contains seven WD (also known as WD40, motif of ~40 amino acids terminating with a tryptophan-aspartate – WD – dipeptide) repeats important for protein-protein interactions, forming a bigger complex of ~800 kDa (Mizushima *et al.*, 2003). The Atg12-Atg5-Atg16 complex assists in the formation of the autophagosome membrane from the beginning of the elongation, and dissociates upon completion of the double membrane (Mizushima *et al.*, 2001; Mizushima *et al.*, 2003).

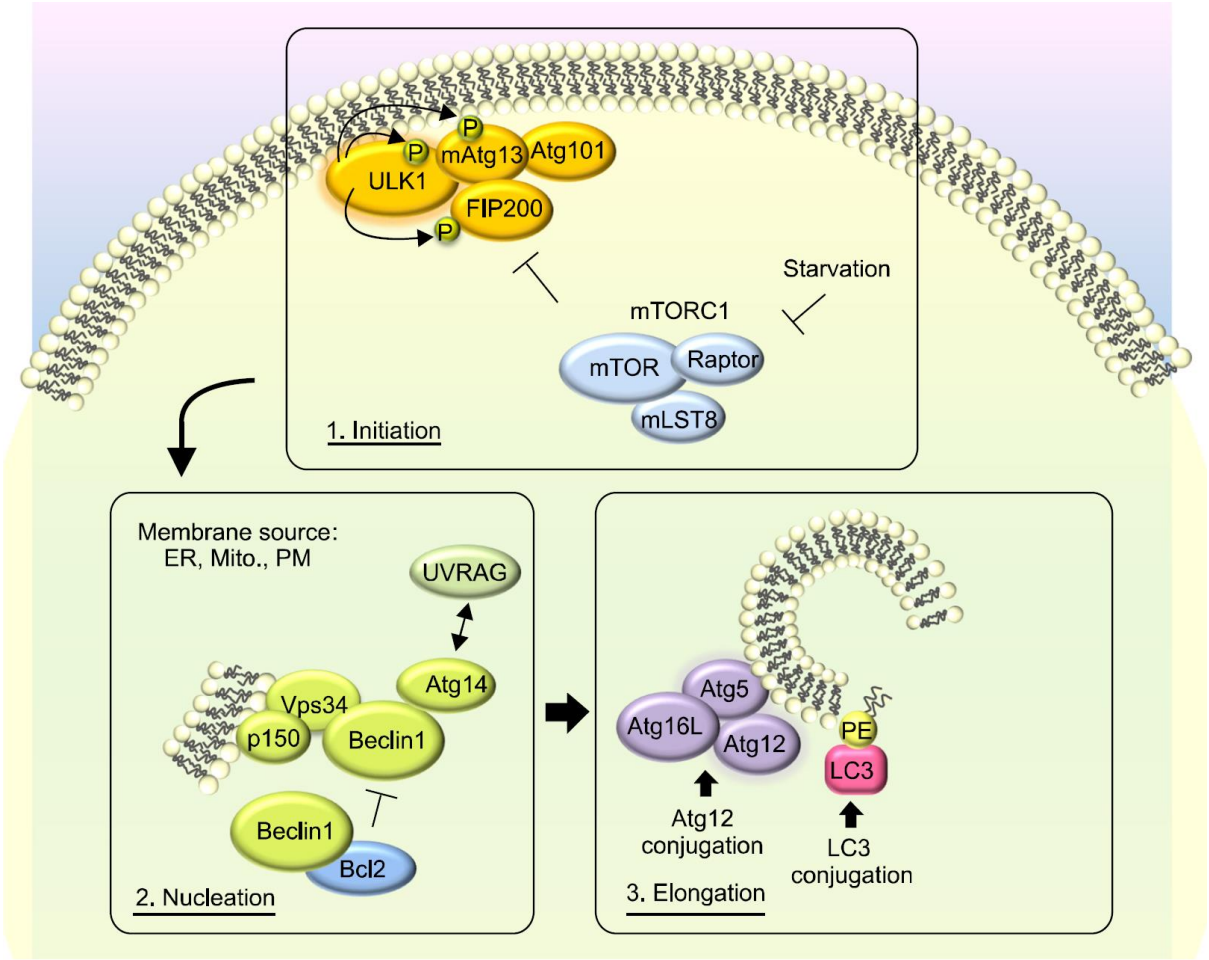

Figure 1.7 | Molecular machinery of macroautophagy. Macroautophagy is initiated by the ULK1 complex, which is activated during starvation by inhibition of the mTORC1 complex. The nucleation of the autophagosome is mediated by the Vps34-Beclin1 complex, which promotes the formation of the autophagosomal membrane. The Atg12- and LC3-conjugation systems ensure the elongation of the membrane to form the mature autophagosome. ER: endoplasmic reticulum; Mito: mitochondria; PM: plasma membrane. Adapted from (Pyo *et al.*, 2012).

The second conjugation system consists in the conjugation of a single lipid molecule, the phosphatidylethanolamine (PE), with the C-terminal Gly of LC3 (microtubule-associated protein – MAP – light chain 3, mammalian orthologous of Atg8) (Ichimura *et al.*, 2000; Shpilka *et al.*, 2011). Together with the other two Atg8 mammalian homologues GABARAP (gamma-aminobutyric acid receptor-associated protein) and GATE-16 (Golgi-associated ATPase enhancer of 16 kDa), LC3 is an UBL protein

structurally similar to ubiquitin (Sugawara *et al.*, 2004). The human LC3 family consists of four proteins, named LC3A (having two alternative splicing variants), LC3B, LC3B2 and LC3C, each being expressed in different tissues and having different roles during the autophagosome biogenesis (Shpilka *et al.*, 2011; Klionsky *et al.*, 2016). LC3 is synthesised as a precursor which is cleaved at its C-terminal by Atg4, a Cys protease that exposes the Gly residue involved in the lipidation process (Kabeya *et al.*, 2000; Kirisako *et al.*, 2000). The exposed Gly of the cleaved LC3 (known as LC3-I) is activated by the E1-like enzyme Atg7 and then transferred onto the E2-like enzyme Atg3, leading to the formation of an amide bond between the PE and LC3 (known as LC3-II) (Ichimura *et al.*, 2000). Differently from Atg12, LC3-II remains attached to both sides of the autophagosome membrane, and for this reason it is widely used as a marker for autophagosome formation (Rubinsztein *et al.*, 2009; Mizushima *et al.*, 2010). The LC3 molecules on the outer membrane can be cleaved off from PE by Atg4 (a process known as deconjugation) for recycle, while the molecules on the inner membrane are degraded together with the cargo after fusion with the lysosome (Mizushima *et al.*, 2010; Yu *et al.*, 2012).

In the last steps of the autophagy process, the newly-synthesised autophagosome can either fuse with a lysosome and produce an autolysosome, where the cytoplasmic components are eventually degraded, or interact with the endosomal compartment forming an amphisome (Mizushima, 2007). The amphisome can eventually fuse to a lysosome following acidification by the membrane proton pumps, and mature into an autolysosome (Hansen and Johansen, 2011).

1.5.4 Selective autophagy

After being regarded as a non-selective degradation pathway for the bulk degradation of cytoplasm from its discovery until recently, new experimental evidence over the last decade has shown how autophagy can also be a selective process, where specific targets are exclusively degraded based on the necessity of the cell (van der Vaart *et al.*, 2008; Reggiori *et al.*, 2012). Since it has been proven difficult to exactly discern between starvation-induced autophagy and selective

autophagy, it has been recently proposed to classify the autophagic events in a more appropriate way, thus distinguishing between cargo-independent (i.e. non-selective) and cargo-induced (i.e. selective) autophagy (Zaffagnini and Martens, 2016). Therefore, it is possible to distinguish different types of selective autophagy depending on the type of cargo involved, such as mitochondria (mitophagy), ER (reticulophagy), ribosomes (ribophagy), peroxisomes (pexophagy), protein aggregates (aggrephagy) and invading pathogens (xenophagy) (Stolz *et al.*, 2014).

An example of selective autophagy is the Cvt pathway in *Saccharomyces cerevisiae*, a biosynthetic pathway involved in the delivery of cytoplasmic hydrolyses to the vacuole, which shares most of the molecular machinery of the autophagy pathway (Lynch-Day and Klionsky, 2010). Here, the cytoplasmic proenzyme prApe1 (precursor of Ape1 – aminopeptidase 1) is the principal cargo, which first assembles into dodecamers and then forms higher order oligomers known as the Ape1 complex (Kim *et al.*, 1997). The cargo is recognised by the protein receptor Atg19/Cvt19 which in turn binds to Ams1 (α-mannosidase), thus forming the Cvt complex (Morales Quinones *et al.*, 2012). Finally, Atg19/Cvt19 interacts first with Atg11/Cvt9, mediating the recruitment of the Cvt complex to the PAS, and then with Atg8/Aut7/Cvt5, which determines the engulfment of the complex into the autophagosome-like Cvt vesicle (Scott *et al.*, 2001; Shintani *et al.*, 2002). The tight interaction between Atg19 and Atg8, mediated by the exposure of multiple Atg8-binding sites on Atg19 following cargo binding, determines the bending of the Cvt vesicle membrane, permitting the exclusion of non-specific cargo material (Sawa-Makarska *et al.*, 2014). Once the Cvt vesicle is complete, its outer membrane fuses with the vacuole, thus releasing a single-membrane Cvt body into the vacuolar lumen (Umekawa and Klionsky, 2012). The Cvt body is then degraded by the lipase Atg15/Cvt17, releasing the prApe1 whose N-terminal is cleaved off by the vacuolar enzyme Pep4 (proteinase 4), reaching the Ape1 mature and active form (Trumbly and Bradley, 1983; Teter *et al.*, 2001).

Although the Cvt pathway does not involve the degradation of the cytoplasmic hydrolases (rather, their delivery to the vacuole and their activation), it shares the same criteria as for selective autophagy: recognition and engulfment of specific cargo

into nascent autophagosomal structures by means of a receptor protein, such as Atg19 (Zaffagnini and Martens, 2016). In fact, selective autophagy uses several receptor proteins to drive the degradation of its targets, while adaptor proteins (such as ULK1 and Atg12) are necessary for autophagosome formation but not for cargo recognition (Svenning and Johansen, 2013; Stolz *et al.*, 2014). Receptor proteins are therefore degraded together with their cargo, while adaptor proteins are not. More than two dozen receptor proteins have been identified in mammals, although the best characterised are p62, NBR1 (neighbour of BRCA1 – breast cancer 1 – gene 1), NIX, NDP52 (nuclear domain 10 protein of 52 kDa) and OPTN (optineurin) (Stolz *et al.*, 2014). Interestingly, there seems to be a high degree of functional redundancy between these proteins, where different combinations of receptors are needed for the correct degradation of certain cargoes, such as protein aggregates, mitochondria and bacteria (Mancias and Kimmelman, 2016).

For instance, p62 and NBR1 participate in the degradation of protein aggregates (see **Chapter 1.6.3**), while p62, NDP52 and OPTN cooperate for the removal of invading pathogens (Kirkin *et al.*, 2009a; Wild *et al.*, 2011). These autophagy receptors share some structural domains, and can interact with both LC3 and ubiquitin (Wild *et al.*, 2014). Indeed, ubiquitination is the most prevalent route for targeting cargoes towards selective disposal, as for the proteasome (Kirkin *et al.*, 2009b). However, it is important to consider that a wider array of ubiquitin-independent mechanisms exists, such as direct interactions between receptors and cargoes (as for Atg19), recognition of lipids- and sugars-based signals, and UBL modifiers (Khaminets *et al.*, 2016). Indeed, the receptor NIX is a mitochondrial outer-membrane protein that can link the mitochondria with the autophagosomal machinery without the need of ubiquitination (Novak *et al.*, 2010).

The most studied receptor protein in selective autophagy is certainly p62, which has an active and important role in the disposal of protein aggregates (van der Vaart *et al.*, 2008). However, p62 is not only involved in protein degradation, but rather in a wide array of intracellular functions.

1.6 Overview of SQSTM1/p62

The roles of p62 in the cell are many and various. As a multi-domain protein, p62 acts as a scaffold for many signalling pathways and takes part in various physiological and pathological processes like apoptosis, inflammation, cancer and ageing (Moscat and Diaz-Meco, 2009; Bitto *et al.*, 2014). Its functions can vary from the degradation of polyubiquitinated cargoes to the activation of anti-stress responses. Furthermore, p62 mediates the interplay between the two major degradative routes in the cell, the UPS and the autophagy pathway (Lilienbaum, 2013). The presence of p62 in virtually all protein inclusions found in neurodegenerative diseases suggests an active role of the protein in the formation of such aggregates, whose role still needs to be addressed (Zatloukal *et al.*, 2002).

1.6.1 Structure of p62

SQSTM1/p62 (sequestosome 1, also known as A170 and ZIP) is a 440 amino acid, ubiquitously expressed multi-domain protein conserved in all metazoa, but not in plants and fungi (National Center for Biotechnology Information – NCBI – Entrez Gene ID for *Homo sapiens*: 8878). It was first discovered as a phosphotyrosine-independent interacting partner of the $p56^{lck}$ (lymphocyte-specific protein tyrosine) kinase (Park *et al.*, 1995). Soon after it was discovered that p62 could bind mono- and polyubiquitin moieties non-covalently through its C-terminal UBA (ubiquitin-associated) domain (amino acids – a.a. – 393-438), mutations of which are commonly linked to Paget's disease of bone (PDB), a condition characterized by increased osteoclastic activity and excessive bone resorption (Vadlamudi *et al.*, 1996; Layfield *et al.*, 2004). For its ability to bind polyubiquitinated proteins, the name of "sequestosome" was given to the cytoplasmic compartment where p62 stores its targets (Shin, 1998).

Other important protein-protein interacting domains are the N-terminal PB1 (Phox and Bem1p, a.a. 4-102), the ZZ-type zinc finger (a.a. 126-168), the TBS (an E3 ubiquitin ligase, TNF – tumor necrosis factor – receptor-associated factor 6 – TRAF6

– binding site, a.a. 228-233), the LIR and KIR (LC3- and Keap1-interacting regions, a.a. 336-341 and 346-359, respectively) (**Figure 1.8**) (Salminen *et al.*, 2012; Lin *et al.*, 2013). In addition, there are two nuclear localisation signals (NLS1 and NLS2) and one nuclear export signal (NES), consistent with p62 shuttling between nucleus and cytoplasm, thus regulating the protein quality control in these two compartments (Pankiv *et al.*, 2010). Two PEST sequences rich in proline (P), glutamate (E), serine (S) and threonine (T) are also present, acting as a signal for fast degradation, indicating that p62 should have a short intracellular half-life, a feature of many other regulatory proteins (Rechsteiner and Rogers, 1996). Indeed, it has been shown that p62 half-life is about 6 hours in HeLa cells (Bjorkoy *et al.*, 2005).

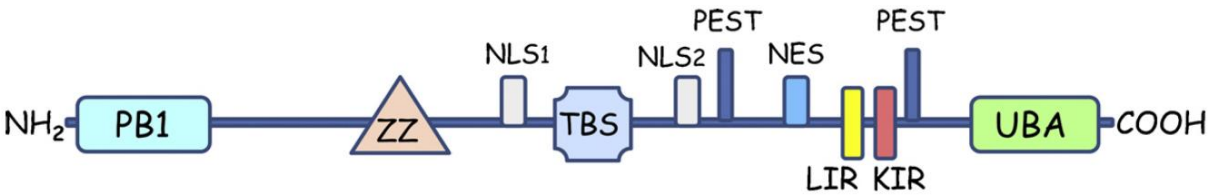

Figure 1.8 | Schematic representation of p62 functional domains. The multi-domain structure of p62 is represented. The explanation for each of the p62 domains is provided in the text. PB1: Phox and Bem1p; ZZ: zinc finger; TBS: TRAF6 binding site; NLS: nuclear localisation signal; NES: nuclear export signal; PEST: sequence rich in proline, glutamic acid, serine and threonine; LIR: LC3 interacting region; KIR: Keap1 interacting region; UBA: ubiquitin-associated. Adapted from (Salminen *et al.*, 2012).

1.6.2 Signalling functions of p62

As mentioned earlier, p62 is a multi-domain protein which can interact with numerous binding partners, therefore acting as a signalling hub in a multitude of cellular responses (Katsuragi *et al.*, 2015). The ZZ-type zinc finger domain, which binds two zinc ions, is responsible for the interaction between p62 and RIP1 (receptor-interacting protein 1), a serine/threonine, TNFα-signalling adaptor kinase involved in

the induction of different signalling events that could lead to the death or the survival of the cell (Festjens *et al.*, 2007). By the ZZ domain, p62 can also bind to AMPA (α-amino-3-hydroxy-5-methyl-4-isoxazolepropionic acid) receptors, mediating their translocation to the plasma membrane as well as their atypical protein kinases C (aPKCs)-mediated phosphorylation, thus regulating the long term potentiation (LTP) response in neurons (Jiang *et al.*, 2009).

The N-terminal PB1 domain is a conserved scaffolding module with an UBL β-grasp fold topology, responsible for the oligomerisation of proteins (Moscat *et al.*, 2006a; Sumimoto *et al.*, 2007). PB1 domains are classified into type I (or A), containing an OPCA (OPR/PC/AID – octicosapeptide repeat/Phox and Cdc/aPKC-interacting domain) motif rich in acidic residues (Glu/Asp), type II (or B), possessing a basic cluster of Lys/Arg, and type I/II (or AB), which contains both (Seibenhener *et al.*, 2007). The PB1 domain of p62 is a type I/II, thus allowing p62 to self-oligomerise through a front-to-back interaction between the acidic OPCA motif (front) of one molecule with the basic cluster (back) of another one (Wilson *et al.*, 2003). Artificial mutations in either the OPCA motif (D69A) or the basic cluster (K7A), or both (K7A,D69A), greatly impairs the ability of p62 to oligomerise (Lamark *et al.*, 2003). It has been shown that oligomerisation of p62 is a necessary step for the selective degradation of ubiquitinated substrates, highlighting the importance of the PB1 domain for the function of p62 as a receptor protein (**Figure 1.9**) (Ichimura *et al.*, 2008; Itakura and Mizushima, 2011). Additionally, the PB1 domain mediates the recognition and the degradation of p62 ubiquitinated cargoes through the UPS by interacting with the proteasomal subunits Rpn10/S5a and Rpt1 (Seibenhener *et al.*, 2004). Therefore, p62 may serve as a shuttle for the proteasomal degradation of polyubiquitinated proteins, since the depletion of p62 delays the turnover of several proteasomal substrates (Seibenhener *et al.*, 2004).

One important PB1-PB1 interaction is between p62 and the aPKCs, creating the scaffold for the NF-κB (nuclear factor-kappa B) stress response (Moscat *et al.*, 2006b). The atypical PKCs (such as aPKCζ and aPKCι/λ) are a subfamily of PKCs that are independent of both Ca^{2+} and diacylglycerol for their activation (Jaken, 1996). The p62-aPKCs binding activates the NF-κB pathway downstream of TNF-α,

interleukin 1 (IL1), RANK (receptor activator of NF-κB) ligand (RANKL) or NGF (nerve growth factor) cell stimulation (Moscat *et al.*, 2007). Also, the interaction with TRAF6 by the TBS domain of p62 is important for NF-κB activation as well as for bone remodelling (Duran *et al.*, 2004). Moreover, by interacting with TRAF6, p62 acts in the downstream events after the binding of neurotrophines such as NGF, brain-derived neurotrophic factor (BDNF) and neurotrophin-3, inducing the activation of the ERK (extracellular signal-activated kinases)/MAPK signalling and playing a role in cell differentiation (Wooten *et al.*, 2001; Geetha and Wooten, 2003). As mentioned above, the ZZ domain of p62 is also involved in the activation of NF-κB, following the interaction with RIP1 in response to TNF-α (Sanz *et al.*, 1999).

The NF-κB pathway is known to regulate a wide range of cellular functions, including immunity, inflammation and metabolism (Tornatore *et al.*, 2012). NF-κB is usually found as a heterodimer formed by RelA/p65 and p50 proteins, which is sequestered in the cytoplasm by the inhibitory protein IκB (inhibitor of κB), thus preventing the NF-κB nuclear translocation and the transcription of genes (Ghosh and Karin, 2002). The activation of NF-κB is controlled by the IKK (IκB kinase) complex, formed by two catalytic (IKKα and IKKβ) and one regulatory subunit (IKKγ, also known as NEMO – NF-κB essential modulator) (Karin and Ben-Neriah, 2000). In particular, the IKKβ appears to be important for the phosphorylation of IκB, its degradation by the UPS and the subsequent NF-κB nuclear translocation and activation (Ghosh and Karin, 2002). The formation of p62-aPKCs complexes after cell stimulation leads to the recruitment and the oligomerisation of TRAF6, which has an E3 ubiquitin ligase activity and catalyses the K63-linked polyubiquitination of both itself and NEMO, inducing the phosphorylation and the activation of the IKK complex (Chen, 2005).

Interestingly, mutations in the UBA domain (causing Paget's disease) lead to an enhancement of NF-κB and osteoclasts activity (Chamoux *et al.*, 2009). As the ubiquitination of proteins is important for their regulation and function, also deubiquitination has a considerable role. In the NF-κB pathway, the DUB CYLD (cylindromatosis tumor suppressor protein) appears to act as a negative regulator by inhibiting the IKK complex by cleaving off K63-linked polyubiquitin chains of TRAF6 and NEMO (Kovalenko *et al.*, 2003; Jin *et al.*, 2008). Paradoxically, p62 interacts via

its C-terminus with CYLD facilitating its interaction with TRAF6, thus providing a negative contribution to the NF-κB signalling (Jin *et al.*, 2008). The induction of NF-κB signalling also seems to induce CYLD transcription, giving an autoregulatory feedback to the pathway (Jono *et al.*, 2004).

Additionally, p62 can interact with the Kelch domain of Keap1 through its KIR domain, likely competing for the binding with Nrf2 (Komatsu *et al.*, 2010; Lau *et al.*, 2010). The Keap1-Cullin3-E3 ubiquitin ligase activity towards Nrf2 becomes impaired upon p62-Keap1 interaction, leading to Keap1 autoubiquitination instead (Lau *et al.*, 2010). Importantly, the ectopic expression of p62 leads to a decrease in Keap1 levels, while the knock-down of p62 through siRNA (small interfering RNA) has shown an increase in the amount of Keap1 and a consequent diminution of Nrf2 protein levels, suggesting that p62 is important in the degradation of Keap1 and in the activation of Nrf2 activity (Copple *et al.*, 2010). The p62-Keap1 interaction enhances during autophagy-deficiency conditions, where the amount of p62 is increased due to the lack of its autophagic degradation (Komatsu *et al.*, 2010; Lau *et al.*, 2010). Thus, the hyperactivity of Nrf2 during autophagy inhibition could be due to the accumulation of p62, rather than the ROS-mediated modification on Keap1 (Lau *et al.*, 2010). Furthermore, the p62 promoter is under the control of Nrf2, which generates a positive feedback for the expression of p62 and its role in upregulating the Nrf2 pathway (Jain *et al.*, 2010).

It has been proposed that p62 could be a point of cross-talk between Nrf2 and NF-κB pathways. In fact, as Keap1 is involved in the ubiquitination and degradation of IKKβ, its binding to p62 could rescue IKKβ from degradation, thus upregulating the NF-κB pathway in concert with Nrf2 (Stepkowski and Kruszewski, 2011).

1.6.3 Selective autophagy and p62

As previously mentioned, p62 participates in the selective degradation of autophagic substrates by acting as a receptor protein (see **Chapter 1.5.4**), linking the cargos to the autophagic machinery (**Figure 1.9**) (Johansen and Lamark, 2011). The

interaction between p62 and LC3 is mediated by the LIR domain, in which a sequence of 11 amino acids named LRS (LC3 recognition sequence) is sufficient for the effective binding to LC3 (Pankiv *et al.*, 2007; Ichimura *et al.*, 2008). The signalling molecule that leads to the autophagic degradation of substrates is ubiquitin, the hallmark of proteasomal degradation, which also has an important role in the disposal of both protein aggregates and organelles (Kirkin *et al.*, 2009b). It has been reported that K63-linked polyubiquitin chains, which show a higher tendency in promoting protein aggregation, are mainly involved during autophagy (Tan *et al.*, 2008). Indeed, the lack of autophagy after genetic knock-out causes the formation of ubiquitin-positive inclusions in mice, which are suppressed upon p62 ablation (Komatsu *et al.*, 2007a).

The interaction between polyubiquitinated substrates and p62 is mediated by the UBA domain, which has a higher affinity for K63-linked polyubiquitin chains compared to K48-linked (Long *et al.*, 2008). The ubiquitin binding causes a conformational switch in the UBA domain, determining a transition from a dimeric state (unbound) to a monomeric state (bound), possibly as an autoinhibitory mechanism (Isogai *et al.*, 2011). The affinity between the UBA domain and polyubiquitin chains is increased by a phosphorylation event at the Ser403 of p62 mediated by casein kinase 2 (CK2) when the proteasome is impaired, leading to the enhanced autophagic degradation of ubiquitinated substrates (Matsumoto *et al.*, 2011). More recently, it has been shown that TBK1 (TANK – TRAF family member-associated NF-κB activator – binding kinase 1) can also phosphorylate p62 at Ser403, which leads to the efficient engulfment of depolarised mitochondria during Parkin-mediated mitophagy (Matsumoto *et al.*, 2015). An additional phosphorylation site at Ser409 mediated by ULK1 has been shown to destabilise the UBA dimer interface of p62 and increase its affinity towards polyubiquitinated substrates (Lim *et al.*, 2015).

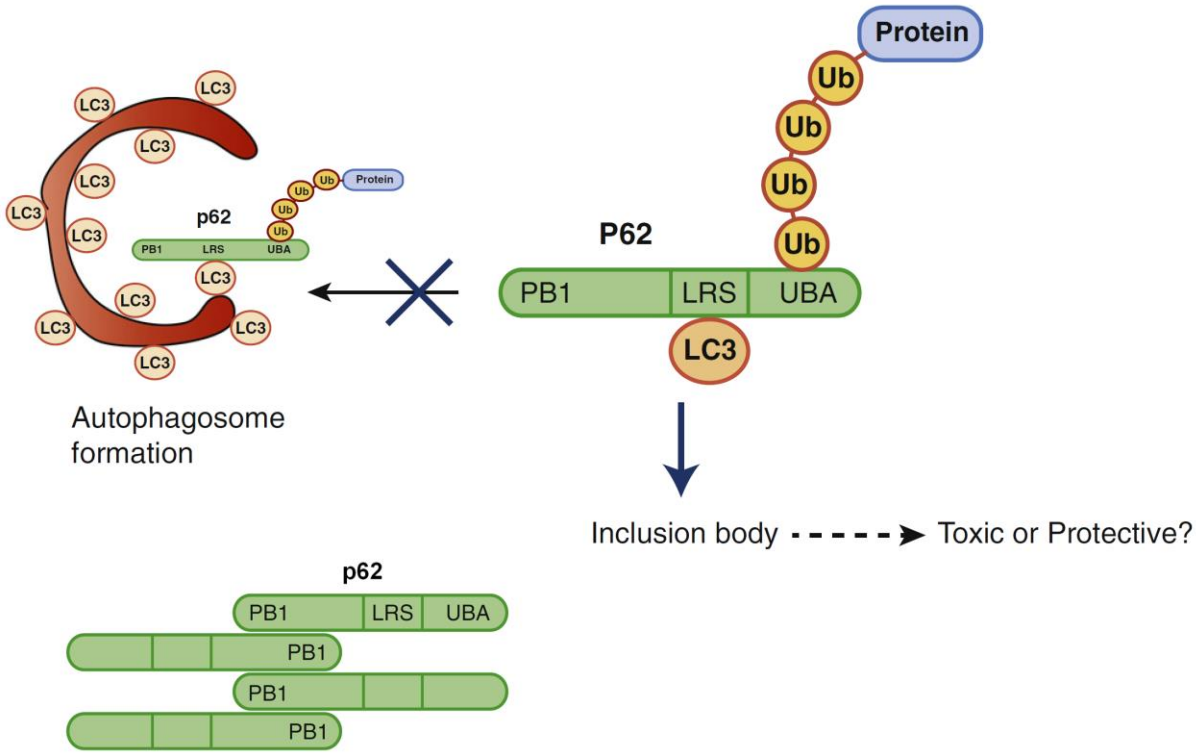

Figure 1.9 | Representation of p62 function in selective autophagy. p62 binds to polyubiquitinated substrates through its UBA domain, while the LRS sequence recognises LC3 on the autophagosomal membrane. The PB1 domain is involved in the self-oligomerisation of p62, an important step for its selective degradation. Impairment of autophagy can lead to the accumulation of p62 together with its cargo, leading to the formation of inclusion bodies. Adapted from (Tanaka and Matsuda, 2014).

Both PB1 and UBA domains of p62 are required for the formation of ubiquitinated aggregates, also known as p62 bodies, which can be found as both membrane-free (sequestosomes) and membrane-enclosed (autophagosomes) structures ranging from 0.1 to 2 µm (Bjorkoy *et al.*, 2005). The PB1 domain is responsible for the self-oligomerisation of p62, a critical step for aggregate formation and their targeting to the autophagosome (Bjorkoy *et al.*, 2005; Itakura and Mizushima, 2011). The oligomerisation of different p62 molecules by means of the PB1 domain determines a stronger interaction with ubiquitinated proteins, as well as a tighter binding with LC3 clusters on the autophagosomal membrane, driving the bending of the latter around the cargo (Wurzer *et al.*, 2015). It has been recently shown that the PB1 domain

assembles into a helical scaffold, creating long p62 filaments that can more efficiently bind to LC3 and determining the elongation of the autophagosomal membrane (Ciuffa *et al.*, 2015; Johansen and Sachse, 2015). Interestingly, an electrostatic bridge (a.a. 100-122) rich in charged amino acids, located C-terminally to the PB1 domain, has been shown to be crucial for stabilising the p62 filaments (Ciuffa *et al.*, 2015). It is important to notice that the binding with polyubiquitin chains leads to the shortening of such filaments which, together with the dimer-to-monomer destabilisation of the UBA domain upon ubiquitin binding, can be an inhibitory mechanism to avoid excessive aggregation (Isogai *et al.*, 2011; Ciuffa *et al.*, 2015). Notably, the targeting of p62 to the autophagosomal nucleation site requires its self-oligomerisation through the PB1 domain but not LC3 binding, which is only needed during the actual enclosure of the cargo (Itakura and Mizushima, 2011). Following autophagy inhibition, p62 tends to accumulate together with ubiquitinated proteins, leading to the formation of insoluble inclusion bodies (Zatloukal *et al.*, 2002; Komatsu *et al.*, 2007b).

Another selective autophagy receptor important in aggregate degradation is NBR1, a 966 amino acids protein which has a domain organization similar to p62, containing an N-terminal PB1 domain, a ZZ-type zinc finger domain, a LIR and a C-terminal UBA domains (Kirkin *et al.*, 2009a). Like p62, NBR1 binds to polyubiquitinated substrates through the UBA domain and links them to the autophagosomal membrane by binding to LC3 (Lamark *et al.*, 2009). However, the interaction with LC3 is not the only way for proteins to interact with the autophagic machinery. An example is Alfy (autophagy-linked FYVE protein), a protein that contains the FYVE, a phospholipid-binding zinc finger domain which can interact with PI3P and therefore with the autophagosomal membrane, creating a scaffold for the degradation of ubiquitinated cargos (Simonsen *et al.*, 2004; Filimonenko *et al.*, 2010). The complex of p62, NBR1 and Alfy, together with ubiquitinated substrates, seems to be important for the formation of p62 bodies, as well as for their degradation through selective autophagy (Johansen and Lamark, 2011).

As already mentioned, the formation of ubiquitinated aggregates and insoluble inclusions could be an attempt of the cell to avoid the cytotoxicity of misfolded proteins (see **Chapter 1.2.3**). This is especially evident following proteasomal inhibition, where the main way for the cell to degrade such aggregates is through a subtype of selective autophagy called aggrephagy (Lamark and Johansen, 2012). It has been shown that protein aggregates can be targeted by microtubules to the MTOC (microtubule organising centre), located in perinuclear position, to form a membrane-free structure called aggresome (Johnston *et al.*, 1998). Ubiquitinated particles reach the MTOC by a dynein/dynactin motor that brings them from the periphery to the perinuclear site (Garcia-Mata *et al.*, 1999). Significant is the abundant presence of lysosomes at the MTOC, where they can fuse with autophagosomes which are also transported to the same location along microtubules (Fass *et al.*, 2006). It has been shown that every aggresome particle has a fixed size of ~50–90 nm, meaning that uniform number of proteins is needed to form a single particle (Garcia-Mata *et al.*, 1999). Aggresome particles are then surrounded by a cage of intermediate filaments, such as vimentin, leading to the stability of the structure (Johnston *et al.*, 1998).

The transportation of aggresomes to the MTOC is regulated by the α-tubulin deacetylase HDAC6 (histone deacetylase 6). The role of HDAC6 in aggresome formation is essential, since it can bind ubiquitin through its BUZ (binding-of-ubiquitin zinc) finger domain, with a preference for K63-linked polyubiquitin chains, and also interacts with dynein motors, participating in the transport of ubiquitinated cargo towards the MTOC (Kawaguchi *et al.*, 2003). However, unlike p62 and NBR1, HDAC6 cannot interact with LC3 due to the lack of the LIR domain. Thus, it is possible that HDAC6 and p62 may act sequentially, as p62 can mediate the aggregation of target proteins whereas HDAC6 can interact with dynein and carry aggregates to the MTOC (Yao, 2010). Moreover, it is known that HDAC6 controls the fusion between autophagosomes and lysosomes through actin remodelling, which is required after the recruitment of the autophagic machinery by p62 (Lee *et al.*, 2010a). In this way, p62 and HDAC6 may act in concert to promote disposal of ubiquitinated protein aggregates.

Due to the importance of mitochondria in the development of various degenerative diseases, a lot of interest has been focussed on their selective degradation through mitophagy (Kubli and Gustafsson, 2012). Mitochondria generate ATP for the cells, but during this process they also produce ROS that could become harmful during pathological conditions. Increased ROS production in damaged mitochondria is an important reason for their fast elimination. It has been shown that p62, in concert with PINK1 (phosphatase and tensin homolog – PTEN – induced putative kinase 1) and Parkin, mediates the autophagic clearance of mitochondria (Geisler *et al.*, 2010). Following mitochondrial depolarisation, the serine/threonine kinase PINK1 accumulates onto the outer membrane of damaged mitochondria and recruits Parkin, an E3-ubiquitin ligase that labels mitochondrial proteins through ubiquitination (mainly by K27- and K63-linked polyubiquitin chains), leading to mitochondrial clearance (Geisler *et al.*, 2010; Narendra *et al.*, 2010b; Vives-Bauza *et al.*, 2010). An important target of ubiquitination, preferentially by K27-linked polyubiquitin chains, is VDAC1 (voltage-dependent anion channel 1, also known as Porin), a protein involved in mitochondrial membrane permeabilisation and apoptosis (Kroemer *et al.*, 2007; Geisler *et al.*, 2010). Thus, a Parkin-dependent degradation of damaged mitochondria could prevent leaking of pro-apoptotic factors and ultimately cell death (Geisler *et al.*, 2010).

Subsequently to Parkin-mediated ubiquitination, damaged mitochondria are targeted to the same perinuclear site where aggresomes accumulate through the concerted action of p62 and HDAC6, leading to their autophagic degradation, (Lee *et al.*, 2010b; Okatsu *et al.*, 2010). Importantly, It has been reported that p62 can only induce mitochondrial clustering through its PB1 domain, but not the mitophagy process itself, suggesting a role for other receptor proteins in mitochondrial degradation (Narendra *et al.*, 2010a). For instance, Parkin-mediated ubiquitination of two GTPases involved in mitochondrial fusion, mitofusins Mfn1 and Mfn2, leads to their degradation through the mediation of p97/VCP (valosin-containing protein) (Tanaka *et al.*, 2010). More recently, it has been discovered that NDP52 and OPTN, known for their role in xenophagy, are principally involved in mitophagy in HeLa cells, while p62 is dispensable for this process (Lazarou *et al.*, 2015).

1.7 Neurodegenerative Diseases (NDs)

Neurodegenerative diseases (NDs) are devastating, chronic and terminal conditions, mostly age-related with a late-onset, characterised by the decline in cognitive functions due to neuronal vulnerability and death (Ross and Poirier, 2004). Many diseases fall under this category, such as Alzheimer's disease (AD), Parkinson's disease (PD), dementia with Lewy bodies (DLB), Huntington's disease (HD), amyotrophic lateral sclerosis (ALS), frontotemporal dementia (FTD), and many more. Despite the presence of some hereditary conditions, most of these diseases have a sporadic onset, whose causes are not yet established. A pathological feature that NDs share is the formation of cytoplasmic, nuclear and/or extracellular neuronal inclusion bodies (**Figure 1.10**) (Ross and Poirier, 2005). Different proteins are involved in the aggregation process in different NDs, becoming the hallmark for such diseases, e.g. β-amyloid (extracellular) and tau (intracellular) in AD, α-synuclein in PD and DLB, huntingtin in HD, SOD1 in ALS and TDP-43 (transactive response – TAR – DNA-binding protein of 43 kDa) in FTD and ALS (Ross and Poirier, 2004). These inclusions, which are used as a neuropathological marker for *post-mortem* diagnosis, are formed by the polymerisation of misfolded, fibril forming-prone proteins that tend to aggregate in one or more foci in the cell (Kopito, 2000; Douglas and Dillin, 2010).

The first event that leads to aggregation is the loss of the three-dimensional native structure of proteins which results in an abnormal conformation (Stefani, 2004). As evidenced by extensive genetic studies, genetic mutations conferring a gain-of-function are often the cause of protein misfolding and toxicity, a leading cause of NDs (Rubinsztein, 2006). Misfolded proteins could be toxic *per se*, or alternatively the loss of conformation can lead to the exposure of hydrophobic sites, or reactive NH and CO groups, which could interact with other cellular components and generate a toxic environment (Ross and Poirier, 2005). Also aggregates could have a role in inducing toxicity, or they might be a way for the cell to segregate toxic proteins and limit cellular damage (Kopito, 2000; Ross and Poirier, 2005).

Oxidative stress plays an important role in neurodegeneration, as certain neuron populations exhibit a higher susceptibility to ROS known as selective neuronal vulnerability (Wang and Michaelis, 2010). Such vulnerability relies upon the intrinsic characteristics of neuronal cells, such as higher dependence on oxidative phosphorylation, high oxygen consumption, enrichment in metal ions (which can catalyse ROS formation) and in polyunsaturated fats (prone to oxidation), and the relative low concentration of antioxidants compared to other organs (e.g. liver) (Chen *et al.*, 2012). Thus, maintaining a balanced redox environment could be a hard task, especially during increased oxidative stress in the course of ageing (Finkel and Holbrook, 2000). High levels of ROS can cause irreversible oxidation of proteins, leading to protein misfolding and aggregation and ultimately to neurodegeneration, therefore reducing the oxidative burden could be a strategy for intervention in NDs (Melo *et al.*, 2011). However, it is unclear whether oxidative stress is a cause or a consequence of neurodegeneration, although surely implicated in the propagation of cellular damage in NDs (Andersen, 2004).

The protein quality control system in neurons has a principal role in the defence against the formation of aberrant proteins, and it relies on molecular chaperones, the UPS and the autophagic pathway (Chen *et al.*, 2011; Takalo *et al.*, 2013). Hence, impairment in proteostasis can lead to the formation of misfolded and aggregated proteins, causing the collapse of the PN and ultimately neurodegeneration (Labbadia and Morimoto, 2015). Experimental evidence indicates the autophagy pathway as a common theme for the clearance of aggregate-prone proteins associated with NDs (Garcia-Arencibia *et al.*, 2010; Nah *et al.*, 2015). Genetic studies have shown that the knock-out of autophagy-related genes *Atg5* and *Atg7* is sufficient to result in the formation of protein inclusions and neurodegeneration in mice (Hara *et al.*, 2006; Komatsu *et al.*, 2006).

Indeed, impairment of autophagy has been observed in most NDs, where accumulation of autophagic vacuoles (AVs) were detected in neurons, particularly within dystrophic neurites (Nixon *et al.*, 2005; Son *et al.*, 2012). Although such accumulation of AVs was first interpreted as an activation of the autophagy pathway, it became clear that AVs clearance was instead reduced due to hindered fusion

between autophagosomes and lysosomes (Yu *et al.*, 2005; Boland *et al.*, 2008). On the other hand, the upregulation of the autophagic pathway could be a strategy of intervention, promoting the clearance of aggregates and the amelioration of NDs (Rubinsztein *et al.*, 2007; Garcia-Arencibia *et al.*, 2010). Interestingly, it has recently been proposed that autophagy could serve as an antioxidant protective pathway by removing damaged proteins and organelles, thus reducing the spreading of damage in neurons (Giordano *et al.*, 2014). Hence, the upregulation of autophagy could be a better strategy in treating NDs rather than enhancing the antioxidant system directly, which could hinder the physiological cellular signalling (Giordano *et al.*, 2014).

Moreover, the clearance of mutated proteins associated with NDs is more dependent on autophagy than on the UPS, which is mainly implicated in the degradation of native/soluble form (Ravikumar *et al.*, 2002; Webb *et al.*, 2003). One explanation could be that the narrow size of the proteasome entrance is accessible for soluble proteins but not for aggregates, which must be degraded by autophagy (Yao, 2010). In fact, it has been shown that aggregated α-synuclein inhibits the 26S of the proteasome by interacting with the protein S6'/Rpt5, a subunit of the 19S cap particle (Snyder *et al.*, 2003). Additionally, inhibition of autophagy impairs the UPS activity and leads to the accumulation of specific proteasome targets, while it has been shown that during UPS impairment the autophagic pathway is upregulated, but not *vice versa* (Pandey *et al.*, 2007; Korolchuk *et al.*, 2009; Korolchuk *et al.*, 2010). Thus, upon UPS inhibition or under pathological conditions, the cell may not be able to eliminate soluble misfolded proteins, which may accumulate and become prone to form insoluble cytoplasmic inclusions. After this event, last chance for the cell to dispose of such inclusions is the autophagy pathway (Ravikumar *et al.*, 2010). However, it remains to be clarified whether alterations in the UPS can be the cause of the development of NDs or the consequence of these pathologies (Ciechanover and Brundin, 2003; Layfield *et al.*, 2005).

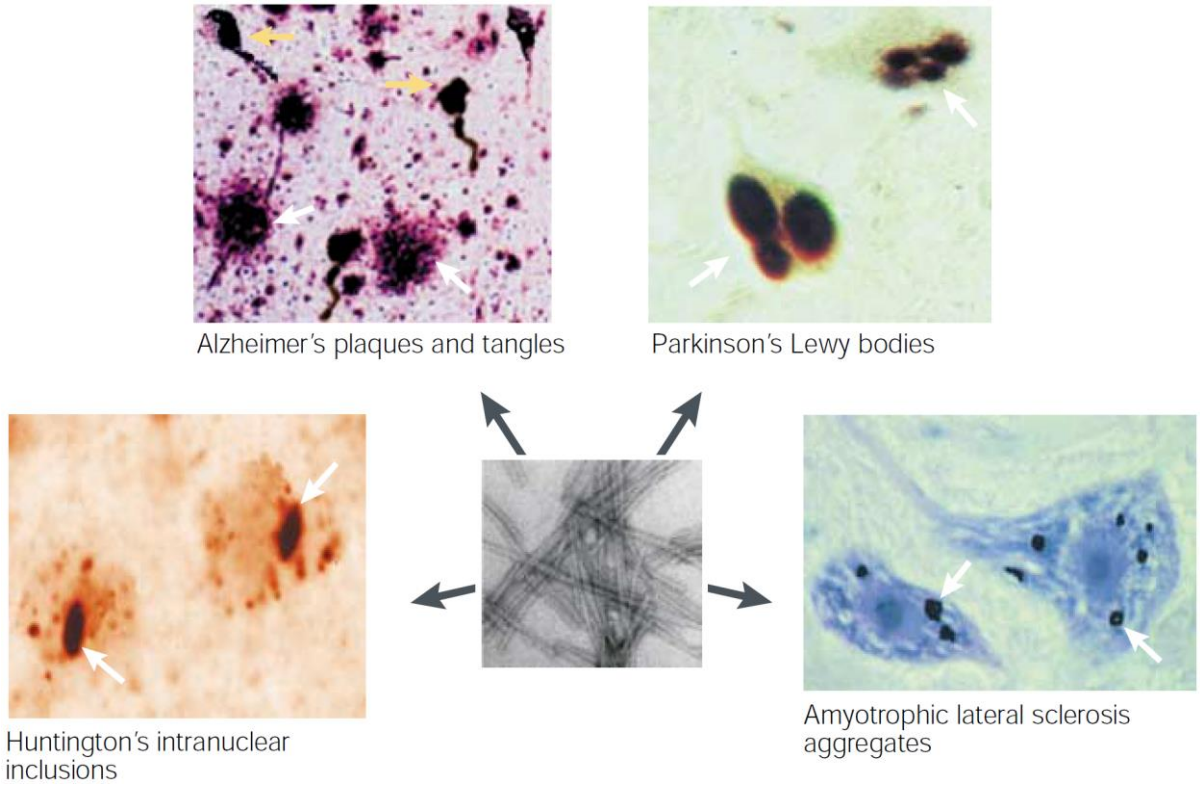

Figure 1.10 | Protein inclusions in neurodegenerative diseases. Representation of the diverse protein inclusions found in major neurodegenerative diseases: beta-amyloid in amyloid plaques (yellow arrows) and hyperphosphorylated tau in neurofibrillary tangles (white arrows) in Alzheimer's disease, α-synuclein in Lewy bodies in Parkinson's disease, huntingtin inclusions in Huntington's disease and SOD1 aggregates in amyotrophic lateral sclerosis (white arrows). Adapted from (Soto, 2003).

1.7.1 Role of p62 in NDs

As a substrate and receptor of selective autophagy, together with its ability to self-oligomerise, p62 has a crucial role in the development of inclusions in NDs. Indeed, the presence of p62 has been essentially detected in all NDs-related protein aggregates such as neurofibrillary tangles in AD (but absent in amyloid plaques), Lewy bodies in PD and DLB, inclusion bodies in HD as well as in ALS and FTD (Kuusisto *et al.*, 2001; Zatloukal *et al.*, 2002; Gal *et al.*, 2007). For this reason, p62 has become a "general inclusion stain" to facilitate the diagnosis of NDs (Kuusisto *et*

al., 2008). The ability to bind both ubiquitin and LC3 through its UBA and LIR domains, respectively, allows p62 to work as a bridge between the UPS and autophagy, thus becoming an important player in the quality control system of proteins (Kirkin *et al.*, 2009b).

Following autophagy inhibition, p62 tends to accumulate and aggregate through its PB1 domain together with polyubiquitinated proteins and can be found in cellular inclusions (Komatsu *et al.*, 2007b). Importantly, genetic loss of p62 during autophagy inhibition strongly reduces the ubiquitin-positive aggregate formation, although the neurodegenerative process is not affected, suggesting the presence of additional factors mediating neurodegeneration in neurons (Komatsu *et al.*, 2007b). On the other hand, the knock-out of p62 is also detrimental for neural physiology and enhances the accumulation of hyperphosphorylated tau protein in mice, where the inhibition of aPKCι, an interactor of p62, leads to the upregulation of protein kinases implicated in the hyperphosphorylation process (Ramesh Babu *et al.*, 2008). The knock-out of TRAF6 also leads to the loss of tau K63-linked polyubiquitination, which normally drives tau for proteasomal degradation upon p62 interaction (Babu *et al.*, 2005). Therefore, either the abatement of p62 expression or the inhibition of proteasomal activity could enhance the formation of tau neurofibrillary tangles (Babu *et al.*, 2005).

It has been reported that p62 is involved in the polyubiquitination and aggregation of mutant huntingtin that drives its degradation by autophagy, thus reducing the toxicity correlated with the presence of the mutated protein (Bjorkoy *et al.*, 2005). Cell death was enhanced by depletion of p62 or by expression of p62 lacking the UBA domain, whereas mutant huntingtin was still able to aggregate, highlighting the crucial role of p62 in driving such aggregates to the autophagic machinery (Nagaoka *et al.*, 2004; Bjorkoy *et al.*, 2005).

Additionally, mutations of p62 have been connected to ALS as well as frontotemporal lobar degeneration (FTLD, a pathological process that occurs in FTD) (Fecto *et al.*, 2011; Rubino *et al.*, 2012). Notably, several of these mutations are common to both ALS-FTLD and PDB, although the latter is likely to be often unrecognised in patients

due to its relative late onset (Teyssou *et al.*, 2013; Rea *et al.*, 2014). Differently from the PDB-associated mutations of p62 (usually affecting the UBA domain), ALS-FTLD mutations are present along the whole sequence of p62, often affecting its domains such as PB1, LIR, KIR and UBA (Rea *et al.*, 2014). Recently, a LIR-associated L341V mutation of p62 has been shown to impair its binding to LC3, therefore altering the correct formation of phagophores (Goode *et al.*, 2016).

Although an impairment in autophagy has been associated with increased p62 levels due to a reduction of its selective degradation (Yue, 2007), it has been shown that the expression levels of p62 are down-regulated following oxidative stress conditions, which causes damage to the p62 gene promoter (Du *et al.*, 2009a; Du *et al.*, 2009b). The amount of damage in the p62 promoter sequence, revealed by the increased oxidation of guanine into its derivative 8-OHdG (8-hydroxy-2'-deoxyguanosine, used as a marker for DNA oxidation), is significantly increased in NDs, showing a reduction in the activation of the gene and in the expression of p62 (Kasai, 1997; Du *et al.*, 2009b).

The accumulation of p62 in cytoplasmic aggregates could be also a mechanism for modulating the signalling activity of p62 in the cell. For instance, NF-κB and Nrf2 pathways, which are known to be involved in the response against oxidative stress during the development of NDs, could be modulated by p62 aggregation (Mattson *et al.*, 2000; Calkins *et al.*, 2009). Therefore, p62 has a complex role in NDs, where it can be involved in protein degradation for aggregates removal, but it can also play a detrimental role by driving aggregation especially when, as in many NDs, proteolytic degradation is impaired.

1.8 Objective and Aims

Oxidative stress and autophagy inhibition have been shown to have an important role in the pathogenesis of NDs, in which protein aggregates accumulate. The selective autophagy receptor p62 drives the formation of protein aggregates for their degradation, however the mechanisms of p62 oligomerisation, especially during oxidative stress, are still incompletely understood. Preliminary data from our laboratory have shown that the electrophoretic mobility of p62 could be modified by different stressors, such as oxidation or DUBs inhibition, suggesting a new potential mechanism of p62 oligomerisation. This could lead to a better understanding on the role of p62 in forming protein aggregates during pathological conditions. The main objective of this thesis work is to investigate the molecular mechanism underlying the oligomerisation and the aggregation of p62, and finding potential molecular targets for the amelioration of human NDs.

The first aim is to identify novel post-translational modifications of p62, together with the amino acids involved in intra- and inter-molecular interactions, in order to better characterise p62 oligomerisation and aggregate formation. The second aim is to understand whether such new mechanism of p62 oligomerisation could be relevant to human physiology, particularly in the pathogenesis of NDs.

Chapter 2. Materials and Methods

2.1 Materials

Table 2.1 | Consumables for cell culture used in this study.

Cell Culture Consumables		
Reagent	**Manufacturer**	**Product No.**
CryoTube vials	Thermo Fisher Scientific	377267
Mr. Frosty™ freezing container	Thermo Fisher Scientific	5100-0001
0.6 ml 'Crystal Clear' microcentrifuge tube	Starlab	E1405-0600
1.5 ml microcentrifuge tubes	Starlab	S1615-5500
6-well plates	Fisher	11825275
12-well plate	Fisher	TKB-100-110R
24-well plates	Fisher	TKB-100-115H
15 ml Centrifuge Tube, Conical (Sterile), Loose	Star labs	E1415-0200
175 cm^2 TC treated flask with filter cap	Greiner-Bio one	661175
2 ml 'Crystal Clear' Microcentrifuge Tube	Starlab	E1420-2000
50 ml Centrifuge Tube, Conical (Sterile), Loose	Starlab	E1450-0200
75 cm^2 TC treated flask with filter cap	Greiner-Bio one	658175
Acrodisc® Mini Spike syringe filters	Sigma-Aldrich	Z260444-1PAK

Acryl Aquaclean	WAK-Chemie Medical GmbH	WAK-AQA-250-50L
Bijou sample container, plain label	Sigma-Aldrich	Z645346-700EA
Cell culture dish treated with vents sterile polystyrene non-pyrogenic	Thermo Fisher Scientific	10075371
Coverglass 13 mm/0.16 mm	VWR	631-0150
Glass Pasteur pipettes 230 mm	VWR	612-1702
Serological pipettes 10 ml	Sarstedt	86.1254.001
Serological pipettes 25 ml	Sarstedt	86.1685.001
Serological pipettes 5 ml	Sarstedt	86.1253.001

Table 2.2 | Reagents for cell culture used in this study.

Cell Culture Reagents		
Reagent	**Manufacturer**	**Product No.**
Trypsin-EDTA solution	Sigma-Aldrich	T3924
Penicillin-Streptomycin	Sigma-Aldrich	P4333
Mycoalert Detection Kit	Lonza	LT07-218
L-Glutamine solution	Sigma-Aldrich	G7513
Lipofectamine® 2000	Thermo Fisher Scientific	11668019
Dulbecco's Modified Eagle's Medium (DMEM), high glucose	Sigma-Aldrich	D5796
Opti-MEM® I Reduced-Serum Medium, no phenol red	Thermo Fisher Scientific	11058021
Dimethyl sulfoxide (DMSO)	Sigma-Aldrich	D2650

20x PBS	New England BioLabs Inc.	9808
Fetal Bovine Serum (FBS), heat inactivated	BioSera	FB1001H
Isopropanol	Sigma-Aldrich	278475

Table 2.3 | Reagents for mutagenesis and cloning used in this study.

Mutagenesis and Cloning Reagents		
Reagent	**Manufacturer**	**Product No.**
QuikChange II XL Site-Directed Mutagenesis Kit	Agilent Technologies	200521
PfuUltra High-Fidelity DNA Polymerase	Agilent Technologies	600380
XL10-Gold® Ultracompetent Cells	Agilent Technologies	200314
Phusion High Fidelity PCR kit	Thermo Fisher Scientific	F553S
QIAquick Gel Extraction Kit	Quiagen	28704
Calf Intestinal Alkaline Phosphatase	Thermo Fisher Scientific	18009019
T4 DNA Ligase	New England BioLabs Inc.	M0202S
α-select Gold Efficiency Competent Cells	Bioline	BIO-85027
Agarose	Thermo Fisher Scientific	BP1356-500
Ampicillin	Sigma-Aldrich	A5354
Kanamycin	Sigma-Aldrich	K0254
Burner Bunsen Natural Gas 13mm	SLS	BUR3000
Cell culture dish treated with vents sterile polystyrene non-pyrogenic	Thermo Fisher Scientific	10075371

Glass spreaders	Sigma-Aldrich	S4522-6EA
LB Agar Miller	Thermo Fisher Scientific	10734724
LB Broth Miller Powder	Thermo Fisher Scientific	10638013
Molecular Grade RNase-free water	Thermo Fisher Scientific	B-003000-WB-100
peqGREEN	Peqlab	37-5000
PureYield™ Plasmid Midiprep System	Promega	A2492
S.O.C. Medium	Thermo Fisher Scientific	15544-034
QIAprep Spin Miniprep Kit	Qiagen	27104

Table 2.4 | Reagents for immunoblot used in this study.

Immunoblot Reagents		
Reagent	**Manufacturer**	**Product No.**
Ammonium persulphate (APS)	Sigma-Aldrich	A3678
Bovine Serum Albumin (BSA)	Sigma-Aldrich	A2153
Polyoxyethylene sorbitan (Tween-20)	Sigma-Aldrich	93774
N,N,N',N'-Tetramethylethylenediamine (TEMED)	Sigma-Aldrich	T9281
Clarity western ECL substrate	Bio-Rad	170-5061
2x Laemmli buffer	Bio-Rad	1610737
Precision Plus Protein™ Dual Color Standards	Bio-Rad	610374
DC Protein Assay Kit	Bio-Rad	500-0112

Marvel non-fat dry milk powder	Asda	N/A
Immobilon-P polyvinylidene difluoride (PVDF) membrane	Millipore	IPVH00010
Phosphatase inhibitor cocktail 100X	Thermo Fisher Scientific	1861280
N-ethylmaleimide (NEM)	Sigma-Aldrich	E3876
Restore™ PLUS Western Blot Stripping Buffer	Thermo Fisher Scientific	46430
GelCode™ Blue stain reagent	Thermo Fisher Scientific	10608494
Acrylamide/Bis-acrylamide	Severn Biotech	20-2100-10
Sodium chloride (NaCl)	Sigma-Aldrich	S7653
Sodium deoxycholate (NaDoC)	Sigma-Aldrich	D6750
IGEPAL® CA-630 (NP-40)	Sigma-Aldrich	I3021
Methanol	Sigma-Aldrich	32213
Thick blotting paper	VWR	732-0594
Gel loading tips	Starlab	1022 0600
20x PBS	New England Bio	9808
Glycine	Sigma-Aldrich	G8898
Trizma® base (Tris)	Sigma-Aldrich	T1503
β-mercaptoethanol (β-ME)	Sigma-Aldrich	M3148

Table 2.5 | Reagents for immunofluorescence used in this study.

Immunofluorescence Reagents		
Reagent	**Manufacturer**	**Product No.**
20x PBS	New England Bio	9808
Bovine Serum Albumin (BSA)	Sigma-Aldrich	5482
Triton X-100	Sigma-Aldrich	X100
Polyoxyethylene sorbitan (Tween-20)	Sigma-Aldrich	93774
Microscope slide ground edges, twin frosted	Thermo Fisher Scientific	FB58628
ProLong® Gold Antifade Mountant with DAPI	Thermo Fisher Scientific	P36935
TO-PRO-3 iodide	Thermo Fisher Scientific	T3605
37% Formaldehyde	Sigma-Aldrich	252549
Normal Goat Serum	Vector Laboratories	S-1000
Normal Rabbit Serum	Vector Laboratories	S-5000

Table 2.6 | Reagents for immunohistochemistry used in this study.

Immunohistochemistry Reagents		
Reagent	**Manufacturer**	**Product No.**
Microscope slide ground edges, twin frosted	Thermo Fisher Scientific	FB58628
Histoclear	National Diagnostics	HS-200
Ethanol	Thermo Fisher Scientific	E/0650DF/17
Normal Goat Serum	Vector Laboratories	S-1000
VECTASTAIN ABC kit	Vector Laboratories	PK-4000
NovaRED	Vector Laboratories	SK-4800
haematoxylin	Vector Laboratories	H-3401
DPX mounting medium	Thermo Fisher Scientific	12658646

2.3 Cell Culture

2.3.1 Cell Lines

HeLa cells were obtained from ECACC (European Collection of Cell Cultures). *p62* knock-out (*p62*$^{-/-}$) mouse embryonic fibroblasts (MEFs) (Komatsu *et al.*, 2007b) were kindly provided by Eiji Warabi (University of Tsukuba, Japan). The p62/A170 mouse gene of the *p62*$^{-/-}$ MEFs was isolated by designing a targeting vector against the exons 1-4 of the gene. HEK293FT (human embryonic fibroblasts) lentivirus packaging cells were from Invitrogen. Stable *p62*$^{-/-}$ cell lines expressing FLAG-p62 transgenes either wild-type or C105,113A double mutant of p62 were produced in this study by lentiviral transduction. Cells were grown in DMEM (Dulbecco's modified eagle's medium, Sigma-Aldrich) supplemented with 10% heat-inactivated FBS (fetal bovine serum, Biosera), 1% penicillin/streptomycin (Invitrogen) and 2 mM L-glutamine (Sigma-Aldrich) in a humidified atmosphere containing 5% CO_2 at 37°C (**Table 2.1, 2.2**). Cells at ~80% confluency were treated with the compounds listed in **Table 2.7**. Cell medium was switched to serum-free DMEM for the duration of the treatments.

2.3.2 Cryogenic storage

Exponentially growing adherent cells were trypsinised (when at ~80% confluence) with trypsin-EDTA (ethylene-diamine-tetraacetic acid, Sigma-Aldrich). Trypsin was neutralized with the addition of pre-warmed media and cells centrifuged at 900 rpm for 3 min at room temperature. The supernatant was removed and cells were resuspended in FBS containing 10% (v/v) dimethyl sulfoxide (DMSO) at a density of $1x10^6$ cells/ml. The cell suspension was immediately transferred to cryovials in 1 ml aliquots (containing $1x10^6$ cells) and placed in a Mr. Frosty™ freezing container (Thermo Fisher Scientific) filled with isopropanol (Sigma-Aldrich). Cells were placed at -80°C for 24 hours to allow slow freezing, before being transferred to liquid nitrogen for long term storage.

2.3.3 Resuscitation of frozen cells

Cryovials containing the cell suspension were removed from liquid nitrogen and placed in a water bath at 37°C to thaw for 5 min. The thawed cell suspension was immediately added to pre-warmed media and seeded in cell flask. Cell culture media was replaced after 24 hours to remove the DMSO and cell debris.

2.3.4 Cell density calculation

Cell density was calculated using a 0.1 mm Improved Neubauer haemocytometer (Hawksley, #AC1000), where 10 µL of trypsinised cells suspension were analysed using an inverted microscope (DM IL LED, Leica Microsystems). Cells were counted from two different corner squares of the haemocytometer, and their average was equivalent to the number of cells x10^4/ml. This allowed for the calculation of the total number of cells by multiplying the volume of the cell suspension to the cells concentration (cells/ml). For seeding purposes, the C1*V1=C2*V2 formula was used, where:

C1= Starting cells concentration (cells/ml)
V1= Cells volume needed for seeding (ml)
C2= Desired cells concentration (cells/ml)
V2= Desired cells volume (ml)

The desired amount of cells (C2) was multiplied to the desired volume of media (V2), then divided to the starting concentration of cells (C1) by using the formula: V1= (C2*V2)/C1. Cells were tracked by recording the dilution factor and the number of passages.

Table 2.7 | Compounds for cell culture treatments used in this study.

Cell Culture Treatments		
Reagent	**Manufacturer**	**Product No.**
Bafilomycin A1 (Baf)	Enzo Life Sciences	BML-CM110-0100
Chloroquine (CQ)	Sigma-Aldrich	C6628
H_2O_2	Sigma-Aldrich	323381
PR-619	LifeSensors	SI9619
N-acetylcysteine (NAC)	Sigma-Aldrich	A7250
Paraquat (PQ)	Sigma-Aldrich	36541
Puromycin	Santa Cruz Biotechnology	sc-108071
Staurosporine	Sigma-Aldrich	S4400
Z-VAD-FMK	Calbiochem	219007
N-ethylmaleimide (NEM)	Sigma-Aldrich	E3876
Curcumin	Sigma-Aldrich	C1386
Auranofin	Sigma-Aldrich	A6733
Cycloheximide (CHX)	Sigma-Aldrich	C7698
MG132	Sigma-Aldrich	C2211

2.4 Transfection

HeLa cells and MEFs were seeded in either 6- or 12-well plates, cultured for 24 (HeLa) or 48 (MEFs) hours and transfected with Lipofectamine® 2000 (Thermo Fisher Scientific) according to the manufacturer's instructions for 24 hours prior to lysis. For each transfection, 1 µg DNA, 3 µl of transfection reagent and 100 µl Opti-MEM® I Reduced-Serum Medium (Thermo Fisher Scientific) per well were used. Plasmids used in this study: pEGFP-p62, pEGFP-ΔUBAp62 and pDEST-GST-p62 were kindly provided by Terje Johansen (University of Tromsø, Norway) (Lamark *et al.*, 2003), His-FLAG-p62 was kindly provided by Robert Layfield (University of Nottingham, UK) (Najat *et al.*, 2009), pEGFP-C2 (Clontech, #632481), pLENTI6/V5-DEST (Invitrogen, #V496-10), and all the p62 mutants and deletion constructs generated in this study.

2.5 Mutagenesis

Point mutagenesis of the *p62* gene was carried out using the QuikChange II XL Site-Directed Mutagenesis Kit (Agilent Technologies) (**Table 2.3**) following the provided protocol. Mutagenesis primers were designed using the QuikChange Primer Design program available online on the Agilent website (http://www.genomics.agilent.com/) (**Table 2.8**). The pEGFP-p62 and FLAG-p62 wild-type plasmids were used as a template. Every PCR mixture was prepared according to the provided protocol: 1x reaction buffer, 10 ng dsDNA template, 125 ng oligonucleotide primers (both forward and reverse), 200 µM dNTP, 3 µl QuikSolution reagent, *PfuUltra* High-Fidelity DNA polymerase (Agilent Technologies, 2.5 U/µl) and ddH_2O up to final volume 50 µl. PCR reactions were placed on a Veriti 96-Well Thermal Cycler (Applied Biosystems) using the provided program: 1 cycle at 95°C for 1 min, 18 cycles (Denaturation 95°C for 50 sec, Annealing 60°C for 50 sec, Extension 68°C for 7 min) and 1 cycle at 68°C for 6 min. PCR samples were then kept at 4°C until digestion with 10 U/µl of *DpnI* (1 hour at 37°C), which digests parental methylated and hemimethylated DNA and

selects the mutagenised DNA. Bacteria transformation was then carried out using 45 µl of XL10-Gold® Ultracompetent Cells (Agilent Technologies) and 2 µl of β-ME mix provided with the kit, together with 2 µl of the *DpnI*-treated DNA per each reaction. Transformation mixtures were incubated on ice for 30 min, heat-pulsed in a 42°C water bath for 30 sec, incubated on ice for 2 min, followed by the addition of 500 µl of S.O.C. medium (Thermo Fisher Scientific). After 1 hour incubation at 37°C with shaking at 220 rpm, 250 µl of each transformation reaction were plated on LB agar (Thermo Fisher Scientific) plates containing 100 ng/µl of ampicillin (Sigma-Aldrich) and incubated overnight at 37°C. Then, colonies were picked up and grown in 5 ml of LB broth (Thermo Fisher Scientific) overnight at 37°C with shaking at 220 rpm. Bacterial DNA was extracted using the QIAprep Spin Miniprep Kit (Qiagen) to a final volume of 50 µl and sent for sequencing (Genevision, Newcastle University). Sequenced DNA was aligned with the wild-type sequence of p62 to confirm the presence of mutations using the BLAST software available online (NCBI).

2.6 Cloning

Deletions of *p62* were produced through PCR (**Table 2.3,** see **Appendix A, B, C**), using the pEGFP-p62 wild-type as a template and specific primers generated by SnapGene software (GSL Biotech) (**Table 2.8**). The generated fragments were then ligated into the pEGFP-C2 vector. Forward primers included a *BglII* (sticky end, New England BioLabs Inc.) restriction site. PCRs were performed using the Phusion High-Fidelity PCR kit (Thermo Fisher Scientific) and every PCR mixture was prepared according to the provided protocol: 1x Phusion High-Fidelity buffer, 10 ng DNA template, 125 ng oligonucleotide primers (both forward and reverse), 200 µM dNTP, Phusion High-Fidelity DNA polymerase (2 U/µl) and ddH_2O up to final volume of 50 µl. PCR reactions were placed on a Veriti 96-Well Thermal Cycler (Applied Biosystems) using the provided program: 1 cycle at 98°C for 30 sec, 25 cycles (Denaturation 98°C for 10 sec, Annealing 57°C for 30 sec, Extension 72°C for 1 min) and 1 cycle at 72°C for 5 min. The *p62* fragments were then digested with *BglII* for 3 hours at 37°C and run on 0.8% agarose gel which was then purified. The pEGFP-C2

vector was digested with *SmaI* (blunt end, New England BioLabs Inc.) and run on 0.8% agarose gel followed by purification with QIAquick Gel Extraction Kit (Quiagen). The pEGFP-C2 vector was then digested with *BglII*, followed by gel purification. After the double digestion, the pEGFP-C2 vector was dephosphorylated by calf intestinal alkaline phosphatase (Thermo Fisher Scientific) for 50 min at 37°C. The digested *p62* fragments were ligated into the double digested pEGFP-C2 vector (sticky-end/blunt-end ligation) using the T4 DNA Ligase (New England BioLabs Inc.) at 16°C overnight. Bacterial transformation was performed using α-select GOLD Efficiency chemically competent cells (Bioline) adding 2 µl of ligation mixture to 45 µl of cells. Cells were plated on LB agar plates containing 50 ng/ml of kanamycin (Sigma-Aldrich). FLAG-p62 and FLAG-C105,113Ap62 for lentiviral expression were subcloned into the pLENTI6/V5-DEST vector using *EcoRI* and *XhoI* (New England BioLabs Inc.) as described above.

Table 2.8 | Primers for mutagenesis and cloning used in this study. Fw: forward; Rev: reverse.

Primers for Mutagenesis and Cloning	
Name/direction	**Sequence**
K7A_Fw	5'-CGTCGCTCACCGTGGCGGCCTACCTTCTGG-3'
K7A_Rev	5'-CCAGAAGGTAGGCCGCCACGGTGAGCGACG-3'
C26A_Fw	5'-CCGCTTCAGCTTCGCCTGCAGCCCCGAG-3'
C26A_Rev	5'-CTCGGGGCTGCAGGCGAAGCTGAAGCGG-3'
C27A_Fw	5'-GCTTCAGCTTCTGCGCCAGCCCCGAGCCTG-3'
C27A_Rev	5'-CAGGCTCGGGGCTGGCGCAGAAGCTGAAGC-3'
C44A_Fw	5'-GGTCCGGGACCCGCCGAGCGGCTGCT-3'
C44A_Rev	5'-AGCAGCCGCTCGGCGGGTCCCGGACC-3'

D69A_Fw D69A_Rev	5'-CGCACTACCGCGCTGAGGACGGGGA-3' 5'-TCCCCGTCCTCAGCGCGGTAGTGCG-3'
C105A_Fw C105A_Rev	5'-ACATTAAAGAGAAAAAAGAGGCCCGGCGGGACCACCG-3' 5'-CGGTGGTCCCGCCGGGCCTCTTTTTTCTCTTTAATGT-3'
C113A_Fw C113A_Rev	5'-CCACCGCCCACCGGCTGCTCAGGAGGCG-3' 5'-CGCCTCCTGAGCAGCCGGTGGGCGGTGG-3'
C128A_Fw C128A_Rev	5'-GCACCCCAATGTGATCGCCGATGGCTGCAATGGG-3' 5'-CCCATTGCAGCCATCGGCGATCACATTGGGGTGC-3'
C131A_Fw C131A_Rev	5'-GTGATCTGCGATGGCGCCAATGGGCCTGTGGT-3' 5'-ACCACAGGCCCATTGGCGCCATCGCAGATCAC-3'
C142A_Fw C142A_Rev	5'-GAACCCGCTACAAGGCCAGCGTCTGCCCAG-3' 5'-CTGGGCAGACGCTGGCCTTGTAGCGGGTTC-3'
C145A_Fw C145A_Rev	5'-CTACAAGTGCAGCGTCGCCCCAGACTACGACTTG-3' 5'-CAAGTCGTAGTCTGGGGCGACGCTGCACTTGTAG-3'
C151A_Fw C151A_Rev	5'-CCAGACTACGACTTGGCTAGCGTCTGCGAGGG-3' 5'-CCCTCGCAGACGCTAGCCAAGTCGTAGTCTGG-3'
C154A_Fw C154A_Rev	5'-CAAGCCCTTTCCCTCGGCGACGCTACACAAGTCG-3' 5'-CGACTTGTGTAGCGTCGCCGAGGGAAAGGGCTTG-3'
C289A/C290A_Fw C289A/C290A_Rev	5'-GCTTGCTGGGGTCAGAGGCGGCGCTGCTTGGCTGTGAGC-3' 5'-GCTCACAGCCAAGCAGCGCCGCCTCTGACCCCAGCAAGC-3'
C331A_Fw C331A_Rev	5'-GTCATCATCTCCTCCTGAAGCGTTATCCGACTCCATCTGT-3' 5'-ACAGATGGAGTCGGATAACGCTTCAGGAGGAGATGATGAC-3'
p62_1BglII_Fw	5'-CTCAGATCTCGATGGCGTCGCTCACCG-3'
p62_114BglII_Fw	5'-CTCAGATCTCGGCTCAGGAGGCGCCC-3'
p62_122SalI_Rev	5'-ACCGTCGACTCTACACCATGTTGCGGGGC-3'
p62_200SalI_Rev	5'-ACCGTCGACTCTAACCCATTTCCCATCCTGGC-3'
p62_440_Rev	5'-TCACAACGGCGGGGG-3'

2.7 Lentiviral Transduction

Stable expression of FLAG-p62 and FLAG-C105A-C113Ap62 in *p62*$^{-/-}$ MEFs was achieved through lentiviral transduction. FLAG-p62 (see **Appendix D**) and FLAG-C105A-C113Ap62 transgenes were cloned into the pLenti6/V5-DEST expression vector containing the blasticidin resistance gene (see **Appendix E**). HEK293FT cells were seeded in antibiotic-free medium supplemented with 0.1 mM MEM non-essential amino acids (Gibco, #11140050) and then cotransfected with either empty or *p62* lentiviral expression vectors and 3rd generation packaging system plasmids (Thermo Fisher Scientific, #K497500). After 24 hours, media was replaced with fresh media without antibiotics. 48 hours after transfection, viral transduction was performed by transferring media from HEK293FT cells 70% confluent *p62* knock-out (*p62*$^{-/-}$) MEFs in the presence of 6 µg/ml Polybrene (Sigma-Aldrich, #H9268). Media containing virus was replaced after 24 hours with fresh media containing 8 µg/ml of blasticidin (Thermo Fisher Scientific, #R21001) for selection of transduced cells. Media was replaced every 2-3 days for 10-12 days by keeping the antibiotic selection. Transduced MEFs were then maintained in lower levels of blasticidin (4 µg/ml) until seeding for experimental purposes.

2.8 GST-p62 Purification

GST-p62 fusion protein was produced in *E. cloni* EXPRESS BL21 (DE3) Chemically Competent Cells (Lucigen, #60401) using the pDEST-GST-p62 plasmid as previously described (Lamark *et al.*, 2003). Fusion protein expression was induced by adding 0.2 mM IPTG (isopropyl β-D-1-thiogalactopyranoside, Sigma-Aldrich, #I5502) for 2 hours. Bacterial pellets were lysed by sonication in buffer (50 mM Tris pH 7.4, 150 mM NaCl) and GST-fusion protein purified using Glutathione-Sepharose 4B beads (GE Healthcare, #17075601). Purified GST-p62 fusion protein was then treated with H_2O_2 and PR-619 as indicated and subjected to immunoblot analysis.

2.9 Immunoblot Analysis

2.9.1 Protein extraction

HeLa, MEFs or HEK293E cells were seeded in 6- or 12-well plates 24 (HeLa and HEK293E) or 48 (MEFs) hours prior treatments (**Table 2.4**). After treatments, cells were washed in ice-cold 1x PBS then lysed in RIPA (radioimmunoprecipitation assay) buffer (150 mM NaCl, 1% NP-40, 0.5% NaDoC, 0.1% SDS, 50 mM Tris pH 7.4, supplemented with 1X Halt protease & phosphatase inhibitor cocktail (Thermo Fisher Scientific) in ddH_2O) plus 50 mM N-ethylmaleimide (NEM, Sigma-Aldrich), which determines alkylation of reduced cysteine residues and protects them from being oxidised during sample preparation (Gregory, 1955; Paulech *et al.*, 2013). Cells were scraped with rubber scrapers on ice and lysates were centrifuged at 4°C at 13,000 rpm for 10 min to remove insoluble cellular components. Supernatants containing proteins were then quantified.

2.9.2 Protein quantification

Protein concentration was measured by Bradford assay using the DC Protein Assay Kit I (Bio-Rad), a detergent-compatible colorimetric assay. Four different dilutions of protein standards (0, 0.25, 0.75 and 1.5 µg of BSA) in duplicate were used to generate a calibration curve. After adding the standards (5 µl) and the unknown protein samples (2 µl) in a 96-well plate, 25 µl of Reagent A' (an alkaline copper tartrate solution) were added to each well, followed by 200 µl of Reagent B (Folin reagent). The colorimetric reaction is mediated by a reaction between proteins and copper in an alkaline medium, and a subsequent reduction of Folin reagent by the copper-treated proteins. Absorbance was then measured with a FLUOstar Omega plate reader (BMG Labtech) at 750 nm, and the colorimetric values were analysed on Excel (Microsoft). Samples were prepared at the same concentration by mixing the appropriate volume of protein lysate and 2x Laemmli buffer (Bio-Rad) and boiled at 100°C for 5 min in the presence or absence of 2.5% β-ME (β-mercaptoethanol,

Sigma-Aldrich). Samples were either stored at -20°C or immediately used for immunoblot analysis.

2.9.3 Acrylamide gel preparation

Gels for electrophoresis were assembled by pouring a mix solution for the resolving gel (10-15% acrylamide, 1.5 M Tris pH 8.8, 10% SDS, 10% ammonium persulphate and 0.05% TEMED in ddH_2O), pouring it into 1.5 mm empty gel cassette (Thermo Fisher Scientific) leaving 1 inch empty and overlaying with 1 ml of water to ensure a straight edge. After the polymerisation of the resolving edge, a mix solution for the stacking gel (5% acrylamide, 1 M Tris pH 6.8, 10% SDS, 10% ammonium persulphate and 0.1% TEMED in ddH_2O) was then poured into the cassette on top of the resolving gel, and a gel comb (10-15 wells, Thermo Fisher Scientific) was inserted.

2.9.4 Electrophoresis and transfer

The cassettes with the polymerised gel were placed in an XCell SureLock™ Mini-Cell electrophoresis system (Invitrogen) which was filled with Tris-Glycine running buffer (250 µM Tris, 1.92 mM glycine and 0.1% w/v SDS). Samples (20-40 µg of proteins) were loaded into the wells of the gel along with the Precision Plus Protein™ Dual Color Standards (Bio-Rad) and electrophoresis was performed at 120 volts, 35 mA and 5 watts for 90 min. Following electrophoresis, gels were removed from the cassettes and proteins were transferred to Immobilon-P PVDF membranes (0.45 µm, Millipore) using a Trans-Blot SD Semi-Dry Transfer Cell (Bio-Rad) at 17 volts for 1 hour. Thick blotting paper pads (VWR International) soaked in transfer buffer (250 µM Tris, 1.92 mM glycine) were used above and under the gels. Alternatively, gels were stained with GelCode™ Blue stain reagent (Thermo Fisher Scientific), based on colloidal Coomassie dye G-250 for nanogram-level detection of proteins, for 1 hour at room temperature.

After the transfer, membranes were stained with Ponceau S solution (0.5% Ponceau and 5% acetic acid in ddH_2O) for band detection, to assess efficiency of the transfer and to trim membranes as required.

2.9.5 Membranes staining and evaluation

Membranes were washed in PBS and incubated with a blocking solution (PBS containing 5% fat-free dry milk, 0.1% Tween-20) for 1 hour. After washing with PBS, membranes were incubated with primary antibody (**Table 2.9**) diluted in blocking solution at 4˚C overnight with gentle shaking. The day after, membranes were washed three times, 5 min each: one time with PBS, once in PBS with 0.1% Tween-20 and one more time in PBS. Then, membranes were incubated with HRP (horseradish peroxidase)-conjugated secondary antibody diluted in blocking solution for 1 hour at room temperature with gentle shacking. The secondary antibodies were: α-mouse (Sigma-Aldrich, #A2554, 1:5000), α-rabbit (Sigma-Aldrich, #A0545, 1:5000) and α-guinea pig (Dako, #P0141, 1:1000). Membranes were washed three times as above, then incubated for 5 min with Clarity™ Western ECL Substrate (Bio-Rad), which is prepared by mixing equal amounts of peroxide reagent and luminol/enhancer reagent. Membranes were visualised by chemiluminescence using a LAS-4000 CCD camera system (Fujifilm).

Table 2.9 | Primary antibodies for immunoblot used in this study.

Primary antibodies for immunoblot			
Protein	**Host**	**Dilution**	**Manufacturer/ Product No.**
p62	Guinea pig	1:2000	GP62-C
Ubiquitin	Mouse	1:1000	LifeSensors #VU101
LC3	Mouse	1:1000	Enzo Life Sciences #ALX-803-081-C100
Mfn2	Mouse	1:1000	Sigma-Aldrich #WH0009927M3
rpL10 (QM)	Rabbit	1:200	Santa Cruz Biotechnology #sc-798
Prx-3	Rabbit	1:2000	(Olahova *et al.*, 2008)
Prx-SO_3	Rabbit	1:2000	Abcam #ab16830
GFP	Mouse	1:1000	Santa Cruz Biotechnology #sc-9996
GAPDH	Rabbit	1:10,000	Cell Signaling #5174
Actin	Rabbit	1:2000	Abcam #ab8227

2.10 Ultracentrifugation

Lysates from HeLa cells and MEFs were spun first at 4°C at 13,000 rpm for 10 min, and samples of whole-cell lysates were prepared by boiling in 2x Laemmli buffer (Bio-Rad) at 100°C for 5 min. Supernatants where loaded into 1 ml thickwall polycarbonate cuvettes (Beckman Coulter, #343778) and centrifuged using an Optima^{TM} TLX Ultracentrifuge (Beckman Coulter) at 100,000 rpm at 4°C for 1 hour. Soluble and insoluble fraction samples were prepared by boiling supernatants and pellets in 2x Laemmli buffer (Bio-Rad) at 100°C for 5 min.

2.11 Immunoprecipitation (IP)

HeLa cells were seeded in 100 mm dishes and subjected to transfection after 24 hours. The following day, cells were lysed in IP buffer (20 mM Tris pH 7.4, 150 mM NaCl, 0.5% NP-40, 2 mM $MgCl_2$, 50 mM NEM supplemented with 1X Halt protease & phosphatase inhibitor cocktail (Thermo Fisher Scientific) in ddH_2O) on ice and centrifuged at 13,000 rpm for 10 min at 4°C. After centrifugation, the supernatants were collected (5%) for subsequent analysis of protein expression levels. Supernatants were then incubated with 20 µl of α-FLAG M2 magnetic beads (Sigma-Aldrich, #M8823) for 1 hour at 4°C with constant rotation. Beads were then washed three times in IP buffer and eluted by adding 0.2 M glycine-HCl pH 2.5 and boiling the elution in 2x Laemmli buffer (Bio-Rad) for 5 min at 100°C. Alternatively, the beads were boiled in 2x Laemmli buffer (Bio-Rad) at 100°C for 5 min in the presence or absence of 2.5% β-ME.

2.12 6xHis Pull-Down Assay

The 6xHis pull-down assay was carried out using TALON magnetic beads (Clontech, #635636) as per company instructions. Briefly, HeLa cells were seeded in 100 mm dishes and transfected after 24 hours. The following day, cells were lysed on ice in 1x Equilibration buffer in the presence of 8 M urea, 50 mM NEM and 1X Halt protease & phosphatase inhibitor cocktail (Thermo Fisher Scientific). Lysates were centrifuged at 13,000 rpm for 10 min at 4°C. After centrifugation, the supernatants were collected (5%) for subsequent analysis of protein expression levels. Supernatants were then incubated with 100 µl of TALON magnetic beads (Clontech) for 1 hour at 4°C with constant rotation. Beads were then washed three times in 1x Equilibration buffer and eluted by adding 1x Elution buffer and boiling the elution in 2x Laemmli buffer (Bio-Rad) for 5 min at 100°C. Alternatively, the beads were boiled in 2x Laemmli buffer (Bio-Rad) for 5 min at 100°C.

2.13 Click-iT AHA Assay

Cells were seeded into 10 mm dishes and grown until 70-80% confluency. For labelling of newly synthesised proteins, cells were washed once with PBS and incubated overnight with 4 µM Click-iT AHA (L-azidohomoalanine) (Thermo Fisher Scientific, #C10102) in DMEM without cysteine and methionine (Thermo Fisher Scientific, #21013024). The following day, AHA was removed and cells were washed with PBS and incubated in serum-free DMEM for the required chase time (0-6 hours). Cells were harvested into 400 µl p62 IP buffer (20 mM Tris pH 7.4, 150 mM NaCl, 0.5% NP-40, 2 mM $MgCl_2$ and protease inhibitor cocktail (Roche)) and incubated on ice for 10 min. Lysates were centrifuged for 10 min at 13,000 rpm, the supernatant was incubated with 20 µl of prewashed EZview M2 agarose beads (Sigma-Aldrich, #F2426) for 2 hours at 4°C with constant rotation. Beads were then washed 3 times in p62 IP buffer. The AHA containing proteins were then labelled with biotin (biotin alkyne, Thermo Fisher Scientific, #B10185) on the beads via Click-iT Cell Reaction

Buffer Kit (Thermo Fisher Scientific, #C10269) and following the manufacturer's protocol. Finally, beads were washed 3 times in p62 IP buffer before protein was eluted by boiling in 2x Laemmli sample buffer (Bio-Rad). Eluted samples were run on 10% SDS-PAGE gels and transferred to low fluorescence PVDF membrane (Millipore). Western blots were probed with streptavidin conjugated to IRdye Infrared Dyes (LiCor Biosciences, #800CW) and visualised using an Odyssey Scanner (LiCor Biosciences). Band intensity was quantified using Image Studio software (LiCor Biosciences).

2.14 Immunofluorescence

For immunofluorescence (**Table 2.5**), HeLa cells and MEFs were seeded on coverslips in 12-well plates. After treatments, cells were fixed in 3.7% formaldehyde in PBS for 10 minutes at room temperature. Formaldehyde was removed and cells were washed three times with PBS. Cells were permeabilised with 0.5% Triton X-100 for 5 minutes at room temperature. Following permeabilisation, cells were washed three times in PBS and incubated in blocking solution (5% normal goat or rabbit serum in PBS, 0.1% Tween-20) for 1 hour at room temperature in constant agitation. Cells were incubated with primary antibodies diluted in blocking solution overnight at 4°C. Primary antibodies used in this study include guinea pig α-p62 (Progen, #GP62-C 1:200), goat α-Ubiquitin (Santa Cruz Biotechnology #sc-34870, 1:200) and mouse α-LC3 (Enzo Life Sciences, #ALX-803-081-C100, 1:200). Cells were washed three times and incubated with the appropriate secondary antibodies (Life Technologies, 1:5000) for one hour at room temperature. Cells were washed three times in PBS, nuclear DNA was stained by incubation with TO-PRO-3 iodide (Life Technologies, 1:3000) for 10 minutes at room temperature. Coverslips were mounted on slides with ProLong® Gold Antifade Mountant with DAPI (Thermo Fisher Scientific) and imaged with an LSM 510 META Confocal Microscope (Zeiss) using a 63X Plan-Apo/1.4 NA Oil objective.

2.15 Cell Death Assay

MEFs were seeded 24 hours prior to treatments in 12-well plate. After treatments, cells viability was assessed using Ready Probes Cell Viability Imaging kit (Thermo Fisher Scientific, #R37609) as per company instructions. Briefly, NucBlue Live reagent (Hoechst 33342) and NucGreen Dead reagent (FITC/GFP) were added to the media for 30 min after treatments to determine cell viability by counting total vs. dead cells. NucBlue Live reagent stains all cell nuclei, while NucGreen Dead reagent stains only the nuclei of cells with compromised plasma membrane. Cells were imaged on inverted DM IL LED Leica microscope equipped with an Invenio 3SII digital camera (3.1 Mpix Colour CMOS; DeltaPix). Images were analysed using ImageJ and the percentage of cell death was quantified.

2.16 ROS Measurement

Hydrogen peroxide formation was detected using non-fluorescent dihydrorhodamine 123 (DHR, Thermo Fisher Scientific, #D23806), which after its oxidation by H_2O_2 is converted to fluorescent rhodamine. MEFs were seeded in a 12-well plate, the next day they were treated with the different ROS inducing agents. Cells were then washed with PBS, followed by trypsinisation. Cells were transferred to a 15 ml tube, centrifuged for 3 min at 1,600 rpm. The pellet was resuspended in 500 µl DMEM containing the DHR dye (5 µM). Following 30 minutes incubation at 37˚C, cells were centrifuged again for 3 min at 1,600 rpm and the pellet was resuspended in 2 ml DMEM. Cells were immediately analysed by fluorescence-activated cell sorting (FACS, Partec PAS).

2.17 Human Brain and Spinal Cord Tissue

Frozen brain and spinal cord tissue were obtained from the Newcastle Brain Tissue Resource bank. Frozen tissue from Alzheimer's disease (AD, temporal cortex), frontotemporal dementia (FTD, temporal cortex), dementia with Lewy bodies (DLB, cingulate cortex), Parkinson's disease (PD, substantia nigra), amyotrophic lateral sclerosis (ALS), and matched controls (**Table 2.10, 2.11**) were homogenised using a Ultra-Turrax T10 (IKA) in homogenisation buffer (0.1 M Tris pH 7.4, 0.5% Triton X-100, 50 mM NEM supplemented with 1X Halt protease & phosphatase inhibitor cocktail (Thermo Fisher Scientific) in ddH_2O) in a 1:10 ratio (e.g. 50 mg of tissue in 500 µl of buffer). Homogenised samples were centrifuged (13,000 rpm for 10 min at 4°C), protein concentration in supernatants was measured as described previously and samples were made by adding 2x Laemmli sample buffer to supernatants in the presence or absence of 2.5% β-ME. Samples were then analysed by immunoblot analysis.

Table 2.10 | Human brain tissue used in this study. PM: *post-mortem*

Human Brain Tissue						
Case ID	**Diagnosis**	**Area (Cortex)**	**Hemisphere**	**Age**	**Sex**	**PM delay (h)**
0205	AD	Temporal	Left	86	F	5
0026	AD	Temporal	Left	83	M	12
0083	AD	Temporal	Left	63	F	11
0378	FTD	Temporal	Left	88	M	42
0051	FTD	Temporal	Left	73	F	47
0085	FTD	Temporal	Left	83	F	39
0932	DLB	Cingulate	Left	78	M	8
0310	DLB	Cingulate	Left	91	F	10
0017	DLB	Cingulate	Left	77	M	8
0115	Control	Cingulate/Temporal	Left	82	F	12
1035	Control	Cingulate/Temporal	Right	66	M	9
0102	Control	Cingulate/Temporal	Left	72	M	17
0038	PD	Substantia Nigra	Left	76	M	49
0827	PD	Substantia Nigra	Left	83	M	105
1912	PD	Substantia Nigra	Left	70	M	48
0400	Control	Substantia Nigra	Left	65	F	47
0411	Control	Substantia Nigra	Left	88	M	28
1903	Control	Substantia Nigra	Left	52	M	102

Table 2.11 | Spinal cord tissue used in this study. PM: *post-mortem*

Spinal Cord Tissue					
Case ID	**Diagnosis**	**Area of Onset**	**Age**	**Sex**	**PM delay (h)**
0768	ALS	Limbs	75	F	26
0219	ALS	Limbs	72	F	52
1913	ALS	Limbs	80	F	26
0496	Control	N/A	80	F	31
1016	Control	N/A	74	F	49
0891	Control	N/A	73	M	25

2.18 Mouse Brain Tissue and Immunohistochemistry

Young (3 months) and old (24 months) mice were housed in same-sex cages in groups of 4 to 6 (56×38×18 cm; North Kent Plastics, Kent, UK) and individually identified by an ear notch. Mice were housed at 20 ± 2°C under a 12 hours light/12 hours dark photoperiod with lights on at 7.00 am. The diet used was standard rodent pelleted chow (CRM (P); Special Diets Services, Witham, UK). For immunoblot, samples were prepared as for human tissue. For immunohistochemistry (**Table 2.6**), paraffin sections were deparaffinised with Histo-Clear (National Diagnostics) and ethanol, antigen was retrieved by incubation in 0.01 M pH 6.0 citrate buffer at 95°C for 20 min. Slides were incubated in 0.9% H_2O_2 for 30 min and afterwards placed in blocking buffer (5% normal goat serum, Vector Laboratories) for 30 min at room temperature. Primary antibody (guinea pig α-p62) was applied overnight at 4°C. Slides were washed three times with PBS and incubated for 30 min with secondary

antibody (Vector Laboratories). Antibodies were detected using peroxidase VECTASTAIN ABC kit (Vector Laboratories) according to the manufacturer's instructions. Substrate was developed using NovaRED (Vector Laboratories). Sections were counterstained with haematoxylin (Vector Laboratories) and mounted with DPX (Thermo Fisher Scientific).

2.19 p62 Alignment and *in Silico* Calculations

The sequences of p62 protein in 30 organisms (**Table 2.12**) were identified by searching UniProt for the gene name SQSTM, then removing sequence fragments and choosing the longest isoform from each organism. Multiple sequence alignment was carried out using the Muscle server at the EBI (European Bioinformatic Institute) website (http://www.ebi.ac.uk/Tools/msa/muscle/) with default parameters. The resulting alignment was visualised using ALINE software (Bond and Schuttelkopf, 2009). Conservation is indicated by depth of colour from light to dark red, with conservation below 40% indicated in white. All 30 sequences were used to generate the alignment and calculate conservation, but only 14 were included in the graphical output. Secondary structure in the PB1 domain was indicated by using the X-ray crystal structure (PDB entry 4MJS chain B), and in the ZZ zinc-finger domain using homology to CBP (PDB entry 1TOT).

Table 2.12 | List of organisms used for multiple alignment of p62 protein sequences. Organisms included in **Figure 4.3** are marked with an asterisk.

Organisms for Multiple Alignment
Genus/Species/Common name
Homo sapiens (Human)*
Pongo abelii (Sumatran orang-utan)*
Gorilla gorilla gorilla (Western Lowland gorilla)
Pan troglodytes (Chimpanzee)
Macaca mulatta (Macaque)*
Papio anubis (Olive baboon)
Callithrix jacchus (Common marmoset)
Nomascus leucogenys (White-cheeked gibbon)
Otolemur garnettii (Small-eared galago)
Spermophilus tridecemlineatus (Thirteen-lined ground squirrel)
Drosophila melanogaster (Common fruit fly)*
Caenorhabditis elegans (Roundworm/nematode)*
Ovis aries (Sheep)
Bos taurus (Cow)*
Sus scrofa (Pig)
Oryctolagus cuniculus (Rabbit)
Rattus norvegicus (Rat)

Mus musculus (Mouse)*
Canis familiaris (Dog)*
Felis catus (Cat)
Cavia porcellus (Guinea pig)*
Loxodonta africana (African elephant)
Sarcophilus harrisii (Tasmanian devil)*
Gallus gallus (Chicken)*
Ficedula albicollis (Collared flycatcher)
Xenopus laevis (African clawed frog)*
Xenopus tropicalis (Western clawed frog)
Anolis carolinensis (Carolina anole)*
Danio rerio (Zebrafish)
Latimeria Chalumnae (African coelacanth)*

2.20 Quantifications and Statistical Analysis

Quantification of cells was performed by blind scoring of slides as described previously (Korolchuk *et al.*, 2011). More than 200 cells were counted per slide and quantification was based on at least three independent experiments. Quantification of immunoblots was carried out using ImageJ software (National Institutes of Health) by measuring the integrated density from each band after background subtraction. Two-tailed, unpaired Student's t-tests were carried out on experimental data from at least three individual experiments.

Chapter 3. p62 Senses Oxidation by Forming Disulphide-Linked Conjugates (DLC)

3.1 Introduction

Autophagy is a catabolic pathway important for protein homeostasis involved in the degradation of damaged proteins and organelles. Autophagy employs double-membrane vesicles called autophagosomes to engulf ubiquitinated substrates recognised by receptor proteins, and delivers them to lysosomes (Stolz *et al.*, 2014). Impairment of autophagy has been linked to many pathophysiological processes such as ageing and neurodegeneration, and modulation of autophagy activity appeared to be an effective approach to ameliorate such conditions in different animal models (Rubinsztein *et al.*, 2011; Rubinsztein *et al.*, 2012; Carroll *et al.*, 2013). Oxidative stress, which represents the imbalance between reactive oxygen species (ROS) formation and their neutralisation by the antioxidant defences, has also been connected to ageing and age-related diseases (Finkel and Holbrook, 2000; Chen *et al.*, 2012). Although ROS have important regulatory functions in the cell, their excessive production can lead to damage of a vast array of molecules. The thiol group of cysteine (Cys) residues are particularly susceptible to ROS action, and tend to form disulphide bonds when oxidised (Cremers and Jakob, 2013). SQSTM1/p62 is a selective autophagy receptor involved in the accumulation and degradation of polyubiquitinated substrates by targeting them to autophagosomes (Pankiv *et al.*, 2007). Importantly, p62 tends to form aggregates and inclusions during autophagy deficiency (Bjorkoy *et al.*, 2005; Komatsu *et al.*, 2007b). Indeed, p62 has been found in virtually all protein aggregates related to neurodegenerative diseases (NDs), which are a hallmark of neurodegeneration (Zatloukal *et al.*, 2002).

Although p62 has been extensively studied in relation to its receptor function in selective autophagy, its role during conditions of oxidative stress is unknown. In this chapter, we sought to examine the role and the function of p62 during oxidation.

3.2 Results

3.2.1 p62 forms disulphide-linked conjugates (DCL) and aggregates in old mouse brain tissue

In order to investigate age-related changes in proteostasis, we homogenised brain tissue from young (3 months) and old (24 months) mice and analysed them by immunoblot (**Figure 3.1A, B**). In agreement with (Ohtsuka *et al.*, 1995), the old brain tissue contained a higher amount of ubiquitinated proteins which could indicate an imbalance in the degradation processes (**Figure 3.1A**). Additionally, it was possible to detect an increased amount of hyperoxidised Prx (Prx-SO_3), a marker of oxidative stress (Wagner *et al.*, 2002), in the old brain tissue. Since the imbalance in proteostasis could have been a direct consequence of the increased oxidation, also regulatory proteins such as p62 could have been affected by the oxidative environment.

Thus, an immunoblot analysis of the young and old brain tissue was performed in the presence (reducing) or absence (non-reducing) of β-mercaptoethanol (β-ME), a reducing agent that breaks disulphide bonds between Cys residues (**Figure 3.1B**). In the absence of β-ME it was possible to detect an accumulation of p62 at higher MW in the old brain tissue, which was not observed after addition of β-ME. Hence, these structures were named disulphide-linked conjugates (DLC) of p62 since they were observed only in non-reducing conditions and were likely to be dependent on different Cys through covalent interactions. Considering that p62 DLC were exclusively present in the old mouse brain tissue together with increased oxidative stress, we hypothesised that p62 DLC formation could have been oxidation-dependent.

On the other hand, levels of autophagy markers such as LC3-II and p62 itself were comparable in both young and old tissue, suggesting no significant difference in the autophagy function between them (**Figure 3.1A, B**). This finding was in conflict with the general idea of impaired autophagy during ageing, a concept that has become

more prominent after multiple studies reporting the inhibition of autophagic degradation during ageing and neurodegenerative diseases (Rubinsztein *et al.*, 2011). On the contrary, evidence has been given for an increase in autophagy levels during ageing in mouse brain (Gamerdinger *et al.*, 2009; Narita, 2010). These discrepancies indicate that autophagy is a dynamic and complex process which could be difficult to examine, especially *in vivo*. In our hands, we could not find differences in autophagy between young and old mouse brain tissue.

Additionally, we investigated whether p62 formed aggregates in the old brain tissue. In fact, accumulation and aggregation of p62 has been previously reported following autophagy inhibition (Komatsu *et al.*, 2007b; Korolchuk *et al.*, 2009), a common feature during ageing. Since we did not find any impairment in the autophagy function, we questioned whether increased oxidation could also induce p62 inclusion bodies formation. Thus, cerebellum tissue form young and old mice was immunostained for p62 and analysed by light microscopy, and the percentage of Purkinje cells with aggregates was then quantified (**Figure 3.1C**) The formation of p62 aggregates was enhanced in the old mouse tissue, although the overall levels of p62 protein were not different between young and old (cf. **Figure 3.1B**). This suggested that oxidation and the formation of DLC of p62 could have been important for its aggregation. Thus, it could be hypothesised that disulphide bond formation could promote an initial oligomerisation of p62 and facilitate the formation of aggregates.

In summary, p62 showed to sense oxidation potentially through formation of disulphide bonds in an age-dependent manner, which would lead to its increased aggregation.

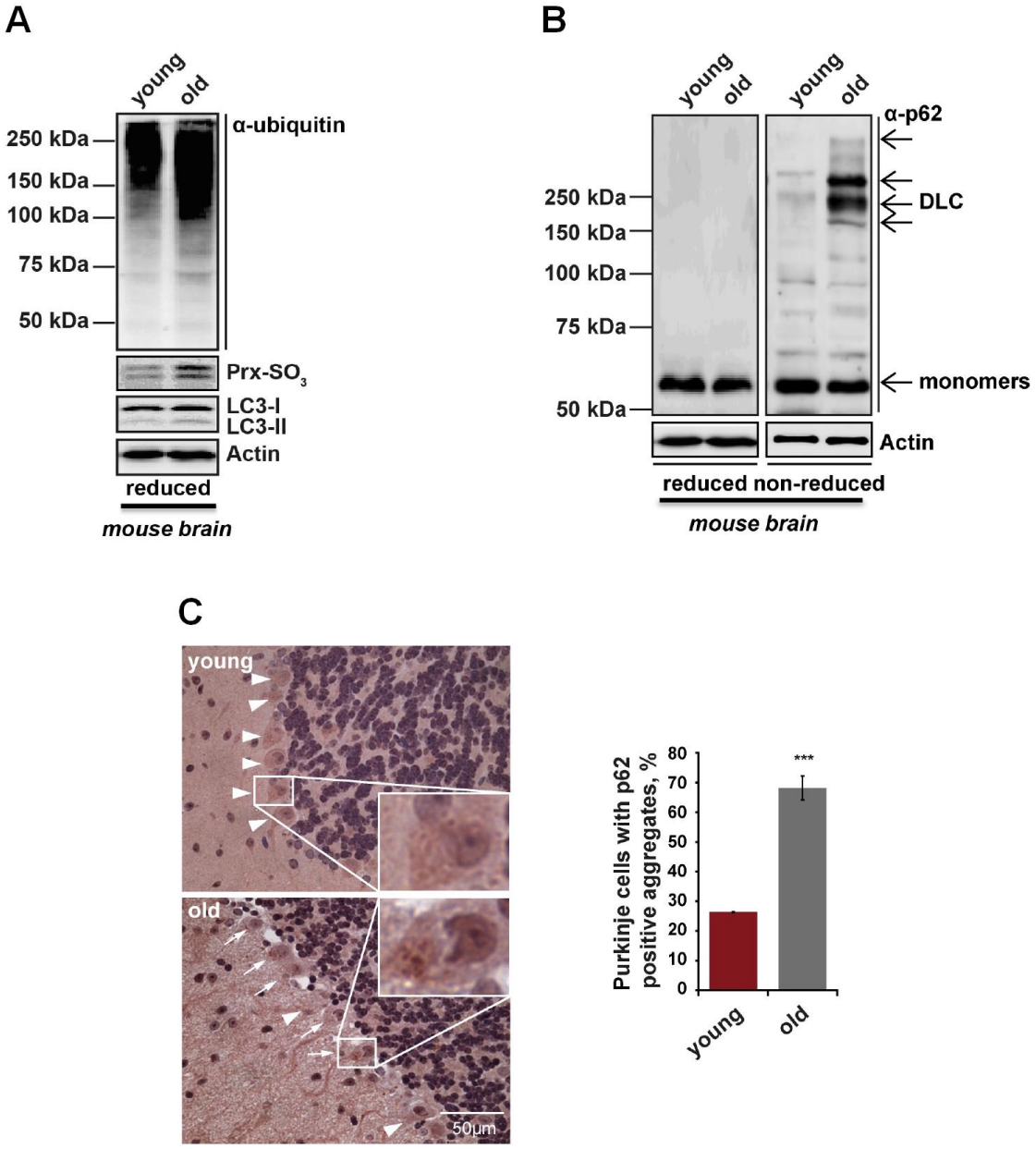

Figure 3.1 | Oxidative stress and ageing determine p62 aggregation and DLC formation in old mouse brain tissue. (A and B) Young (3 months) and old (24 months) mouse brain tissues (*n*=3) were homogenised and subjected to immunoblot analysis for ubiquitin, Prx-SO_3 and LC3 in reducing conditions (2.5% β-ME) **(A)**, and for p62 in either reducing or non-reducing conditions **(B)**. Actin was used as a loading control. Arrows represent monomers and DLC of p62. **(C)** Young and old mouse cerebellum sections were immunostained for p62 and analysed by light microscopy; the percentage of Purkinje cells positive for p62 aggregates was quantified. Error bars represent s.e.m., *n*=3, ***p<0.005. Data are representative of at least two independent experiments. The work in (A, B) was done in collaboration with Elsje G. Otten, while the work in (C) was carried out by Dr Diana Jurk at Newcastle University.

3.2.2 Oxidative stress induces formation of p62 DLC in cell culture

To model the behaviour of p62 seen in old mouse brain tissue, we used mammalian cells in tissue culture and tested whether oxidation could induce the formation of DLC of p62. HeLa (named after the donor Henrietta Lacks) cells, an immortalised cervical cancer cell line (Landry *et al.*, 2013), were used throughout the experiments as they were easy to grow and transfect. Since autophagy was not perturbed in the old mouse brain tissue (cf. **Figure 3.1A**), we compared the effects of autophagy inhibitors and oxidative stress inductors on the ability of p62 to form DLC. Our expectations were that inhibition of autophagy would only lead to the accumulation of p62 as shown by previous studies (Bjorkoy *et al.*, 2005; Komatsu *et al.*, 2007b; Korolchuk *et al.*, 2009), while oxidation would induce the formation of disulphide bond of p62 and slow down its electrophoretic mobility.

To inhibit autophagy, we used bafilomycin A1 (Baf) and chloroquine (CQ), two late phase inhibitors of autophagy. Bafilomycin A1, a macrolide antibiotic derived from *Streptomyces griseus*, is an inhibitor of vacuolar H^+-ATPase (V-ATPase) which prevents the acidification of lysosomes and the fusion between autophagosomes and lysosomes (Yoshimori *et al.*, 1991; Yamamoto *et al.*, 1998). Chloroquine is a lysosomotropic agent which tends to accumulate in lysosomes and reduce their acidity, therefore inhibiting the formation of autolysosomes (Shintani and Klionsky, 2004). The induction of oxidation was carried out using hydrogen peroxide (H_2O_2), added as a bolus to the cell medium. H_2O_2 is a strong oxidiser due to its unstable peroxide bond, and is the most abundant ROS produced in the cells (cf. **Chapter 1.1**) (Giorgio *et al.*, 2007). Additionally, we tested whether ubiquitination of p62 could have also been implicated in DLC formation. We employed a non-specific and reversible inhibitor of DUB enzymes known as PR-619 (2,6-diaminopyridine-3,5-bis(thiocyanate)), in order to induce accumulation of polyubiquitinated proteins (Altun *et al.*, 2011; Seiberlich *et al.*, 2012).

Immunoblot analyses on HeLa cell lysates showed that inhibition of autophagy by Baf and CQ led primarily to the accumulation of p62 at its expected MW (62 kDa) (**Figure 3.2A**). This was in agreement with previous observations, where aggregation of p62 consequent to autophagy inhibition has been shown to be mediated by non-covalent PB1 domain-dependent interactions (Lamark *et al.*, 2003). In contrast, H_2O_2 was able to induce a decrease in the electrophoretic mobility of p62 in non-reducing conditions, leading to the formation of p62 DLC similarly to what was seen in old mouse brain tissue (cf. **Figure 3.1B**).

Interestingly, PR-619 also increased the formation of p62 DLC in HeLa cells, exerting an even stronger effect than H_2O_2 (**Figure 3.2A**). Thus, we questioned how PR-619 could induce p62 modification. Since oxidation was the main candidate in DLC formation, we performed FACS analysis on HeLa cells treated with PR-619 in the presence or absence of N-acetylcysteine (NAC), an N-acetyl derivative of L-cysteine which replenishes GSH levels thus acting as an antioxidant (Atkuri *et al.*, 2007), and compared them to H_2O_2-treated cells (**Figure 3.2B**). Surprisingly, we found that PR-619 was a strong oxidising agent, producing high levels of ROS in the cells. To further confirm the ability of PR-619 to oxidise, we treated HeLa cells with PR-619 in the presence or absence of NAC and subjected the protein lysates to immunoblot analysis (**Figure 3.2C**). As expected, both ROS production and p62 DLC formation were strongly inhibited after addition of NAC. Thus, we confirmed that PR-619 induced oxidative stress which in turn led to the formation of p62 DLC.

DLC were completely abolished in the presence of β-ME, again suggesting the important role of covalent interactions between Cys in the formation of these high MW structures (**Figure 3.2A**). Importantly, the amount of p62 visible at 62 kDa was also diminished compared to the control, indicating an actual shift of the protein towards higher MW. This shift was ranging from 180 kDa to 250 kDa and above in the stacking gel, suggesting formation of inter-molecular bonds between different p62 molecules (trimers and tetramers) or other interactors, or both.

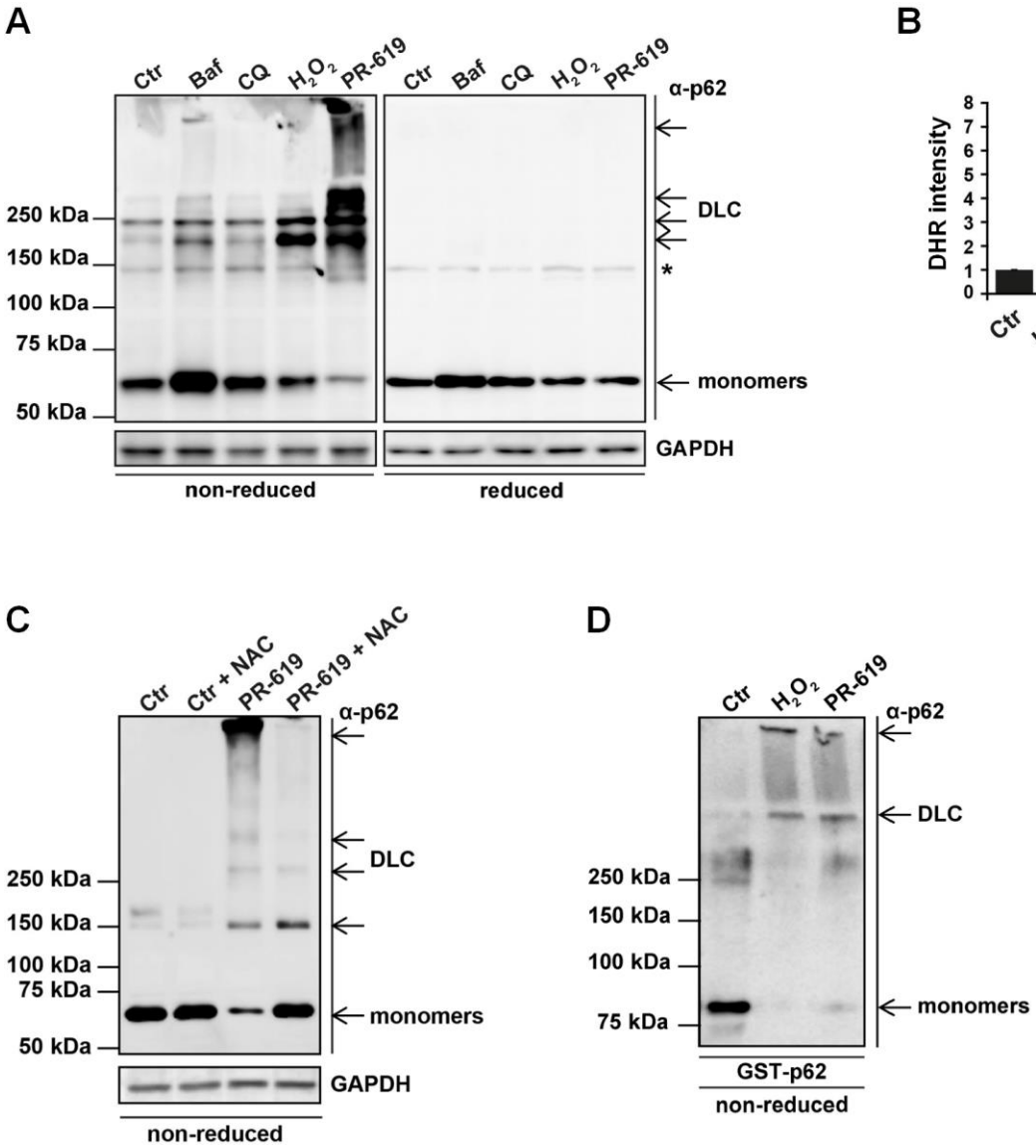

Figure 3.2 | Oxidative stress induced by H_2O_2 and PR-619 determines p62 DLC formation. (A) HeLa cells were treated with autophagy inhibitors bafilomycin A1 (Baf, 400 nM, 4 hours) and chloroquine (CQ, 50 μM, 4 hours), with the oxidative stressor H_2O_2 (5 mM, 10 min) and the DUB-inhibitor PR-619 (50 μM, 30 min). Lysates were analysed by immunoblotting for endogenous p62 in either non-reducing or reducing (2.5% β-ME) conditions. GAPDH was used as a loading control. Asterisk indicates an unspecific band. **(B)** HeLa cells were treated with H_2O_2 (1 mM, 10 min) or PR-619 (10 μM, 10 min) in the presence or absence of the antioxidant N-acetylcysteine (NAC, 5 mM), then oxidation levels were assessed by staining cells with dihydrorhodamine 123 (DHR) and analysing by fluorescence-activated cell sorting (FACS). Data were normalised, error bars represent standard deviation, *n*=2. **(C)** HeLa cells were treated with PR-619 as in (B) in the presence of absence of 5 mM NAC, then lysed and subjected to immunoblot analysis for endogenous p62. GAPDH was used as a loading control. **(D)** GST-p62 was purified from *E. coli*, treated with H_2O_2 and PR-619 as in (A) and immunoblotted for p62. Arrows represent monomers and DLC of p62. Data are representative of at least two independent experiments.

Thus, to assess whether other proteins besides p62 (e.g. ubiquitin) were required for DLC formation, we expressed a recombinant GST-p62 in *E. coli* and purified it with glutathione-sepharose beads, and then tested p62 electrophoretic mobility *in vitro* (**Figure 3.2D**). Treatments with H_2O_2 and PR-619 were sufficient to induce p62 DLC in the absence of other proteins, suggesting that formation of DLC could occur between different p62 molecules. However, the participation of other partners to the process *in vivo* was not excluded, which could explain the different pattern of DLC bands compared to HeLa cells (cf. **Figure 3.2A**).

In brief, oxidative stress appeared to be the stimulus leading to p62 DLC formation, while autophagy inhibition only led to the accumulation of p62 at its expected MW. The sole presence of p62 *in vitro* was sufficient to produce DLC formation upon oxidation, without excluding that hetero-oligomerisation with other proteins could possibly take place *in vivo*.

3.2.3 Oxidative stress and DLC formation enhance p62 aggregation and insolubility

Next, we wanted to test whether the oligomerisation of p62 through DLC formation could be involved in the development of p62 aggregates. This would have been in agreement with the previous findings of enhanced oxidation and p62 aggregation in the old mouse brain tissue (cf. **Figure 3.1**). Since autophagy inhibition is known to increase formation of p62 aggregates (Bjorkoy *et al.*, 2005; Komatsu *et al.*, 2007b; Korolchuk *et al.*, 2009), we tested whether also oxidation would induce a similar effect in p62 aggregation. To induce oxidation, we used paraquat (PQ) along with H_2O_2 and PR-619. Paraquat is an herbicide belonging to a family of redox-active heterocycles, which catalyses the formation of ROS and depletes the reducing equivalents in the cell (Bus and Gibson, 1984).

HeLa cells were treated with the autophagy inhibitors Baf and CQ and the oxidation inducers PQ, H_2O_2 and PR-619, stained for the endogenous p62 and analysed by confocal microscopy (**Figure 3.3A**). Both Baf and CQ increased the formation of p62

aggregates as expected. Similarly to autophagy inhibition, the formation of p62 inclusions was also induced under conditions of oxidative stress. This suggested that the formation of p62 aggregates could be mediated by different mechanisms, where increased levels of p62 due to its impaired degradation as well as direct disulphide bond formation would lead to its aggregation.

Additionally, we sought to investigate whether oxidation, and in turn DLC formation, could affect p62 solubility. To do so, we implemented the use of ultracentrifugation on HeLa cell lysates to separate the soluble fraction from the insoluble one (RIPA buffer insoluble), after treating the cells with H_2O_2 and PR-619 to induce oxidation (**Figure 3.3B**). During control conditions, monomeric p62 was distributed between the soluble and insoluble fractions, although more concentrated in the latter (lanes 2 and 3). After treatments, the amount of monomeric p62 in the soluble fraction was reduced, while it accumulated in the insoluble fraction. Strikingly, p62 DLC were only evident in the insoluble fraction (lanes 6 and 9), but absent from the soluble one (lanes 5 and 8), suggesting that DLC formation causes p62 to aggregate and form insoluble inclusions. Such effect of DLC on p62 aggregation might be important for its function as a receptor for selective autophagy, since oligomerisation of p62 and aggregate formation is known to be required for the efficient degradation of substrates (Itakura and Mizushima, 2011).

In summary, different types of stress like autophagy inhibition and oxidation could induce accumulation and aggregation of p62 in tissue culture, similarly to what has been found in old mouse brain tissue. Also, the solubility of p62 seemed dependent on oxidation and DLC formation, which drive the shift of p62 from the soluble to the insoluble fraction.

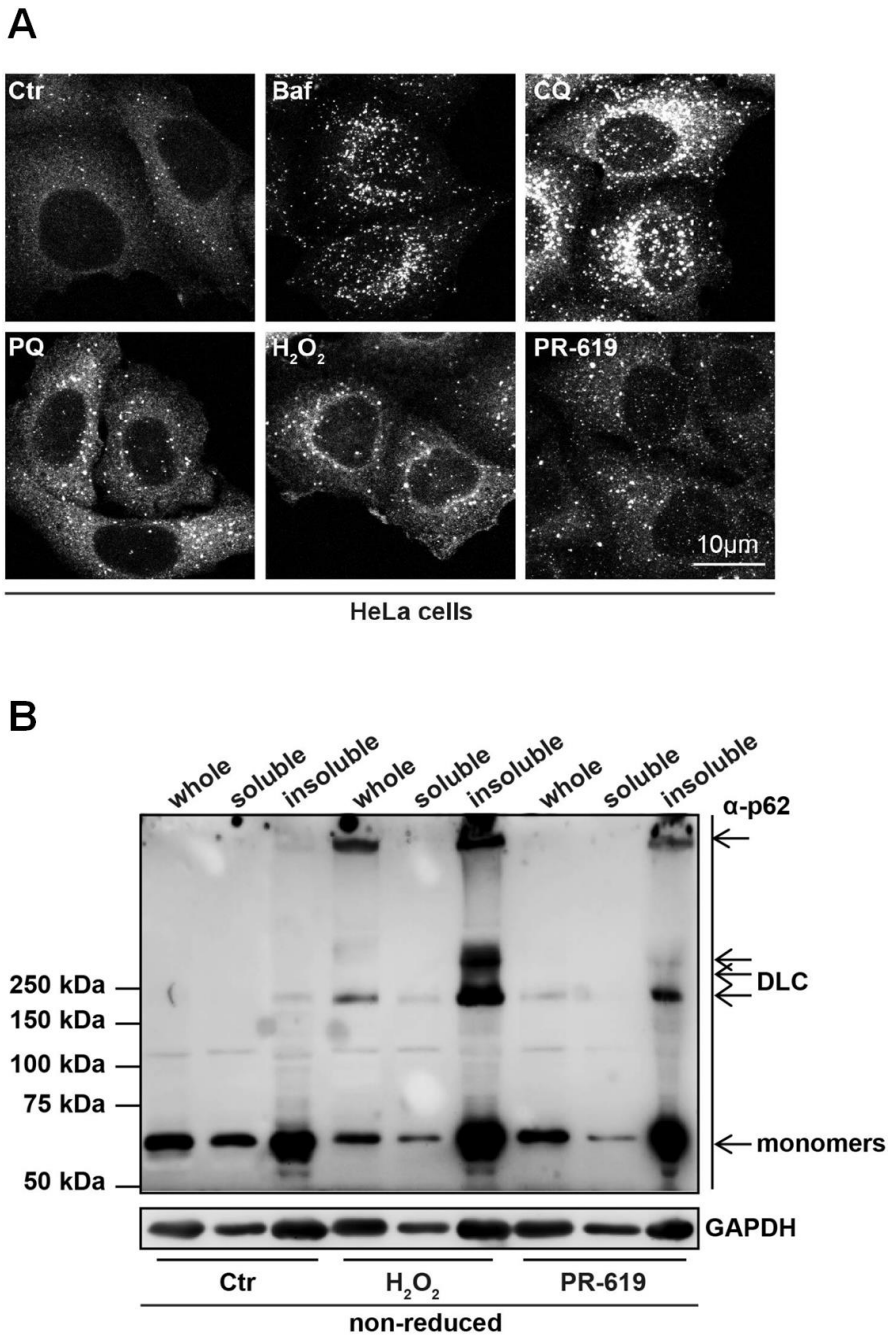

Figure 3.3 | Oxidative stress induces p62 aggregation and insolubility. (A) HeLa cells were treated with autophagy inhibitors bafilomycin A1 (Baf, 400 nM, 4 hours) and chloroquine (CQ, 50 μM, 4 hours), and with oxidative stressors Paraquat (PQ, 1 mM, 30 min), H_2O_2 (5 mM, 10 min) and PR-619 (50 μM, 30 min). Cells were immunostained for p62 and analysed by confocal microscopy. **(B)** HeLa cells were treated with H_2O_2 (5 mM, 1 min) and PR-619 (10 μM, 10 min), lysed and subjected to ultracentrifugation to separate the soluble and insoluble fractions. Whole cell, soluble and insoluble fractions were then immunoblotted for endogenous p62. GAPDH was used as a loading control. Arrows represent monomeric and DLC p62. Data are representative of at least two independent experiments.

3.2.4 p62 is a specific sensor of oxidative stress

To understand whether p62 was a specific sensor of oxidation, we evaluated whether other proteins unrelated to p62 could be able to sense oxidation and produce DLC. We tested the mitochondrial outer membrane protein mitofusin 2 (Mfn2), a known selective autophagic substrate and Parkin receptor (Chen and Dorn, 2013) with 13 Cys residues in its sequence, and the ribosomal protein L10 (rpL10, also known as QM), involved in the regulation of transcription (Inada *et al.*, 1997) with 8 Cys residues in its sequence.

In addition to oxidation, we tested further treatments known to induce oligomerisation and aggregation of p62, such as inhibition of protein synthesis by puromycin (Pankiv *et al.*, 2007) and apoptosis induction (Jin *et al.*, 2009) by staurosporine. Puromycin is an aminonucleoside antibiotic derived from *Streptomyces alboniger* which, due to its structural analogy to aminoacyl-tRNA, prevents the formation of full-length protein by hindering the ribosomes (Azzam and Algranati, 1973). It has been shown that puromycin induces the formation of ALIS (aggresome-like induced structures) containing p62 and ubiquitin (Szeto *et al.*, 2006; Pankiv *et al.*, 2007). Staurosporine is an alkaloid derived from *Streptomyces staurosporeus*, a strong inhibitor of protein kinases and an inducer of apoptosis by both caspase-dependent and –independent pathways (Zhang *et al.*, 2004). The treatment with staurosporine was combined with the caspase inhibitor Z-VAD-FMK, in order to inhibit the actual cell death.

HeLa cells were subjected to the above compounds as well as H_2O_2 and PR-619, and protein lysates were analysed by immunoblot (**Figure 3.4**). Neither puromycin nor staurosporine induced formation of p62 DLC in comparison to H_2O_2 and PR-619, further confirming the role of oxidation in DLC formation while also showing that p62 oligomerisation and DLC formation might be driven by different mechanisms (**Figure 3.4A**). Both Mfn2 and rpL10 proteins did not produce DLC following treatments with puromycin, staurosporine as well as H_2O_2 and PR-619, supporting the idea that p62 would act as a specific sensor of oxidation. In summary, p62 formed DLC specifically upon oxidation, while other structurally-unrelated proteins did not share the same behaviour.

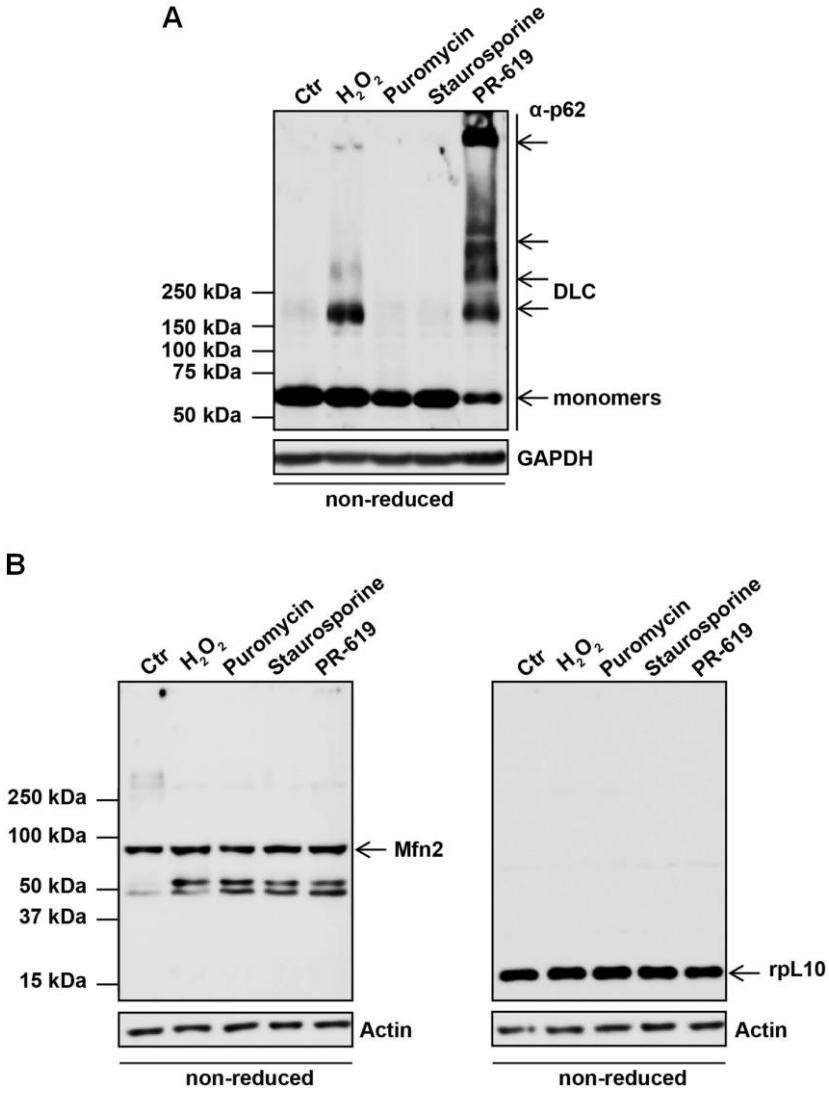

Figure 3.4 | p62, but not other structurally-unrelated proteins, forms DLC uniquely in response to oxidation. (A, B) HeLa cells were treated with H_2O_2 (5 mM, 1 min), puromycin (10 µg/ml, 3 hours), staurosporine (0.5 µM and Z-VAD-FMK 6.6 µM, 3 hours) and PR-619 (20 µM, 10 min), lysed and subjected to immunoblot analysis for p62 **(A)**, Mfn2 and rpL10 **(B)**. GAPDH (A) and Actin (B) were used as loading controls. Arrows in (A) represent monomeric and DLC p62. Data are representative of at least two independent experiments.

3.2.5 H_2O_2 and PR-619 induce p62 DLC with different kinetics

Since H_2O_2 and PR-619 showed a different degree of efficacy towards p62 shifting to higher MW (cf. **Figure 3.2A**), we sought to determine whether these two treatments could induce p62 DLC in a different manner. Thus, we analysed the kinetics of DLC formation upon H_2O_2 and PR-619 treatments. HeLa cells were treated with increasing concentrations and time points (1, 10 and 30 min) of H_2O_2 and PR-619, then lysed and analysed by immunoblot (**Figure 3.5**).

Interestingly, H_2O_2 induced a rapid formation of DLC after 1 min of exposure (lanes 2, 5 and 8, **Figure 3.5A**), although its effect appeared transient already after 5 min, and almost disappeared after 30 min at lower concentrations (100 µM and 500 µM, lanes 3 and 6). This transient formation of p62 DLC might depend on H_2O_2 quick decay after bolus addition to the media (Gulden *et al.*, 2010), and their subsequent break down by the cellular antioxidant systems. In contrast, PR-619 produced a more sustained oxidative stress reflected by progressive accumulation of DLC following longer treatments (10 and 30 min, **Figure 3.5B**). Notably, the shift of p62 towards higher MW was more prominent at the highest dose (50 µM), accompanied by a decrease in the amount of monomeric p62. Such loss of monomeric p62 was also visible in previous data (cf. **Figure 3.2A, C** and **Figure 3.4A**), and might reflect an increase in the protein insolubility that leads to lower amounts of the monomeric protein (cf. **Figure 3.3B**). As mentioned previously, PR-619 is a non-selective and reversible DUB inhibitor, thus we wanted to rule out any involvement of ubiquitin during DLC formation. To do so, we treated cells with N-ethylmaleimide (NEM), a Cys protease inhibitor that irreversibly blocks DUB enzymes (Liu *et al.*, 2003; Paulech *et al.*, 2013), and we checked for p62 DLC formation by immunoblot analysis (**Figure 3.4C**). Treatments with NEM at different time points did not produce any DLC of p62, suggesting that increased levels of ubiquitination driven by DUBs inhibition were not involved in p62 DLC formation, while PR-619 was used as a positive control (once again showing reduced levels of monomeric p62).

These results further showed that ubiquitination was not involved during DLC formation, and that oxidation was responsible for p62 modification. In order to

understand whether additional oxidative stressors could also cause p62 to form DLC, we tested other ROS-inducing compounds such as rotenone and paraquat, but neither of them gave consistent results (data not shown). Therefore, we continued using H_2O_2 and PR-619 as *bona fide* inducers of p62 DLC throughout the successive experiments.

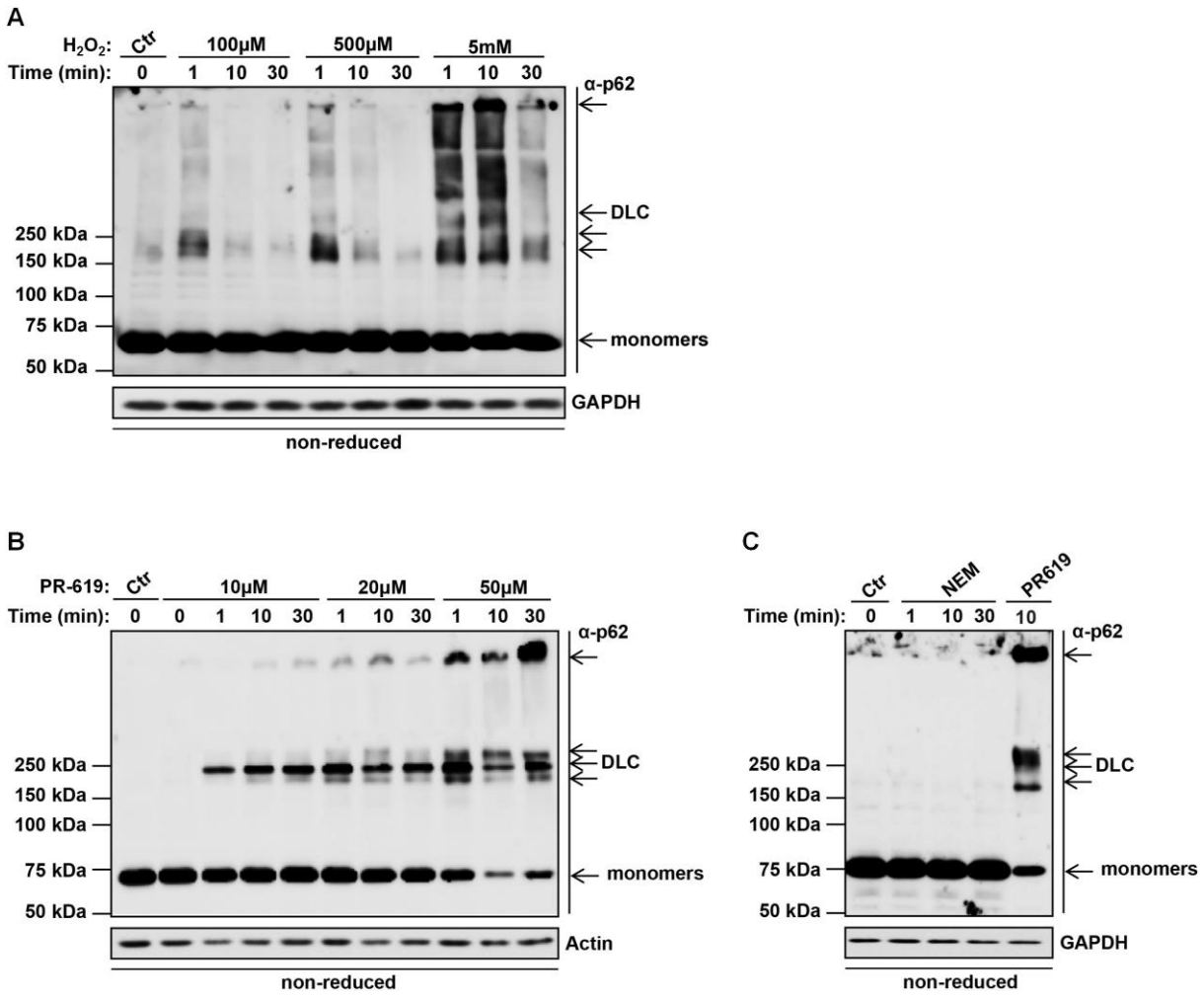

Figure 3.5 | H_2O_2 or PR-619 induce oxidation of p62 with different kinetics. (A, B) HeLa cells were treated with increasing concentration of H_2O_2 **(A)** or PR-619 **(B)** at different time points as indicated, lysed and subjected to immunoblot analysis for p62. (**C**) HeLa cells were treated with NEM (50 mM) at different time points as indicated, lysed and subjected to immunoblot analysis for p62. GAPDH (A, C) and Actin (B) were used as loading controls. Arrows represent monomeric and DLC p62. Data are representative of at least two independent experiments.

3.2.6 Inhibition of the peroxiredoxin/thioredoxin (Prx/Trx) antioxidant system enhances p62 DLC formation

Since oxidation was clearly involved in the formation of p62 DLC, we tested whether the antioxidant system, specifically the peroxiredoxin/thioredoxin (Prx/Trx) system (**Chapter 1.1.2**) could be involved in the reduction of DLC as for NAC (cf. **Figure 3.1C**). Thus, we employed immunoblot analysis to visualise Prx-SO_3 and Prx-3 (a mitochondrial Prx) as additional readouts for oxidation and for their role in regulating the redox state of the cell. At the same time, we employed HEK293E (human embryonic fibroblasts), to assess whether p62 would form DLC also in a different cell model.

Hence, HEK293E cells were treated with increasing concentrations of H_2O_2 (starting from 10 μM up to 500 μM) and different time points (20 sec, 1 and 10 min), then lysed and analysed by immunoblotting for p62, Prx-3 and Prx-SO_3 (**Figure 3.6A**). Interestingly, p62 reacted only slightly to the lower concentrations of H_2O_2 (10 and 50 μM) by appearing at about 250 kDa. The formation of more prominent amounts of p62 DLC was only achievable with higher doses of H_2O_2 (100 and 500 μM) and in a transient manner (DLC were reduced after 10 min), in agreement with the result of the previous time course (cf. **Figure 3.5A**). Treatments with H_2O_2 up to 100 μM increased the dimerisation of Prx-3, indicating its activation upon low-to-medium doses of H_2O_2. Such dimerisation appeared reduced upon high levels of H_2O_2 (100-500 μM, last four lanes) while levels of hyperoxidised Prx-SO_3 were increased, suggesting the inability of Prx in buffering high levels of oxidation as shown previously (Cox *et al.*, 2010).

Thus, it is possible that p62 forms DLC when the H_2O_2-buffering capacity of the cells is saturated (i.e. when Prx-3 is hyperoxidised), while during low levels of H_2O_2 the oxidising burden can be handled by the cellular antioxidant defence (i.e. Prx dimerisation). This would explain the need of high doses of H_2O_2, as well as high levels of oxidation mediated by PR-619, in order to produce DLC of p62.

Since Prx-3 appeared to be more sensitive to ROS than p62, we examined whether by blocking the Prx/Trx antioxidant system we could accelerate the formation of p62 DLC upon oxidation. To do this, we employed two compounds, curcumin and auranofin, both known to block the activity of thioredoxin reductase (TrxR). Curcumin is the main polyphenol of the plant *Curcuma longa* (widely known as turmeric) known for its antitumor properties, which irreversibly modifies the catalytic site of TrxR causing inhibition of its reductase activity and production of ROS (Fang *et al.*, 2005). Auranofin is a gold-containing compound used as an antirheumatic agent, which reacts with the selenocysteine residue of TrxR thus blocking its activity (Gromer *et al.*, 1998).

HeLa cells were pre-treated with either curcumin or auranofin for 30 min in order to block the activity of TrxR, then treated with H_2O_2 at different time points (1, 10 and 30 min) (**Figure 3.6B**). In the absence of pre-treatments, H_2O_2 did not induce a significant amount of p62 DLC, although the concentration used was rather high (3 mM). Nevertheless, in the presence of both curcumin and auranofin, it was possible to identify DLC of p62 already in the absence of H_2O_2 (lanes 5 and 9), especially following auranofin pre-treatment. Upon addition of H_2O_2, the production of p62 DLC was greatly intensified, showing enhanced accumulation of p62 in the stacking gel together with the reduction of the monomeric form (once again, auranofin had the biggest effect). This would suggest that p62 DLC are normally reduced by the Prx/Trx system. Notably, the dimerisation of Prx-3 was also increased during oxidation following curcumin and auranofin treatments, as found in previous studies (Cox *et al.*, 2010). The amounts of Prx-SO_3 were instead decreased, since Prx-3 dimerises but cannot cycle back to monomer due to the absence of reducing equivalents following TrxR inhibition. Both increased dimerisation of Prx-3 and loss of Prx-SO_3 were more evident following auranofin treatment, further confirming the higher efficacy of the compound over curcumin.

In summary, p62 DLC seemed to be reduced by the Prx/Trx antioxidant system. While low levels of oxidation were not sufficient to induce DLC formation, higher levels of H_2O_2 were sufficient to deplete the redox buffering capacity of the cells and induce p62 DLC.

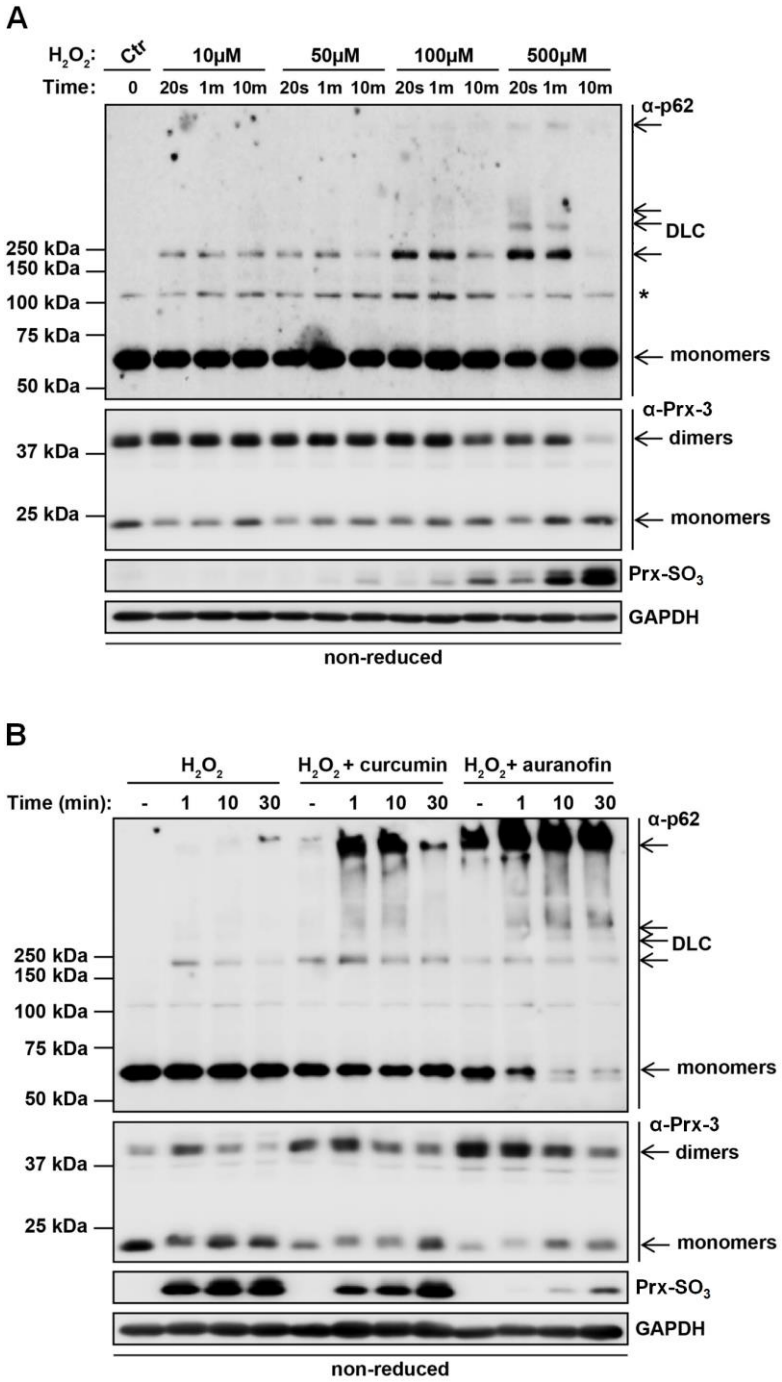

Figure 3.6 | The peroxiredoxin/thioredoxin (Prx/Trx) antioxidant system is involved in the reduction of p62 DLC. (A) HEK293E cells were treated with increasing concentrations of H_2O_2 at different time points as indicated, then lysed and immunoblotted for p62, Prx-3 and Prx-SO_3. **(B)** HeLa cells were pre-treated with either curcumin (50 μM) or auranofin (5 μM) for 30 min, then treated with H_2O_2 (3 mM) at different time points as shown. Cell were then lysed and immunoblotted for p62, Prx-3 and Prx-SO_3. GAPDH was used as a loading control. Arrows indicate monomeric and DLC p62, as well as monomeric and dimeric Prx-3. Asterisk indicates an unspecific band. Data are representative of at least two independent experiments.

3.2.7 p62 DLC are "sticky" and cannot be purified by immunoprecipitation

To better understand the composition of p62 DLC, we sought to purify these high MW species by immunoprecipitation (IP) followed by mass spectrometry, in order to analyse both the type of interactions involved in DLC formation and the presence of possible p62 interactors.

HeLa cells were transfected with FLAG-p62 (in order to overexpress p62 and increase DLC amount) for 24 hours and treated with PR-619 to induce formation of DLC; then, an IP was performed on cell lysates using α-FLAG magnetic beads and samples were analysed by immunoblot (**Figure 3.7A**). Any aspecific binding of p62 to the beads was ruled out by the absence of detectable p62 in untransfected cells (lane 4). Although p62 DLC were easily detectable in the Input following PR-619 treatment (lane 3), these were not eluted by acid buffer (which is commonly used to disrupt the interaction between the antibody and the antigen) (lane 6). Notably, monomeric levels of p62 were decreased both in the Input and after elution (lanes 3 and 6), indicating that p62 was oxidised but somehow lost during the elution process. The unbound fraction, which did not bind to the beads, showed lower levels of p62 both monomeric and DLC compared to the Input, suggesting that p62 overexpression worked beyond the binding capacity of the magnetic beads.

Interestingly, once the beads were boiled directly in the SDS-loading buffer in reducing conditions (β-ME), the amount of monomeric p62 after PR-619 treatment was increased. This would suggest that p62 DLC might be "sticking" to the beads, for example through hydrophobic interactions, and that a reducing environment would release them from binding to the beads. Indeed, manipulating proteins outside from their intracellular environment or overexpressing them as tagged proteins may result in a change in their conformation, determining increased aggregation and "stickiness" (Feller and Lewitzky, 2012). The absence of p62 DLC after IP was also confirmed by boiling the samples in non-reducing SDS-loading buffer followed by Blue Coomassie staining (**Figure 3.7B**). Although monomeric p62 was visibly reduced after PR-619 treatment, there was no presence of p62 DLC, in a similar way to what we found after eluting the proteins (cf. with Eluted in **Figure 3.7A**).

Since p62 “stickiness” could have been dependent on the protein ternary structure, we employed a different construct, a 6xHistidine-tagged p62 (His-p62), in order to pull-down the protein in denaturing conditions (8 M urea) and reduce the occurrence of hydrophobic interactions. In fact, the binding of His-tag to the purification beads (which commonly employ bivalent ions) is not dependent on the protein tertiary structure, thus allowing the addition of denaturing agents to the IP buffer without affecting the purification process (Bornhorst and Falke, 2000).

Thus, we transfected HeLa cells with His-p62 for 24 hours and treated them with H_2O_2; cell lysates were then subjected to pull-down using TALON magnetic beads (employing cobalt ions, Co^{2+}, to bind the His-tag) and samples were analysed by immunoblot (**Figure 3.7C**). Although monomeric p62 was visible also in untransfected samples due to unspecific binding, the amount of proteins bound to the beads was higher in the transfected samples. The presence of p62 DLC was evident in the Input, although completely lost in the eluted fraction as well as after boiling in non-reducing SDS-loading buffer. To further assess the potential presence of DLC, we performed a Blue Coomassie staining on eluted and boiled samples (**Figure 3.7D**). We could not find any difference in either monomeric p62 levels or DLC formation between untransfected and transfected cells, once again confirming the impossibility of isolating such formations.

In short, by performing IP and pull-down with different p62-tagged constructs we could not isolate and purify p62 DLC, possibly due to hydrophobic interactions that would lead to the “stickiness” of the protein to the isolation beads.

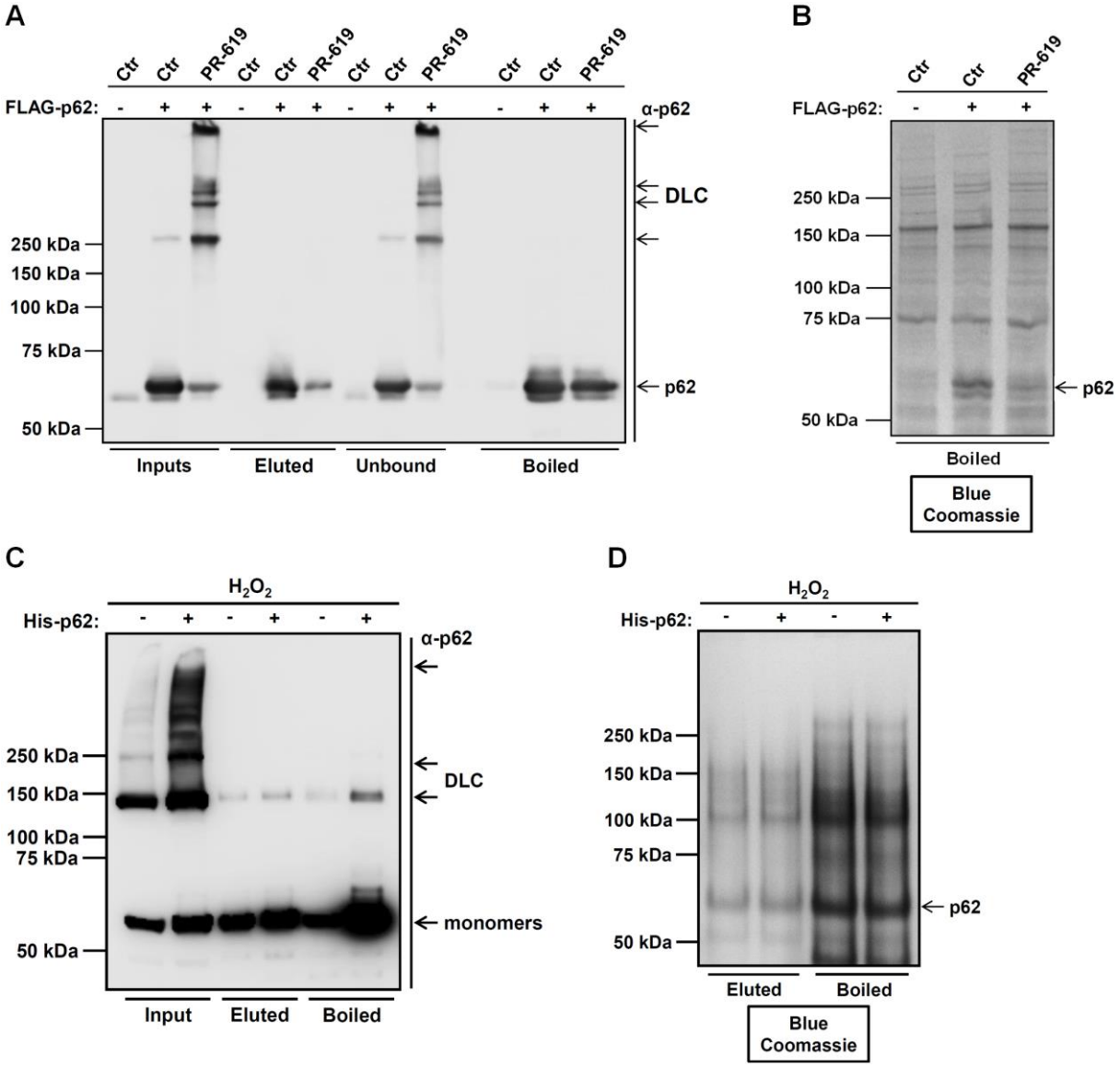

Figure 3.7 | p62 DLC are lost during immunoprecipitation. (A, B) HeLa cells were transfected with FLAG-p62 for 24 hours, treated with PR-619 (20 μM, 10 min) and lysed. Lysates were subjected to immunoprecipitation using α-FLAG magnetic beads which were either eluted with glycine-HCl buffer pH 2.5 or boiled in reducing SDS-loading buffer (+β-ME) as indicated. Input indicates whole cell lysates. Samples were then subjected to immunoblot analysis for p62 **(A)** or stained with Blue Coomassie **(B)**. **(C, D)** HeLa cells were transfected with His-p62 for 24 hours, treated with H_2O_2 (5 mM, 1 min) and lysed. Lysates were subjected to pull-down using TALON Co^{2+} magnetic beads in denaturing conditions (8 M urea) which were either eluted with elution buffer or boiled in non-reducing SDS-loading buffer as indicated. Input indicates whole cell lysates. Samples were then subjected to immunoblot analysis for p62 **(C)** or stained with Blue Coomassie **(D)**. Arrows represent monomeric and DLC p62. Data are representative of at least two independent experiments.

3.2.8 p62 accumulates and forms DLC in human brain tissue

After confirming the formation of p62 DLC both in old mouse brain tissue and in mammalian cell culture upon oxidative stress, we sought to investigate whether the DLC were also relevant to human age-related diseases. Since oxidative stress and impairment of autophagy are known to be associated with neurodegenerative diseases (NDs) (Melo *et al.*, 2011; Vidal *et al.*, 2014), we also examined the relevance of these processes to the NDs aetiology. To do so, we analysed human brain tissue provided by the Newcastle Brain Tissue Resource bank.

Human brain tissue from Alzheimer's disease (AD, temporal cortex), dementia with Lewy bodies (DLB, cingulate cortex) and frontotemporal dementia (FTD, temporal cortex) samples, plus age-matched controls, were homogenised and subjected to immunoblot analysis for p62, LC3 and the oxidation marker Prx-SO_3 (**Figure 3.8A**). Regarding LC3, we could only detect LC3-I (higher MW) but not LC3-II (lower MW). This was in agreement with previous studies, which have shown greater accumulation of LC3-I over LC3-II in crude brain homogenates, causing difficulties in detecting the latter (Yang *et al.*, 2011; Klionsky *et al.*, 2016). Thus, it was not possible to assess the actual levels of autophagic activity in these samples.

The ratio between monomeric and DLC p62 to the loading control was quantified and normalised to the healthy controls (**Figure 3.8B**). Strikingly, we could detect accumulation of monomeric p62 as well as p62 DLC in the disease samples, showing that DLC of p62 were also pertinent to human brain tissue. The DLC were accumulating at ~250 kDa, in accordance with our previous findings. The monomeric p62 was ranging between 37 and 60 kDa, possibly due to degradation processes occurring during the *post-mortem* (PM) delay. Such accumulation of p62 might suggest either impairment in autophagy, since p62 could not be degraded efficiently, or upregulation of p62 (and p62 DLC) expression levels in order to sequester toxic proteins into aggregates. Additionally, Prx-SO_3 seemed to accumulate in the diseased tissue, suggesting higher oxidation levels compared to the control tissue. This could explain the accumulation of p62 DLC in the NDs samples, in accordance with our finding that oxidation would be the stimulus leading to p62 modification. The

DLC were completely abolished after addition of β-ME to the sample buffer, thus showing that the cysteine residues of p62 were mediating DLC formation by covalent interactions. This was in agreement with our previous findings in both mouse brain tissue and mammalian cells (cf. **Figure 3.1B, 3.2A**).

To further investigate whether oxidation of p62 was also detectable in a wider context of neurodegeneration, we homogenised Parkinson's disease (PD, substantia nigra) brain tissue and amyotrophic lateral sclerosis (ALS, lumbar transverse section) spinal cord samples, plus age-matched controls, and analysed them by immunoblot analysis for p62 (**Figure 3.8C, E**). The ratio between monomeric p62 and p62 DLC to the loading control was quantified and normalised to the healthy control (**Figure 3.8D, F**). As for the other diseased tissue, also PD and ALS samples showed accumulation of monomeric p62 at lower MW, ranging from 37 kDa to 45 kDa, possibly due to PM delay. The DLC were also accumulating at ~250 kDa as for the other NDs.

In summary, p62 appeared to accumulate and form DLC in brain tissue affected by NDs, together with the presence of enhanced oxidation. This was in agreement with our previous findings that p62 would form DLC upon oxidative stress and induce protein aggregation, possibly leading to aggregates degradation through autophagy.

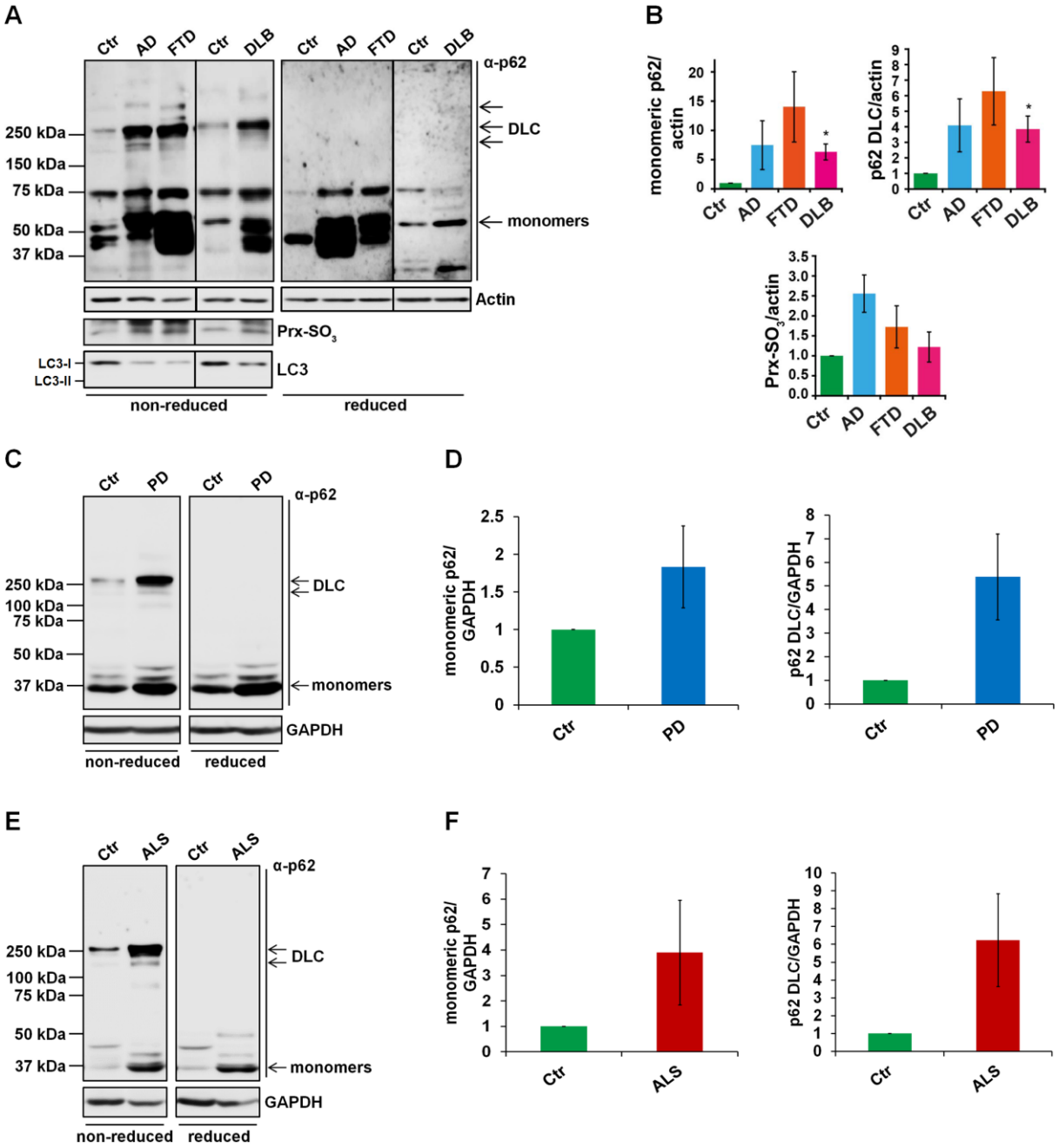

Figure 3.8 | Monomeric and DLC p62 accumulate in diseased human brain tissue. (A, C, E) Human brain tissue from patients with Alzheimer's disease (AD), frontotemporal dementia (FTD), dementia with Lewy bodies (DLB) **(A)**, Parkinson's disease (PD) **(C)**, amyotrophic lateral sclerosis (ALS) **(E)** and matching controls (*n*=3) were subjected to immunoblot analysis for p62, LC3 (A) and Prx-SO_3 (A) in either non-reducing or reducing (2.5% β-ME) conditions. GAPDH was used as a loading control. Arrows represent monomeric and DLC p62. **(B, D, F)** Levels of monomeric and DLC p62, as well as Prx-SO_3 (B), were quantified and normalised to the control. Error bars represent s.e.m., *n*=3, *p<0.05. Data are representative of at least two independent experiments.

3.3 Discussion

The cross-talk between autophagy and oxidative stress has been extensively studied in regards to nutrient deprivation, as ROS have been shown to induce the autophagy process while antioxidants can partially or completely halt it (Filomeni *et al.*, 2010). Nevertheless, little is still known regarding how the autophagic machinery is activated by oxidative stress, with only few evidences suggesting how the process is regulated. For instance, the Cys protease Atg4, important in the elongation of the autophagosomal membrane, has been shown to be modified by mitochondrial H_2O_2 on a Cys residue in its catalytic site, leading to Atg4 inactivation and subsequent lipidation of LC3 (Scherz-Shouval *et al.*, 2007). It has also been suggested that AMPK, which senses energy levels in the cells and induces autophagy by inhibiting mTOR, can be regulated by H_2O_2 exposure on one reactive Cys (Zmijewski *et al.*, 2010). Interestingly, oxidation of GSH has been shown to induce autophagy in the absence of other stimuli (Desideri *et al.*, 2012), thus indicating that Cys thiol oxidation could have an important function in regulating the autophagy process. Other proteins involved in autophagy activation have been suggested to be regulated by ROS, such as the ubiquitin-like Atg3, Atg7 and Atg10 (Filomeni *et al.*, 2010). Among these, also the selective autophagy receptor p62 has been noted since its ZZ-type zinc finger domain, containing several Cys residues, could provide redox sensitivity like other zinc finger-containing proteins (Giles *et al.*, 2003; Filomeni *et al.*, 2015).

In this chapter, we have for the first time shown that p62 can sense oxidation and can be covalently modified, most likely by cysteine oxidation and disulphide bond formation. Indeed, p62 formed HM weight species in non-reducing immunoblot analysis which were completely abolished by addition of a reducing agent such as β-ME (β-mercaptoethanol, which breaks disulphide bonds between the proteins), thus we have named these formations disulphide-linked conjugates (DLC) (**Figure 3.1B, 3.2A**). Importantly, no other selective autophagy receptors have been so far described to sense oxidation levels, a feature which could have an important role for p62 function in degrading autophagic cargoes. We have found that formation of p62 DLC is evident in aged mouse brain tissue, as well as in mammalian cell culture and

diseased human brain tissue, demonstrating the relevance of p62 modification both *in vivo* and *in vitro* (**Figure 3.1B, 3.2A, 3.8**).

Comparing young and old mouse brain tissue, we could not find differences in autophagy levels, nevertheless both oxidation stress (increased levels of Prx-SO_3) and proteostasis imbalance (increase in polyubiquitination) was evident in the old mice (**Figure 3.1A**). It has been shown previously that aged mouse brain tissue accumulates ubiquitinated proteins compared to young mice, especially in the cerebellum, which was not due to the elevation of the free ubiquitin pool (Ohtsuka *et al.*, 1995). In our case, we can assume that increased levels of oxidation would cause damage to proteins and drive their ubiquitination in aged brain tissue. Such mice also exhibited formation of p62 DLC sensitive to β-ME reduction (**Figure 3.1B**), suggesting that oxidation would be the signal involved in the process. Since p62 showed to accumulate in old mouse brain cerebellum (**Figure 3.1C**), we have hypothesised that DLC formation could lead to increased p62 aggregate formation, a feature that has only been associated with p62 self-oligomerisation mediated by its PB1 domain (Lamark *et al.*, 2003). The importance of p62 aggregation for its function in degrading ubiquitinated substrates is well established (Ichimura *et al.*, 2008; Itakura and Mizushima, 2011), thus our hypothesis would mean a stronger response of p62 during oxidative stress conditions, in order to accumulate toxic proteins and dispose them through autophagy.

We confirmed that p62 DLC were induced by oxidation by employing H_2O_2 and PR-619 (which showed to be a strong oxidiser) in mammalian cell culture, specifically in HeLa cells and HEK293E (**Figure 3.2A**, **3.6A**). Both treatments showed to induce p62 shift towards HM weights, while autophagy inhibition predominantly increased monomeric p62 levels. H_2O_2 induced p62 DLC transiently (**Figure 3.5A**), while PR-619 produced a much stable response over time (**Figure 3.5B**). Additionally, oxidative stress and DLC formation increased p62 insolubility and induced aggregate formation, again suggesting that both oxidation and p62 aggregation could be interconnected (**Figure 3.3**).

Regarding the size of p62 DLC, they appeared at ~180-250 kDa, potentially resembling a trimer and a tetramer of p62 proteins. At the same time, other proteins that could covalently bind p62 could not be excluded, which would explain why oxidation of purified GST-p62 led to different DLC size (**Figure 3.2D**). Unfortunately, we were unable to purify p62 DLC to assess whether other proteins would be involved in the process, as the DLC appeared to "stick" to the purification beads (**Figure 3.7**). Especially following PR-619 treatment, the DLC were often accumulating at much higher MW, up in the stacking gel. It is therefore possible that DLC could drive p62 oligomerisation through Cys residues, a first step in allowing p62 aggregate formation during oxidative stress conditions. Additionally, the shift from the soluble to the insoluble fraction following oxidation suggests that p62 DLC may lead to the formation of insoluble protein aggregates (**Figure 3.3B**). It is also important to notice that monomeric p62 tended to disappear following high levels of oxidative stress (i.e. using high amounts of H_2O_2 and PR-619), as if the majority of the protein would react to the oxidising environment and produce DLC (cf. **Figure 3.2A, 3.5B, 3.6B**). Such reduction in p62 monomeric levels have been previously described following incubation of purified GST-p62, together with the concomitant accumulation of p62 high MW and intracellular aggregates (Paine *et al.*, 2005). These spontaneous aggregates were in fact p62 β-sheet fibrils resembling those of α-synuclein and β-amyloid, demonstrating that p62 has aggregation-prone properties which are important for substrates sequestration and cell survival (Paine *et al.*, 2005). In a similar manner, p62 DLC could be important for aggregate formation under conditions of oxidative stress, leading to the degradation of damaged substrates.

Additionally, high MW species of p62 have been previously shown during cellular ageing, where the levels of monomeric p62 seemed to decrease while SDS-resistant polymers would accumulate (Gamerdinger *et al.*, 2009). The authors hypothesised that these polymers of p62 could represent inclusion bodies of aggregated proteins, which were enhanced due to the increased activity of autophagic degradation to maintain the protein quality control (Gamerdinger *et al.*, 2009). Instead, we argue that p62 DLC are solely dependent on oxidative stress. More recently, covalently-crosslinked oligomers of p62 have been shown to be induced by singlet oxygen, a

type of ROS where electrons have been rearranged in the oxygen atom (Donohue *et al.*, 2014). The authors also showed that such high MW species of p62 were present in aged cells and could be produced by purified GST-p62, similarly to what we have shown in our lab (Donohue *et al.*, 2014). Nevertheless, the authors concluded that crosslinked p62 would lead to the impairment of autophagy and autophagosome formation, while we suggest that p62 DLC would be important for aggregate formation and subsequent autophagic degradation of substrates.

In order to further confirm the role of oxidation in p62 DLC formation, we blocked the peroxiredoxin/thioredoxin (Prx/Trx) antioxidant system by using two inhibitors of Trx reductase (TrxR), curcumin and auranofin (**Figure 3.6B**). Both compounds showed to increase p62 DLC formation, suggesting that p62 is constantly reduced by TrxR and starts producing DLC once the redox buffering system is saturated (e.g. during high levels of oxidation). Inactivation of Prx by high levels of oxidative stress has been previously shown to be important for Trx to act on other oxidised substrates (Day *et al.*, 2012). Thus, increased in Prx-SO_3 and decreased Prx-3 dimers following high levels of H_2O_2 (**Figure 3.6**) could indicate a similar scenario, where p62 DLC would become targets of TrxR action. This result further supports our hypothesis that p62 senses oxidation and forms DLC during oxidative stress conditions.

Finally, we looked into human diseases to investigate whether p62 DLC were also relevant in a wider context of neurodegeneration. Thus, we analysed human brain tissue affected by several NDs, such as Alzheimer's disease (AD), frontotemporal dementia (FTD), dementia with Lewy bodies (DLB), Parkinson's disease (PD) and amyotrophic lateral sclerosis (ALS), comparing them to healthy age-matching controls (**Figure 3.8**). In all NDs cases we could find accumulation of monomeric p62, suggestive of autophagic impairment. As mentioned earlier, autophagy dysfunction has been connected to ageing and neurodegeneration, although there has been also evidence of enhanced autophagy during ageing (Wohlgemuth *et al.*, 2010; Rubinsztein *et al.*, 2011). Such discrepancy might be due to difficulties in addressing a dynamic process like autophagy with simple "snapshots" of activity (Narita, 2010). Unfortunately, we were not able to detect LC3-II in our samples (**Figure 3.8A**), a difficulty that has been previously reported (Yang *et al.*, 2011; Klionsky *et al.*, 2016).

Nevertheless, we were able to detect higher levels of Prx-SO_3 in the diseased samples, indicating the presence of oxidative stress in the analysed NDs (**Figure 3.8A**). Strikingly, the tissue affected by NDs showed accumulation of p62 DLC compared to the healthy controls, which could be therefore correlated with the higher levels of oxidation (**Figure 3.8**). However, p62 DLC presence could also be dependent on the accumulation of monomeric p62, which might depend on autophagy impairment. We propose that both autophagy impairment and oxidative stress in NDs cause accumulation of p62 and formation of DLC, enhancing the aggregation of misfolded ubiquitinated proteins and their sequestration into less harmful inclusions. In such a scenario, the therapeutic induction of autophagy and subsequent degradation of protein aggregates could have positive effects and slow the progression of NDs as previously hypothesised (Rubinsztein *et al.*, 2012).

Chapter 4. Two Cysteine Residues of p62 are Critical for DLC Formation

4.1 Introduction

In Chapter 3, we have identified a new mechanism of oligomerisation of p62 through disulphide-linked conjugates (DLC) triggered by oxidative stress. DLC of p62 were detected in old mouse brain tissue which appeared to have increased levels of oxidation. Additionally, the possibility of inducing the formation of p62 DLC in mammalian cells by means of hydrogen peroxide (H_2O_2) and PR-619 (having proved to be a strong oxidiser) also accredited the oxidation-sensing rationale. The main hypothesis for the formation of DLC was that cysteine (Cys) residues in the p62 molecule were involved in this process. In fact, Cys residues can sense oxidation by modifications of their thiol (SH) group, which becomes oxidised forming a sulphenic acid (SOH) leading to disulphide bonds formation (Poole *et al.*, 2004). Since DLC were disrupted in the presence of a reducing agent like β-mercaptoethanol (β-ME), we have hypothesized that the DLC could be dependent on oxidation of specific redox-sensitive Cys residues in p62 protein, which could subsequently form disulphide bonds through their thiol groups. In this chapter, we sought to identify which region of p62 was involved in DLC formation, in order to identify the Cys residues involved in the process.

4.2 Results

4.2.1 Production of p62 deletion constructs

In order to understand which particular region of p62 was implicated in the formation of DLC, we performed molecular cloning of different p62 fragments in a pEGFP-C2 vector to produce deletion constructs of p62 (**Figure 4.1**) (see **Section 2.6**, **Appendix A, B, C**). Therefore, the encoded fusion proteins contained the GFP protein (27 kDa) attached to the N-terminal of p62. The rationale of using a GFP-tagged p62 was to investigate the effects of the expression of deletion constructs also by live cell imaging, although we later dismissed it. The GFP-p62 constructs were designed to include different domains of the p62 protein: full-length GFP-p62 (a.a. 1-440, 89 kDa), ΔUBAp62 (a.a. 1-385, lacking the C-terminal UBA domain, 69 kDa), 1-200p62 (including the PB1 and ZZ-zinc finger domains, 50 kDa), 1-122p62 (including the PB1 domain plus a neighbouring unstructured region, 41 kDa) and 114-440p62 (excluding the PB1 domain, 75 kDa).

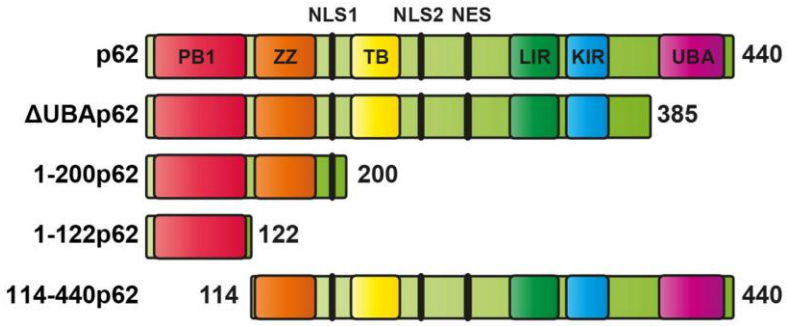

Figure 4.1 | Schematic representation of p62 deletion constructs produced in this study. Deletion constructs of p62 were produced by performing PCR using the GFP-p62 construct as a template. The different p62 constructs were then ligated into a previously digested pEGFP-C2 plasmid. The different domains of p62 are represented in different colours.

4.2.2 The N-terminal fragment of p62 is necessary for DLC formation

Once the p62 deletion constructs were cloned, we used them to overexpressed GFP-p62 fusion proteins, focusing on the N-terminal fragment as it comprised the PB1 and the ZZ-zinc finger domains incorporating the majority of the Cys residues in p62 sequence (11 out of 14). Moreover, it has been already postulated that the ZZ-zinc finger domain of p62, rich in Cys residues involved in metal binding that may be redox regulated, could be important for sensing oxidation levels (Filomeni *et al.*, 2015).

HeLa cells were transfected with different GFP-p62 constructs showed in **Figure 4.1**, and treated with H_2O_2 and PR-619 to induce DLC formation (**Figure 4.2**). Interestingly, all the constructs were able to form DLC upon oxidation except for the 114-440p62 fragment (blot n. 5) which did not contain the PB1 domain (amino acids 4-102) and its flanking region (amino acids 103-114). The 1-122p62 fragment, comprising the PB1 domain and the flanking unstructured region, was essential for p62 redox-sensitivity, as it was required and sufficient for both the formation of DLC and the preservation of monomeric p62 (blot n. 4). On the contrary, the ZZ-zinc finger domain appeared not to be involved in p62 DLC formation although it contained several Cys residues (6 out of 14), since DLC were visible both in the presence and absence of this domain (cf. blot 3 and 4). Also the UBA domain, lacking in Cys residues, did not seem to participate in the production of DLC (blot n. 2), suggesting that the binding to ubiquitin was not important in the process.

These results suggested that the N-terminus of p62 alone, containing the PB1 domain and the unstructured neighbouring region, was likely to be involved in DLC formation upon oxidation, while other fragments of the protein were not essential for the process.

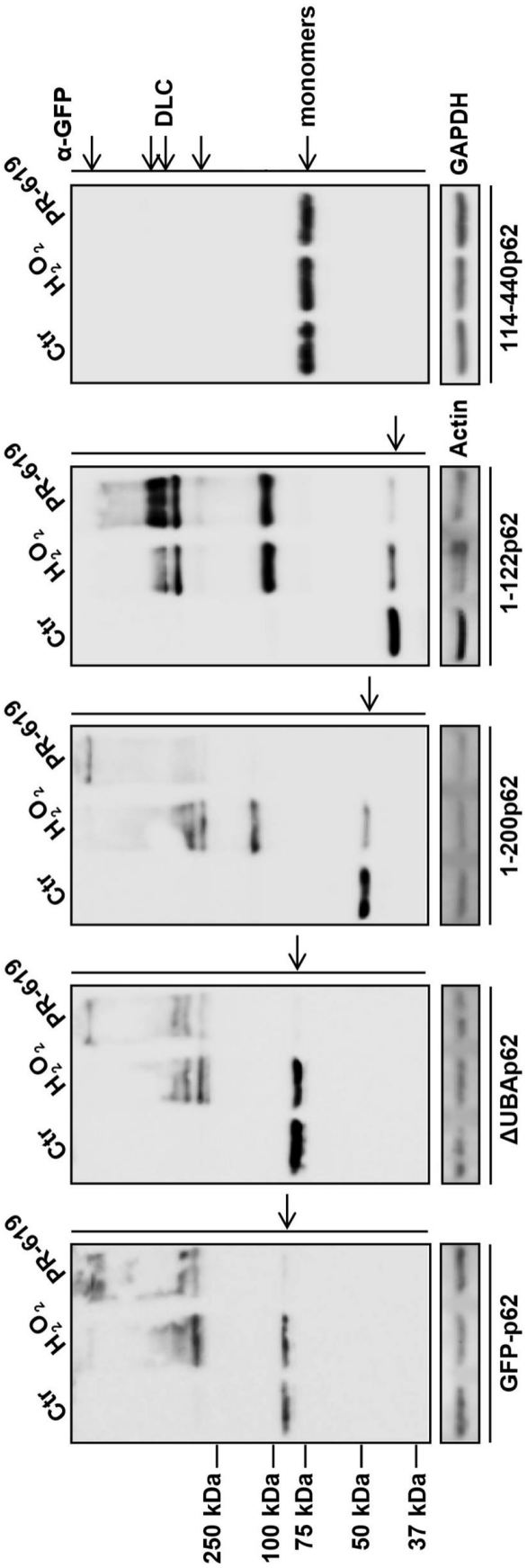

Figure 4.2 | The N-terminal fragment of p62 is required for DLC formation. HeLa cells were transfected with different GFP-tagged p62 constructs, treated with H_2O_2 (1 mM, 1 min) or PR-619 (20 µM, 10 min) and subjected to immunoblot analysis for GFP-tagged p62. Actin and GAPDH were used as loading controls. Arrows represent monomeric and DLC p62. Data are representative of at least two independent experiments.

4.2.3 Two cysteine residues in the p62 N-terminus are conserved in vertebrates

Since the N-terminal fragment of p62 appeared to be essential for DLC production, we hypothesised that the Cys residues contained in the 1-122 fragment would be involved in sensing oxidative stress. Unexpectedly, the Cys residues in the ZZ-zinc finger domain, which are conserved throughout the metazoa, seemed not to be participating in DLC formation (cf. **Figure 4.2**), although their potential sensitivity to ROS has been postulated (Filomeni *et al.*, 2015).

Hence, we performed a multiple alignment of p62 sequences (a.a. 1-175) from 30 different species (cf. **Table 2.12**) using the software ALINE (Bond and Schuttelkopf, 2009), in order to compare the levels of conservation of the Cys residues between the p62 N-terminus fragment (1-122) and the ZZ domain (**Figure 4.3**). The analysis showed that the three Cys in the PB1 domain (positions 26, 27 and 44) did not show a high degree of conservation among the chosen species. Interestingly, two Cys residues (positions 105 and 113, green boxes) in the unstructured region (a.a. 103-125) flanking the PB1 domain, unexpectedly showed a higher degree of conservation among species. Notably, these two Cys residues were surrounded by a considerable amount of amino acids with charged side chains, such as Lys (+), Arg (+), His (+), Asp (-) and Glu (-), hence they could have been sensitive to the charged environment. However, both C105 and C113 were missing in invertebrates (*D. melanogaster* and *C. elegans*) but present only in vertebrates, suggesting that C105 and C113 appeared later in evolution. As expected, all six Cys residues lying in the ZZ domain (positions 128, 131, 142, 145, 151 and 154) were all conserved in both vertebrates and invertebrates. Since C105 and C113 were the only conserved Cys residues lying in the N-terminal of p62 which was essential to produce DLC, we hypothesised that they could be redox-regulated.

In summary, our analysis showed that two Cys residue, C105 and C113, lying in an unstructured region between PB1 and ZZ domains, exhibited a high degree of conservation among vertebrates but were missing in invertebrates.

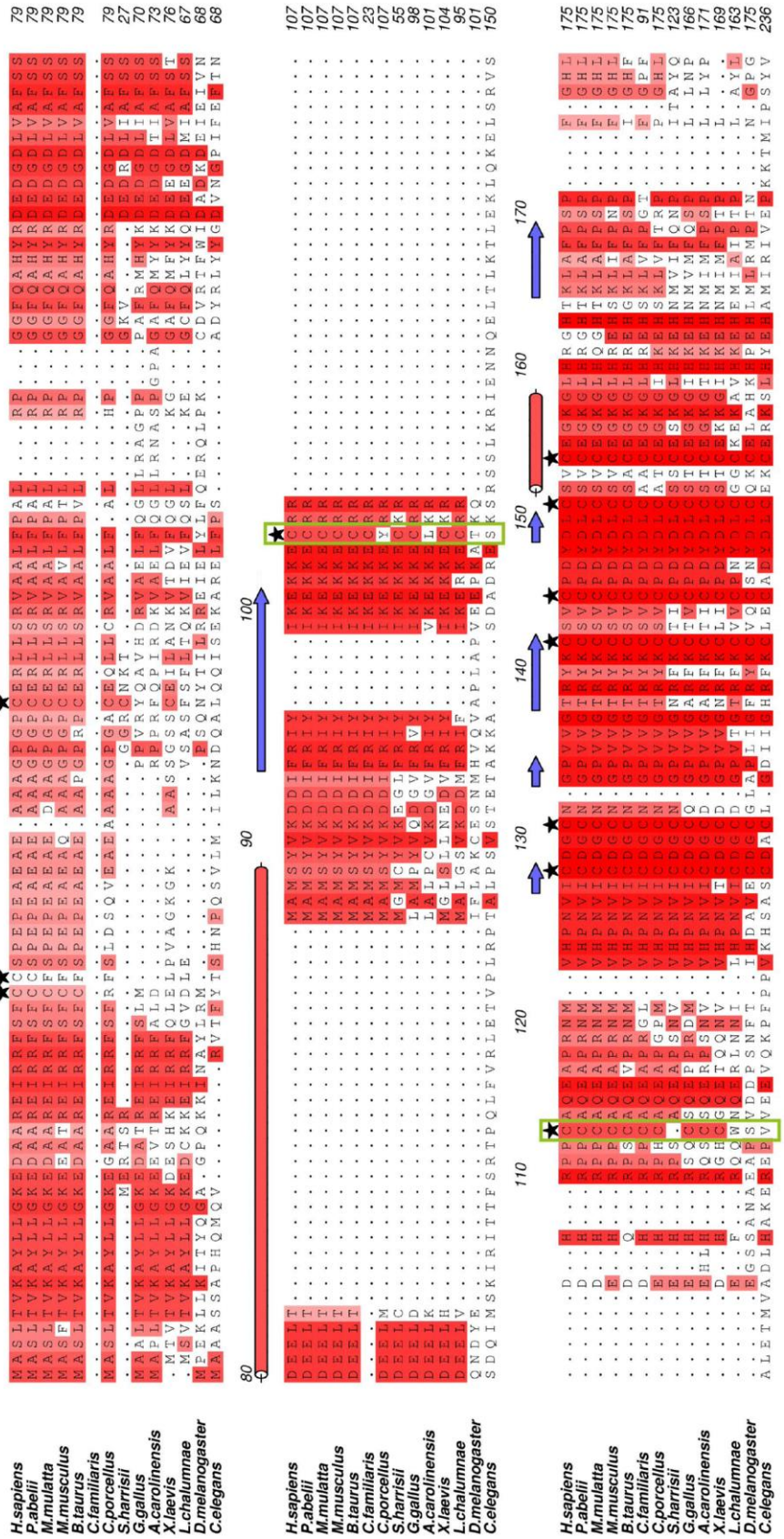

Figure 4.3 | Multiple alignment of p62 sequences shows a high degree of conservation of C105 and C113 in vertebrates. A multiple alignment of p62 N-terminus (a.a. 1-175) was performed in 30 different species (showing only 14) using the protein-sequence alignment editor ALINE. Increasing conservation of amino acid residues is shown by light-to-dark red. Cysteine residues are indicated by stars; C105 and C113 are highlighted by green boxes. Predicted ordered regions are indicated by lines above the sequence alignment with β-sheets and α-helixes shown as blue arrows and red cylinders, respectively. PB1 domain: a.a. 4-102; ZZ domain: a.a. 126-168. The work was carried out by Dr Graham Smith at Newcastle University.

4.2.4 Cysteine residues C105 and C113 are important for p62 DLC formation

To test our hypothesis whether the Cys residues in the N-terminus of p62 (PB1 domain and the flanking unstructured region) were effectively sensing ROS and playing a role in DLC formation, we performed single Cys-to-Ala site-directed mutagenesis on the full-length GFP-tagged p62, specifically on positions 26, 27, 44, 105, and 113.

Each single mutant was then expressed in HeLa cells, following treatments with H_2O_2 and PR-619 to induce p62 oxidation and immunoblot analysis (**Figure 4.4A**). The ratio between DLC and monomeric p62 was quantified and normalised to the wild-type GFP-p62 (**Figure 4.4B**). Although it was possible to detect some differences in the amount of p62 protein that was shifting toward higher MW, none of the p62 single mutants were able to prevent the formation of DLC. However, C105A and C113A mutants seemed to develop slightly lower levels of DLC, as well as preserving the monomeric form of p62 from shifting to higher MW. Notably, the C113A mutant produced less DLC compared to the C105A mutant. This result showed that Cys residues in p62 sequence were indeed involved in sensing oxidative stress, specifically the C105 and C113 that appeared to be conserved in our alignment analysis (cf. **Figure 4.3**).

In short, Cys-to-Ala single mutagenesis in the p62 N-terminus showed that C105 and C113, located in the unstructured region ahead of the PB1 domain, were involved in DLC formation upon oxidation.

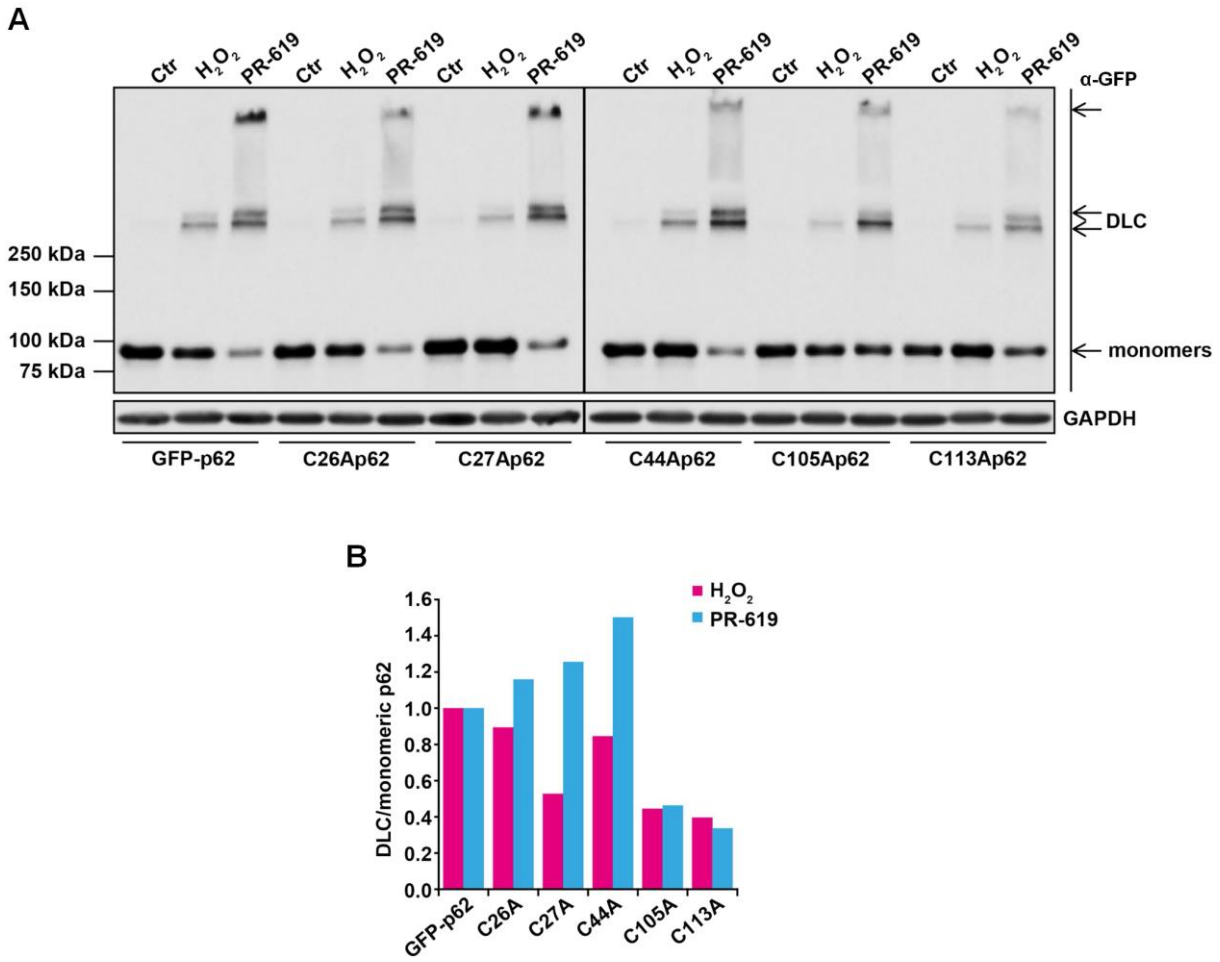

Figure 4.4 | Single mutagenesis of C105 and C113 of p62 reduces DLC formation. (A) HeLa cells were transfected with GFP-tagged wild-type or different p62 mutants as shown, treated with H_2O_2 (1 mM, 1 min) or PR-619 (10 μM, 10 min) and subjected to immunoblot analysis for GFP-tagged p62. GAPDH was used as a loading control. Arrows represent monomeric and DLC p62. **(B)** The ratio between DLC and monomeric p62 was quantified and normalised to the wild-type GFP-p62. Data are representative of at least two independent experiments, while quantification represents *n*=1.

4.2.5 Double mutation of C105A and C113A dramatically reduces p62 DLC formation

Since the C113A mutant of p62 seemed to produce less DLC among the other p62 N-terminal mutants (cf. **Figure 4.4**), we selected it as a template for a second round of Cys-to-Ala site-directed mutagenesis. In our prediction, the double mutation of the two conserved Cys residues C105 and C113 would have led to the loss of p62 redox sensitivity. We also employed the well-characterised K7A,D69A double mutant of p62, known to disrupt the ability of the PB1 domain to self-oligomerise (Lamark *et al.*, 2003), in order to understand whether PB1-mediated aggregation was important during oxidation and DLC formation.

The double mutants of p62 were then expressed in HeLa cells, treated with H_2O_2 and PR-619 to induce oxidation and analysed by immunoblot (**Figure 4.5A**). The ratio between DLC and monomeric p62 was quantified and normalised to the wild-type GFP-p62 (**Figure 4.5B**). All Cys double mutants of p62 showed a reduction of DLC formation or a preservation of the monomeric form of p62 since they all contained the C113A mutation affecting DLC formation (cf. **Figure 4.4A**). Strikingly, the C105A-113A double mutant dramatically reduced the levels of DLC formation, although without abolishing them completely. This result was in accordance with our hypothesis that the two conserved Cys residues C105 and C113 would have a primary role in DLC formation. However, residual presence of p62 DLC was still evident after substitution of the two Cys residues, suggestive of redundancy between the Cys residues along p62 sequence. Interestingly, the K7A,D69A double mutant of p62 did not show any changes in the formation of DLC compared to the wild-type, demonstrating that the self-oligomerisation of p62 mediated by non-covalent interactions was not important in the formation of DLC during oxidative stress.

In summary, the Cys residues C105 and C113 in the N-terminal of p62 were crucial in DLC formation but not indispensable for the process. Instead, the PB1-mediated oligomerisation of p26 was not contributing to DLC production during oxidative stress.

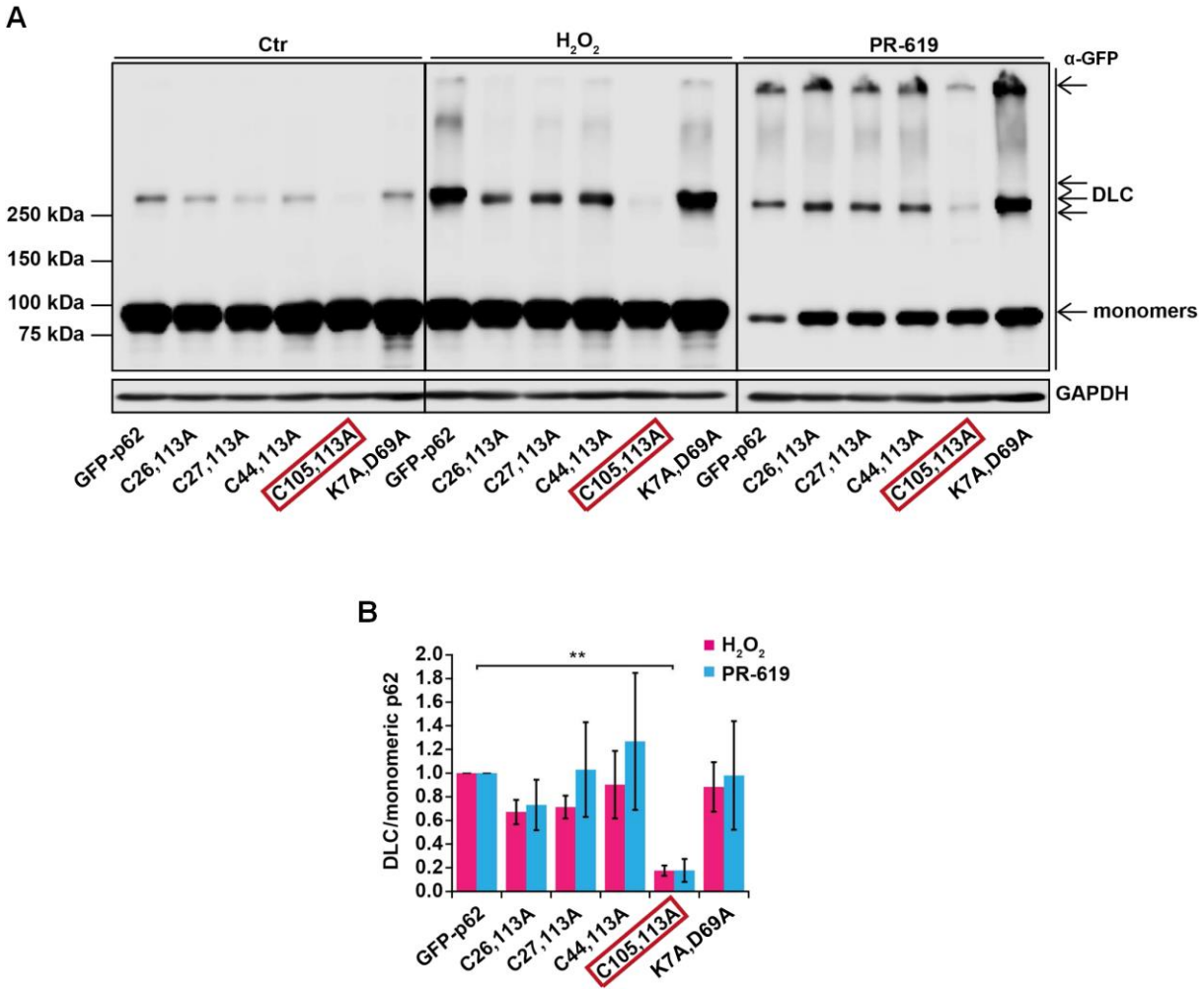

Figure 4.5 | Cysteine residues C105 and C113 of p62 are crucial for DLC formation. (A) HeLa cells were transfected with GFP-tagged wild-type or different p62 mutants as shown, treated with H_2O_2 (1 mM, 1 min) or PR-619 (10 μM, 10 min) and subjected to immunoblot analysis for GFP-tagged p62. GAPDH was used as a loading control. The C105,113A p62 double mutant is highlighted by red boxes. Arrows represent monomeric and DLC p62. **(B)** The ratio between DLC and monomeric p62 was quantified and normalised to the wild-type GFP-p62. Error bars represent s.e.m., n=3, $^{**}p<0.01$. Data are representative of at least three independent experiments.

4.2.6 Additional mutations in the PB1 domain of p62 do not further decrease DLC formation

Since the substitution of C105 and C113 did not lead to a complete loss of p62 DLC (cf. **Figure 4.5**), we sought to investigate whether other Cys residues in the N-terminus of p62 were implicated in DLC formation. As already mentioned, low remaining levels of DLC after C105 and C113 mutation could have been caused by neighbouring redundant Cys residues, hence additional mutation of Cys residues could have been needed to completely abolish p62 DLC.

To do so, we used the C105,113A p62 double mutant to perform a further round of Cys-to-Ala site-directed mutagenesis, specifically on positions 26, 27 and 44. The triple mutants of p62 were then expressed in HeLa cells, treated with H_2O_2 and PR-619 to induce oxidation and analysed by immunoblot (**Figure 4.6A**). The ratio between DLC and monomeric p62 was quantified and normalised to the wild-type GFP-p62 (**Figure 4.6B**). Although the reduction of DLC was evident in all triple mutants, none of them completely suppressed p62 DLC formation. Since the Cys residues in the PB1 domain did not appear to be conserved in our multiple-sequence alignment (cf. **Figure 4.3**), we hypothesised that more conserved Cys residues in p62 sequence would instead have been implicated in DLC formation, such as those present in the ZZ domain.

In summary, further mutations of Cys residues in the PB1 domain of p62 did not show a complete abolishment of DLC, suggesting that other Cys residues along p62 sequence could provide redundancy during oxidation.

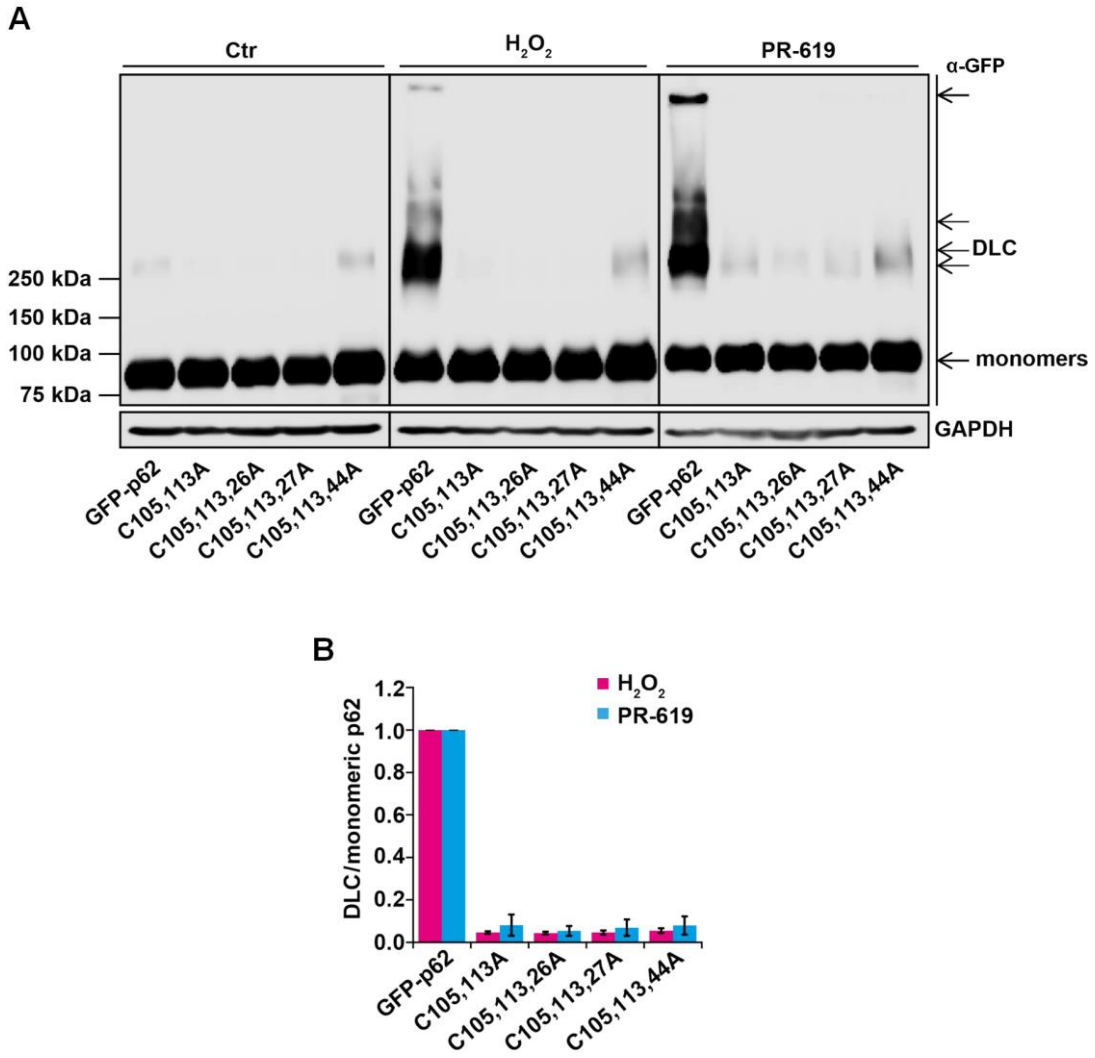

Figure 4.6 | Additional mutations in the N-terminus of p62 do not show reduction of DLC. (A) HeLa cells were transfected with GFP-tagged wild-type or different p62 mutants as shown, treated with H_2O_2 (1 mM, 1 min) or PR-619 (10 μM, 10 min) and subjected to immunoblot analysis for GFP-tagged p62. GAPDH was used as a loading control. Arrows represent monomeric and DLC p62. **(B)** The ratio between DLC and monomeric p62 was quantified and normalised to the wild-type GFP-p62. Error bars represent standard deviation, *n*=2. Data are representative of at least two independent experiments.

4.2.7 Additional mutations along p62 sequence lead to variability in DLC formation

Since the additional mutation of Cys residues in the PB1 domain did not completely suppress p62 DLC formation (cf. **Figure 4.6**), we decided to look at other Cys residues along p62 sequence. The ZZ domain of p62 contained several conserved Cys residues (cf. **Figure 4.3**) close to C105 and C113, which could have been playing a role in sensing oxidation through redundancy.

Hence, one more round of Cys-to-Ala site-directed mutagenesis was performed using the C105A-C113A p62 double mutant as a template, specifically on positions 131, 142, 145, 154, 289/290 and 331. Oxidation was induced with H_2O_2 and PR-619 after expressing the p62 mutants in HeLa cells, and the protein lysates were analysed by immunoblot (**Figure 4.7A**). The ratio between monomeric and DLC p62 was quantified and normalised to the wild-type GFP-p62 (**Figure 4.7B**). Although the new mutants did not show any significant decrease in DLC formation compared to the C105A-C113A, some mutations resulted in a higher development of DLC upon oxidation. The point-mutations implicated in this increase of DLC formation (C131A, C142A, C145A and C154A) involved the Cys residues located in the ZZ domain, which appeared to be the most conserved among the species we analysed (cf. **Figure 4.3**). One explanation could be that the substitution of such Cys residues would result in the destabilisation of the zinc finger, leading to the exposure of other Cys residues previously involved in the binding of the Zn^{2+} ions.

In short, additional mutations of Cys residues along p62 sequence did not suppress DLC formation. Instead, mutation of the conserved Cys residues in the ZZ domain induced an increase in DLC production, possibly due to the destabilisation of the zinc finger.

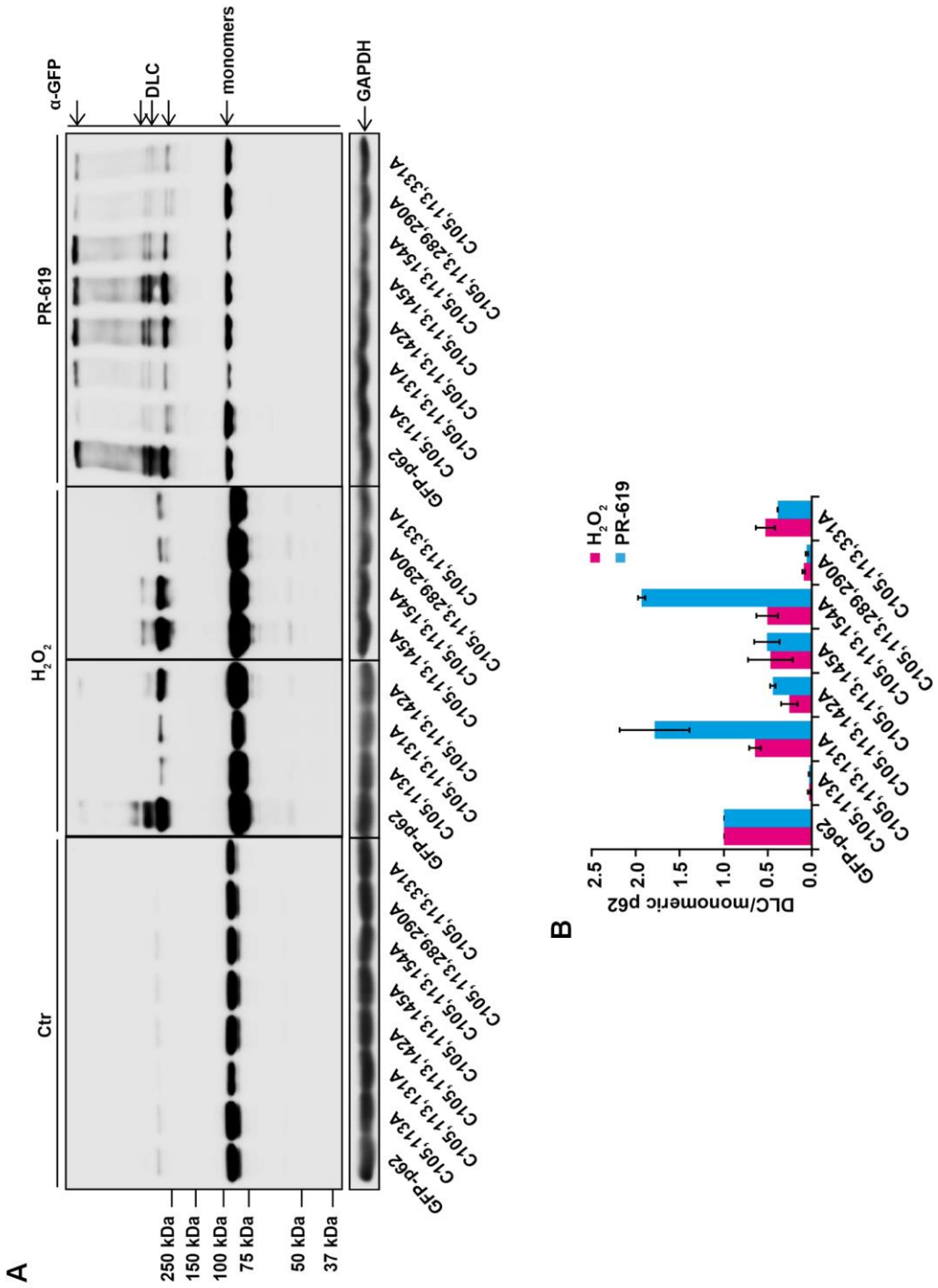

Figure 4.7 | Redundancy of cysteine residues of p62 leads to variability in DLC formation. (A) HeLa cells were transfected with GFP-tagged wild-type or different p62 mutants as shown, treated with H_2O_2 (1 mM, 1 min) or PR-619 (10 μM, 10 min) and subjected to immunoblot analysis for GFP-tagged p62. GAPDH was used as a loading control. Arrows represent monomeric and DLC p62. **(B)** The ratio between DLC and monomeric p62 was quantified and normalised to the wild-type GFP-p62. Error bars represent standard deviation, *n*=2. Data are representative of at least two independent experiments.

4.2.8 Single and double mutation of C105 and C113 in the N-terminal fragment of p62 determines loss of DLC formation

To avoid the participation of redundant Cys residues in the formation of DLC, we employed the N-terminal fragment of GFP-tagged p62 (a.a. 1-122, 42 kDa) and carried out single and double Cys-to-Ala mutagenesis of C105 and C113 residues. In this way, we could avoid the presence of conserved Cys residues in the ZZ domain which could also become available for DLC formation, although the three Cys residues in the PB1 domain were still present.

HeLa cells were transfected with N-terminal GFP-p62 mutants, treated with H_2O_2 and PR-619 and analysed by immunoblot (**Figure 4.8**). Notably, the DLC produced by the p62 N-terminal fragment started appearing at ~80 kDa, which resembled a dimer of p62 rather than a trimer or tetramer as we had found previously (cf. **Figure 3.2A**). As expected, the single mutation of C105 and C113 determined a decrease in the formation of DLC. Strikingly, the double mutation of the two Cys residues seemed to completely suppress p62 DLC formation, although a band slightly higher than the dimers was still visible. We could not define whether such band was an artefact or an actual DLC, since the Cys residues lying in the PB1 domain could have become available in the process. However the result further confirmed the importance of C105 and C113 in the formation of p62 DLC upon oxidation.

In summary, the double mutation of C105 and C113 in the N-terminal fragment of p62 showed to greatly impair DLC formation, although it was not clear whether such impairment was complete.

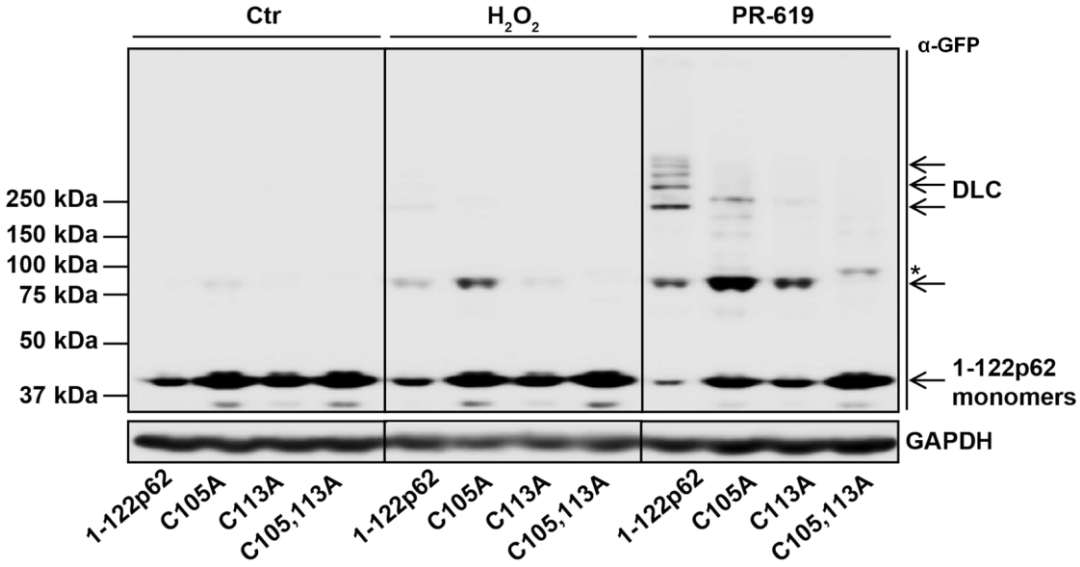

Figure 4.8 | Mutations of C105 and C113 in the N-terminal fragment of p62 suppress DLC formation. HeLa cells were transfected with GFP-tagged wild-type or different p62 mutants as shown, treated with H_2O_2 (1 mM, 1 min) or PR-619 (10 μM, 10 min) and subjected to immunoblot analysis for GFP-tagged p62. GAPDH was used as a loading control. Arrows represent monomeric and DLC p62. Data are representative of at least two independent experiments.

4.3 Discussion

Cysteine (Cys) residues have important roles in the regulation of proteins, as they can affect their structure and function (Cremers and Jakob, 2013). The high versatility of these residues is determined by their thiol groups (SOH), which often participate in enzymatic reactions as well as form disulphide bonds between different Cys residues (Paulsen and Carroll, 2010). In Chapter 3, we have found that p62 can sense oxidation by forming disulphide-linked conjugates (DLC), since they were sensitive to reducing agents. Thus, we wanted to determine which residues where involved in the formation of p62 DLC.

In this chapter, we have identified two Cys residues in p62 sequence which appeared responsible for DLC formation during oxidative stress conditions. By producing different deletion constructs of p62 (**Figure 4.1**), we found that the N-terminus of p62 (a.a. 1-122) was essential for DLC formation (**Figure 4.2**). Following Cys-to-Ala point-mutagenesis of p62, we have found that C105 and C113, located in an unstructured region between PB1 and ZZ domains, were mainly involved in the process (**Figure 4.4, 4.5**). However, mutagenesis of both C105 and C113 was not sufficient to completely suppress p62 DLC, suggesting the involvement of additional Cys residues. The subsequent mutation of other Cys residues in the N-terminus of p62 or along its sequence did not show any further inhibition of DLC formation (**Figure 4.6, 4.7**). However, several Cys-to-Ala substitutions in the ZZ domain paradoxically increased the tendency of p62 to form DLC (**Figure 4.7**). The substitution of both C105 and C113 in the N-terminal fragment of p62 (1-122p62) determined an almost complete loss of DLC formation, although we could not exclude the involvement of other Cys residues in the PB1 domain (**Figure 4.8**).

The ZZ-type zinc finger domain of p62 contains 6 conserved Cys residues engaged in coordinating two Zn^{2+} ions, whose involvement in redox sensitivity has been previously suggested (Filomeni *et al.*, 2015). It could be possible that the mutagenesis of certain Cys residues in the ZZ domain could induce the destabilisation of the zinc finger and the subsequent exposure of metal-binding Cys

residues, which would then become available to form disulphide bonds in place of C105 and C113. Thus, we can hypothesise a redundancy in Cys residues which can become involved in DLC formation following modifications in p62 structure. In a similar manner, redundancy of Lys residues involved in ubiquitination in different proteins has been suggested to take place following Lys mutagenesis (Fung *et al.*, 2005; Li *et al.*, 2012a; Guharoy *et al.*, 2016). Thus, the precise site of ubiquitination in proteins is generally overlooked, since multiple Lys residues can become ubiquitin acceptors in the absence of the typical ubiquitination sites (King *et al.*, 1996).

A way to overcome this redundancy could be the substitution of all the 14 Cys residues in p62 sequence and the subsequent reintroduction of C105 and C113. In this way, we could assess whether the sole presence of these two residues is sufficient for DLC formation. The following reintroduction of other Cys residues would then clarify the presence of additional residues involved in the process. Several studies have employed Cys-less mutant proteins in order to understand their structures and functions, indicating the efficacy of such approach (Loo and Clarke, 2006; Arendt *et al.*, 2007; Nishi *et al.*, 2008). Interestingly, the production of a Lys-less protein mutant has also been employed in order to completely abolish its ubiquitination (Li *et al.*, 2012a), again suggesting the similarity between Cys and Lys residues redundancy and a common route to overcome the issue. Alternatively, the genetic deletion of the linker region between PB1 and ZZ domains of p62 could provide the means to assess the importance of this unstructured region in sensing oxidative stress.

We have also analysed the K7A,D69A double mutant of p62, which lacks the ability to self-oligomerise via the PB1 domain (Lamark *et al.*, 2003), and found that formation of DLC was not affected by the mutation (**Figure 4.5**). This would suggest that self-oligomerisation of p62 is not necessary for DLC formation. By contrast, a recent study has shown that K7A,D69A mutant p62 could not form high-molecular crosslinks, suggesting that p62 crosslinking would be dependent on its self-oligomerisation (Donohue *et al.*, 2014). Since the authors induced p62 crosslinks with the autophagy inhibitor verteporfin, we can hypothesise that such treatment would have different effects on the ability of p62 to form DLC.

Our multiple alignment analysis of p62 sequences in different organisms has shown a high degree of conservation of C105 and C113, although they were not found in invertebrates such as *D. melanogaster* and *C. elegans* (**Figure 4.3**). Both residues are located in a linker region predicted to be natively unstructured due to the high presence of polar, charged amino acids (Romero *et al.*, 2001; Vucetic *et al.*, 2003). Disordered regions are very common in proteins, and despite their functional role has been overlooked for a long time, they have been shown to be involved in important processes such as cell signalling, regulation and molecular recognition (Dunker *et al.*, 2005; Uversky *et al.*, 2005). Thus, we propose that p62 DLC formation could be a protective mechanism against oxidative stress acquired later in evolution with important consequences for p62 function, such as aggregate formation and autophagy induction.

Due to the high reactivity of their thiols, Cys residues are not very abundant in proteins, showing a lower frequency of appearance during evolution compared to other amino acids, and tend to be very conserved (Miseta and Csutora, 2000). Thiols reactivity depend on their pK_a (acid dissociation constant), which represents the tendency of losing a hydrogen atom and form the thiolate ion (S^-), a strong nucleophile (Roos *et al.*, 2013). Charged and uncharged polar amino acids in the vicinity of Cys residues can strongly influence thiols reactivity by producing hydrogen bonds, which reduce the pK_a by stabilising the thiolate ion (Snyder *et al.*, 1981; Billiet *et al.*, 2012; Roos *et al.*, 2013). Interestingly, residues C105 and C113 are located in close proximity to electrically-charged as well as polar uncharged amino acids, all showing high degree of conservation among different species (**Figure 4.2**). Notably, C105 is surrounded by both positively- (K102, K103, R106 and R107) and negatively-charged (E101 and E104) residues. Also, one negative (D108) and two positive (H109 and R110) residues are located between C105 and C113, while one uncharged polar (Q115) and one negative (E116) residues are located right after C113. Thus, it is possible that the vicinity of C105 and C113 to these charged polar residues could lower their pK_a, resulting in increased thiols reactivity and disulphide bond formation during oxidative stress conditions.

Additionally, perturbations in the ionic environment can lead to changes in thiols reactivity, thus impacting on the ability of Cys residues to form disulphide bonds (Cremers and Jakob, 2013; Roos *et al.*, 2013). Recently, a charge-reversal mutant of p62 (R106E/R107E) has been employed in order to destabilise the assembly of PB1 filaments of p62, determining the formation of larger aggregates than wild-type p62 (Ciuffa *et al.*, 2015). In fact, the authors identified the unstructured region flanking the PB1 domain as an electrostatic bridge, whose role is crucial for the correct formation of PB1 filaments and ultimately p62 aggregates (Ciuffa *et al.*, 2015). In a similar manner, mutations of charged amino acids in the vicinity of C105 and C113 could have an impact onto the stability of p62 DLC, as well as on its ability to form polyubiquitinated aggregates.

Interestingly, a charge-reversal heterozygote mutation of p62 (K102E) has been identified in a sporadic amyotrophic lateral sclerosis (SALS) case, associated with large round p62 inclusions in neurons affected by the disease (Teyssou *et al.*, 2013). Evidence from our lab have shown that overexpression of p62 K102E mutant impaired DLC formation following oxidative stress (unpublished), thus suggesting the important role of charged residues in regulating the reactivity of C105 and C113 and the potential importance of DLC formation in protein homeostasis and neuronal survival.

Chapter 5. Formation of DLC is Important for p62 Function in Autophagy

5.1 Introduction

In the previous chapter, we have identified two cysteine (Cys) residues of p62, C105 and C113, which were found to be required for its ability to sense oxidation and form DLC. Such Cys residues, lying in an unstructured region between PB1 and ZZ domains, appeared to be highly conserved in vertebrates but not in invertebrates, suggesting that the ability of p62 in sensing oxidative stress might have been acquired later in evolution. Since p62 oxidation seemed to contribute to aggregate formation (cf. **Figure 3.3**), we wanted to understand whether the double Cys mutant of p62 would not only impair DLC formation but also aggregation of p62 and its substrates. It is known that p62 aggregation is a crucial step for its function as a selective autophagy receptor (Ichimura *et al.*, 2008; Itakura and Mizushima, 2011), which leads to a tighter interaction with the autophagy marker LC3 (Wurzer *et al.*, 2015). Thus, we hypothesised that the loss of the oxidation-sensing properties of p62 would also impair its ability to form aggregates and drive cargos to degradation. In this chapter we analysed the relevance of p62 oxidation to its function as an autophagy receptor protein, and investigated whether the loss of DLC formation would impact on protein degradation and cell survival during oxidative stress conditions.

5.2 Results

5.2.1 Production and validation of FLAG-p62 stable cell lines

To investigate the role of C105 and C113 in p62 function as receptor for selective autophagy, we used *p62*$^{-/-}$ (knock-out) mouse embryonic fibroblasts (MEFs) to stably express either wild-type or Cys mutant p62, in order to avoid the presence of endogenous p62 and instead focus on the effect of the p62 oxidation-insensitive mutant compared to the wild-type protein.

Thus, we performed lentiviral transduction to stably introduce a transgenic FLAG-tagged p62, either wild-type or C105A-C113A mutant in *p62*$^{-/-}$ MEFs (**Figure 5.1A**). To do so, we transfected the VSV-G (vesicular stomatitis virus G glycoprotein, used to amplify the host range due to its wide infectivity) (Burns *et al.*, 1993) and packaging plasmids plus the FLAG-tagged p62 transgenes (or empty vector) in HEK293FT (human embryonic kidney) cells (optimised for virus production), in order to produce and concentrate the lentivirus containing p62 transgenes. The virus particles were then used to infect *p62*$^{-/-}$ MEFs, integrating the viral genome into the cells. Transduced cells were then selected with antibiotics until their expansion. The presence of the FLAG-p62 transgene in the stable cell lines was then confirmed by immunoblot, although it showed lower levels of expression compared to the endogenous p62 from wild-type MEFs (Hewitt *et al.*, 2016). To validate the effect of the C105A-C113A mutation in the stable cell lines, we induced oxidation with H_2O_2 and PR-619 and performed immunoblot analysis (**Figure 5.1B**). As expected, the formation of DLC in the FLAG-C105,133Ap62 cell line was greatly reduced compared to FLAG-p62 wild-type, although DLC were not completely suppressed, similarly to what we have seen in HeLa cells after overexpression of the GFP-p62 double mutant (cf. **Figure 4.5**).

In short, we produced stable cell lines expressing FLAG-p62 and FLAG-C105,113Ap62 in order to investigate the effects of the double Cys mutation on p62 function during oxidative stress.

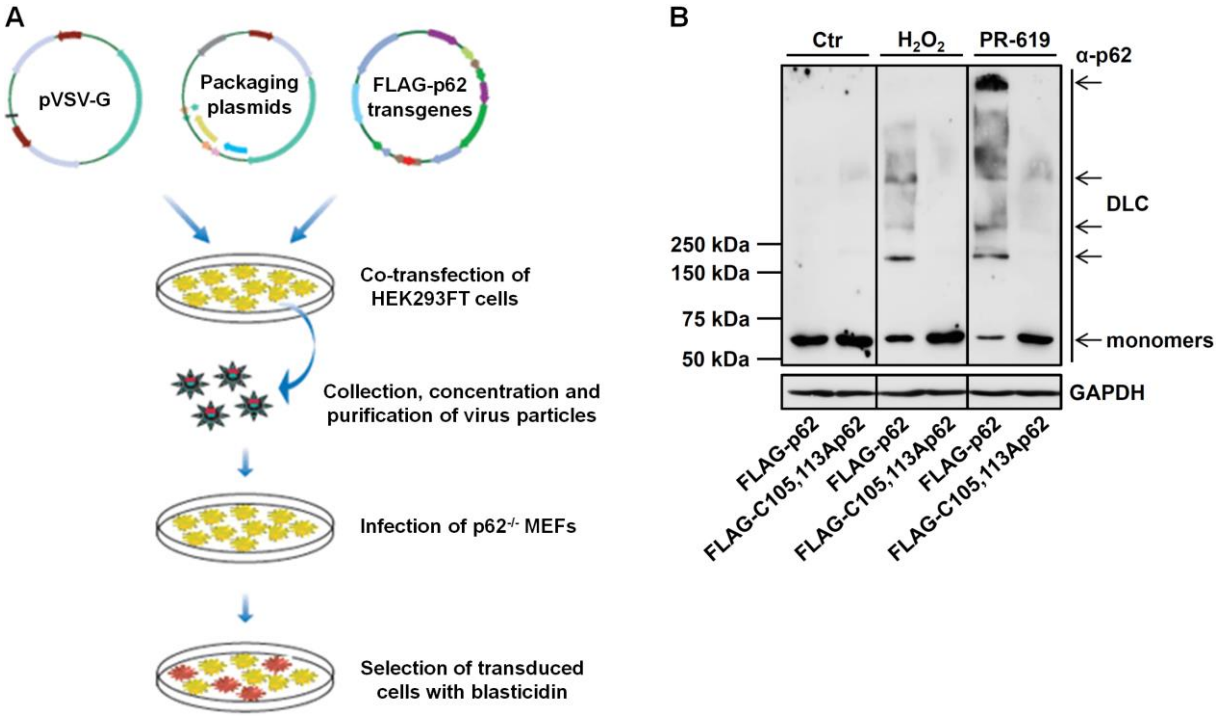

Figure 5.1 | Stable cell lines produced and validated in this study. (A) Schematic representation of the lentivirus packaging and transduction protocol followed to produce stable cell lines used in this study. Adapted from www.biocat.com. **(B)** *p62*$^{-/-}$ MEFs stably expressing either wild-type or C105,113A FLAG-p62 were treated with H_2O_2 (1 mM, 1 min) or PR-619 (10 μM, 10 min) and immunoblotted for p62 in non-reducing conditions. GAPDH was used a loading control. Arrows represent monomeric and DLC p62. Data are representative of at least two independent experiments.

5.2.2 Mutation of C105 and C113 of p62 determines impaired formation of insoluble aggregates

After producing the stable cell lines, we sought to investigate whether the double Cys mutation of p62 would impair not only the formation of DLC but also the function of p62 as a receptor for selective autophagy. We previously showed that oxidation increased the formation of p62 aggregates in HeLa cells (cf. **Figure 3.3A**), and that formation of DLC was also correlated with the shift of p62 from the soluble to the insoluble fraction (cf. **Figure 3.3B**). It is known that the presence of p62 is necessary for the formation of polyubiquitinated aggregates (Komatsu *et al.*, 2007b; Korolchuk

et al., 2009), and that p62 aggregation is a crucial step for the degradation of substrates through autophagy (Bjorkoy *et al.*, 2005; Itakura and Mizushima, 2011). Thus, we investigated whether the loss of p62 sensitivity to oxidative stress through DLC formation would impact its ability to form polyubiquitinated aggregates.

Wild-type and C105,113A FLAG-p62 stable cells lines were treated with H_2O_2 and PR-619 to induce protein aggregation, stained for p62 and ubiquitin, analysed by confocal microscopy and the percentage of p62 aggregates quantified (**Figure 5.2A**). In control conditions, both cell lines showed a modest presence of protein aggregates. Following oxidative stress, a high increase in protein aggregates positive for p62 and ubiquitin was detected in the wild-type cell line. In contrast, formation of protein aggregates in the C105,113A mutant cell line was significantly impaired compared to the wild-type, suggesting that the loss of DLC would impact on the ability of p62 to form polyubiquitinated aggregates.

To further confirm the role of oxidation and DLC in protein aggregates, we performed ultracentrifugation to separate the soluble from the insoluble fraction following treatments with H_2O_2 and PR-619, and quantified the ratio between DLC and monomeric p62 in the insoluble fraction (**Figure 5.2B**). Similarly to what we had previously seen in HeLa cells (cf. **Figure 3.3A**), we could detect the accumulation of p62 DLC in the insoluble fraction of the wild-type cell line (lane 3 in both blots), although the effect of H_2O_2 was only moderate, again suggesting that oxidation of p62 increased its insolubility. On the contrary, the C105,113A mutant cell line did not show formation of DLC in either whole-cell or insoluble fraction following treatments (lane 6 in both blots), suggesting that the loss of the Cys residues sensitive to oxidation would impair p62 insolubility and formation of insoluble aggregates.

In summary, the loss of p62 sensitivity to oxidation was correlated with reduced formation of polyubiquitinated aggregates and protein insolubility, suggesting that the function of p62 in aggregating cargos for degradation was impaired.

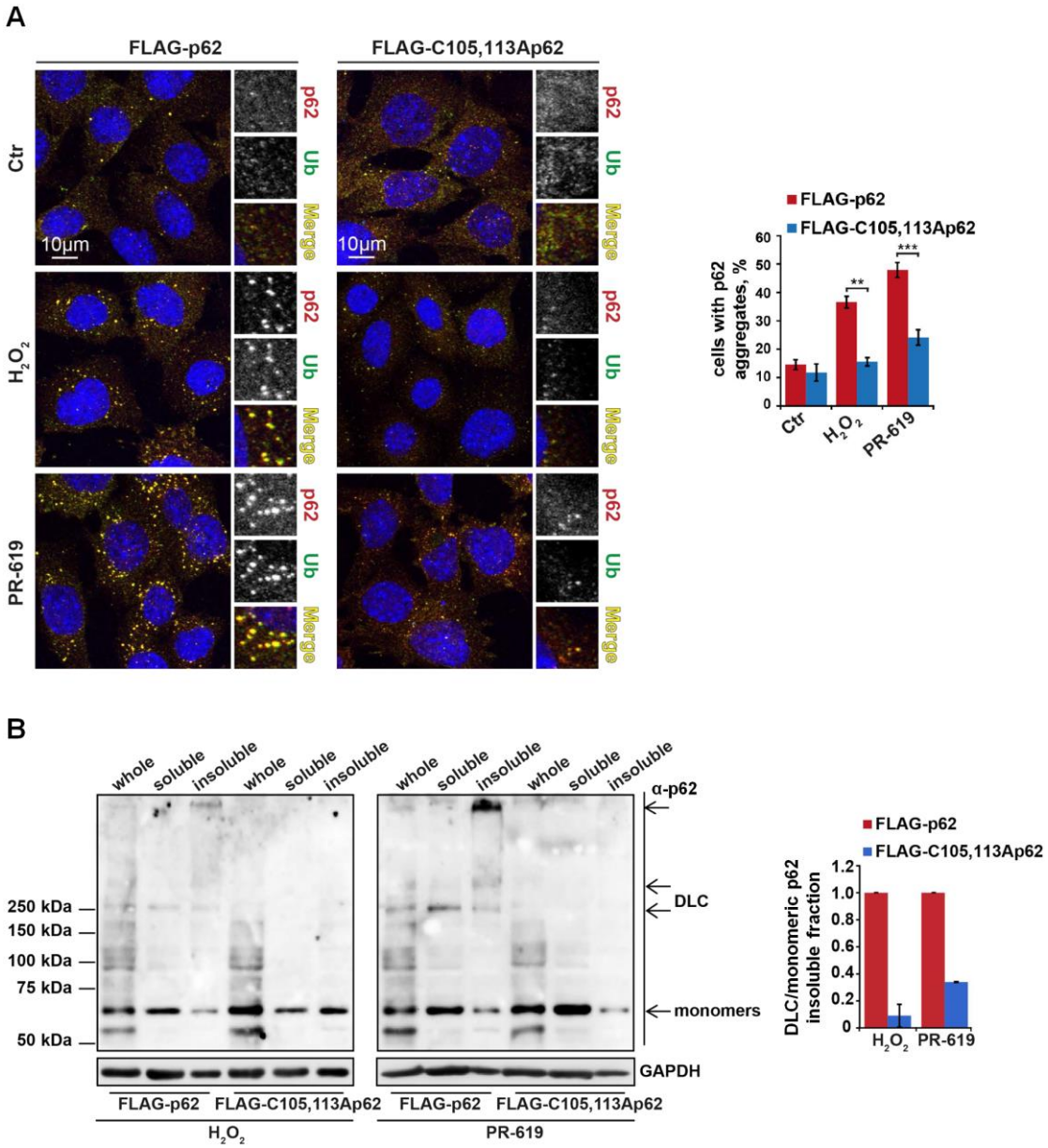

Figure 5.2 | Loss of p62 redox-sensitivity reduces the formation of insoluble aggregates. (A) *p62*$^{-/-}$ MEFs stably expressing FLAG-tagged wild-type or C105,113A p62 were treated with H_2O_2 (1 mM, 30 min) or PR-619 (5 µM, 30 min), immunostained for ubiquitin and p62 and analysed by confocal microscopy. Nuclei were stained with TO-PRO-3 iodide. Cells with positive aggregates for p62 were counted and their proportion quantified. Error bars represent s.e.m., $n=3$, $^{**}p<0.01$, $^{***}p<0.005$. Data are representative of at least three independent experiments. **(B)** Stable cell lines as in (A) were treated with H_2O_2 (5 mM, 1 min) and PR-619 (10 µM, 10 min), lysed and subjected to ultracentrifugation to separate the soluble and insoluble fractions. Whole cell, soluble and insoluble fractions were then immunoblotted for endogenous p62. GAPDH was used as a loading control. Arrows indicate the positions of monomeric and DLC p62. The ratio of DLC to monomeric p62 was quantified and normalised to wild-type FLAG-p62. Error bars represent standard deviations, $n=2$. Data are representative of at least two independent experiments.

5.2.3 K7A,D69A mutant suppresses the formation of p62 aggregates during oxidative stress and autophagy inhibition

Since disulphide bond formation following oxidative stress appeared to contribute to p62 aggregation, and considering that self-oligomerisation of p62 through its PB1 domain is known to be essential for cytoplasmic bodies formation (Bjorkoy *et al.*, 2005), we examined the relationship of these two mechanisms further. We had previously shown that the PB1 domain mutant K7A,D69A, which disrupts the ability of p62 to self-oligomerise (Lamark *et al.*, 2003), could normally form DLC following oxidative stress (cf. **Figure 4.5**), suggesting that PB1-mediated oligomerisation and DLC formation where two separate mechanisms. Hence, we wanted to examine whether the PB1 mutant, which does not form cytoplasmic aggregates following overexpression and autophagy knock-out (Lamark *et al.*, 2003; Ichimura *et al.*, 2008), could still aggregate upon oxidative stress.

Thus, we overexpressed GFP-tagged wild-type or K7A,D69A p62 in HeLa cells, and compared the effects of H_2O_2 and PR-619 on aggregation with those of autophagy inhibition through bafilomycin A1 (Baf) by confocal microscopy analysis (**Figure 5.3A**). Interestingly, the absence of PB1-mediated oligomerisation determined the disappearance of p62 aggregates compared to the wild-type in conditions of both oxidative stress and autophagy inhibition. This suggested that the PB1 domain would have a primary role in the process of aggregate formation as shown previously (Ichimura *et al.*, 2008), even in the presence of DLC.

To compare the ability of the C105,113A mutant in forming polyubiquitinated aggregates during autophagy inhibition, we treated the stable cell lines expressing FLAG-tagged wild-type or mutant p62 with Baf, analysed them with confocal microscopy and quantified the cells with aggregates (**Figure 5.3B**). Autophagy inhibition greatly enhanced the formation of aggregates positive for p62 and ubiquitin both in wild-type and C105,113A p62, showing that oxidation sensitivity of p62 did not have a role during such conditions.

In summary, accumulation of p62 following autophagy inhibition drove its aggregation predominantly through the PB1 domain. At the same time, p62 DLC appeared to be important for aggregation during oxidative stress, although the microscopically-detectable aggregates also required the function of the PB1 domain of p62.

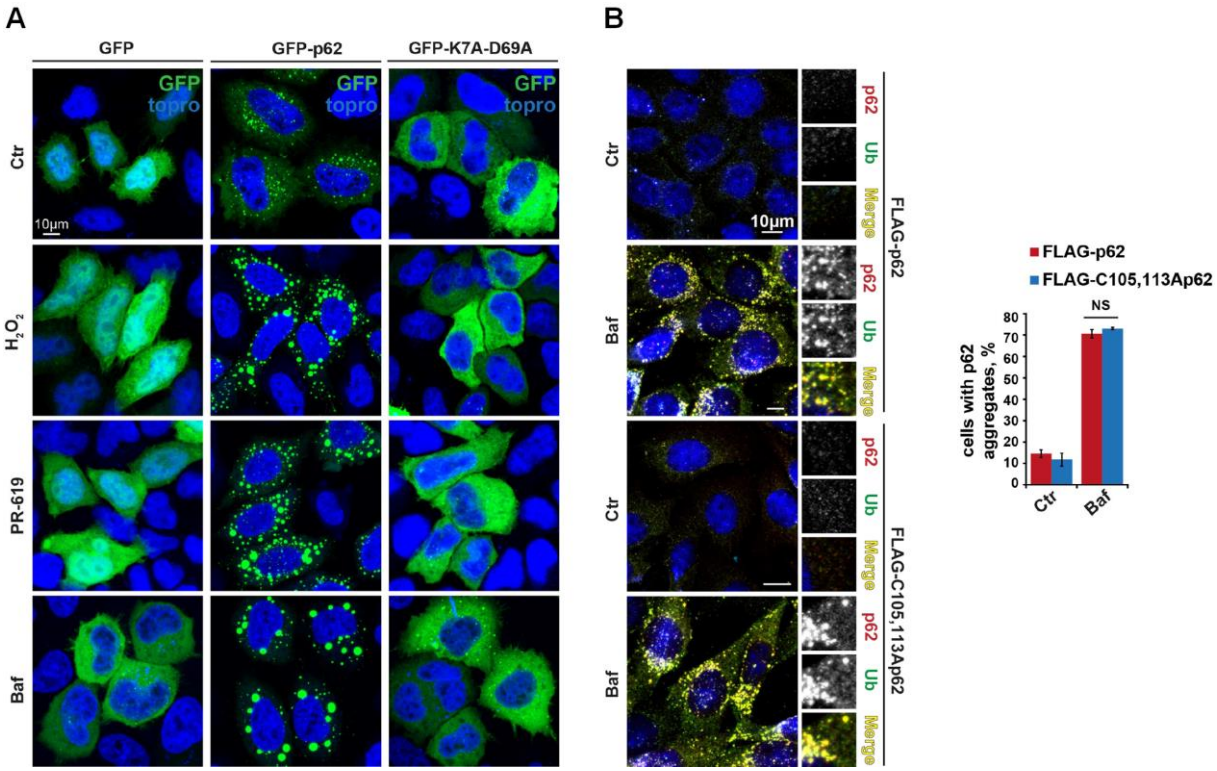

Figure 5.3 | The PB1 domain of p62 is required for intracellular aggregate formation. (A) HeLa cells were transfected with GFP, GFP-tagged wild-type or K7A,D69A p62 and treated with H_2O_2 (5 mM, 1 min), PR-619 (10 µM, 10 min) and bafilomycin A1 (Baf, 400 nM, 4 hours). Nuclei were stained with TO-PRO-3 iodide. Cells were fixed and analysed by confocal microscopy. **(B)** *p62*$^{-/-}$ MEFs stably expressing wild-type and C105,113A FLAG-tagged p62 were treated with bafilomycin A1 (Baf) as in (A) or left untreated (Ctr), immunostained for ubiquitin and p62 and analysed by confocal microscopy. Nuclei were stained with TO-PRO-3 iodide. Cells with positive aggregates for p62 were counted and their proportion quantified. Error bars represent s.e.m., *n*=3, NS: not significant. Data are representative of at least three independent experiments.

5.2.4 Degradation of C105,113A p62 is impaired compared to wild-type p62

Since aggregate formation upon oxidation appeared to be impaired in the presence of the double Cys mutant of p62 (**Figure 5.2**), we questioned whether the function of p62 in autophagy would have been affected by the mutation. The degradation of p62 is known to be correlated with its function as an autophagy receptor, as autophagy inhibition leads to the accumulation of p62 (Bjorkoy *et al.*, 2005; Komatsu *et al.*, 2007b; Komatsu and Ichimura, 2010). Thus, we tested whether the degradation rates of the double Cys mutant of p62 would have been affected during oxidative stress.

For this purpose, we used cycloheximide (CHX) to block protein synthesis in the cells and to determine the decay of p62 over time (Zhou, 2004). Cycloheximide is an antibiotic produced by *Streptomyces griseus* which blocks protein translation by binding to the 60S ribosomal subunit, causing cell growth arrest (Schneider-Poetsch *et al.*, 2010). We performed a CHX chase experiment to determine the rate of degradation of p62 in the wild-type and the mutant stable cell lines. Thus, we treated the cells for 1, 4 and 8 hours with CHX and analysed them by immunoblot (**Figure 5.4A**). The ratio of p62 to the loading control was quantified and normalised to the untreated samples. Interestingly, we discovered that C105,113A p62 had a significantly slower degradation compared to the wild-type after 4 and 8 hours of treatment, suggesting impaired autophagic function. This could reflect an impairment of the autophagic removal of the mutant p62.

Another way to investigate p62 degradation in our stable cell lines was to label the newly synthesised p62 and look at its degradation over time. Thus, a Click-iT assay was performed by labelling newly synthesised proteins with AHA (L-azidohomoalanine), using biotin to pull-down p62 over a period of 6 hours and then detecting the signal with streptavidin (**Figure 5.4B**). Also in this case, the C105,113A p62 mutant showed a slower degradation compared to the wild-type protein, significantly at 2 and 6 hours after labelling with AHA. This result further supported the role of p62 redox-sensitivity for its normal function as an autophagy receptor.

In brief, the loss of DLC formation impaired the degradation of the C105,113A p62, suggesting that the autophagic degradation of our mutant was impaired.

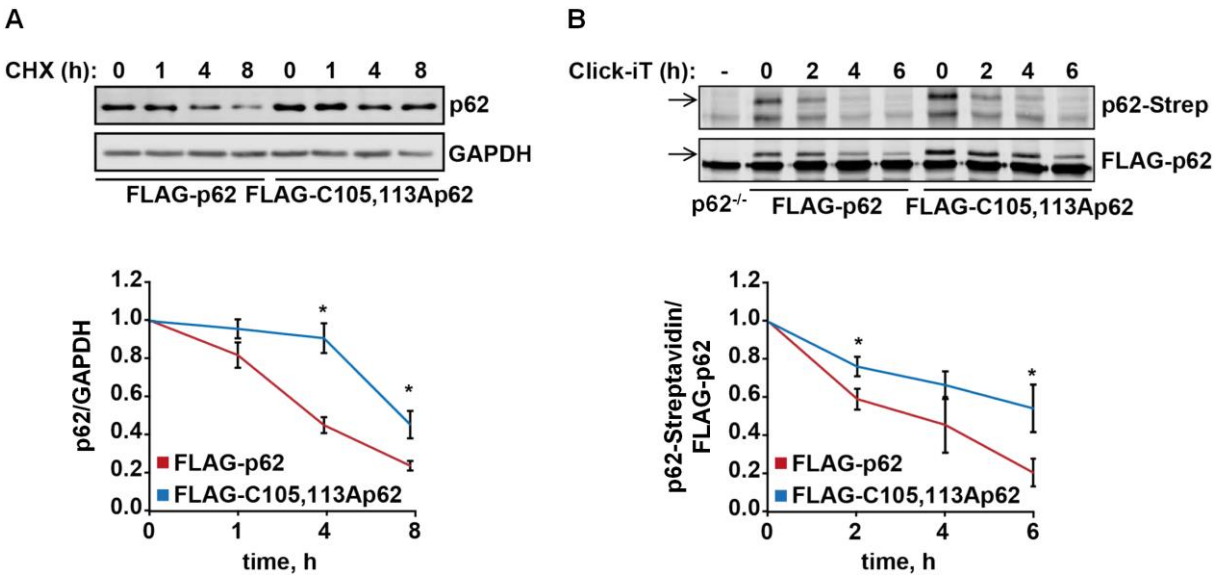

Figure 5.4 | Degradation of C105,113A p62 is delayed compared to wild-type. (**A**) *p62*$^{-/-}$ MEFs stably expressing FLAG-tagged wild-type or C105,113A p62 were treated with cycloheximide (CHX, 50 µg/ml), lysed at the indicated times post-treatment and immunoblotted for p62. GAPDH was used as a loading control. The amounts of p62 protein were quantified and normalised to the untreated. **(B)** *p62*$^{-/-}$ MEFs stably expressing empty vector plus stable cell lines as in (A) were analysed by Click-iT assay, where AHA (L-azidohomoalanine) reagent was incorporated into newly synthesised proteins, monitored via biotin pull-down over a chase period of 6 hours and probed with streptavidin for detection. FLAG-tagged p62 protein was used as an Input. The amount of newly synthesised p62 (p62-Strep) was quantified and normalised to the untreated. Error bars represent s.e.m., n=3, *p<0.05. Data are representative of at least three independent experiments. The work in (B) was carried out by Dr Fiona Menzies at Cambridge University.

5.2.5 Wild-type and C105,113A p62 show no difference in ubiquitin binding

Since the C105,113A p62 mutant showed impaired aggregation and degradation during oxidative stress conditions in our previous experiments (**Figure 5.2, 5.4**), and

both are considered important features for proper function of p62 as a receptor for selective autophagy (Komatsu and Ichimura, 2010), we questioned whether the double Cys mutation would affect the ability of p62 to bind to polyubiquitinated substrates.

Thus, we performed an immunoprecipitation (IP) using α-FLAG magnetic beads in in order to purify FLAG-tagged p62 from our wild-type and Cys mutant stable cell lines. Following the purification of FLAG-p62 wild-type and C105,133A, we performed immunoblot analysis for ubiquitin and p62 followed by quantification of ubiquitin-to-p62 protein levels (**Figure 5.5**). Importantly, the binding to ubiquitin showed no differences in both stable cell lines, suggesting that the double Cys mutation did not influence the binding of p62 to polyubiquitinated proteins.

To conclude, the ubiquitin binding was not affected in the C105,113A p62 cell line compared to the wild-type p62, suggesting that the impaired aggregation and degradation of the Cys mutant was not dependent on its ubiquitin-binding properties.

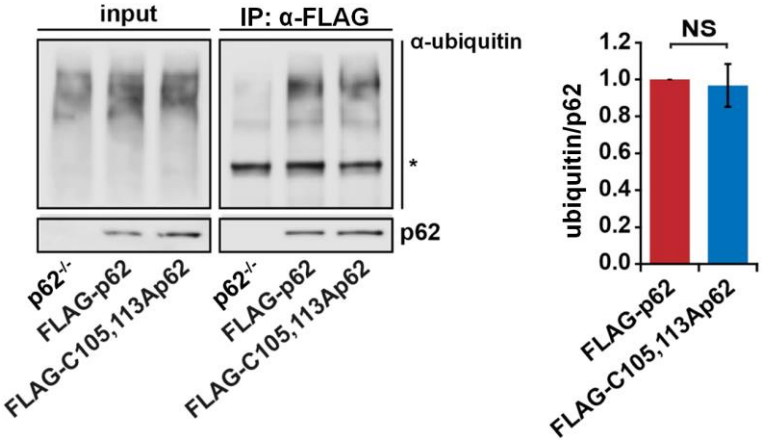

Figure 5.5 | Ubiquitin binding is not affected by the double Cys mutation of p62. (A) *p62*$^{-/-}$ MEFs stably expressing empty vector, FLAG-tagged wild-type or C105,113A p62 were subjected to immunoprecipitation (IP) using α-FLAG magnetic beads followed by immunoblot for ubiquitin and p62. Asterisk indicates an unspecific band. The ratio of immunoprecipitated ubiquitin to p62 was quantified and normalised to wild-type FLAG-p62. Error bars represent s.e.m., *n*=4, NS: not significant. Data are representative of at least three independent experiments.

5.2.6 Loss of DLC formation and self-oligomerisation of p62 inhibits autophagy function

After determining that p62 aggregation and degradation was impaired due to loss of DLC formation, and that polyubiquitinated proteins could bind independently of p62 oxidation, we wanted to investigate whether the double Cys mutation of p62 could affect its function as an autophagy receptor. Additionally, we compared the oxidation-insensitive mutant with the PB1 mutant in order to understand if both covalently- and non-covalently-mediated interactions of p62 were important for autophagy induction.

Thus, *p62*$^{-/-}$ MEFs stably expressing empty vector, FLAG-tagged wild-type, C105,113A or K7A,D69A p62 were treated for 5 hours with H_2O_2 in serum free media to induce autophagy during oxidative stress, then lysed and analysed by immunoblot analysis for ubiquitin, LC3 and p62 (**Figure 5.6A**). The levels of ubiquitin, LC3 and p62 were then quantified and normalised to the untreated *p62*$^{-/-}$ cells (**Figure 5.6B**). Interestingly, the reintroduction of wild-type p62 in the cell line could efficiently induce the autophagic degradation of polyubiquitinated substrates, as shown by the reduction of ubiquitin and increased levels of LC3-II (lane 6). In contrast, both C105,113A and K7A,D69A mutants of p62 failed to induce autophagy, as the ubiquitin levels were higher than in control conditions and the accumulation of LC3 was modest (lanes 7 and 8). As a confirmation, also p62 levels were higher in the mutant cell lines compared to the wild-type, highlighting the impaired degradation of p62 in the absence of DLC formation or self-oligomerisation. Unfortunately, we were not able to assess the levels of LC3 directly binding to p62 by IP in our mutant cell lines compared to wild-type (data not shown).

To confirm the impaired induction of autophagy in the two mutant cell lines compared to wild-type, we immunostained them for p62 and LC3 in order to look at the autophagosome formation (**Figure 5.6C**). While we could detect the presence of autophagosomes after reintroduction of wild-type FLAG-p62, the mutants C105,113 and K7A,D69A failed to form autophagosomes, suggesting an impairment in the process of autophagosome formation.

Another way to understand the rates of autophagic degradation of substrates in different cell lines has been recently experimented in (Lim *et al.*, 2015). In this study, the authors induced accumulation of polyubiquitinated proteins by blocking the proteasome, and then looked at the rates of autophagic degradation of such proteins by either activating or inhibiting autophagy. We used MG132 (also known as carbobenzoxy-Leu-Leu-leucinal), a peptide aldehyde which selectively and reversibly blocks the 26S proteasome complex, to induce accumulation of misfolded and polyubiquitinated substrates in the cells (Lee and Goldberg, 1998; Goldberg, 2012).

Hence, *p62*$^{-/-}$ MEFs stably expressing empty vector, FLAG-tagged wild-type or mutant p62 were treated with MG132 for 24 hours in medium with serum in order to accumulate polyubiquitinated proteins. Then, cells were switched to serum-free medium in the absence or presence of Baf (-Baf, +Baf) for another 24 hours, in order to either activate or block autophagy, respectively (**Figure 5.6D**). As expected, MG132 induced accumulation of polyubiquitinated proteins in all three cell lines (lanes 2, 6 and 10). After recovery in serum free medium (-Baf), cells started degrading the substrates via autophagy, although in the presence of wild-type FLAG-p62 such degradation was more pronounced (lane 7) compared to *p62*$^{-/-}$ and C105,113A cell lines (lanes 3 and 11). This resembled an impairment of autophagy in the mutant cell lines compared to wild-type, which was also confirmed by the higher accumulation of p62 following proteasome inhibition (cf. lanes 6 and 10) and its slower degradation following autophagy induction (cf. lanes 7 and 11). In conditions of autophagy inhibition (+Baf), both wild-type and mutant cell lines accumulated polyubiquitinated substrates, although accumulation in the mutant cell line was more marked. However, technical difficulties during such experiment (due to significant cell loss after treatments and subsequent poor extraction of proteins) led to high variability in our results and unreliable quantifications regarding the rates of substrates degradation. Nevertheless, other repeats similarly indicated an impairment in autophagy activation in the presence of the C105,133A p62 mutant.

In conclusion, the loss of either redox-sensitivity or the self-oligomerisation of p62 led to the impairment of autophagy and autophagosome formation, suggesting that both

properties would be important for the function of p62 as an autophagy receptor protein.

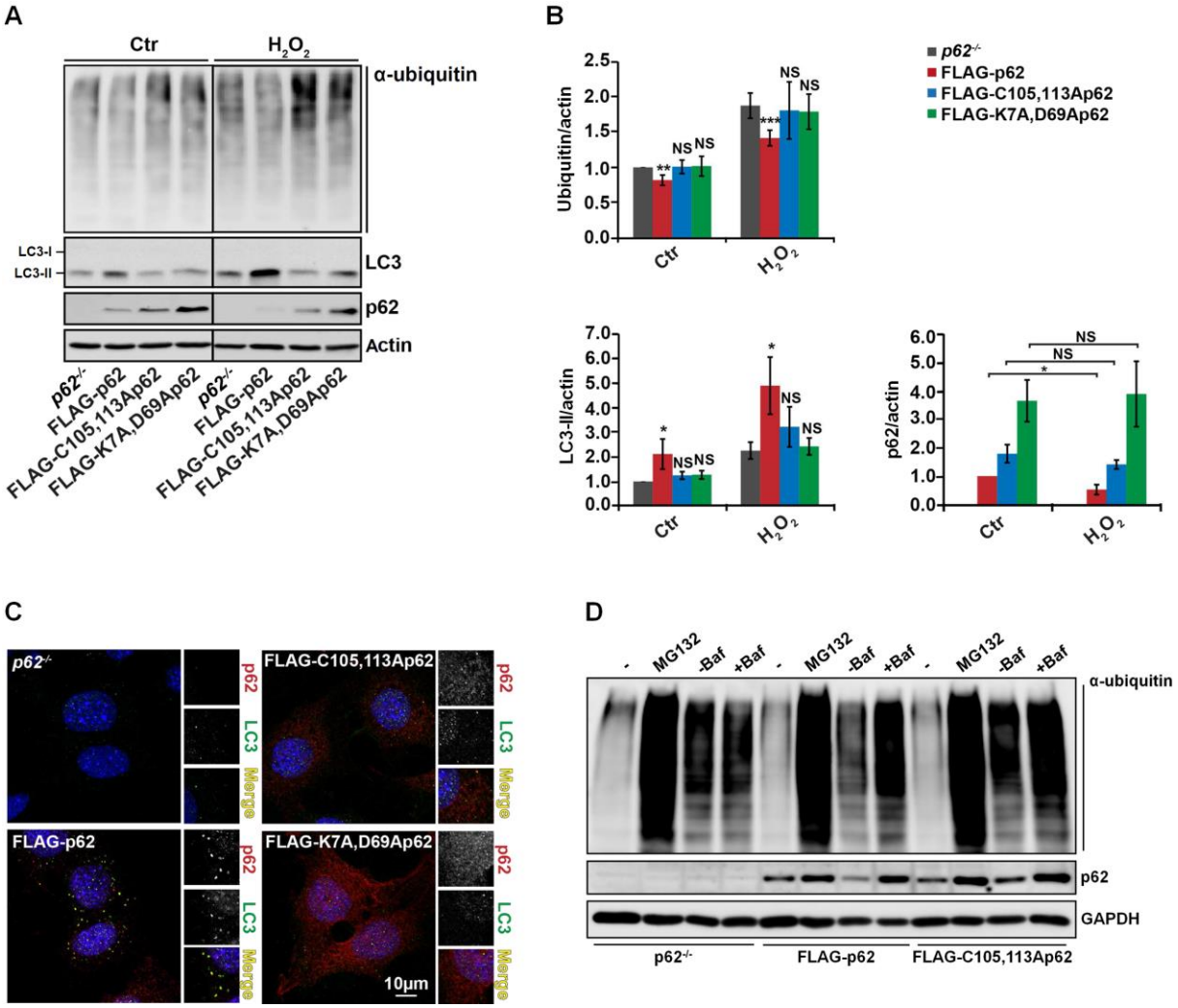

Figure 5.6 | Oxidation and self-oligomerisation of p62 are important for autophagy induction. **(A)** *p62*$^{-/-}$ MEFs stably expressing empty vector, FLAG-tagged wild-type, C105,113A or K7A,D69A p62 were treated with H_2O_2 (1 mM, 5 hours), lysed and immunoblotted for ubiquitin, LC3 and p62. Actin was used as a loading control. **(B)** The amounts of ubiquitin, LC3 and p62 were quantified and normalised to the *p62*$^{-/-}$. Error bars represent s.e.m., n=3, *p<0.05, **p<0.01, ***p<0.005, NS: not significant. **(C)** Stable cell lines as in (A) were grown on coverslips, fixed then stained for p62 and LC3 and analysed by confocal microscopy. **(D)** *p62*$^{-/-}$ MEFs stably expressing empty vector, FLAG-tagged wild-type or C105,113A p62 were treated with MG132 (2.5 μM, 24 hours), then media was replaced with or without bafilomycin A1 (-/+ Baf, 100 nm, 24 hours). Cells were lysed and analysed by immunoblot for ubiquitin and p62. GAPDH was used as a loading control. Data are representative of at least three independent experiments. The work in (A, B, C) was carried out in collaboration with Elsje G. Otten.

5.2.7 Loss of redox-sensitivity and self-oligomerisation of p62 affect cell survival under oxidative stress

Since both oxidation and self-oligomerisation of p62 appeared to be important for the induction of autophagy (cf. **Figure 5.6**), we questioned whether the loss of these properties would affect cell viability in conditions of oxidative stress. In fact, autophagy is a catabolic process of vital importance in the cell, whose inhibition is linked to apoptosis (Boya *et al.*, 2005).

Thus, *p62*$^{-/-}$ MEFs stably expressing empty vector, FLAG-tagged wild-type, C105,113A or K7A,D69A p62 were exposed to oxidative stress (H_2O_2) for 5 hours, stained with fluorescence dyes to assess cell death and analysed by light microscopy (**Figure 5.7A**). The percentage of dead cells was then quantified and normalised to the *p62*$^{-/-}$ MEFs (**Figure 5.7B**). Oxidation appeared to have a strong effect on cell viability in the absence of p62 (*p62*$^{-/-}$), while the reintroduction of wild-type FLAG-p62 significantly prevented cellular loss. These data suggested the importance of p62 for cell survival, potentially by driving the degradation of substrates affected by the oxidative environment. Strikingly, neither C105,113A nor K7A,D69A p62 could rescue cell viability, confirming the role of both ROS-sensitivity and PB1-domain dependent p62 self-oligomerisation in cell survival.

In short, redox-insensitive and oligomerisation-deficient mutants of p62 failed in protecting cells from oxidative stress, possibly due to autophagy impairment determined by p62 mutations.

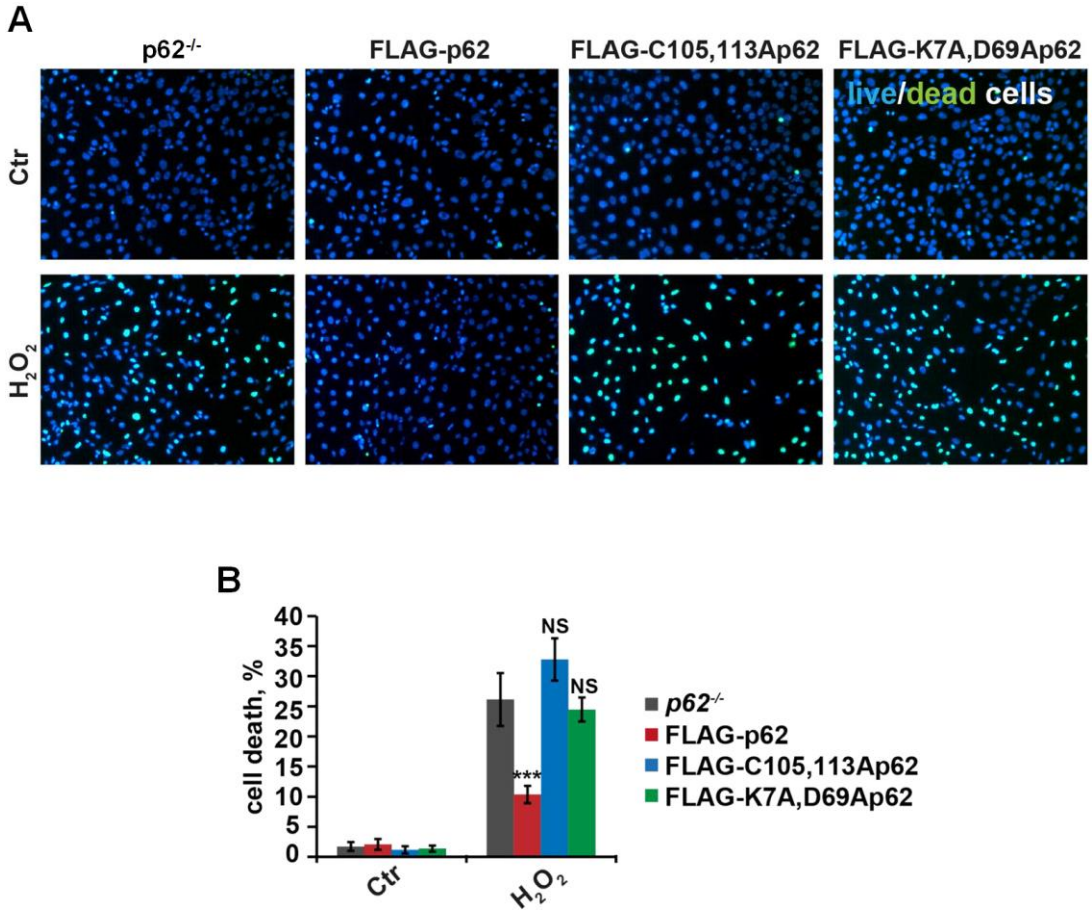

Figure 5.7 | Loss of redox-sensitivity and self-oligomerisation of p62 reduce cell viability. (A) *p62*$^{-/-}$ MEFs stably expressing empty vector, FLAG-tagged wild-type, C105,113A or K7A,D69A p62 were treated with H_2O_2 (1 mM, 5 hours), and cells were stained with ReadyProbes fluorescent dyes to assess cell death. Blue fluorescence indicates total cells while green fluorescence indicates dead cells. Images were taken at x20 magnification by fluorescence microscope. **(B)** The percentage of cell death was quantified and normalised to the *p62*$^{-/-}$. Error bars represent s.e.m., n=3, *p<0.05, **p<0.01, ***p<0.005. Data are representative of at least three independent experiments. The work was carried out in collaboration with Elsje G. Otten.

5.3 Discussion

Selective autophagy is a catabolic process that requires autophagy receptors in order to recognise and accumulate cargos for degradation (Johansen and Lamark, 2011). Autophagy receptors, such as SQSTM1/p62, NDP52 and OPTN, bind to polyubiquitinated substrates and link them to the forming autophagosomal membrane, driving the engulfment of cargos (Stolz *et al.*, 2014). In chapters 3 and 4, we have found that p62 senses by oxidative stress by forming disulphide-linked conjugates (DLC) in response to ROS. We have then identified two Cys residues in an unstructured region of p62, C105 and C113, important for DLC formation. Since oxidative stress also appeared to induce formation of p62 aggregates, which are essential for the autophagic degradation of cargos (Bjorkoy *et al.*, 2005; Ichimura *et al.*, 2008), we questioned whether the loss of DLC formation would have impaired the function of p62 as an autophagy receptor.

In this chapter, we have investigated the effects of the loss of p62 DLC by producing stable cell lines (MEFs) in a p62 knock-out background (*p62*$^{-/-}$) expressing either wild-type or mutant C105,113A p62 (**Figure 5.1**). In this way, we could question whether insensitivity to oxidative stress would have affected the aggregation and function of p62. By inducing oxidation in our stable cell lines, we were able to detect lower formation of p62- and ubiquitin-positive aggregates in mutant C105,113 p62 compared to wild-type, suggesting that DLC had an important role in driving p62 accumulation and aggregation (**Figure 5.2A**). Such aggregates were also positive for ubiquitin, in accordance with the requirement of p62 for their formation (Komatsu *et al.*, 2007b; Korolchuk *et al.*, 2009). Additionally, the loss of DLC formation did not induce the shift of p62 to the insoluble fraction, suggestive of impaired formation of insoluble aggregates (**Figure 5.2B**). Since formation of p62 aggregates has been linked to its ability to degrade its substrates (Bjorkoy *et al.*, 2005; Ichimura *et al.*, 2008), we hypothesised that the function of p62 as an autophagy receptor could be affected by the loss of DLC.

Until now, p62 aggregation has been linked to its ability of self-oligomerise mediated by the PB1 domain (Lamark *et al.*, 2003; Ichimura *et al.*, 2008). We therefore employed the well-characterised K7A,D69A PB1 mutant of p62, which lacks the ability to self-oligomerise and form intracellular aggregates (Lamark *et al.*, 2003), in order to compare it with our Cys mutant. Since the PB1 mutant retained the ability to form DLC following oxidation in our previous analysis (cf. **Figure 4.5**), we were curious to understand whether it would have been important also during aggregation in the same conditions. Oxidative stress failed to induce aggregation of mutant p62 in K7A,D69A stable cell line (**Figure 5.3A**), showing that PB1 domain-mediated oligomerisation of p62 was essential for aggregate formation in such conditions. Additionally, autophagy inhibition induced by Baf failed to induce aggregation of p62 in the K7A,D69A cell line as shown in literature (Ichimura *et al.*, 2008) (**Figure 5.3A**), while both wild-type and C105,133A p62 mutant cell lines accumulated aggregates of p62 to the same level (**Figure 5.3B**), suggesting that DLC of p62 were dispensable for the process. Thus, we hypothesised that p62 DLC-mediated oligomerisation could facilitate aggregate formation in conditions of oxidative stress, while PB1 domain-mediated interactions would be further required for the assembly of oligomeric p62 into microscopically observable aggregates.

Accumulation and aggregation of p62 have been directly connected to its function in autophagy, where p62 is not only a receptor but also a substrate of autophagic degradation (Komatsu and Ichimura, 2010). In fact, the K7A,D69A mutant p62 has been shown to have a delayed degradation when compared to wild-type, confirming the role of p62 aggregation in autophagy (Ichimura *et al.*, 2008). Therefore, we assessed whether the degradation of the oxidation-insensitive p62 mutant was affected, which could have indicated impaired autophagy. Interestingly, we were able to detect a lower degradation rate of p62 in C105,113A cell line compared to wild-type during CHX chase, suggestive of impaired autophagic degradation (**Figure 5.4A**). Notably, it has been reported that CHX treatment could inhibit autophagy (Lawrence and Brown, 1993), which could have affected the rate of p62 degradation. Therefore, as an alternative approach we employed a pulse-chase labelling technique (Click-IT assay), which allowed us to isolate the newly synthesised p62

and monitor its degradation rates, thus avoiding the need to inhibit protein synthesis (**Figure 5.4B**). Also in this case, the degradation of C105,133A p62 was slower compared to the wild-type, again suggesting that DLC formation was important during autophagy.

Since accumulation and degradation of p62 were both connected to p62 autophagic function and affected by the Cys mutation, we questioned whether the loss of DLC could inhibit the binding to polyubiquitinated substrates. Immunoprecipitation of p62 from wild-type and C105,113A mutant cell lines did not show any differences in ubiquitin binding (**Figure 5.5**), suggesting that the loss of DLC formation did not influence the sequestration of polyubiquitinated substrates. A previous study has instead shown that p62 high-molecular crosslinks impaired the association of p62 to polyubiquitinated cargos, thus leading to the inhibition of autophagosome formation (Donohue *et al.*, 2014). Additionally, the authors have shown that the PB1 domain K7A,D69A mutant of p62 did not form high-molecular species, linking the loss of self-oligomerisation with the disappearance of p62 crosslinks (Donohue *et al.*, 2014). In contrast, we were able to detect the impairment in ubiquitin-positive aggregate formation in our redox-insensitive mutant cell line (cf. **Figure 5.2A**), as well as the formation of DLC of the K7A,D69A mutant following oxidation (cf. **Figure 4.5**). As discussed in Chapter 4, such discrepancy might be due to the different treatments used by the authors, such as the autophagy inhibitor verteporfin, which can have additional effects on the formation of autophagosomes.

Following these findings, we investigated the effects of the loss of p62 redox-sensitivity on the degradation of autophagy substrates during oxidation. Both C105,113A and K7A,D69A mutants failed to induce autophagy following H_2O_2 treatment compared to wild-type p62, shown by the accumulation of polyubiquitinated substrates and lower accumulation of lipidated LC3-II (**Figure 5.6A, B**). Additionally, autophagosome formation appeared reduced in the Cys mutant and PB1 mutant cell lines (**Figure 5.6C**), indicating an impairment in autophagosome assembly. Thus, we suggest that p62 not only works as a receptor protein for the selective degradation of autophagy substrates, but also functions as a core component of the autophagy machinery. Recent evidence has shed light on the importance of p62 oligomerisation

for the proper formation of autophagosomes and membrane bending (Wurzer *et al.*, 2015). In a similar way, we propose that p62 forms DLC in conditions of oxidative stress in order to promote its oligomerisation and aggregation together with the PB1 domain, contributing to the assembly of autophagosomes. Although we could not assess the levels of p62 Cys mutant binding to LC3 (data not shown), our data indicate a clear impairment in the function of p62 as an autophagy receptor. It would be important to further investigate how the impairment of p62 oligomerisation and aggregation leads to the defect in LC3 lipidation, and how it may impact on membrane bending and engulfment of cargos.

The role of p62 in autophagy induction is still unclear. For instance, it has been reported that p62 can disrupt the association between Bcl-2 and Beclin1, positively regulating the autophagy process (Zhou *et al.*, 2013). However, it has also been suggested that p62 can promote mTORC1 activation and translocation to the lysosomes, thus blocking autophagy (Duran *et al.*, 2011). Thus, a potential role of p62 in regulating autophagy upstream of autophagosome assembly cannot be ruled out. It would be interesting to examine whether the loss of DLC formation would affect the ability of p62 to properly interact with molecular partners, and if such impairment could affect the autophagy process.

Finally, we investigated the effects of the Cys mutant on cell survival during oxidative stress. Indeed, autophagy is an essential pro-survival process during conditions of nutrient deprivation and in response to stress, involved in the removal of damaged proteins and organelles as well as providing nutrients through recycling of cellular components (Levine and Yuan, 2005). Hence, the role of p62 in inducing autophagy in conditions of oxidative stress could have important implications in cell viability. Additionally, a previous study has indicated that formation of p62 aggregates increased cell survival (Paine *et al.*, 2005), further showing the importance of p62 aggregate formation. Our analysis showed impaired cell viability in C105,113A p62 as well as K7A,D69A cell lines, which was consistent with the loss of DLC and oligomerisation of p62 (**Figure 5.7**). Therefore, we propose that the ability of p62 to sense ROS and form DLC could serve as a protection mechanism during oxidative

stress, enhancing the aggregation of substrates and their disposal through autophagy, thus promoting to cell survival.

It has been previously shown that self-oligomerisation of p62 through the PB1 domain is important for its localisation to the autophagosomes formation site (Itakura and Mizushima, 2011). More recently, a study has shown that p62 oligomerisation stabilises its interaction with LC3 clusters on the autophagosomal membrane, thus inducing the bending of the membrane and the engulfment of polyubiquitinated cargos (Wurzer *et al.*, 2015). In this chapter, we have shown that DLC formation in conditions of oxidative stress is a mechanism allowing p62 to oligomerise and induce aggregation of associated-polyubiquitinated substrates, while simultaneously promoting autophagosome formation and ultimately degradation of autophagy cargos. We propose that DLC formation, in concert with PB1 domain-dependent oligomerisation, drives the accumulation of p62, important for the stabilisation of the autophagosomal membrane during oxidative stress (**Figure 5.8**). It could be speculated that the underlying mechanism could be mediated by an increased avidity between p62 DLC and Atg8-family proteins on nascent autophagic membranes (phagophores). This would facilitate the assembly of autophagic vesicles around the cargos, leading to their sequestration and degradation through autophagy.

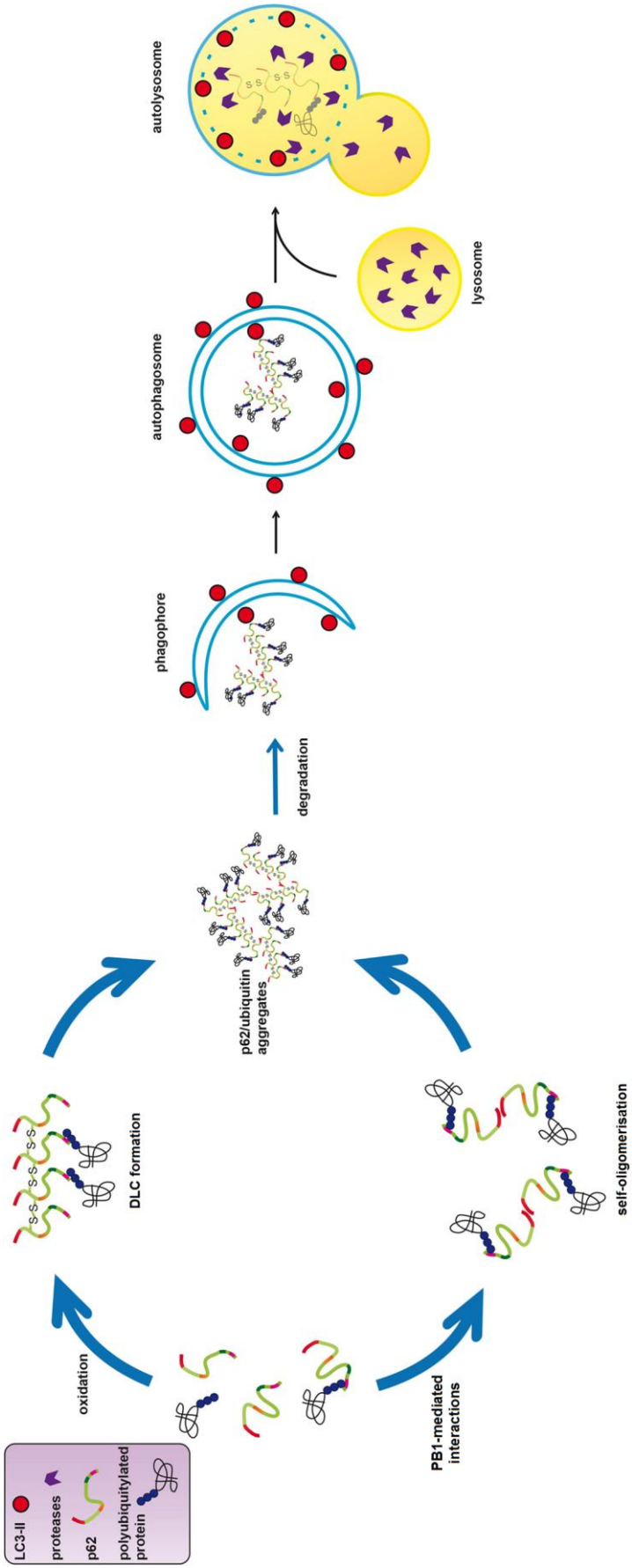

Figure 5.8 | Schematic representation of p62 function in autophagy during oxidative stress conditions. We propose that oxidation induces formation of disulphide-linked conjugates (DLC) of p62 (tetramers and higher order oligomers) which are regulated by the peroxiredoxin/thioredoxin (Prx/Trx) system. Such DLC are important for p62 accumulation and autophagic degradation of cargos. Formation of DLC and oligomerisation of p62 through PB1 domain interactions work in concert to serve as docking sites for the nascent autophagic membranes (phagophores). The interaction with LC3 leads to the engulfment of p62 and its substrates and their subsequent degradation through autophagy.

Chapter 6. Conclusions

The oligomerisation and aggregation of proteins are important features of neurodegenerative diseases (NDs), which are untreatable and devastating conditions affecting the nervous system. Here, specific neuronal proteins tend to lose their native conformation (a process known as misfolding) and form fibrils, which can further aggregate in neurons leading to the formation of insoluble inclusions (Douglas and Dillin, 2010). However, little has been understood whether such protein aggregates are harmful or protective for the cells, and whether they are the cause or the consequence of the disease ((Ross and Poirier, 2005). Oxidative stress, which arises when reactive oxygen species (ROS) accumulate in the cell, can lead to protein misfolding and aggregation through the irreversible oxidation of cysteine (Cys) residues (Reddie and Carroll, 2008). However, healthy levels of oxidation are also required for the regulation of proteins, where Cys residues are oxidised and form disulphide bonds, a reversible modification which often leads to protein functional changes (Paulsen and Carroll, 2010). The catabolic pathway autophagy, in which specific receptor proteins drive the degradation of substrates, is in charge for degrading protein aggregates and alleviate the cellular toxic burden (Johansen and Lamark, 2011; Stolz *et al.*, 2014).

In this thesis work, we have investigated the mechanisms of oligomerisation and aggregation of the selective autophagy receptor SQSTM1/p62, and for the first time shown that p62 can sense and be regulated by oxidative stress. In fact, sensitivity of p62 to oxidation has recently been postulated, however no experimental evidence has been shown before (Filomeni *et al.*, 2015). Evidence of autophagy regulation by oxidative stress is also scarce, with Atg4 regulation by ROS being the only mechanism shown experimentally so far, while other autophagy players have only been suggested to be regulated by it (Scherz-Shouval *et al.*, 2007; Filomeni *et al.*, 2010).

Autophagy is a catabolic pathway aimed at degrading anything from long-lived proteins to whole organelles. Its sub-pathway macroautophagy (usually referred to as simply autophagy), is a tightly regulated process that involves the engulfment of substrates by double-membrane organelles known as autophagosomes, and their fusion to lysosomes to form autolysosomes where degradation occurs (Ravikumar *et al.*, 2009). Specific receptor proteins, such as p62, bind to polyubiquitin-tagged proteins (i.e. tagged for degradation) and drive their degradation through autophagy, thus allowing the selective autophagy of substrates (Johansen and Lamark, 2011). However, impairment of autophagy leads to the accumulation of p62 and its substrates due to their inefficient degradation, often leading to aggregate formation and cell death (Levine and Kroemer, 2008).

Here, we have found that p62 can be covalently modified by ROS, determining a slower electrophoretic mobility of p62 in immunoblot analysis. Following induction with H_2O_2 or the oxidative stress inducer PR-619, p62 forms disulphide-linked conjugates (DLC) through disulphide bonds between cysteine (Cys) residues. These formations, which were sensitive to reducing agents such as β-mercaptoethanol, were distinct from the monomeric p62, and were visible in brain tissue from aged mice as well as in cell culture. Additionally, p62 DLC formation appeared to be important for aggregate formation, since oxidation could shift the presence of p62 from the soluble to the insoluble fraction in our cell lysates. Unfortunately, we were unable to isolate p62 DLC and examine their exact composition, however their MW size resembles trimers and tetramers of p62, together with higher MW structures which often remained confined in the stacking gel. Additionally, p62 DLC were also visible after purifying bacterial GST-p62 and inducing oxidative stress, thus suggesting the absence of other interacting proteins.

The increase of DLC formation following inhibition of TrxR suggests that p62 is indeed oxidised in our experimental conditions, and the intracellular antioxidant system (Prx/Trx) is constantly involved in the reduction of p62 DLC. The formation of covalent oligomers of p62 has been already shown in literature, although such modifications were not investigated further (Paine *et al.*, 2005; Gamerdinger *et al.*, 2009). A recent work has shown the formation of p62 covalent crosslinks following

oxidative stress, although we found several differences with this thesis work, especially in the function of these covalent modifications of p62 (Donohue *et al.*, 2014).

Through the generation of p62 deletion constructs and several rounds of mutagenesis, we have identified two conserved Cys residues C105 and C113 (located in an unstructured region of p62 between the PB1 and ZZ domains) to be pivotal for DLC formation. This linker region appears rich in conserved, charged amino acids that could be important for C105 and C113 reactivity towards ROS. The same linker region has been recently identified as an electrostatic bridge, where the high presence of charged amino acids is crucial for the correct formation of PB1 filaments (Ciuffa *et al.*, 2015). The disruption of the PB1 filaments following mutation of two charged amino acids in the electrostatic bridge, together with our experimental evidence of DLC loss following C105A-C113A mutation, suggests that the electrostatic environment of this unstructured linker region of p62 could be critical not only for the non-covalent PB1-mediated oligomerisation, but also for the covalent disulphide-mediated oligomerisation of p62. The incomplete block of DLC formation following mutation of both C105 and C113 could resemble a redundancy between neighbouring Cys residues, which might become available for DLC formation. The absence of C105 and C113 in lower animals such as invertebrates suggests that p62 gained the ability to sense ROS during evolution, in order to maintain protein homeostasis in more complex and long-lived organisms.

Following the production of stable cell lines expressing transgenic p62 either wild-type or C105A-C113A mutant, we have shown that mutagenesis of these residues impairs both aggregation and insolubility of p62, as well as its degradation rates, thus affecting its function as an autophagy receptor. Indeed, p62 aggregation has been connected to its ability to degrade substrates through autophagy (Bjorkoy *et al.*, 2005; Ichimura *et al.*, 2008). Activation of autophagy was also impaired in the presence of C105A-C113A p62, although we were not able to assess the levels of binding between p62 and LC3. Finally, cell survival was also affected by the absence of DLC formation, since the cells expressing mutant p62 were more susceptible to oxidative stress.

Since aggregate formation is also dependent on p62 self-oligomerisation through its PB1 domain (Itakura and Mizushima, 2011), we propose that DLC formation would act in concert with p62 self-oligomerisation for substrate aggregation and subsequent disposal by selective autophagy. The enhanced oligomerisation of p62 would increase its binding to LC3 and stabilise the autophagosomal membrane (Wurzer *et al.*, 2015), leading to the engulfment and degradation of cargos.

Thus, we propose that DLC formation would be another mechanism of p62 oligomerisation distinct from the PB1-mediated, which would serve to enhance the aggregability of p62 during conditions of oxidative stress and promote the degradation of substrates. Additionally, we provide evidence that the aggregation of p62, which is enhanced by DLC formation following oxidative stress, could be a protective mechanism. This new function of p62 would then serve to combat the burden of misfolded proteins caused by oxidative stress, thus improving cell survival.

Importantly, we have also found that DLC of p62 were also accumulating in human brain tissue affected by NDs, such as Alzheimer's disease and Parkinson's disease, together with increased levels of oxidative stress. In fact, p62 has been found in all protein aggregates associated with NDs, and its antibodies have been recommended to stain human brain tissue as a general diagnostic marker (Kuusisto *et al.*, 2008). The new mechanism of p62 aggregation proposed in this thesis work could eventually lead to the development of new diagnostic tools for the early detection of pathological processes in patients. For example, the production of antibodies directed towards the oxidised form of p62 could be used to detect increased levels of p62 oxidation in patients, suggestive of increased oxidative stress, which could correlate with the onset of neurodegenerative disease.

Chapter 7. Appendices

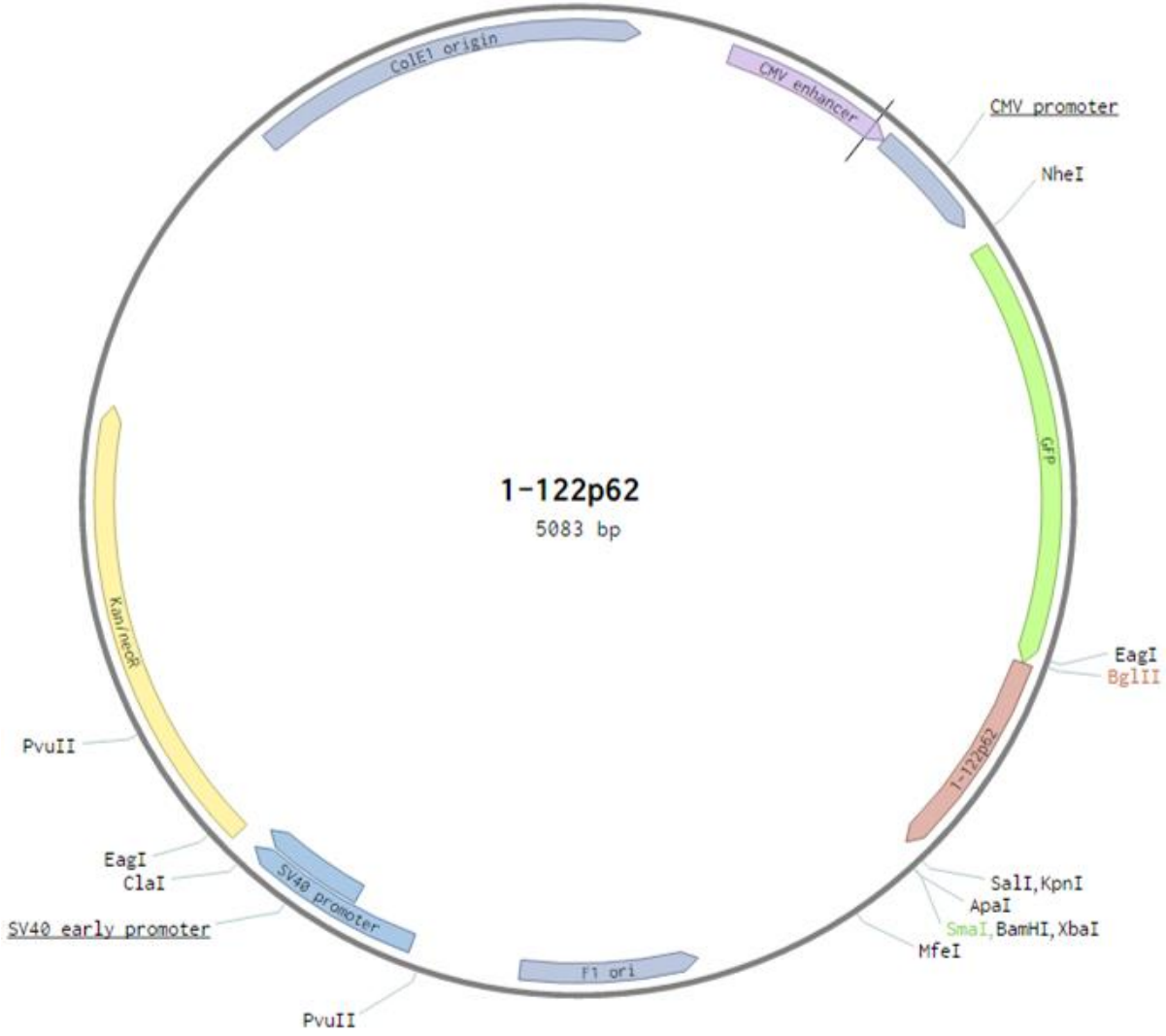

Appendix A | Plasmid map of GFP-tagged 1-122p62 deletion construct produced in this study.

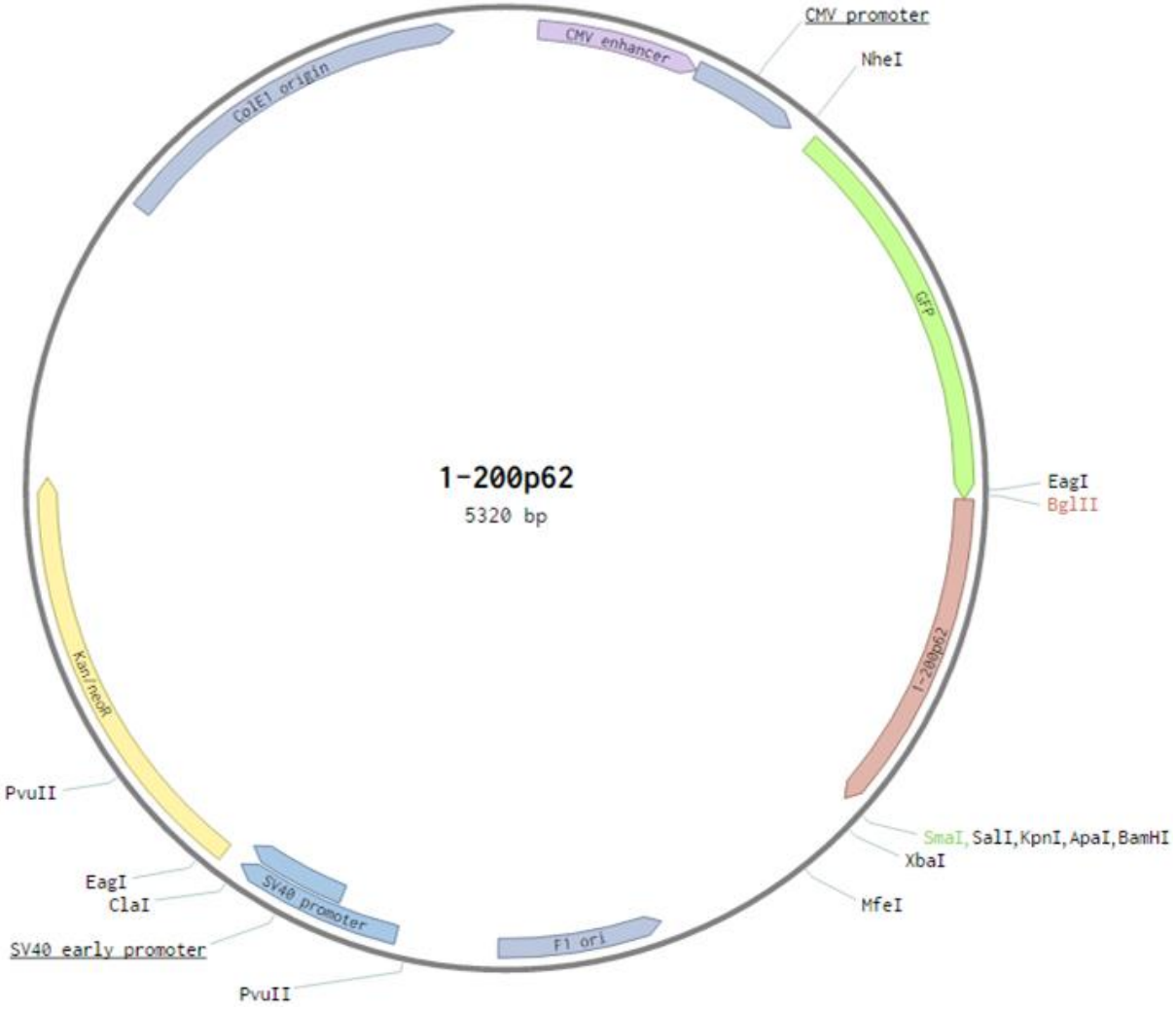

Appendix B | Plasmid map of GFP-tagged 1-200p62 deletion construct produced in this study.

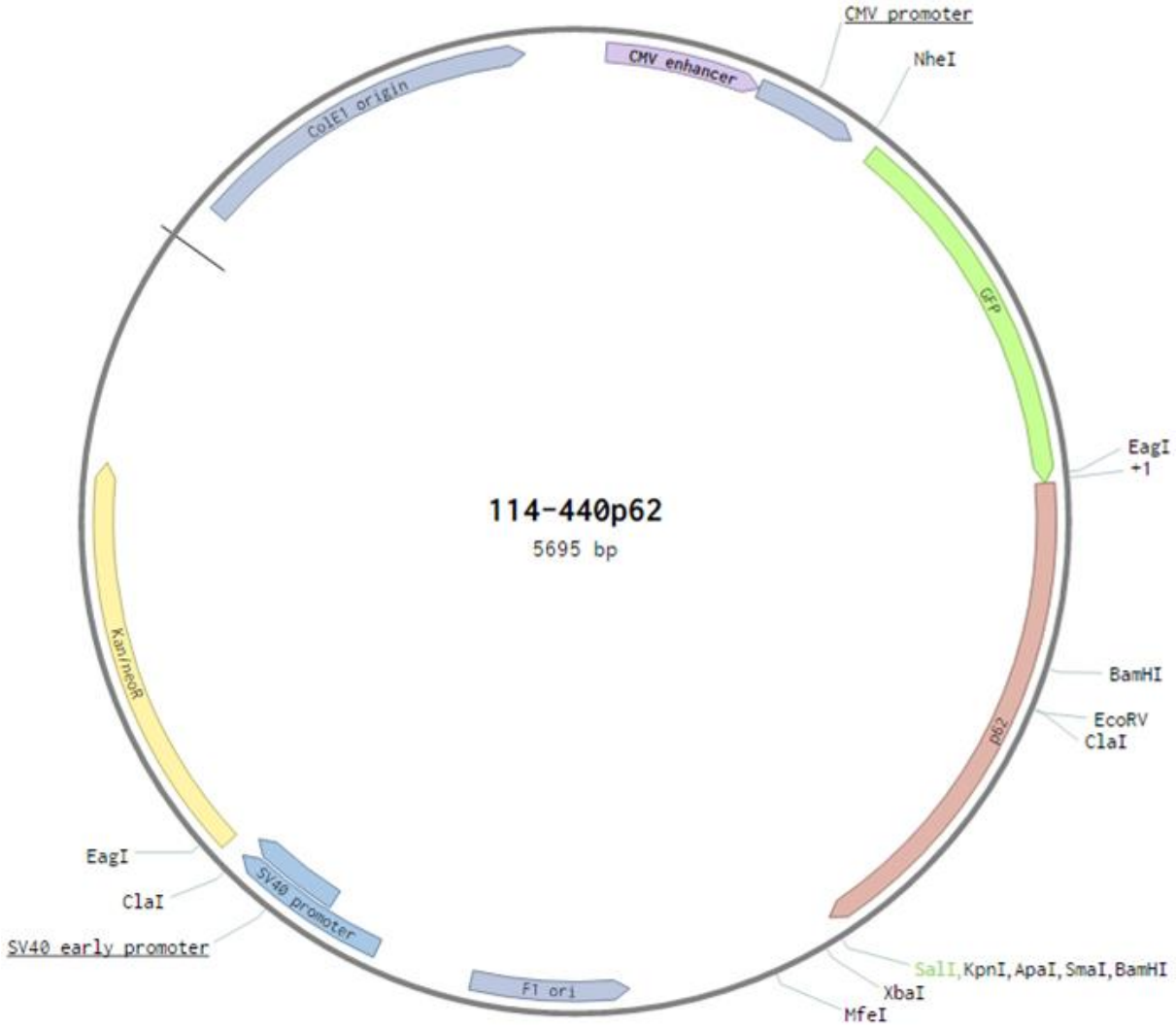

Appendix C | Plasmid map of GFP-tagged 114-440p62 deletion construct produced in this study.

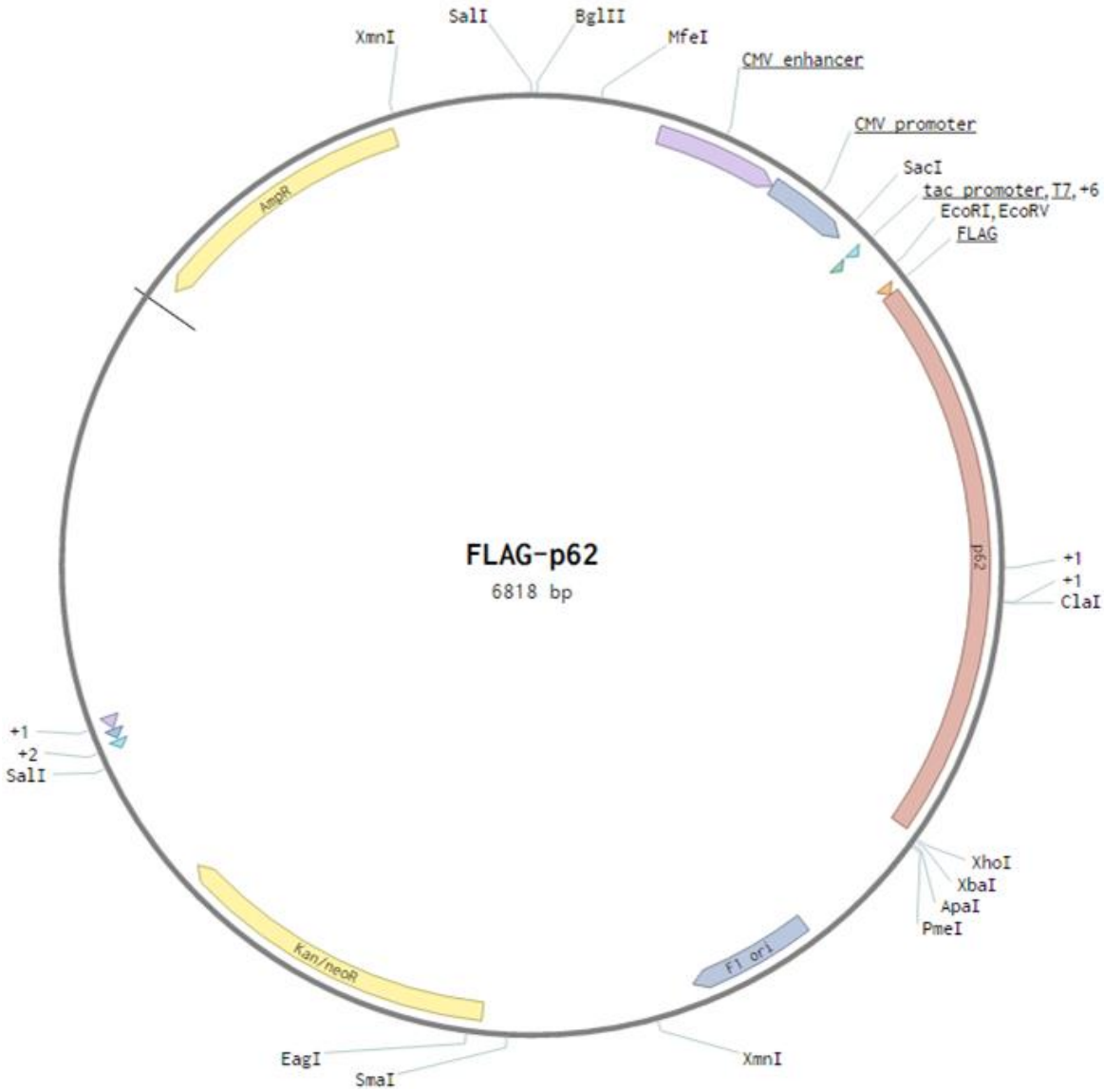

Appendix D | Plasmid map of FLAG-tagged p62 construct used in this study.

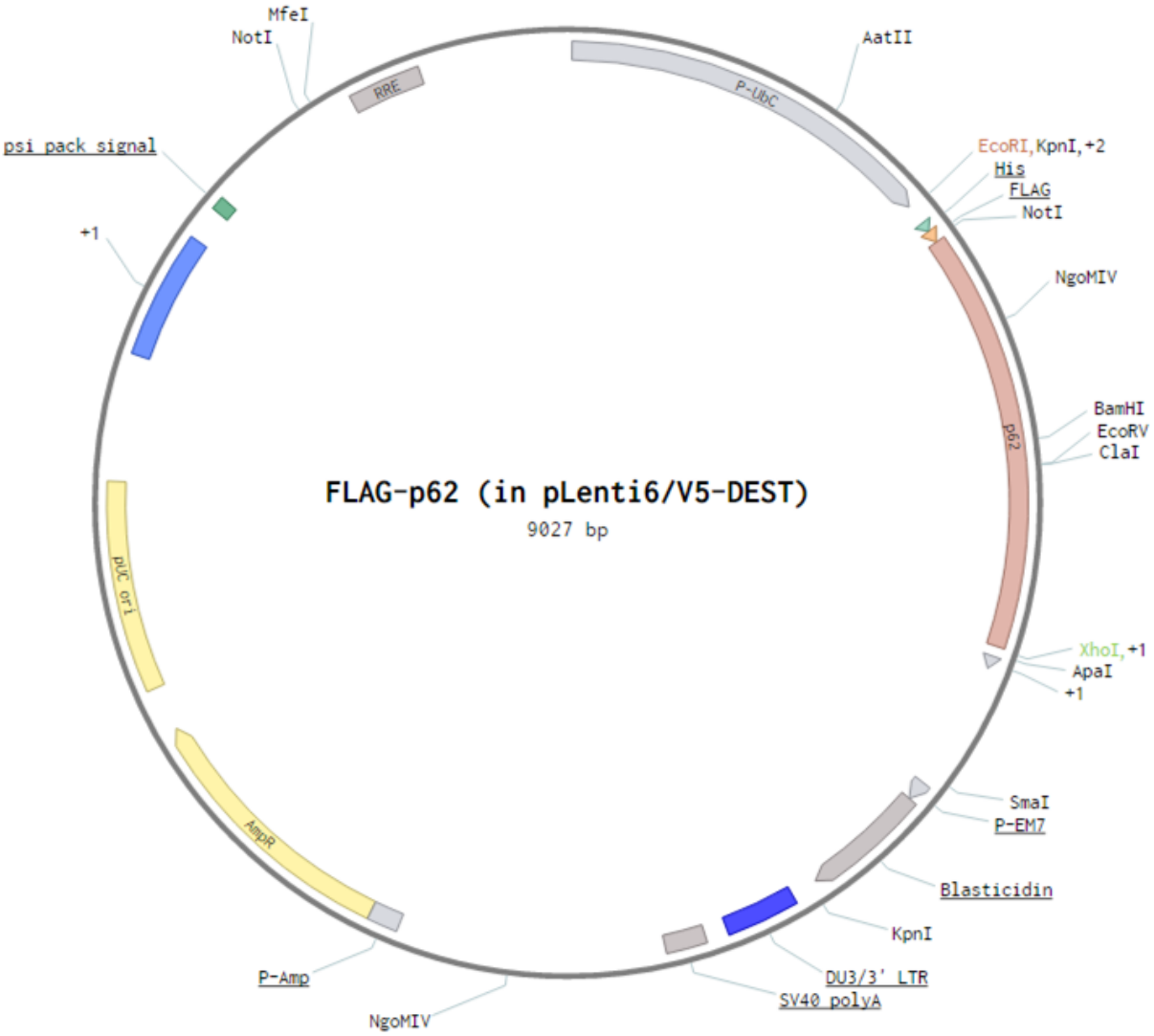

Appendix E | Plasmid map of FLAG-tagged p62 lentiviral vector produced in this study.

References

Abate, C., Patel, L., Rauscher, F.J., 3rd and Curran, T. (1990) 'Redox regulation of fos and jun DNA-binding activity in vitro', *Science*, 249(4973), pp. 1157-61.

Agarraberes, F.A., Terlecky, S.R. and Dice, J.F. (1997) 'An intralysosomal hsp70 is required for a selective pathway of lysosomal protein degradation', *J Cell Biol*, 137(4), pp. 825-34.

Ahlberg, J., Marzella, L. and Glaumann, H. (1982) 'Uptake and degradation of proteins by isolated rat liver lysosomes. Suggestion of a microautophagic pathway of proteolysis', *Lab Invest*, 47(6), pp. 523-32.

Altun, M., Kramer, H.B., Willems, L.I., McDermott, J.L., Leach, C.A., Goldenberg, S.J., Kumar, K.G., Konietzny, R., Fischer, R., Kogan, E., Mackeen, M.M., McGouran, J., Khoronenkova, S.V., Parsons, J.L., Dianov, G.L., Nicholson, B. and Kessler, B.M. (2011) 'Activity-based chemical proteomics accelerates inhibitor development for deubiquitylating enzymes', *Chem Biol*, 18(11), pp. 1401-12.

Andersen, J.K. (2004) 'Oxidative stress in neurodegeneration: cause or consequence?', *Nat Med*, 10 Suppl, pp. S18-25.

Arendt, C.S., Ri, K., Yates, P.A. and Ullman, B. (2007) 'Genetic selection for a highly functional cysteine-less membrane protein using site saturation mutagenesis', *Anal Biochem*, 365(2), pp. 185-93.

Argyrou, A. and Blanchard, J.S. (2004) 'Flavoprotein disulfide reductases: advances in chemistry and function', *Prog Nucleic Acid Res Mol Biol*, 78, pp. 89-142.

Arndt, V., Rogon, C. and Hohfeld, J. (2007) 'To be, or not to be--molecular chaperones in protein degradation', *Cell Mol Life Sci*, 64(19-20), pp. 2525-41.

Atkuri, K.R., Mantovani, J.J., Herzenberg, L.A. and Herzenberg, L.A. (2007) 'N-Acetylcysteine--a safe antidote for cysteine/glutathione deficiency', *Curr Opin Pharmacol*, 7(4), pp. 355-9.

Azzam, M.E. and Algranati, I.D. (1973) 'Mechanism of puromycin action: fate of ribosomes after release of nascent protein chains from polysomes', *Proc Natl Acad Sci U S A*, 70(12), pp. 3866-9.

Babu, J.R., Geetha, T. and Wooten, M.W. (2005) 'Sequestosome 1/p62 shuttles polyubiquitinated tau for proteasomal degradation', *J Neurochem*, 94(1), pp. 192-203.

Backer, J.M., Bourret, L. and Dice, J.F. (1983) 'Regulation of catabolism of microinjected ribonuclease A requires the amino-terminal 20 amino acids', *Proc Natl Acad Sci U S A*, 80(8), pp. 2166-70.

Backer, J.M. and Dice, J.F. (1986) 'Covalent linkage of ribonuclease S-peptide to microinjected proteins causes their intracellular degradation to be enhanced during serum withdrawal', *Proc Natl Acad Sci U S A*, 83(16), pp. 5830-4.

Bae, Y.S., Kang, S.W., Seo, M.S., Baines, I.C., Tekle, E., Chock, P.B. and Rhee, S.G. (1997) 'Epidermal growth factor (EGF)-induced generation of hydrogen peroxide. Role in EGF receptor-mediated tyrosine phosphorylation', *J Biol Chem*, 272(1), pp. 217-21.

Balch, W.E., Morimoto, R.I., Dillin, A. and Kelly, J.W. (2008) 'Adapting proteostasis for disease intervention', *Science*, 319(5865), pp. 916-9.

Bandyopadhyay, U., Kaushik, S., Varticovski, L. and Cuervo, A.M. (2008) 'The chaperone-mediated autophagy receptor organizes in dynamic protein complexes at the lysosomal membrane', *Mol Cell Biol*, 28(18), pp. 5747-63.

Bates, G.P. (2006) 'BIOMEDICINE: One Misfolded Protein Allows Others to Sneak By', *Science*, 311(5766), pp. 1385-6.

Behl, C. (2011) 'BAG3 and friends: co-chaperones in selective autophagy during aging and disease', *Autophagy*, 7(7), pp. 795-8.

Behrends, C. and Harper, J.W. (2011) 'Constructing and decoding unconventional ubiquitin chains', *Nat Struct Mol Biol*, 18(5), pp. 520-8.

Billiet, L., Geerlings, P., Messens, J. and Roos, G. (2012) 'The thermodynamics of thiol sulfenylation', *Free Radic Biol Med*, 52(8), pp. 1473-85.

Biteau, B., Labarre, J. and Toledano, M.B. (2003) 'ATP-dependent reduction of cysteine-sulphinic acid by S. cerevisiae sulphiredoxin', *Nature*, 425(6961), pp. 980-4.

Bitto, A., Lerner, C.A., Nacarelli, T., Crowe, E., Torres, C. and Sell, C. (2014) 'p62/SQSTM1 at the interface of aging, autophagy, and disease', *Age (Dordr)*.

Bjorkoy, G., Lamark, T., Brech, A., Outzen, H., Perander, M., Overvatn, A., Stenmark, H. and Johansen, T. (2005) 'p62/SQSTM1 forms protein aggregates degraded by autophagy and has a protective effect on huntingtin-induced cell death', *J Cell Biol*, 171(4), pp. 603-14.

Bochtler, M., Ditzel, L., Groll, M., Hartmann, C. and Huber, R. (1999) 'The proteasome', *Annu Rev Biophys Biomol Struct*, 28, pp. 295-317.

Bokov, A., Chaudhuri, A. and Richardson, A. (2004) 'The role of oxidative damage and stress in aging', *Mech Ageing Dev*, 125(10-11), pp. 811-26.

Boland, B., Kumar, A., Lee, S., Platt, F.M., Wegiel, J., Yu, W.H. and Nixon, R.A. (2008) 'Autophagy induction and autophagosome clearance in neurons: relationship to autophagic pathology in Alzheimer's disease', *J Neurosci*, 28(27), pp. 6926-37.

Bond, C.S. and Schuttelkopf, A.W. (2009) 'ALINE: a WYSIWYG protein-sequence alignment editor for publication-quality alignments', *Acta Crystallogr D Biol Crystallogr*, 65(Pt 5), pp. 510-2.

Bornhorst, J.A. and Falke, J.J. (2000) 'Purification of proteins using polyhistidine affinity tags', *Methods Enzymol*, 326, pp. 245-54.

Boya, P., Gonzalez-Polo, R.A., Casares, N., Perfettini, J.L., Dessen, P., Larochette, N., Metivier, D., Meley, D., Souquere, S., Yoshimori, T., Pierron, G., Codogno, P. and Kroemer, G. (2005) 'Inhibition of macroautophagy triggers apoptosis', *Mol Cell Biol*, 25(3), pp. 1025-40.

Brannigan, J.A., Dodson, G., Duggleby, H.J., Moody, P.C., Smith, J.L., Tomchick, D.R. and Murzin, A.G. (1995) 'A protein catalytic framework with an N-terminal nucleophile is capable of self-activation', *Nature*, 378(6555), pp. 416-9.

Braun, B.C., Glickman, M., Kraft, R., Dahlmann, B., Kloetzel, P.M., Finley, D. and Schmidt, M. (1999) 'The base of the proteasome regulatory particle exhibits chaperone-like activity', *Nat Cell Biol*, 1(4), pp. 221-6.

Brigelius-Flohe, R. and Maiorino, M. (2013) 'Glutathione peroxidases', *Biochim Biophys Acta*, 1830(5), pp. 3289-303.

Bryan, H.K., Olayanju, A., Goldring, C.E. and Park, B.K. (2013) 'The Nrf2 cell defence pathway: Keap1-dependent and -independent mechanisms of regulation', *Biochem Pharmacol*, 85(6), pp. 705-17.

Burns, J.C., Friedmann, T., Driever, W., Burrascano, M. and Yee, J.K. (1993) 'Vesicular stomatitis virus G glycoprotein pseudotyped retroviral vectors: concentration to very high titer and efficient gene transfer into mammalian and nonmammalian cells', *Proc Natl Acad Sci U S A*, 90(17), pp. 8033-7.

Bus, J.S. and Gibson, J.E. (1984) 'Paraquat: model for oxidant-initiated toxicity', *Environ Health Perspect*, 55, pp. 37-46.

Calkins, M.J., Johnson, D.A., Townsend, J.A., Vargas, M.R., Dowell, J.A., Williamson, T.P., Kraft, A.D., Lee, J.M., Li, J. and Johnson, J.A. (2009) 'The Nrf2/ARE pathway as a potential therapeutic target in neurodegenerative disease', *Antioxid Redox Signal*, 11(3), pp. 497-508.

Callahan, M.K., Chaillot, D., Jacquin, C., Clark, P.R. and Menoret, A. (2002) 'Differential acquisition of antigenic peptides by Hsp70 and Hsc70 under oxidative conditions', *J Biol Chem*, 277(37), pp. 33604-9.

Callis, J. (2014) 'The ubiquitination machinery of the ubiquitin system', *Arabidopsis Book*, 12, p. e0174.

Caplan, A.J. (2003) 'What is a co-chaperone?', *Cell Stress Chaperones*, 8(2), pp. 105-7.

Carrigan, P.E., Sikkink, L.A., Smith, D.F. and Ramirez-Alvarado, M. (2006) 'Domain:domain interactions within Hop, the Hsp70/Hsp90 organizing protein, are required for protein stability and structure', *Protein Sci*, 15(3), pp. 522-32.

Carroll, B., Hewitt, G. and Korolchuk, V.I. (2013) 'Autophagy and ageing: implications for age-related neurodegenerative diseases', *Essays Biochem*, 55, pp. 119-31.

Caughey, B. and Lansbury, P.T. (2003) 'Protofibrils, pores, fibrils, and neurodegeneration: separating the responsible protein aggregates from the innocent bystanders', *Annu Rev Neurosci*, 26, pp. 267-98.

Chamoux, E., Couture, J., Bisson, M., Morissette, J., Brown, J.P. and Roux, S. (2009) 'The p62 P392L mutation linked to Paget's disease induces activation of human osteoclasts', *Mol Endocrinol*, 23(10), pp. 1668-80.

Chen, B., Retzlaff, M., Roos, T. and Frydman, J. (2011) 'Cellular strategies of protein quality control', *Cold Spring Harb Perspect Biol*, 3(8), p. a004374.

Chen, X., Guo, C. and Kong, J. (2012) 'Oxidative stress in neurodegenerative diseases', *Neural Regen Res*, 7(5), pp. 376-85.

Chen, Y. and Dorn, G.W., 2nd (2013) 'PINK1-phosphorylated mitofusin 2 is a Parkin receptor for culling damaged mitochondria', *Science*, 340(6131), pp. 471-5.

Chen, Y. and Klionsky, D.J. (2011) 'The regulation of autophagy - unanswered questions', *J Cell Sci*, 124(Pt 2), pp. 161-70.

Chen, Z.J. (2005) 'Ubiquitin signalling in the NF-kappaB pathway', *Nat Cell Biol*, 7(8), pp. 758-65.

Chiang, H.L. and Dice, J.F. (1988) 'Peptide sequences that target proteins for enhanced degradation during serum withdrawal', *J Biol Chem*, 263(14), pp. 6797-805.

Chiang, H.L., Terlecky, S.R., Plant, C.P. and Dice, J.F. (1989) 'A role for a 70-kilodalton heat shock protein in lysosomal degradation of intracellular proteins', *Science*, 246(4928), pp. 382-5.

Chiti, F., Stefani, M., Taddei, N., Ramponi, G. and Dobson, C.M. (2003) 'Rationalization of the effects of mutations on peptide and protein aggregation rates', *Nature*, 424(6950), pp. 805-8.

Choi, H.J., Kang, S.W., Yang, C.H., Rhee, S.G. and Ryu, S.E. (1998) 'Crystal structure of a novel human peroxidase enzyme at 2.0 A resolution', *Nat Struct Biol*, 5(5), pp. 400-6.

Ciechanover, A. (1994) 'The ubiquitin-proteasome proteolytic pathway', *Cell*, 79(1), pp. 13-21.

Ciechanover, A. (2005) 'Proteolysis: from the lysosome to ubiquitin and the proteasome', *Nat Rev Mol Cell Biol*, 6(1), pp. 79-87.

Ciechanover, A. and Brundin, P. (2003) 'The ubiquitin proteasome system in neurodegenerative diseases: sometimes the chicken, sometimes the egg', *Neuron*, 40(2), pp. 427-46.

Ciechanover, A., Heller, H., Elias, S., Haas, A.L. and Hershko, A. (1980) 'ATP-dependent conjugation of reticulocyte proteins with the polypeptide required for protein degradation', *Proc Natl Acad Sci U S A*, 77(3), pp. 1365-8.

Ciuffa, R., Lamark, T., Tarafder, A.K., Guesdon, A., Rybina, S., Hagen, W.J., Johansen, T. and Sachse, C. (2015) 'The Selective Autophagy Receptor p62 Forms a Flexible Filamentous Helical Scaffold', *Cell Rep*.

Connell, P., Ballinger, C.A., Jiang, J., Wu, Y., Thompson, L.J., Hohfeld, J. and Patterson, C. (2001) 'The co-chaperone CHIP regulates protein triage decisions mediated by heat-shock proteins', *Nat Cell Biol*, 3(1), pp. 93-6.

Copple, I.M., Lister, A., Obeng, A.D., Kitteringham, N.R., Jenkins, R.E., Layfield, R., Foster, B.J., Goldring, C.E. and Park, B.K. (2010) 'Physical and functional interaction of sequestosome 1 with Keap1 regulates the Keap1-Nrf2 cell defense pathway', *J Biol Chem*, 285(22), pp. 16782-8.

Cotto-Rios, X.M., Bekes, M., Chapman, J., Ueberheide, B. and Huang, T.T. (2012) 'Deubiquitinases as a signaling target of oxidative stress', *Cell Rep*, 2(6), pp. 1475-84.

Cox, A.G., Winterbourn, C.C. and Hampton, M.B. (2010) 'Measuring the redox state of cellular peroxiredoxins by immunoblotting', *Methods Enzymol*, 474, pp. 51-66.

Cox, J.S., Shamu, C.E. and Walter, P. (1993) 'Transcriptional induction of genes encoding endoplasmic reticulum resident proteins requires a transmembrane protein kinase', *Cell*, 73(6), pp. 1197-206.

Cremers, C.M. and Jakob, U. (2013) 'Oxidant sensing by reversible disulfide bond formation', *J Biol Chem*, 288(37), pp. 26489-96.

Cuervo, A.M. (2004) 'Autophagy: many paths to the same end', *Mol Cell Biochem*, 263(1-2), pp. 55-72.

Cuervo, A.M. (2010) 'Chaperone-mediated autophagy: selectivity pays off', *Trends Endocrinol Metab*, 21(3), pp. 142-50.

Cuervo, A.M. (2011) 'Chaperone-mediated autophagy: Dice's 'wild' idea about lysosomal selectivity', *Nat Rev Mol Cell Biol*, 12(8), pp. 535-41.

Cuervo, A.M. and Dice, J.F. (1996) 'A receptor for the selective uptake and degradation of proteins by lysosomes', *Science*, 273(5274), pp. 501-3.

Cuervo, A.M. and Dice, J.F. (2000a) 'Age-related decline in chaperone-mediated autophagy', *J Biol Chem*, 275(40), pp. 31505-13.

Cuervo, A.M. and Dice, J.F. (2000b) 'Regulation of lamp2a levels in the lysosomal membrane', *Traffic*, 1(7), pp. 570-83.

Cuervo, A.M., Hildebrand, H., Bomhard, E.M. and Dice, J.F. (1999) 'Direct lysosomal uptake of alpha 2-microglobulin contributes to chemically induced nephropathy', *Kidney Int*, 55(2), pp. 529-45.

Cuervo, A.M., Knecht, E., Terlecky, S.R. and Dice, J.F. (1995) 'Activation of a selective pathway of lysosomal proteolysis in rat liver by prolonged starvation', *Am J Physiol*, 269(5 Pt 1), pp. C1200-8.

Cuervo, A.M., Mann, L., Bonten, E.J., d'Azzo, A. and Dice, J.F. (2003) 'Cathepsin A regulates chaperone-mediated autophagy through cleavage of the lysosomal receptor', *EMBO J*, 22(1), pp. 47-59.

Cuervo, A.M., Terlecky, S.R., Dice, J.F. and Knecht, E. (1994) 'Selective binding and uptake of ribonuclease A and glyceraldehyde-3-phosphate dehydrogenase by isolated rat liver lysosomes', *J Biol Chem*, 269(42), pp. 26374-80.

Day, A.M., Brown, J.D., Taylor, S.R., Rand, J.D., Morgan, B.A. and Veal, E.A. (2012) 'Inactivation of a peroxiredoxin by hydrogen peroxide is critical for thioredoxin-mediated repair of oxidized proteins and cell survival', *Mol Cell*, 45(3), pp. 398-408.

De Duve, C. (1963) 'The lysosome', *Sci Am*, 208, pp. 64-72.

De Duve, C., Pressman, B.C., Gianetto, R., Wattiaux, R. and Appelmans, F. (1955) 'Tissue fractionation studies. 6. Intracellular distribution patterns of enzymes in rat-liver tissue', *Biochem J*, 60(4), pp. 604-17.

De Duve, C. and Wattiaux, R. (1966) 'Functions of lysosomes', *Annu Rev Physiol*, 28, pp. 435-92.

Demand, J., Alberti, S., Patterson, C. and Hohfeld, J. (2001) 'Cooperation of a ubiquitin domain protein and an E3 ubiquitin ligase during chaperone/proteasome coupling', *Curr Biol*, 11(20), pp. 1569-77.

Demuro, A., Mina, E., Kayed, R., Milton, S.C., Parker, I. and Glabe, C.G. (2005) 'Calcium dysregulation and membrane disruption as a ubiquitous neurotoxic mechanism of soluble amyloid oligomers', *J Biol Chem*, 280(17), pp. 17294-300.

Denu, J.M. and Tanner, K.G. (1998) 'Specific and reversible inactivation of protein tyrosine phosphatases by hydrogen peroxide: evidence for a sulfenic acid intermediate and implications for redox regulation', *Biochemistry*, 37(16), pp. 5633-42.

Deponte, M. (2013) 'Glutathione catalysis and the reaction mechanisms of glutathione-dependent enzymes', *Biochim Biophys Acta*, 1830(5), pp. 3217-66.

Deshaies, R.J. and Joazeiro, C.A. (2009) 'RING domain E3 ubiquitin ligases', *Annu Rev Biochem*, 78, pp. 399-434.

Desideri, E., Filomeni, G. and Ciriolo, M.R. (2012) 'Glutathione participates in the modulation of starvation-induced autophagy in carcinoma cells', *Autophagy*, 8(12), pp. 1769-81.

Deveraux, Q., Ustrell, V., Pickart, C. and Rechsteiner, M. (1994) 'A 26 S protease subunit that binds ubiquitin conjugates', *J Biol Chem*, 269(10), pp. 7059-61.

Di Domenico, F., Head, E., Butterfield, D.A. and Perluigi, M. (2014) 'Oxidative Stress and Proteostasis Network: Culprit and Casualty of Alzheimer’s-Like Neurodegeneration', *Advances in Geriatrics*, 2014, p. 14.

Dice, J.F. (1990) 'Peptide sequences that target cytosolic proteins for lysosomal proteolysis', *Trends Biochem Sci*, 15(8), pp. 305-9.

Dice, J.F. (2009) 'Chaperone-mediated autophagy: the heretofore untold story of J. Fred "Paulo" Dice. Interview by Daniel J. Klionsky', *Autophagy*, 5(8), pp. 1079-84.

Dice, J.F., Chiang, H.L., Spencer, E.P. and Backer, J.M. (1986) 'Regulation of catabolism of microinjected ribonuclease A. Identification of residues 7-11 as the essential pentapeptide', *J Biol Chem*, 261(15), pp. 6853-9.

Dinkova-Kostova, A.T., Holtzclaw, W.D., Cole, R.N., Itoh, K., Wakabayashi, N., Katoh, Y., Yamamoto, M. and Talalay, P. (2002) 'Direct evidence that sulfhydryl groups of Keap1 are the sensors regulating induction of phase 2 enzymes that protect against carcinogens and oxidants', *Proc Natl Acad Sci U S A*, 99(18), pp. 11908-13.

Dobashi, Y., Watanabe, Y., Miwa, C., Suzuki, S. and Koyama, S. (2011) 'Mammalian target of rapamycin: a central node of complex signaling cascades', *Int J Clin Exp Pathol*, 4(5), pp. 476-95.

Dohi, E., Tanaka, S., Seki, T., Miyagi, T., Hide, I., Takahashi, T., Matsumoto, M. and Sakai, N. (2012) 'Hypoxic stress activates chaperone-mediated autophagy and modulates neuronal cell survival', *Neurochem Int*, 60(4), pp. 431-42.

Donohue, E., Balgi, A.D., Komatsu, M. and Roberge, M. (2014) 'Induction of Covalently Crosslinked p62 Oligomers with Reduced Binding to Polyubiquitinated Proteins by the Autophagy Inhibitor Verteporfin', *PLoS One*, 9(12), p. e114964.

Douglas, P.M. and Dillin, A. (2010) 'Protein homeostasis and aging in neurodegeneration', *J Cell Biol*, 190(5), pp. 719-29.

Du, Y., Wooten, M.C., Gearing, M. and Wooten, M.W. (2009a) 'Age-associated oxidative damage to the p62 promoter: implications for Alzheimer disease', *Free Radic Biol Med*, 46(4), pp. 492-501.

Du, Y., Wooten, M.C. and Wooten, M.W. (2009b) 'Oxidative damage to the promoter region of SQSTM1/p62 is common to neurodegenerative disease', *Neurobiol Dis*, 35(2), pp. 302-10.

Dunker, A.K., Cortese, M.S., Romero, P., Iakoucheva, L.M. and Uversky, V.N. (2005) 'Flexible nets. The roles of intrinsic disorder in protein interaction networks', *FEBS J*, 272(20), pp. 5129-48.

Duran, A., Amanchy, R., Linares, J.F., Joshi, J., Abu-Baker, S., Porollo, A., Hansen, M., Moscat, J. and Diaz-Meco, M.T. (2011) 'p62 is a key regulator of nutrient sensing in the mTORC1 pathway', *Mol Cell*, 44(1), pp. 134-46.

Duran, A., Serrano, M., Leitges, M., Flores, J.M., Picard, S., Brown, J.P., Moscat, J. and Diaz-Meco, M.T. (2004) 'The atypical PKC-interacting protein p62 is an important mediator of RANK-activated osteoclastogenesis', *Dev Cell*, 6(2), pp. 303-9.

Eskelinen, E.-L. (2005) 'Macroautophagy in Mammalian Cells', in *Lysosomes*. Boston, MA: Springer US, pp. 166-180.

Eskelinen, E.L., Reggiori, F., Baba, M., Kovacs, A.L. and Seglen, P.O. (2011) 'Seeing is believing: the impact of electron microscopy on autophagy research', *Autophagy*, 7(9), pp. 935-56.

Fang, J., Lu, J. and Holmgren, A. (2005) 'Thioredoxin reductase is irreversibly modified by curcumin: a novel molecular mechanism for its anticancer activity', *J Biol Chem*, 280(26), pp. 25284-90.

Fass, E., Shvets, E., Degani, I., Hirschberg, K. and Elazar, Z. (2006) 'Microtubules support production of starvation-induced autophagosomes but not their targeting and fusion with lysosomes', *J Biol Chem*, 281(47), pp. 36303-16.

Fecto, F., Yan, J., Vemula, S.P., Liu, E., Yang, Y., Chen, W., Zheng, J.G., Shi, Y., Siddique, N., Arrat, H., Donkervoort, S., Ajroud-Driss, S., Sufit, R.L., Heller, S.L., Deng, H.X. and Siddique, T. (2011) 'SQSTM1 mutations in familial and sporadic amyotrophic lateral sclerosis', *Arch Neurol*, 68(11), pp. 1440-6.

Feller, S.M. and Lewitzky, M. (2012) 'Very 'sticky' proteins - not too sticky after all?', *Cell Commun Signal*, 10(1), p. 15.

Festjens, N., Vanden Berghe, T., Cornelis, S. and Vandenabeele, P. (2007) 'RIP1, a kinase on the crossroads of a cell's decision to live or die', *Cell Death Differ*, 14(3), pp. 400-10.

Filimonenko, M., Isakson, P., Finley, K.D., Anderson, M., Jeong, H., Melia, T.J., Bartlett, B.J., Myers, K.M., Birkeland, H.C., Lamark, T., Krainc, D., Brech, A., Stenmark, H., Simonsen, A. and Yamamoto, A. (2010) 'The selective macroautophagic degradation of aggregated proteins requires the PI3P-binding protein Alfy', *Mol Cell*, 38(2), pp. 265-79.

Filomeni, G., De Zio, D. and Cecconi, F. (2015) 'Oxidative stress and autophagy: the clash between damage and metabolic needs', *Cell Death Differ*, 22(3), pp. 377-88.

Filomeni, G., Desideri, E., Cardaci, S., Rotilio, G. and Ciriolo, M.R. (2010) 'Under the ROS...thiol network is the principal suspect for autophagy commitment', *Autophagy*, 6(7), pp. 999-1005.

Filomeni, G., Rotilio, G. and Ciriolo, M.R. (2002) 'Cell signalling and the glutathione redox system', *Biochem Pharmacol*, 64(5-6), pp. 1057-64.

Fimia, G.M., Kroemer, G. and Piacentini, M. (2013) 'Molecular mechanisms of selective autophagy', *Cell Death Differ*, 20(1), pp. 1-2.

Finkel, T. and Holbrook, N.J. (2000) 'Oxidants, oxidative stress and the biology of ageing', *Nature*, 408(6809), pp. 239-47.

Finley, D. (2009) 'Recognition and processing of ubiquitin-protein conjugates by the proteasome', *Annu Rev Biochem*, 78, pp. 477-513.

Finley, D., Tanaka, K., Mann, C., Feldmann, H., Hochstrasser, M., Vierstra, R., Johnston, S., Hampton, R., Haber, J., McCusker, J., Silver, P., Frontali, L., Thorsness, P., Varshavsky, A., Byers, B., Madura, K., Reed, S.I., Wolf, D., Jentsch, S., Sommer, T., Baumeister, W., Goldberg, A., Fried, V., Rubin, D.M., Toh-e, A. and et al. (1998) 'Unified nomenclature for subunits of the Saccharomyces cerevisiae proteasome regulatory particle', *Trends Biochem Sci*, 23(7), pp. 244-5.

Forman, H.J., Maiorino, M. and Ursini, F. (2010) 'Signaling functions of reactive oxygen species', *Biochemistry*, 49(5), pp. 835-42.

Fridovich, I. (1995) 'Superoxide radical and superoxide dismutases', *Annu Rev Biochem*, 64, pp. 97-112.

Fung, T.K., Yam, C.H. and Poon, R.Y. (2005) 'The N-terminal regulatory domain of cyclin A contains redundant ubiquitination targeting sequences and acceptor sites', *Cell Cycle*, 4(10), pp. 1411-20.

Fushman, D. and Walker, O. (2010) 'Exploring the linkage dependence of polyubiquitin conformations using molecular modeling', *J Mol Biol*, 395(4), pp. 803-14.

Gal, J., Strom, A.L., Kilty, R., Zhang, F. and Zhu, H. (2007) 'p62 accumulates and enhances aggregate formation in model systems of familial amyotrophic lateral sclerosis', *J Biol Chem*, 282(15), pp. 11068-77.

Gamerdinger, M., Hajieva, P., Kaya, A.M., Wolfrum, U., Hartl, F.U. and Behl, C. (2009) 'Protein quality control during aging involves recruitment of the macroautophagy pathway by BAG3', *EMBO J*, 28(7), pp. 889-901.

Ganley, I.G., Lam du, H., Wang, J., Ding, X., Chen, S. and Jiang, X. (2009) 'ULK1.ATG13.FIP200 complex mediates mTOR signaling and is essential for autophagy', *J Biol Chem*, 284(18), pp. 12297-305.

Garcia-Arencibia, M., Hochfeld, W.E., Toh, P.P. and Rubinsztein, D.C. (2010) 'Autophagy, a guardian against neurodegeneration', *Semin Cell Dev Biol*, 21(7), pp. 691-8.

Garcia-Mata, R., Bebok, Z., Sorscher, E.J. and Sztul, E.S. (1999) 'Characterization and dynamics of aggresome formation by a cytosolic GFP-chimera', *J Cell Biol*, 146(6), pp. 1239-54.

Geetha, T. and Wooten, M.W. (2003) 'Association of the atypical protein kinase C-interacting protein p62/ZIP with nerve growth factor receptor TrkA regulates receptor trafficking and Erk5 signaling', *J Biol Chem*, 278(7), pp. 4730-9.

Geisler, S., Holmstrom, K.M., Skujat, D., Fiesel, F.C., Rothfuss, O.C., Kahle, P.J. and Springer, W. (2010) 'PINK1/Parkin-mediated mitophagy is dependent on VDAC1 and p62/SQSTM1', *Nat Cell Biol*, 12(2), pp. 119-31.

Gerschman, R., Gilbert, D.L., Nye, S.W., Dwyer, P. and Fenn, W.O. (1954) 'Oxygen poisoning and x-irradiation: a mechanism in common', *Science*, 119(3097), pp. 623-6.

Ghosh, S. and Karin, M. (2002) 'Missing pieces in the NF-kappaB puzzle', *Cell*, 109 Suppl, pp. S81-96.

Gidalevitz, T., Kikis, E.A. and Morimoto, R.I. (2010) 'A cellular perspective on conformational disease: the role of genetic background and proteostasis networks', *Curr Opin Struct Biol*, 20(1), pp. 23-32.

Gidalevitz, T., Prahlad, V. and Morimoto, R.I. (2011) 'The stress of protein misfolding: from single cells to multicellular organisms', *Cold Spring Harb Perspect Biol*, 3(6).

Giles, N.M., Gutowski, N.J., Giles, G.I. and Jacob, C. (2003) 'Redox catalysts as sensitisers towards oxidative stress', *FEBS Lett*, 535(1-3), pp. 179-82.

Giordano, S., Darley-Usmar, V. and Zhang, J. (2014) 'Autophagy as an essential cellular antioxidant pathway in neurodegenerative disease', *Redox Biol*, 2, pp. 82-90.

Giorgio, M., Trinei, M., Migliaccio, E. and Pelicci, P.G. (2007) 'Hydrogen peroxide: a metabolic by-product or a common mediator of ageing signals?', *Nat Rev Mol Cell Biol*, 8(9), pp. 722-8.

Glickman, M.H. and Ciechanover, A. (2002) 'The ubiquitin-proteasome proteolytic pathway: destruction for the sake of construction', *Physiol Rev*, 82(2), pp. 373-428.

Glickman, M.H., Rubin, D.M., Coux, O., Wefes, I., Pfeifer, G., Cjeka, Z., Baumeister, W., Fried, V.A. and Finley, D. (1998) 'A subcomplex of the proteasome regulatory

particle required for ubiquitin-conjugate degradation and related to the COP9-signalosome and eIF3', *Cell*, 94(5), pp. 615-23.

Goldberg, A.L. (2012) 'Development of proteasome inhibitors as research tools and cancer drugs', *J Cell Biol*, 199(4), pp. 583-8.

Goldstein, G., Scheid, M., Hammerling, U., Schlesinger, D.H., Niall, H.D. and Boyse, E.A. (1975) 'Isolation of a polypeptide that has lymphocyte-differentiating properties and is probably represented universally in living cells', *Proc Natl Acad Sci U S A*, 72(1), pp. 11-5.

Goode, A., Butler, K., Long, J., Cavey, J., Scott, D., Shaw, B., Sollenberger, J., Gell, C., Johansen, T., Oldham, N.J., Searle, M.S. and Layfield, R. (2016) 'Defective recognition of LC3B by mutant SQSTM1/p62 implicates impairment of autophagy as a pathogenic mechanism in ALS-FTLD', *Autophagy*, 12(7), pp. 1094-104.

Gorrini, C., Harris, I.S. and Mak, T.W. (2013) 'Modulation of oxidative stress as an anticancer strategy', *Nat Rev Drug Discov*, 12(12), pp. 931-47.

Grauschopf, U., Winther, J.R., Korber, P., Zander, T., Dallinger, P. and Bardwell, J.C. (1995) 'Why is DsbA such an oxidizing disulfide catalyst?', *Cell*, 83(6), pp. 947-55.

Gregory, J.D. (1955) 'The Stability of N-Ethylmaleimide and its Reaction with Sulfhydryl Groups', *Journal of the American Chemical Society*, 77(14), pp. 3922-3923.

Groettrup, M., Pelzer, C., Schmidtke, G. and Hofmann, K. (2008) 'Activating the ubiquitin family: UBA6 challenges the field', *Trends Biochem Sci*, 33(5), pp. 230-7.

Groll, M., Bajorek, M., Kohler, A., Moroder, L., Rubin, D.M., Huber, R., Glickman, M.H. and Finley, D. (2000) 'A gated channel into the proteasome core particle', *Nat Struct Biol*, 7(11), pp. 1062-7.

Groll, M., Ditzel, L., Lowe, J., Stock, D., Bochtler, M., Bartunik, H.D. and Huber, R. (1997) 'Structure of 20S proteasome from yeast at 2.4 A resolution', *Nature*, 386(6624), pp. 463-71.

Gromer, S., Arscott, L.D., Williams, C.H., Jr., Schirmer, R.H. and Becker, K. (1998) 'Human placenta thioredoxin reductase. Isolation of the selenoenzyme, steady state kinetics, and inhibition by therapeutic gold compounds', *J Biol Chem*, 273(32), pp. 20096-101.

Guharoy, M., Bhowmick, P., Sallam, M. and Tompa, P. (2016) 'Tripartite degrons confer diversity and specificity on regulated protein degradation in the ubiquitin-proteasome system', *Nat Commun*, 7, p. 10239.

Gulden, M., Jess, A., Kammann, J., Maser, E. and Seibert, H. (2010) 'Cytotoxic potency of H2O2 in cell cultures: impact of cell concentration and exposure time', *Free Radic Biol Med*, 49(8), pp. 1298-305.

Hall, A., Karplus, P.A. and Poole, L.B. (2009) 'Typical 2-Cys peroxiredoxins--structures, mechanisms and functions', *FEBS J*, 276(9), pp. 2469-77.

Hall, A., Nelson, K., Poole, L.B. and Karplus, P.A. (2011) 'Structure-based insights into the catalytic power and conformational dexterity of peroxiredoxins', *Antioxid Redox Signal*, 15(3), pp. 795-815.

Hansen, T.E. and Johansen, T. (2011) 'Following autophagy step by step', *BMC Biol*, 9, p. 39.

Hara, K., Maruki, Y., Long, X., Yoshino, K., Oshiro, N., Hidayat, S., Tokunaga, C., Avruch, J. and Yonezawa, K. (2002) 'Raptor, a binding partner of target of rapamycin (TOR), mediates TOR action', *Cell*, 110(2), pp. 177-89.

Hara, T., Nakamura, K., Matsui, M., Yamamoto, A., Nakahara, Y., Suzuki-Migishima, R., Yokoyama, M., Mishima, K., Saito, I., Okano, H. and Mizushima, N. (2006) 'Suppression of basal autophagy in neural cells causes neurodegenerative disease in mice', *Nature*, 441(7095), pp. 885-9.

Harding, T.M., Hefner-Gravink, A., Thumm, M. and Klionsky, D.J. (1996) 'Genetic and phenotypic overlap between autophagy and the cytoplasm to vacuole protein targeting pathway', *J Biol Chem*, 271(30), pp. 17621-4.

Harding, T.M., Morano, K.A., Scott, S.V. and Klionsky, D.J. (1995) 'Isolation and characterization of yeast mutants in the cytoplasm to vacuole protein targeting pathway', *J Cell Biol*, 131(3), pp. 591-602.

Harman, D. (1956) 'Aging: a theory based on free radical and radiation chemistry', *J Gerontol*, 11(3), pp. 298-300.

Harman, D. (1972) 'The biologic clock: the mitochondria?', *J Am Geriatr Soc*, 20(4), pp. 145-7.

Hartl, F.U., Bracher, A. and Hayer-Hartl, M. (2011) 'Molecular chaperones in protein folding and proteostasis', *Nature*, 475(7356), pp. 324-32.

Hay, N. and Sonenberg, N. (2004) 'Upstream and downstream of mTOR', *Genes Dev*, 18(16), pp. 1926-45.

He, C. and Klionsky, D.J. (2009) 'Regulation mechanisms and signaling pathways of autophagy', *Annu Rev Genet*, 43, pp. 67-93.

Heitman, J., Movva, N.R. and Hall, M.N. (1991) 'Targets for cell cycle arrest by the immunosuppressant rapamycin in yeast', *Science*, 253(5022), pp. 905-9.

Hershko, A. and Ciechanover, A. (1998) 'The ubiquitin system', *Annu Rev Biochem*, 67, pp. 425-79.

Hershko, A., Ciechanover, A. and Varshavsky, A. (2000) 'Basic Medical Research Award. The ubiquitin system', *Nat Med*, 6(10), pp. 1073-81.

Hershko, A., Heller, H., Elias, S. and Ciechanover, A. (1983) 'Components of ubiquitin-protein ligase system. Resolution, affinity purification, and role in protein breakdown', *J Biol Chem*, 258(13), pp. 8206-14.

Hetz, C. (2012) 'The unfolded protein response: controlling cell fate decisions under ER stress and beyond', *Nat Rev Mol Cell Biol*, 13(2), pp. 89-102.

Hewitt, G., Carroll, B., Sarallah, R., Correia-Melo, C., Ogrodnik, M., Nelson, G., Otten, E.G., Manni, D., Antrobus, R., Morgan, B.A., von Zglinicki, T., Jurk, D., Seluanov, A., Gorbunova, V., Johansen, T., Passos, J.F. and Korolchuk, V.I. (2016) 'SQSTM1/p62 mediates crosstalk between autophagy and the UPS in DNA repair', *Autophagy*, p. 0.

Hofmann, B., Hecht, H.J. and Flohe, L. (2002) 'Peroxiredoxins', *Biol Chem*, 383(3-4), pp. 347-64.

Hohfeld, J., Minami, Y. and Hartl, F.U. (1995) 'Hip, a novel cochaperone involved in the eukaryotic Hsc70/Hsp40 reaction cycle', *Cell*, 83(4), pp. 589-98.

Holmstrom, K.M. and Finkel, T. (2014) 'Cellular mechanisms and physiological consequences of redox-dependent signalling', *Nat Rev Mol Cell Biol*, 15(6), pp. 411-21.

Hosokawa, N., Hara, T., Kaizuka, T., Kishi, C., Takamura, A., Miura, Y., Iemura, S., Natsume, T., Takehana, K., Yamada, N., Guan, J.L., Oshiro, N. and Mizushima, N. (2009a) 'Nutrient-dependent mTORC1 association with the ULK1-Atg13-FIP200 complex required for autophagy', *Mol Biol Cell*, 20(7), pp. 1981-91.

Hosokawa, N., Sasaki, T., Iemura, S., Natsume, T., Hara, T. and Mizushima, N. (2009b) 'Atg101, a novel mammalian autophagy protein interacting with Atg13', *Autophagy*, 5(7), pp. 973-9.

Huang, W.P. and Klionsky, D.J. (2002) 'Autophagy in yeast: a review of the molecular machinery', *Cell Struct Funct*, 27(6), pp. 409-20.

Hurley, J.H., Lee, S. and Prag, G. (2006) 'Ubiquitin-binding domains', *Biochem J*, 399(3), pp. 361-72.

Hybertson, B.M., Gao, B., Bose, S.K. and McCord, J.M. (2011) 'Oxidative stress in health and disease: the therapeutic potential of Nrf2 activation', *Mol Aspects Med*, 32(4-6), pp. 234-46.

Ichimura, Y., Kirisako, T., Takao, T., Satomi, Y., Shimonishi, Y., Ishihara, N., Mizushima, N., Tanida, I., Kominami, E., Ohsumi, M., Noda, T. and Ohsumi, Y. (2000) 'A ubiquitin-like system mediates protein lipidation', *Nature*, 408(6811), pp. 488-92.

Ichimura, Y., Kumanomidou, T., Sou, Y.S., Mizushima, T., Ezaki, J., Ueno, T., Kominami, E., Yamane, T., Tanaka, K. and Komatsu, M. (2008) 'Structural basis for

sorting mechanism of p62 in selective autophagy', *J Biol Chem*, 283(33), pp. 22847-57.

Inada, H., Mukai, J., Matsushima, S. and Tanaka, T. (1997) 'QM is a novel zinc-binding transcription regulatory protein: its binding to c-Jun is regulated by zinc ions and phosphorylation by protein kinase C', *Biochem Biophys Res Commun*, 230(2), pp. 331-4.

Inoki, K., Li, Y., Xu, T. and Guan, K.L. (2003a) 'Rheb GTPase is a direct target of TSC2 GAP activity and regulates mTOR signaling', *Genes Dev*, 17(15), pp. 1829-34.

Inoki, K., Zhu, T. and Guan, K.L. (2003b) 'TSC2 mediates cellular energy response to control cell growth and survival', *Cell*, 115(5), pp. 577-90.

Isogai, S., Morimoto, D., Arita, K., Unzai, S., Tenno, T., Hasegawa, J., Sou, Y.S., Komatsu, M., Tanaka, K., Shirakawa, M. and Tochio, H. (2011) 'Crystal structure of the ubiquitin-associated (UBA) domain of p62 and its interaction with ubiquitin', *J Biol Chem*, 286(36), pp. 31864-74.

Itakura, E. and Mizushima, N. (2011) 'p62 Targeting to the autophagosome formation site requires self-oligomerization but not LC3 binding', *J Cell Biol*, 192(1), pp. 17-27.

Itoh, K., Chiba, T., Takahashi, S., Ishii, T., Igarashi, K., Katoh, Y., Oyake, T., Hayashi, N., Satoh, K., Hatayama, I., Yamamoto, M. and Nabeshima, Y. (1997) 'An Nrf2/small Maf heterodimer mediates the induction of phase II detoxifying enzyme genes through antioxidant response elements', *Biochem Biophys Res Commun*, 236(2), pp. 313-22.

Itoh, K., Wakabayashi, N., Katoh, Y., Ishii, T., Igarashi, K., Engel, J.D. and Yamamoto, M. (1999) 'Keap1 represses nuclear activation of antioxidant responsive elements by Nrf2 through binding to the amino-terminal Neh2 domain', *Genes Dev*, 13(1), pp. 76-86.

Jain, A., Lamark, T., Sjottem, E., Larsen, K.B., Awuh, J.A., Overvatn, A., McMahon, M., Hayes, J.D. and Johansen, T. (2010) 'p62/SQSTM1 is a target gene for transcription factor NRF2 and creates a positive feedback loop by inducing antioxidant response element-driven gene transcription', *J Biol Chem*, 285(29), pp. 22576-91.

Jaken, S. (1996) 'Protein kinase C isozymes and substrates', *Curr Opin Cell Biol*, 8(2), pp. 168-73.

Jang, H.H., Lee, K.O., Chi, Y.H., Jung, B.G., Park, S.K., Park, J.H., Lee, J.R., Lee, S.S., Moon, J.C., Yun, J.W., Choi, Y.O., Kim, W.Y., Kang, J.S., Cheong, G.W., Yun, D.J., Rhee, S.G., Cho, M.J. and Lee, S.Y. (2004) 'Two enzymes in one; two yeast peroxiredoxins display oxidative stress-dependent switching from a peroxidase to a molecular chaperone function', *Cell*, 117(5), pp. 625-35.

Jaramillo, M.C. and Zhang, D.D. (2013) 'The emerging role of the Nrf2-Keap1 signaling pathway in cancer', *Genes Dev*, 27(20), pp. 2179-91.

Jeong, W., Bae, S.H., Toledano, M.B. and Rhee, S.G. (2012) 'Role of sulfiredoxin as a regulator of peroxiredoxin function and regulation of its expression', *Free Radic Biol Med*, 53(3), pp. 447-56.

Jiang, J., Parameshwaran, K., Seibenhener, M.L., Kang, M.G., Suppiramaniam, V., Huganir, R.L., Diaz-Meco, M.T. and Wooten, M.W. (2009) 'AMPA receptor trafficking and synaptic plasticity require SQSTM1/p62', *Hippocampus*, 19(4), pp. 392-406.

Jin, W., Chang, M., Paul, E.M., Babu, G., Lee, A.J., Reiley, W., Wright, A., Zhang, M., You, J. and Sun, S.C. (2008) 'Deubiquitinating enzyme CYLD negatively regulates RANK signaling and osteoclastogenesis in mice', *J Clin Invest*, 118(5), pp. 1858-66.

Jin, Z., Li, Y., Pitti, R., Lawrence, D., Pham, V.C., Lill, J.R. and Ashkenazi, A. (2009) 'Cullin3-based polyubiquitination and p62-dependent aggregation of caspase-8 mediate extrinsic apoptosis signaling', *Cell*, 137(4), pp. 721-35.

Johansen, T. and Lamark, T. (2011) 'Selective autophagy mediated by autophagic adapter proteins', *Autophagy*, 7(3), pp. 279-96.

Johansen, T. and Sachse, C. (2015) 'The higher-order molecular organization of p62/SQSTM1', *Oncotarget*.

Johnston, J.A., Ward, C.L. and Kopito, R.R. (1998) 'Aggresomes: a cellular response to misfolded proteins', *J Cell Biol*, 143(7), pp. 1883-98.

Jones, D.P. (2008) 'Radical-free biology of oxidative stress', *Am J Physiol Cell Physiol*, 295(4), pp. C849-68.

Jono, H., Lim, J.H., Chen, L.F., Xu, H., Trompouki, E., Pan, Z.K., Mosialos, G. and Li, J.D. (2004) 'NF-kappaB is essential for induction of CYLD, the negative regulator of NF-kappaB: evidence for a novel inducible autoregulatory feedback pathway', *J Biol Chem*, 279(35), pp. 36171-4.

Juhasz, G. and Neufeld, T.P. (2006) 'Autophagy: a forty-year search for a missing membrane source', *PLoS Biol*, 4(2), p. e36.

Jung, C.H., Jun, C.B., Ro, S.H., Kim, Y.M., Otto, N.M., Cao, J., Kundu, M. and Kim, D.H. (2009) 'ULK-Atg13-FIP200 complexes mediate mTOR signaling to the autophagy machinery', *Mol Biol Cell*, 20(7), pp. 1992-2003.

Kabeya, Y., Mizushima, N., Ueno, T., Yamamoto, A., Kirisako, T., Noda, T., Kominami, E., Ohsumi, Y. and Yoshimori, T. (2000) 'LC3, a mammalian homologue of yeast Apg8p, is localized in autophagosome membranes after processing', *EMBO J*, 19(21), pp. 5720-8.

Kampinga, H.H. and Craig, E.A. (2010) 'The HSP70 chaperone machinery: J proteins as drivers of functional specificity', *Nat Rev Mol Cell Biol*, 11(8), pp. 579-92.

Kang, R., Zeh, H.J., Lotze, M.T. and Tang, D. (2011) 'The Beclin 1 network regulates autophagy and apoptosis', *Cell Death Differ*, 18(4), pp. 571-80.

Karin, M. and Ben-Neriah, Y. (2000) 'Phosphorylation meets ubiquitination: the control of NF-[kappa]B activity', *Annu Rev Immunol*, 18, pp. 621-63.

Kasai, H. (1997) 'Analysis of a form of oxidative DNA damage, 8-hydroxy-2′-deoxyguanosine, as a marker of cellular oxidative stress during carcinogenesis', *Mutation Research/Reviews in Mutation Research*, 387(3), pp. 147-163.

Katsuragi, Y., Ichimura, Y. and Komatsu, M. (2015) 'p62/SQSTM1 functions as a signaling hub and an autophagy adaptor', *FEBS J*, 282(24), pp. 4672-8.

Kaushik, S., Bandyopadhyay, U., Sridhar, S., Kiffin, R., Martinez-Vicente, M., Kon, M., Orenstein, S.J., Wong, E. and Cuervo, A.M. (2011) 'Chaperone-mediated autophagy at a glance', *J Cell Sci*, 124(Pt 4), pp. 495-9.

Kaushik, S. and Cuervo, A.M. (2012) 'Chaperone-mediated autophagy: a unique way to enter the lysosome world', *Trends Cell Biol*, 22(8), pp. 407-17.

Kaushik, S., Massey, A.C. and Cuervo, A.M. (2006) 'Lysosome membrane lipid microdomains: novel regulators of chaperone-mediated autophagy', *EMBO J*, 25(17), pp. 3921-33.

Kawaguchi, Y., Kovacs, J.J., McLaurin, A., Vance, J.M., Ito, A. and Yao, T.P. (2003) 'The deacetylase HDAC6 regulates aggresome formation and cell viability in response to misfolded protein stress', *Cell*, 115(6), pp. 727-38.

Khaminets, A., Behl, C. and Dikic, I. (2016) 'Ubiquitin-Dependent And Independent Signals In Selective Autophagy', *Trends Cell Biol*, 26(1), pp. 6-16.

Kiffin, R., Christian, C., Knecht, E. and Cuervo, A.M. (2004) 'Activation of chaperone-mediated autophagy during oxidative stress', *Mol Biol Cell*, 15(11), pp. 4829-40.

Kim, H.T., Kim, K.P., Lledias, F., Kisselev, A.F., Scaglione, K.M., Skowyra, D., Gygi, S.P. and Goldberg, A.L. (2007) 'Certain pairs of ubiquitin-conjugating enzymes (E2s) and ubiquitin-protein ligases (E3s) synthesize nondegradable forked ubiquitin chains containing all possible isopeptide linkages', *J Biol Chem*, 282(24), pp. 17375-86.

Kim, J., Scott, S.V., Oda, M.N. and Klionsky, D.J. (1997) 'Transport of a large oligomeric protein by the cytoplasm to vacuole protein targeting pathway', *J Cell Biol*, 137(3), pp. 609-18.

Kim, Y.E., Hipp, M.S., Bracher, A., Hayer-Hartl, M. and Hartl, F.U. (2013) 'Molecular chaperone functions in protein folding and proteostasis', *Annu Rev Biochem*, 82, pp. 323-55.

King, R.W., Glotzer, M. and Kirschner, M.W. (1996) 'Mutagenic analysis of the destruction signal of mitotic cyclins and structural characterization of ubiquitinated intermediates', *Mol Biol Cell*, 7(9), pp. 1343-57.

Kirisako, T., Ichimura, Y., Okada, H., Kabeya, Y., Mizushima, N., Yoshimori, T., Ohsumi, M., Takao, T., Noda, T. and Ohsumi, Y. (2000) 'The reversible modification

regulates the membrane-binding state of Apg8/Aut7 essential for autophagy and the cytoplasm to vacuole targeting pathway', *J Cell Biol*, 151(2), pp. 263-76.

Kirkin, V., Lamark, T., Sou, Y.S., Bjorkoy, G., Nunn, J.L., Bruun, J.A., Shvets, E., McEwan, D.G., Clausen, T.H., Wild, P., Bilusic, I., Theurillat, J.P., Overvatn, A., Ishii, T., Elazar, Z., Komatsu, M., Dikic, I. and Johansen, T. (2009a) 'A role for NBR1 in autophagosomal degradation of ubiquitinated substrates', *Mol Cell*, 33(4), pp. 505-16.

Kirkin, V., McEwan, D.G., Novak, I. and Dikic, I. (2009b) 'A role for ubiquitin in selective autophagy', *Mol Cell*, 34(3), pp. 259-69.

Klionsky, D.J., Abdelmohsen, K., Abe, A., Abedin, M.J., Abeliovich, H., Acevedo Arozena, A., Adachi, H., Adams, C.M., Adams, P.D., Adeli, K., Adhihetty, P.J., Adler, S.G., Agam, G., Agarwal, R., Aghi, M.K., Agnello, M., Agostinis, P., Aguilar, P.V., Aguirre-Ghiso, J., Airoldi, E.M., Ait-Si-Ali, S., Akematsu, T., Akporiaye, E.T., Al-Rubeai, M., Albaiceta, G.M., Albanese, C., Albani, D., Albert, M.L., Aldudo, J., Algul, H., Alirezaei, M., Alloza, I., Almasan, A., Almonte-Beceril, M., Alnemri, E.S., Alonso, C., Altan-Bonnet, N., Altieri, D.C., Alvarez, S., Alvarez-Erviti, L., Alves, S., Amadoro, G., Amano, A., Amantini, C., Ambrosio, S., Amelio, I., Amer, A.O., Amessou, M., Amon, A., An, Z., Anania, F.A., Andersen, S.U., Andley, U.P., Andreadi, C.K., Andrieu-Abadie, N., Anel, A., Ann, D.K., Anoopkumar-Dukie, S., Antonioli, M., Aoki, H., Apostolova, N., Aquila, S., Aquilano, K., Araki, K., Arama, E., Aranda, A., Araya, J., Arcaro, A., Arias, E., Arimoto, H., Ariosa, A.R., Armstrong, J.L., Arnould, T., Arsov, I., Asanuma, K., et al. (2016) 'Guidelines for the use and interpretation of assays for monitoring autophagy (3rd edition)', *Autophagy*, 12(1), pp. 1-222.

Klionsky, D.J., Cregg, J.M., Dunn, W.A., Jr., Emr, S.D., Sakai, Y., Sandoval, I.V., Sibirny, A., Subramani, S., Thumm, M., Veenhuis, M. and Ohsumi, Y. (2003) 'A unified nomenclature for yeast autophagy-related genes', *Dev Cell*, 5(4), pp. 539-45.

Klionsky, D.J. and Emr, S.D. (2000) 'Autophagy as a regulated pathway of cellular degradation', *Science*, 290(5497), pp. 1717-21.

Kobayashi, A., Kang, M.I., Okawa, H., Ohtsuji, M., Zenke, Y., Chiba, T., Igarashi, K. and Yamamoto, M. (2004) 'Oxidative stress sensor Keap1 functions as an adaptor for Cul3-based E3 ligase to regulate proteasomal degradation of Nrf2', *Mol Cell Biol*, 24(16), pp. 7130-9.

Komander, D. (2009) 'The emerging complexity of protein ubiquitination', *Biochem Soc Trans*, 37(Pt 5), pp. 937-53.

Komatsu, M. and Ichimura, Y. (2010) 'Physiological significance of selective degradation of p62 by autophagy', *FEBS Lett*, 584(7), pp. 1374-8.

Komatsu, M., Kurokawa, H., Waguri, S., Taguchi, K., Kobayashi, A., Ichimura, Y., Sou, Y.S., Ueno, I., Sakamoto, A., Tong, K.I., Kim, M., Nishito, Y., Iemura, S., Natsume, T., Ueno, T., Kominami, E., Motohashi, H., Tanaka, K. and Yamamoto, M. (2010) 'The selective autophagy substrate p62 activates the stress responsive

transcription factor Nrf2 through inactivation of Keap1', *Nat Cell Biol*, 12(3), pp. 213-23.

Komatsu, M., Ueno, T., Waguri, S., Uchiyama, Y., Kominami, E. and Tanaka, K. (2007a) 'Constitutive autophagy: vital role in clearance of unfavorable proteins in neurons', *Cell Death Differ*, 14(5), pp. 887-94.

Komatsu, M., Waguri, S., Chiba, T., Murata, S., Iwata, J., Tanida, I., Ueno, T., Koike, M., Uchiyama, Y., Kominami, E. and Tanaka, K. (2006) 'Loss of autophagy in the central nervous system causes neurodegeneration in mice', *Nature*, 441(7095), pp. 880-4.

Komatsu, M., Waguri, S., Koike, M., Sou, Y.S., Ueno, T., Hara, T., Mizushima, N., Iwata, J., Ezaki, J., Murata, S., Hamazaki, J., Nishito, Y., Iemura, S., Natsume, T., Yanagawa, T., Uwayama, J., Warabi, E., Yoshida, H., Ishii, T., Kobayashi, A., Yamamoto, M., Yue, Z., Uchiyama, Y., Kominami, E. and Tanaka, K. (2007b) 'Homeostatic levels of p62 control cytoplasmic inclusion body formation in autophagy-deficient mice', *Cell*, 131(6), pp. 1149-63.

Kopito, R.R. (2000) 'Aggresomes, inclusion bodies and protein aggregation', *Trends Cell Biol*, 10(12), pp. 524-30.

Korolchuk, V.I., Mansilla, A., Menzies, F.M. and Rubinsztein, D.C. (2009) 'Autophagy inhibition compromises degradation of ubiquitin-proteasome pathway substrates', *Mol Cell*, 33(4), pp. 517-27.

Korolchuk, V.I., Menzies, F.M. and Rubinsztein, D.C. (2010) 'Mechanisms of cross-talk between the ubiquitin-proteasome and autophagy-lysosome systems', *FEBS Lett*, 584(7), pp. 1393-8.

Korolchuk, V.I., Saiki, S., Lichtenberg, M., Siddiqi, F.H., Roberts, E.A., Imarisio, S., Jahreiss, L., Sarkar, S., Futter, M., Menzies, F.M., O'Kane, C.J., Deretic, V. and Rubinsztein, D.C. (2011) 'Lysosomal positioning coordinates cellular nutrient responses', *Nat Cell Biol*, 13(4), pp. 453-60.

Kovalenko, A., Chable-Bessia, C., Cantarella, G., Israel, A., Wallach, D. and Courtois, G. (2003) 'The tumour suppressor CYLD negatively regulates NF-kappaB signalling by deubiquitination', *Nature*, 424(6950), pp. 801-5.

Kroemer, G., Galluzzi, L. and Brenner, C. (2007) 'Mitochondrial membrane permeabilization in cell death', *Physiol Rev*, 87(1), pp. 99-163.

Kubli, D.A. and Gustafsson, A.B. (2012) 'Mitochondria and mitophagy: the yin and yang of cell death control', *Circ Res*, 111(9), pp. 1208-21.

Kuma, A., Mizushima, N., Ishihara, N. and Ohsumi, Y. (2002) 'Formation of the approximately 350-kDa Apg12-Apg5.Apg16 multimeric complex, mediated by Apg16 oligomerization, is essential for autophagy in yeast', *J Biol Chem*, 277(21), pp. 18619-25.

Kuusisto, E., Kauppinen, T. and Alafuzoff, I. (2008) 'Use of p62/SQSTM1 antibodies for neuropathological diagnosis', *Neuropathol Appl Neurobiol*, 34(2), pp. 169-80.

Kuusisto, E., Salminen, A. and Alafuzoff, I. (2001) 'Ubiquitin-binding protein p62 is present in neuronal and glial inclusions in human tauopathies and synucleinopathies', *Neuroreport*, 12(10), pp. 2085-90.

Labbadia, J. and Morimoto, R.I. (2014) 'Proteostasis and longevity: when does aging really begin?', *F1000Prime Rep*, 6, p. 7.

Labbadia, J. and Morimoto, R.I. (2015) 'The biology of proteostasis in aging and disease', *Annu Rev Biochem*, 84, pp. 435-64.

Lam, Y.A., Lawson, T.G., Velayutham, M., Zweier, J.L. and Pickart, C.M. (2002) 'A proteasomal ATPase subunit recognizes the polyubiquitin degradation signal', *Nature*, 416(6882), pp. 763-7.

Lamark, T. and Johansen, T. (2012) 'Aggrephagy: selective disposal of protein aggregates by macroautophagy', *Int J Cell Biol*, 2012, p. 736905.

Lamark, T., Kirkin, V., Dikic, I. and Johansen, T. (2009) 'NBR1 and p62 as cargo receptors for selective autophagy of ubiquitinated targets', *Cell Cycle*, 8(13), pp. 1986-90.

Lamark, T., Perander, M., Outzen, H., Kristiansen, K., Overvatn, A., Michaelsen, E., Bjorkoy, G. and Johansen, T. (2003) 'Interaction codes within the family of mammalian Phox and Bem1p domain-containing proteins', *J Biol Chem*, 278(36), pp. 34568-81.

Lamb, C.A., Yoshimori, T. and Tooze, S.A. (2013) 'The autophagosome: origins unknown, biogenesis complex', *Nat Rev Mol Cell Biol*, 14(12), pp. 759-74.

Landry, J.J., Pyl, P.T., Rausch, T., Zichner, T., Tekkedil, M.M., Stutz, A.M., Jauch, A., Aiyar, R.S., Pau, G., Delhomme, N., Gagneur, J., Korbel, J.O., Huber, W. and Steinmetz, L.M. (2013) 'The genomic and transcriptomic landscape of a HeLa cell line', *G3 (Bethesda)*, 3(8), pp. 1213-24.

Laplante, M. and Sabatini, D.M. (2009) 'mTOR signaling at a glance', *J Cell Sci*, 122(Pt 20), pp. 3589-94.

Latimer, H.R. and Veal, E.A. (2016) 'Peroxiredoxins in Regulation of MAPK Signalling Pathways; Sensors and Barriers to Signal Transduction', *Mol Cells*, 39(1), pp. 40-5.

Lau, A., Wang, X.J., Zhao, F., Villeneuve, N.F., Wu, T., Jiang, T., Sun, Z., White, E. and Zhang, D.D. (2010) 'A noncanonical mechanism of Nrf2 activation by autophagy deficiency: direct interaction between Keap1 and p62', *Mol Cell Biol*, 30(13), pp. 3275-85.

Lawrence, B.P. and Brown, W.J. (1993) 'Inhibition of protein synthesis separates autophagic sequestration from the delivery of lysosomal enzymes', *J Cell Sci*, 105 (Pt 2), pp. 473-80.

Layfield, R., Ciani, B., Ralston, S.H., Hocking, L.J., Sheppard, P.W., Searle, M.S. and Cavey, J.R. (2004) 'Structural and functional studies of mutations affecting the UBA domain of SQSTM1 (p62) which cause Paget's disease of bone', *Biochem Soc Trans*, 32(Pt 5), pp. 728-30.

Layfield, R., Lowe, J. and Bedford, L. (2005) 'The ubiquitin-proteasome system and neurodegenerative disorders', *Essays Biochem*, 41, pp. 157-71.

Lazarou, M., Sliter, D.A., Kane, L.A., Sarraf, S.A., Wang, C., Burman, J.L., Sideris, D.P., Fogel, A.I. and Youle, R.J. (2015) 'The ubiquitin kinase PINK1 recruits autophagy receptors to induce mitophagy', *Nature*, 524(7565), pp. 309-14.

Lee, D.H. and Goldberg, A.L. (1998) 'Proteasome inhibitors: valuable new tools for cell biologists', *Trends Cell Biol*, 8(10), pp. 397-403.

Lee, J.Y., Koga, H., Kawaguchi, Y., Tang, W., Wong, E., Gao, Y.S., Pandey, U.B., Kaushik, S., Tresse, E., Lu, J., Taylor, J.P., Cuervo, A.M. and Yao, T.P. (2010a) 'HDAC6 controls autophagosome maturation essential for ubiquitin-selective quality-control autophagy', *EMBO J*, 29(5), pp. 969-80.

Lee, J.Y., Nagano, Y., Taylor, J.P., Lim, K.L. and Yao, T.P. (2010b) 'Disease-causing mutations in parkin impair mitochondrial ubiquitination, aggregation, and HDAC6-dependent mitophagy', *J Cell Biol*, 189(4), pp. 671-9.

Lee, J.G., Baek, K., Soetandyo, N. and Ye, Y. (2013) 'Reversible inactivation of deubiquitinases by reactive oxygen species in vitro and in cells', *Nat Commun*, 4, p. 1568.

Lenaz, G. (2001) 'The mitochondrial production of reactive oxygen species: mechanisms and implications in human pathology', *IUBMB Life*, 52(3-5), pp. 159-64.

Levine, B. and Kroemer, G. (2008) 'Autophagy in the pathogenesis of disease', *Cell*, 132(1), pp. 27-42.

Levine, B. and Yuan, J. (2005) 'Autophagy in cell death: an innocent convict?', *J Clin Invest*, 115(10), pp. 2679-88.

Li, H., Wittwer, T., Weber, A., Schneider, H., Moreno, R., Maine, G.N., Kracht, M., Schmitz, M.L. and Burstein, E. (2012a) 'Regulation of NF-kappaB activity by competition between RelA acetylation and ubiquitination', *Oncogene*, 31(5), pp. 611-23.

Li, W., Bengtson, M.H., Ulbrich, A., Matsuda, A., Reddy, V.A., Orth, A., Chanda, S.K., Batalov, S. and Joazeiro, C.A. (2008) 'Genome-wide and functional annotation of human E3 ubiquitin ligases identifies MULAN, a mitochondrial E3 that regulates the organelle's dynamics and signaling', *PLoS One*, 3(1), p. e1487.

Li, W.W., Li, J. and Bao, J.K. (2012b) 'Microautophagy: lesser-known self-eating', *Cell Mol Life Sci*, 69(7), pp. 1125-36.

Liang, C., Feng, P., Ku, B., Dotan, I., Canaani, D., Oh, B.H. and Jung, J.U. (2006) 'Autophagic and tumour suppressor activity of a novel Beclin1-binding protein UVRAG', *Nat Cell Biol*, 8(7), pp. 688-99.

Liang, X.H., Kleeman, L.K., Jiang, H.H., Gordon, G., Goldman, J.E., Berry, G., Herman, B. and Levine, B. (1998) 'Protection against fatal Sindbis virus encephalitis by beclin, a novel Bcl-2-interacting protein', *J Virol*, 72(11), pp. 8586-96.

Lilienbaum, A. (2013) 'Relationship between the proteasomal system and autophagy', *Int J Biochem Mol Biol*, 4(1), pp. 1-26.

Lim, J., Lachenmayer, M.L., Wu, S., Liu, W., Kundu, M., Wang, R., Komatsu, M., Oh, Y.J., Zhao, Y. and Yue, Z. (2015) 'Proteotoxic Stress Induces Phosphorylation of p62/SQSTM1 by ULK1 to Regulate Selective Autophagic Clearance of Protein Aggregates', *PLoS Genet*, 11(2), p. e1004987.

Lim, J.C., Choi, H.I., Park, Y.S., Nam, H.W., Woo, H.A., Kwon, K.S., Kim, Y.S., Rhee, S.G., Kim, K. and Chae, H.Z. (2008) 'Irreversible oxidation of the active-site cysteine of peroxiredoxin to cysteine sulfonic acid for enhanced molecular chaperone activity', *J Biol Chem*, 283(43), pp. 28873-80.

Lin, H., Bhatia, R. and Lal, R. (2001) 'Amyloid beta protein forms ion channels: implications for Alzheimer's disease pathophysiology', *FASEB J*, 15(13), pp. 2433-44.

Lin, X., Li, S., Zhao, Y., Ma, X., Zhang, K., He, X. and Wang, Z. (2013) 'Interaction Domains of p62: A Bridge Between p62 and Selective Autophagy', *DNA Cell Biol*.

Lipkowitz, S. and Weissman, A.M. (2011) 'RINGs of good and evil: RING finger ubiquitin ligases at the crossroads of tumour suppression and oncogenesis', *Nat Rev Cancer*, 11(9), pp. 629-43.

Liu, M., Li, X.L. and Hassel, B.A. (2003) 'Proteasomes modulate conjugation to the ubiquitin-like protein, ISG15', *J Biol Chem*, 278(3), pp. 1594-602.

Liu, T., Daniels, C.K. and Cao, S. (2012) 'Comprehensive review on the HSC70 functions, interactions with related molecules and involvement in clinical diseases and therapeutic potential', *Pharmacol Ther*, 136(3), pp. 354-74.

Lo, S.C., Li, X., Henzl, M.T., Beamer, L.J. and Hannink, M. (2006) 'Structure of the Keap1:Nrf2 interface provides mechanistic insight into Nrf2 signaling', *EMBO J*, 25(15), pp. 3605-17.

Loewith, R., Jacinto, E., Wullschleger, S., Lorberg, A., Crespo, J.L., Bonenfant, D., Oppliger, W., Jenoe, P. and Hall, M.N. (2002) 'Two TOR complexes, only one of which is rapamycin sensitive, have distinct roles in cell growth control', *Mol Cell*, 10(3), pp. 457-68.

Long, J., Gallagher, T.R., Cavey, J.R., Sheppard, P.W., Ralston, S.H., Layfield, R. and Searle, M.S. (2008) 'Ubiquitin recognition by the ubiquitin-associated domain of p62 involves a novel conformational switch', *J Biol Chem*, 283(9), pp. 5427-40.

Loo, T.W. and Clarke, D.M. (2006) 'Using a cysteine-less mutant to provide insight into the structure and mechanism of CFTR', *J Physiol*, 572(Pt 2), p. 312.

Lowe, J., Stock, D., Jap, B., Zwickl, P., Baumeister, W. and Huber, R. (1995) 'Crystal structure of the 20S proteasome from the archaeon T. acidophilum at 3.4 A resolution', *Science*, 268(5210), pp. 533-9.

Lu, J. and Holmgren, A. (2009) 'Selenoproteins', *J Biol Chem*, 284(2), pp. 723-7.

Lu, J. and Holmgren, A. (2014) 'The thioredoxin antioxidant system', *Free Radic Biol Med*, 66, pp. 75-87.

Luders, J., Demand, J. and Hohfeld, J. (2000) 'The ubiquitin-related BAG-1 provides a link between the molecular chaperones Hsc70/Hsp70 and the proteasome', *J Biol Chem*, 275(7), pp. 4613-7.

Luehrs, D.C., Roher, A.E. and Stephen, W.W. (2007) 'Demonstration of the Fenton Reaction', *Journal of Chemical Education*, 84(8), p. 1290.

Lynch-Day, M.A. and Klionsky, D.J. (2010) 'The Cvt pathway as a model for selective autophagy', *FEBS Lett*, 584(7), pp. 1359-66.

Mancias, J.D. and Kimmelman, A.C. (2016) 'Mechanisms of Selective Autophagy in Normal Physiology and Cancer', *J Mol Biol*, 428(9 Pt A), pp. 1659-80.

Maruyama, K. (1991) 'The Discovery of Adenosine-Triphosphate and the Establishment of Its Structure', *Journal of the History of Biology*, 24(1), pp. 145-154.

Matsumoto, G., Shimogori, T., Hattori, N. and Nukina, N. (2015) 'TBK1 controls autophagosomal engulfment of polyubiquitinated mitochondria through p62/SQSTM1 phosphorylation', *Hum Mol Genet*, 24(15), pp. 4429-42.

Matsumoto, G., Wada, K., Okuno, M., Kurosawa, M. and Nukina, N. (2011) 'Serine 403 phosphorylation of p62/SQSTM1 regulates selective autophagic clearance of ubiquitinated proteins', *Mol Cell*, 44(2), pp. 279-89.

Mattson, M.P., Culmsee, C., Yu, Z. and Camandola, S. (2000) 'Roles of nuclear factor kappaB in neuronal survival and plasticity', *J Neurochem*, 74(2), pp. 443-56.

McCord, J.M. and Fridovich, I. (1969) 'Superoxide dismutase. An enzymic function for erythrocuprein (hemocuprein)', *J Biol Chem*, 244(22), pp. 6049-55.

Meister, A. and Anderson, M.E. (1983) 'Glutathione', *Annu Rev Biochem*, 52, pp. 711-60.

Melo, A., Monteiro, L., Lima, R.M., Oliveira, D.M., Cerqueira, M.D. and El-Bacha, R.S. (2011) 'Oxidative stress in neurodegenerative diseases: mechanisms and therapeutic perspectives', *Oxid Med Cell Longev*, 2011, p. 467180.

Mercer, C.A., Kaliappan, A. and Dennis, P.B. (2009) 'A novel, human Atg13 binding protein, Atg101, interacts with ULK1 and is essential for macroautophagy', *Autophagy*, 5(5), pp. 649-62.

Metzger, M.B., Hristova, V.A. and Weissman, A.M. (2012) 'HECT and RING finger families of E3 ubiquitin ligases at a glance', *J Cell Sci*, 125(Pt 3), pp. 531-7.

Mijaljica, D., Prescott, M. and Devenish, R.J. (2011) 'Microautophagy in mammalian cells: revisiting a 40-year-old conundrum', *Autophagy*, 7(7), pp. 673-82.

Milo, R. (2013) 'What is the total number of protein molecules per cell volume? A call to rethink some published values', *Bioessays*, 35(12), pp. 1050-5.

Miseta, A. and Csutora, P. (2000) 'Relationship between the occurrence of cysteine in proteins and the complexity of organisms', *Mol Biol Evol*, 17(8), pp. 1232-9.

Mizushima, N. (2005) 'The pleiotropic role of autophagy: from protein metabolism to bactericide', *Cell Death Differ*, 12 Suppl 2, pp. 1535-41.

Mizushima, N. (2007) 'Autophagy: process and function', *Genes Dev*, 21(22), pp. 2861-73.

Mizushima, N. (2010) 'The role of the Atg1/ULK1 complex in autophagy regulation', *Curr Opin Cell Biol*, 22(2), pp. 132-9.

Mizushima, N., Kuma, A., Kobayashi, Y., Yamamoto, A., Matsubae, M., Takao, T., Natsume, T., Ohsumi, Y. and Yoshimori, T. (2003) 'Mouse Apg16L, a novel WD-repeat protein, targets to the autophagic isolation membrane with the Apg12-Apg5 conjugate', *J Cell Sci*, 116(Pt 9), pp. 1679-88.

Mizushima, N., Levine, B., Cuervo, A.M. and Klionsky, D.J. (2008) 'Autophagy fights disease through cellular self-digestion', *Nature*, 451(7182), pp. 1069-75.

Mizushima, N., Noda, T. and Ohsumi, Y. (1999) 'Apg16p is required for the function of the Apg12p-Apg5p conjugate in the yeast autophagy pathway', *EMBO J*, 18(14), pp. 3888-96.

Mizushima, N., Noda, T., Yoshimori, T., Tanaka, Y., Ishii, T., George, M.D., Klionsky, D.J., Ohsumi, M. and Ohsumi, Y. (1998) 'A protein conjugation system essential for autophagy', *Nature*, 395(6700), pp. 395-8.

Mizushima, N., Yamamoto, A., Hatano, M., Kobayashi, Y., Kabeya, Y., Suzuki, K., Tokuhisa, T., Ohsumi, Y. and Yoshimori, T. (2001) 'Dissection of autophagosome formation using Apg5-deficient mouse embryonic stem cells', *J Cell Biol*, 152(4), pp. 657-68.

Mizushima, N., Yoshimori, T. and Levine, B. (2010) 'Methods in mammalian autophagy research', *Cell*, 140(3), pp. 313-26.

Mochida, K., Oikawa, Y., Kimura, Y., Kirisako, H., Hirano, H., Ohsumi, Y. and Nakatogawa, H. (2015) 'Receptor-mediated selective autophagy degrades the endoplasmic reticulum and the nucleus', *Nature*, 522(7556), pp. 359-62.

Morales Quinones, M., Winston, J.T. and Stromhaug, P.E. (2012) 'Propeptide of aminopeptidase 1 protein mediates aggregation and vesicle formation in cytoplasm-to-vacuole targeting pathway', *J Biol Chem*, 287(13), pp. 10121-33.

Morano, K.A., Grant, C.M. and Moye-Rowley, W.S. (2012) 'The response to heat shock and oxidative stress in Saccharomyces cerevisiae', *Genetics*, 190(4), pp. 1157-95.

Moreno-Gonzalez, I. and Soto, C. (2011) 'Misfolded protein aggregates: mechanisms, structures and potential for disease transmission', *Semin Cell Dev Biol*, 22(5), pp. 482-7.

Morimoto, R.I. (2008) 'Proteotoxic stress and inducible chaperone networks in neurodegenerative disease and aging', *Genes Dev*, 22(11), pp. 1427-38.

Mortimore, G.E., Lardeux, B.R. and Adams, C.E. (1988) 'Regulation of microautophagy and basal protein turnover in rat liver. Effects of short-term starvation', *J Biol Chem*, 263(5), pp. 2506-12.

Moscat, J. and Diaz-Meco, M.T. (2009) 'p62 at the crossroads of autophagy, apoptosis, and cancer', *Cell*, 137(6), pp. 1001-4.

Moscat, J., Diaz-Meco, M.T., Albert, A. and Campuzano, S. (2006a) 'Cell signaling and function organized by PB1 domain interactions', *Mol Cell*, 23(5), pp. 631-40.

Moscat, J., Diaz-Meco, M.T. and Wooten, M.W. (2007) 'Signal integration and diversification through the p62 scaffold protein', *Trends Biochem Sci*, 32(2), pp. 95-100.

Moscat, J., Rennert, P. and Diaz-Meco, M.T. (2006b) 'PKCzeta at the crossroad of NF-kappaB and Jak1/Stat6 signaling pathways', *Cell Death Differ*, 13(5), pp. 702-11.

Mukhopadhyay, D. and Riezman, H. (2007) 'Proteasome-independent functions of ubiquitin in endocytosis and signaling', *Science*, 315(5809), pp. 201-5.

Muller, F.L., Lustgarten, M.S., Jang, Y., Richardson, A. and Van Remmen, H. (2007) 'Trends in oxidative aging theories', *Free Radic Biol Med*, 43(4), pp. 477-503.

Muller, O., Sattler, T., Flotenmeyer, M., Schwarz, H., Plattner, H. and Mayer, A. (2000) 'Autophagic tubes: vacuolar invaginations involved in lateral membrane sorting and inverse vesicle budding', *J Cell Biol*, 151(3), pp. 519-28.

Murata, S., Yashiroda, H. and Tanaka, K. (2009) 'Molecular mechanisms of proteasome assembly', *Nat Rev Mol Cell Biol*, 10(2), pp. 104-15.

Murphy, M.P. (2009) 'How mitochondria produce reactive oxygen species', *Biochem J*, 417(1), pp. 1-13.

Nagaoka, U., Kim, K., Jana, N.R., Doi, H., Maruyama, M., Mitsui, K., Oyama, F. and Nukina, N. (2004) 'Increased expression of p62 in expanded polyglutamine-expressing cells and its association with polyglutamine inclusions', *J Neurochem*, 91(1), pp. 57-68.

Nah, J., Yuan, J. and Jung, Y.K. (2015) 'Autophagy in neurodegenerative diseases: from mechanism to therapeutic approach', *Mol Cells*, 38(5), pp. 381-9.

Najat, D., Garner, T., Hagen, T., Shaw, B., Sheppard, P.W., Falchetti, A., Marini, F., Brandi, M.L., Long, J.E., Cavey, J.R., Searle, M.S. and Layfield, R. (2009) 'Characterization of a non-UBA domain missense mutation of sequestosome 1 (SQSTM1) in Paget's disease of bone', *J Bone Miner Res*, 24(4), pp. 632-42.

Nakatogawa, H. (2013) 'Two ubiquitin-like conjugation systems that mediate membrane formation during autophagy', *Essays Biochem*, 55, pp. 39-50.

Narendra, D., Kane, L.A., Hauser, D.N., Fearnley, I.M. and Youle, R.J. (2010a) 'p62/SQSTM1 is required for Parkin-induced mitochondrial clustering but not mitophagy; VDAC1 is dispensable for both', *Autophagy*, 6(8), pp. 1090-106.

Narendra, D.P., Jin, S.M., Tanaka, A., Suen, D.F., Gautier, C.A., Shen, J., Cookson, M.R. and Youle, R.J. (2010b) 'PINK1 is selectively stabilized on impaired mitochondria to activate Parkin', *PLoS Biol*, 8(1), p. e1000298.

Narita, M. (2010) 'Quality and quantity control of proteins in senescence', *Aging (Albany NY)*, 2(5), pp. 311-4.

Neff, N.T., Bourret, L., Miao, P. and Dice, J.F. (1981) 'Degradation of proteins microinjected into IMR-90 human diploid fibroblasts', *J Cell Biol*, 91(1), pp. 184-94.

Nioi, P., McMahon, M., Itoh, K., Yamamoto, M. and Hayes, J.D. (2003) 'Identification of a novel Nrf2-regulated antioxidant response element (ARE) in the mouse NAD(P)H:quinone oxidoreductase 1 gene: reassessment of the ARE consensus sequence', *Biochem J*, 374(Pt 2), pp. 337-48.

Nishi, N., Abe, A., Iwaki, J., Yoshida, H., Itoh, A., Shoji, H., Kamitori, S., Hirabayashi, J. and Nakamura, T. (2008) 'Functional and structural bases of a cysteine-less mutant as a long-lasting substitute for galectin-1', *Glycobiology*, 18(12), pp. 1065-73.

Nixon, R.A., Wegiel, J., Kumar, A., Yu, W.H., Peterhoff, C., Cataldo, A. and Cuervo, A.M. (2005) 'Extensive involvement of autophagy in Alzheimer disease: an immuno-electron microscopy study', *J Neuropathol Exp Neurol*, 64(2), pp. 113-22.

Novak, I., Kirkin, V., McEwan, D.G., Zhang, J., Wild, P., Rozenknop, A., Rogov, V., Lohr, F., Popovic, D., Occhipinti, A., Reichert, A.S., Terzic, J., Dotsch, V., Ney, P.A. and Dikic, I. (2010) 'Nix is a selective autophagy receptor for mitochondrial clearance', *EMBO Rep*, 11(1), pp. 45-51.

Obara, K. and Ohsumi, Y. (2008) 'Dynamics and function of PtdIns(3)P in autophagy', *Autophagy*, 4(7), pp. 952-4.

Ohsumi, Y. (2001) 'Molecular dissection of autophagy: two ubiquitin-like systems', *Nat Rev Mol Cell Biol*, 2(3), pp. 211-6.

Ohtsuka, H., Takahashi, R. and Goto, S. (1995) 'Age-related accumulation of high-molecular-weight ubiquitin protein conjugates in mouse brains', *J Gerontol A Biol Sci Med Sci*, 50(5), pp. B277-81.

Okatsu, K., Saisho, K., Shimanuki, M., Nakada, K., Shitara, H., Sou, Y.S., Kimura, M., Sato, S., Hattori, N., Komatsu, M., Tanaka, K. and Matsuda, N. (2010) 'p62/SQSTM1 cooperates with Parkin for perinuclear clustering of depolarized mitochondria', *Genes Cells*, 15(8), pp. 887-900.

Olahova, M., Taylor, S.R., Khazaipoul, S., Wang, J., Morgan, B.A., Matsumoto, K., Blackwell, T.K. and Veal, E.A. (2008) 'A redox-sensitive peroxiredoxin that is important for longevity has tissue- and stress-specific roles in stress resistance', *Proc Natl Acad Sci U S A*, 105(50), pp. 19839-44.

Paine, M.G., Babu, J.R., Seibenhener, M.L. and Wooten, M.W. (2005) 'Evidence for p62 aggregate formation: role in cell survival', *FEBS Lett*, 579(22), pp. 5029-34.

Pandey, U.B., Nie, Z., Batlevi, Y., McCray, B.A., Ritson, G.P., Nedelsky, N.B., Schwartz, S.L., DiProspero, N.A., Knight, M.A., Schuldiner, O., Padmanabhan, R., Hild, M., Berry, D.L., Garza, D., Hubbert, C.C., Yao, T.P., Baehrecke, E.H. and Taylor, J.P. (2007) 'HDAC6 rescues neurodegeneration and provides an essential link between autophagy and the UPS', *Nature*, 447(7146), pp. 859-63.

Pankiv, S., Clausen, T.H., Lamark, T., Brech, A., Bruun, J.A., Outzen, H., Overvatn, A., Bjorkoy, G. and Johansen, T. (2007) 'p62/SQSTM1 binds directly to Atg8/LC3 to facilitate degradation of ubiquitinated protein aggregates by autophagy', *J Biol Chem*, 282(33), pp. 24131-45.

Pankiv, S., Lamark, T., Bruun, J.A., Overvatn, A., Bjorkoy, G. and Johansen, T. (2010) 'Nucleocytoplasmic shuttling of p62/SQSTM1 and its role in recruitment of nuclear polyubiquitinated proteins to promyelocytic leukemia bodies', *J Biol Chem*, 285(8), pp. 5941-53.

Park, I., Chung, J., Walsh, C.T., Yun, Y., Strominger, J.L. and Shin, J. (1995) 'Phosphotyrosine-independent binding of a 62-kDa protein to the src homology 2 (SH2) domain of p56lck and its regulation by phosphorylation of Ser-59 in the lck unique N-terminal region', *Proc Natl Acad Sci U S A*, 92(26), pp. 12338-42.

Pattingre, S., Tassa, A., Qu, X., Garuti, R., Liang, X.H., Mizushima, N., Packer, M., Schneider, M.D. and Levine, B. (2005) 'Bcl-2 antiapoptotic proteins inhibit Beclin 1-dependent autophagy', *Cell*, 122(6), pp. 927-39.

Paulech, J., Solis, N. and Cordwell, S.J. (2013) 'Characterization of reaction conditions providing rapid and specific cysteine alkylation for peptide-based mass spectrometry', *Biochim Biophys Acta*, 1834(1), pp. 372-9.

Paulsen, C.E. and Carroll, K.S. (2010) 'Orchestrating redox signaling networks through regulatory cysteine switches', *ACS Chem Biol*, 5(1), pp. 47-62.

Peskin, A.V., Low, F.M., Paton, L.N., Maghzal, G.J., Hampton, M.B. and Winterbourn, C.C. (2007) 'The high reactivity of peroxiredoxin 2 with H(2)O(2) is not reflected in its reaction with other oxidants and thiol reagents', *J Biol Chem*, 282(16), pp. 11885-92.

Peters, J.M., Franke, W.W. and Kleinschmidt, J.A. (1994) 'Distinct 19 S and 20 S subcomplexes of the 26 S proteasome and their distribution in the nucleus and the cytoplasm', *J Biol Chem*, 269(10), pp. 7709-18.

Pickart, C.M. (2001) 'Mechanisms underlying ubiquitination', *Annu Rev Biochem*, 70, pp. 503-33.

Pickart, C.M. and Cohen, R.E. (2004) 'Proteasomes and their kin: proteases in the machine age', *Nat Rev Mol Cell Biol*, 5(3), pp. 177-87.

Pickart, C.M. and Eddins, M.J. (2004) 'Ubiquitin: structures, functions, mechanisms', *Biochim Biophys Acta*, 1695(1-3), pp. 55-72.

Poole, L.B., Karplus, P.A. and Claiborne, A. (2004) 'Protein sulfenic acids in redox signaling', *Annu Rev Pharmacol Toxicol*, 44, pp. 325-47.

Powers, E.T. and Balch, W.E. (2013) 'Diversity in the origins of proteostasis networks--a driver for protein function in evolution', *Nat Rev Mol Cell Biol*, 14(4), pp. 237-48.

Putker, M., Madl, T., Vos, H.R., de Ruiter, H., Visscher, M., van den Berg, M.C., Kaplan, M., Korswagen, H.C., Boelens, R., Vermeulen, M., Burgering, B.M. and Dansen, T.B. (2013) 'Redox-dependent control of FOXO/DAF-16 by transportin-1', *Mol Cell*, 49(4), pp. 730-42.

Pyo, J.O., Nah, J. and Jung, Y.K. (2012) 'Molecules and their functions in autophagy', *Exp Mol Med*, 44(2), pp. 73-80.

Ramesh Babu, J., Lamar Seibenhener, M., Peng, J., Strom, A.L., Kemppainen, R., Cox, N., Zhu, H., Wooten, M.C., Diaz-Meco, M.T., Moscat, J. and Wooten, M.W. (2008) 'Genetic inactivation of p62 leads to accumulation of hyperphosphorylated tau and neurodegeneration', *J Neurochem*, 106(1), pp. 107-20.

Ravikumar, B., Duden, R. and Rubinsztein, D.C. (2002) 'Aggregate-prone proteins with polyglutamine and polyalanine expansions are degraded by autophagy', *Hum Mol Genet*, 11(9), pp. 1107-17.

Ravikumar, B., Futter, M., Jahreiss, L., Korolchuk, V.I., Lichtenberg, M., Luo, S., Massey, D.C., Menzies, F.M., Narayanan, U., Renna, M., Jimenez-Sanchez, M., Sarkar, S., Underwood, B., Winslow, A. and Rubinsztein, D.C. (2009) 'Mammalian macroautophagy at a glance', *J Cell Sci*, 122(Pt 11), pp. 1707-11.

Ravikumar, B., Sarkar, S., Davies, J.E., Futter, M., Garcia-Arencibia, M., Green-Thompson, Z.W., Jimenez-Sanchez, M., Korolchuk, V.I., Lichtenberg, M., Luo, S., Massey, D.C., Menzies, F.M., Moreau, K., Narayanan, U., Renna, M., Siddiqi, F.H., Underwood, B.R., Winslow, A.R. and Rubinsztein, D.C. (2010) 'Regulation of mammalian autophagy in physiology and pathophysiology', *Physiol Rev*, 90(4), pp. 1383-435.

Ray, P.D., Huang, B.W. and Tsuji, Y. (2012) 'Reactive oxygen species (ROS) homeostasis and redox regulation in cellular signaling', *Cell Signal*, 24(5), pp. 981-90.

Rea, S.L., Majcher, V., Searle, M.S. and Layfield, R. (2014) 'SQSTM1 mutations--bridging Paget disease of bone and ALS/FTLD', *Exp Cell Res*, 325(1), pp. 27-37.

Rechsteiner, M. and Rogers, S.W. (1996) 'PEST sequences and regulation by proteolysis', *Trends Biochem Sci*, 21(7), pp. 267-71.

Reddie, K.G. and Carroll, K.S. (2008) 'Expanding the functional diversity of proteins through cysteine oxidation', *Curr Opin Chem Biol*, 12(6), pp. 746-54.

Reggiori, F., Komatsu, M., Finley, K. and Simonsen, A. (2012) 'Autophagy: more than a nonselective pathway', *Int J Cell Biol*, 2012, p. 219625.

Reyes-Turcu, F.E., Ventii, K.H. and Wilkinson, K.D. (2009) 'Regulation and cellular roles of ubiquitin-specific deubiquitinating enzymes', *Annu Rev Biochem*, 78, pp. 363-97.

Rhee, S.G., Woo, H.A., Kil, I.S. and Bae, S.H. (2012) 'Peroxiredoxin functions as a peroxidase and a regulator and sensor of local peroxides', *J Biol Chem*, 287(7), pp. 4403-10.

Richter, K., Haslbeck, M. and Buchner, J. (2010) 'The heat shock response: life on the verge of death', *Mol Cell*, 40(2), pp. 253-66.

Rieser, E., Cordier, S.M. and Walczak, H. (2013) 'Linear ubiquitination: a newly discovered regulator of cell signalling', *Trends Biochem Sci*, 38(2), pp. 94-102.

Romero, P., Obradovic, Z., Li, X., Garner, E.C., Brown, C.J. and Dunker, A.K. (2001) 'Sequence complexity of disordered protein', *Proteins*, 42(1), pp. 38-48.

Ron, D. and Walter, P. (2007) 'Signal integration in the endoplasmic reticulum unfolded protein response', *Nat Rev Mol Cell Biol*, 8(7), pp. 519-29.

Roos, G., Foloppe, N. and Messens, J. (2013) 'Understanding the pK(a) of redox cysteines: the key role of hydrogen bonding', *Antioxid Redox Signal*, 18(1), pp. 94-127.

Roos, G. and Messens, J. (2011) 'Protein sulfenic acid formation: from cellular damage to redox regulation', *Free Radic Biol Med*, 51(2), pp. 314-26.

Ross, C.A. and Poirier, M.A. (2004) 'Protein aggregation and neurodegenerative disease', *Nat Med*, 10 Suppl, pp. S10-7.

Ross, C.A. and Poirier, M.A. (2005) 'Opinion: What is the role of protein aggregation in neurodegeneration?', *Nat Rev Mol Cell Biol*, 6(11), pp. 891-8.

Rotin, D. and Kumar, S. (2009) 'Physiological functions of the HECT family of ubiquitin ligases', *Nat Rev Mol Cell Biol*, 10(6), pp. 398-409.

Rubino, E., Rainero, I., Chio, A., Rogaeva, E., Galimberti, D., Fenoglio, P., Grinberg, Y., Isaia, G., Calvo, A., Gentile, S., Bruni, A.C., St George-Hyslop, P.H., Scarpini, E., Gallone, S., Pinessi, L. and Group, T.S. (2012) 'SQSTM1 mutations in frontotemporal lobar degeneration and amyotrophic lateral sclerosis', *Neurology*, 79(15), pp. 1556-62.

Rubinsztein, D.C. (2006) 'The roles of intracellular protein-degradation pathways in neurodegeneration', *Nature*, 443(7113), pp. 780-6.

Rubinsztein, D.C., Codogno, P. and Levine, B. (2012) 'Autophagy modulation as a potential therapeutic target for diverse diseases', *Nat Rev Drug Discov*, 11(9), pp. 709-30.

Rubinsztein, D.C., Cuervo, A.M., Ravikumar, B., Sarkar, S., Korolchuk, V., Kaushik, S. and Klionsky, D.J. (2009) 'In search of an "autophagomometer"', *Autophagy*, 5(5), pp. 585-9.

Rubinsztein, D.C., Gestwicki, J.E., Murphy, L.O. and Klionsky, D.J. (2007) 'Potential therapeutic applications of autophagy', *Nat Rev Drug Discov*, 6(4), pp. 304-12.

Rubinsztein, D.C., Marino, G. and Kroemer, G. (2011) 'Autophagy and aging', *Cell*, 146(5), pp. 682-95.

Salminen, A., Kaarniranta, K., Haapasalo, A., Hiltunen, M., Soininen, H. and Alafuzoff, I. (2012) 'Emerging role of p62/sequestosome-1 in the pathogenesis of Alzheimer's disease', *Prog Neurobiol*, 96(1), pp. 87-95.

Salsbury, F.R., Jr., Knutson, S.T., Poole, L.B. and Fetrow, J.S. (2008) 'Functional site profiling and electrostatic analysis of cysteines modifiable to cysteine sulfenic acid', *Protein Sci*, 17(2), pp. 299-312.

Salvador, N., Aguado, C., Horst, M. and Knecht, E. (2000) 'Import of a cytosolic protein into lysosomes by chaperone-mediated autophagy depends on its folding state', *J Biol Chem*, 275(35), pp. 27447-56.

Sandalova, T., Zhong, L., Lindqvist, Y., Holmgren, A. and Schneider, G. (2001) 'Three-dimensional structure of a mammalian thioredoxin reductase: implications for mechanism and evolution of a selenocysteine-dependent enzyme', *Proc Natl Acad Sci U S A*, 98(17), pp. 9533-8.

Sanz, A. (2016) 'Mitochondrial reactive oxygen species: Do they extend or shorten animal lifespan?', *Biochim Biophys Acta*.

Sanz, L., Sanchez, P., Lallena, M.J., Diaz-Meco, M.T. and Moscat, J. (1999) 'The interaction of p62 with RIP links the atypical PKCs to NF-kappaB activation', *EMBO J*, 18(11), pp. 3044-53.

Sarbassov, D.D., Ali, S.M., Kim, D.H., Guertin, D.A., Latek, R.R., Erdjument-Bromage, H., Tempst, P. and Sabatini, D.M. (2004) 'Rictor, a novel binding partner of mTOR, defines a rapamycin-insensitive and raptor-independent pathway that regulates the cytoskeleton', *Curr Biol*, 14(14), pp. 1296-302.

Sattler, T. and Mayer, A. (2000) 'Cell-free reconstitution of microautophagic vacuole invagination and vesicle formation', *J Cell Biol*, 151(3), pp. 529-38.

Sawa-Makarska, J., Abert, C., Romanov, J., Zens, B., Ibiricu, I. and Martens, S. (2014) 'Cargo binding to Atg19 unmasks additional Atg8 binding sites to mediate membrane-cargo apposition during selective autophagy', *Nat Cell Biol*, 16(5), pp. 425-33.

Scherz-Shouval, R. and Elazar, Z. (2007) 'ROS, mitochondria and the regulation of autophagy', *Trends Cell Biol*, 17(9), pp. 422-7.

Scherz-Shouval, R., Shvets, E., Fass, E., Shorer, H., Gil, L. and Elazar, Z. (2007) 'Reactive oxygen species are essential for autophagy and specifically regulate the activity of Atg4', *EMBO J*, 26(7), pp. 1749-60.

Schmidt, E.E. (2015) 'Interplay between cytosolic disulfide reductase systems and the Nrf2/Keap1 pathway', *Biochem Soc Trans*, 43(4), pp. 632-8.

Schneider-Poetsch, T., Ju, J., Eyler, D.E., Dang, Y., Bhat, S., Merrick, W.C., Green, R., Shen, B. and Liu, J.O. (2010) 'Inhibition of eukaryotic translation elongation by cycloheximide and lactimidomycin', *Nat Chem Biol*, 6(3), pp. 209-217.

Scott, S.V., Guan, J., Hutchins, M.U., Kim, J. and Klionsky, D.J. (2001) 'Cvt19 is a receptor for the cytoplasm-to-vacuole targeting pathway', *Mol Cell*, 7(6), pp. 1131-41.

Scott, S.V., Hefner-Gravink, A., Morano, K.A., Noda, T., Ohsumi, Y. and Klionsky, D.J. (1996) 'Cytoplasm-to-vacuole targeting and autophagy employ the same machinery to deliver proteins to the yeast vacuole', *Proc Natl Acad Sci U S A*, 93(22), pp. 12304-8.

Seibenhener, M.L., Babu, J.R., Geetha, T., Wong, H.C., Krishna, N.R. and Wooten, M.W. (2004) 'Sequestosome 1/p62 is a polyubiquitin chain binding protein involved in ubiquitin proteasome degradation', *Mol Cell Biol*, 24(18), pp. 8055-68.

Seibenhener, M.L., Geetha, T. and Wooten, M.W. (2007) 'Sequestosome 1/p62--more than just a scaffold', *FEBS Lett*, 581(2), pp. 175-9.

Seiberlich, V., Goldbaum, O., Zhukareva, V. and Richter-Landsberg, C. (2012) 'The small molecule inhibitor PR-619 of deubiquitinating enzymes affects the microtubule network and causes protein aggregate formation in neural cells: implications for neurodegenerative diseases', *Biochim Biophys Acta*, 1823(11), pp. 2057-68.

Seo, M.S., Kang, S.W., Kim, K., Baines, I.C., Lee, T.H. and Rhee, S.G. (2000) 'Identification of a new type of mammalian peroxiredoxin that forms an intramolecular disulfide as a reaction intermediate', *J Biol Chem*, 275(27), pp. 20346-54.

Shankar, G.M., Li, S., Mehta, T.H., Garcia-Munoz, A., Shepardson, N.E., Smith, I., Brett, F.M., Farrell, M.A., Rowan, M.J., Lemere, C.A., Regan, C.M., Walsh, D.M., Sabatini, B.L. and Selkoe, D.J. (2008) 'Amyloid-beta protein dimers isolated directly from Alzheimer's brains impair synaptic plasticity and memory', *Nat Med*, 14(8), pp. 837-42.

Shibutani, S.T. and Yoshimori, T. (2014) 'A current perspective of autophagosome biogenesis', *Cell Res*, 24(1), pp. 58-68.

Shin, J. (1998) 'P62 and the sequestosome, a novel mechanism for protein metabolism', *Arch Pharm Res*, 21(6), pp. 629-33.

Shintani, T., Huang, W.P., Stromhaug, P.E. and Klionsky, D.J. (2002) 'Mechanism of cargo selection in the cytoplasm to vacuole targeting pathway', *Dev Cell*, 3(6), pp. 825-37.

Shintani, T. and Klionsky, D.J. (2004) 'Autophagy in health and disease: a double-edged sword', *Science*, 306(5698), pp. 990-5.

Shintani, T., Mizushima, N., Ogawa, Y., Matsuura, A., Noda, T. and Ohsumi, Y. (1999) 'Apg10p, a novel protein-conjugating enzyme essential for autophagy in yeast', *EMBO J*, 18(19), pp. 5234-41.

Shpilka, T., Mizushima, N. and Elazar, Z. (2012) 'Ubiquitin-like proteins and autophagy at a glance', *J Cell Sci*, 125(Pt 10), pp. 2343-8.

Shpilka, T., Weidberg, H., Pietrokovski, S. and Elazar, Z. (2011) 'Atg8: an autophagy-related ubiquitin-like protein family', *Genome Biol*, 12(7), p. 226.

Sigismund, S., Polo, S. and Di Fiore, P.P. (2004) 'Signaling Through Monoubiquitination', in Madshus, I. (ed.) *Signalling from Internalized Growth Factor Receptors*. Springer Berlin Heidelberg, pp. 149-185.

Simonsen, A., Birkeland, H.C., Gillooly, D.J., Mizushima, N., Kuma, A., Yoshimori, T., Slagsvold, T., Brech, A. and Stenmark, H. (2004) 'Alfy, a novel FYVE-domain-containing protein associated with protein granules and autophagic membranes', *J Cell Sci*, 117(Pt 18), pp. 4239-51.

Sinha, S. and Levine, B. (2008) 'The autophagy effector Beclin 1: a novel BH3-only protein', *Oncogene*, 27 Suppl 1, pp. S137-48.

Smith, D.M., Chang, S.C., Park, S., Finley, D., Cheng, Y. and Goldberg, A.L. (2007) 'Docking of the proteasomal ATPases' carboxyl termini in the 20S proteasome's alpha ring opens the gate for substrate entry', *Mol Cell*, 27(5), pp. 731-44.

Smith, H.L., Li, W. and Cheetham, M.E. (2015) 'Molecular chaperones and neuronal proteostasis', *Semin Cell Dev Biol*, 40, pp. 142-52.

Snyder, G.H., Cennerazzo, M.J., Karalis, A.J. and Field, D. (1981) 'Electrostatic influence of local cysteine environments on disulfide exchange kinetics', *Biochemistry*, 20(23), pp. 6509-19.

Snyder, H., Mensah, K., Theisler, C., Lee, J., Matouschek, A. and Wolozin, B. (2003) 'Aggregated and monomeric alpha-synuclein bind to the S6' proteasomal protein and inhibit proteasomal function', *J Biol Chem*, 278(14), pp. 11753-9.

Son, J.H., Shim, J.H., Kim, K.H., Ha, J.Y. and Han, J.Y. (2012) 'Neuronal autophagy and neurodegenerative diseases', *Exp Mol Med*, 44(2), pp. 89-98.

Soto, C. (2003) 'Unfolding the role of protein misfolding in neurodegenerative diseases', *Nat Rev Neurosci*, 4(1), pp. 49-60.

Stefani, M. (2004) 'Protein misfolding and aggregation: new examples in medicine and biology of the dark side of the protein world', *Biochim Biophys Acta*, 1739(1), pp. 5-25.

Stepkowski, T.M. and Kruszewski, M.K. (2011) 'Molecular cross-talk between the NRF2/KEAP1 signaling pathway, autophagy, and apoptosis', *Free Radic Biol Med*, 50(9), pp. 1186-95.

Stolz, A., Ernst, A. and Dikic, I. (2014) 'Cargo recognition and trafficking in selective autophagy', *Nat Cell Biol*, 16(6), pp. 495-501.

Sugawara, K., Suzuki, N.N., Fujioka, Y., Mizushima, N., Ohsumi, Y. and Inagaki, F. (2004) 'The crystal structure of microtubule-associated protein light chain 3, a mammalian homologue of Saccharomyces cerevisiae Atg8', *Genes Cells*, 9(7), pp. 611-8.

Sumimoto, H., Kamakura, S. and Ito, T. (2007) 'Structure and function of the PB1 domain, a protein interaction module conserved in animals, fungi, amoebas, and plants', *Sci STKE*, 2007(401), p. re6.

Sun, L. and Chen, Z.J. (2004) 'The novel functions of ubiquitination in signaling', *Curr Opin Cell Biol*, 16(2), pp. 119-26.

Suzuki, K., Kirisako, T., Kamada, Y., Mizushima, N., Noda, T. and Ohsumi, Y. (2001) 'The pre-autophagosomal structure organized by concerted functions of APG genes is essential for autophagosome formation', *EMBO J*, 20(21), pp. 5971-81.

Svenning, S. and Johansen, T. (2013) 'Selective autophagy', *Essays Biochem*, 55, pp. 79-92.

Sykiotis, G.P. and Bohmann, D. (2010) 'Stress-activated cap'n'collar transcription factors in aging and human disease', *Sci Signal*, 3(112), p. re3.

Szeto, J., Kaniuk, N.A., Canadien, V., Nisman, R., Mizushima, N., Yoshimori, T., Bazett-Jones, D.P. and Brumell, J.H. (2006) 'ALIS are stress-induced protein storage compartments for substrates of the proteasome and autophagy', *Autophagy*, 2(3), pp. 189-99.

Taipale, M., Jarosz, D.F. and Lindquist, S. (2010) 'HSP90 at the hub of protein homeostasis: emerging mechanistic insights', *Nat Rev Mol Cell Biol*, 11(7), pp. 515-28.

Takalo, M., Salminen, A., Soininen, H., Hiltunen, M. and Haapasalo, A. (2013) 'Protein aggregation and degradation mechanisms in neurodegenerative diseases', *Am J Neurodegener Dis*, 2(1), pp. 1-14.

Takeshige, K., Baba, M., Tsuboi, S., Noda, T. and Ohsumi, Y. (1992) 'Autophagy in yeast demonstrated with proteinase-deficient mutants and conditions for its induction', *J Cell Biol*, 119(2), pp. 301-11.

Tan, J.M., Wong, E.S., Kirkpatrick, D.S., Pletnikova, O., Ko, H.S., Tay, S.P., Ho, M.W., Troncoso, J., Gygi, S.P., Lee, M.K., Dawson, V.L., Dawson, T.M. and Lim, K.L. (2008) 'Lysine 63-linked ubiquitination promotes the formation and autophagic clearance of protein inclusions associated with neurodegenerative diseases', *Hum Mol Genet*, 17(3), pp. 431-9.

Tanaka, A., Cleland, M.M., Xu, S., Narendra, D.P., Suen, D.F., Karbowski, M. and Youle, R.J. (2010) 'Proteasome and p97 mediate mitophagy and degradation of mitofusins induced by Parkin', *J Cell Biol*, 191(7), pp. 1367-80.

Tanaka, K. and Matsuda, N. (2014) 'Proteostasis and neurodegeneration: The roles of proteasomal degradation and autophagy', *Biochim Biophys Acta*, 1843(1), pp. 197-204.

Tanaka, K., Mizushima, T. and Saeki, Y. (2012) 'The proteasome: molecular machinery and pathophysiological roles', *Biol Chem*, 393(4), pp. 217-34.

Tanida, I., Mizushima, N., Kiyooka, M., Ohsumi, M., Ueno, T., Ohsumi, Y. and Kominami, E. (1999) 'Apg7p/Cvt2p: A novel protein-activating enzyme essential for autophagy', *Mol Biol Cell*, 10(5), pp. 1367-79.

Taylor, R.C. and Dillin, A. (2011) 'Aging as an event of proteostasis collapse', *Cold Spring Harb Perspect Biol*, 3(5).

Tebay, L.E., Robertson, H., Durant, S.T., Vitale, S.R., Penning, T.M., Dinkova-Kostova, A.T. and Hayes, J.D. (2015) 'Mechanisms of activation of the transcription factor Nrf2 by redox stressors, nutrient cues, and energy status and the pathways

through which it attenuates degenerative disease', *Free Radic Biol Med*, 88(Pt B), pp. 108-46.

Terlecky, S.R., Chiang, H.L., Olson, T.S. and Dice, J.F. (1992) 'Protein and peptide binding and stimulation of in vitro lysosomal proteolysis by the 73-kDa heat shock cognate protein', *J Biol Chem*, 267(13), pp. 9202-9.

Teter, S.A., Eggerton, K.P., Scott, S.V., Kim, J., Fischer, A.M. and Klionsky, D.J. (2001) 'Degradation of lipid vesicles in the yeast vacuole requires function of Cvt17, a putative lipase', *J Biol Chem*, 276(3), pp. 2083-7.

Teyssou, E., Takeda, T., Lebon, V., Boillee, S., Doukoure, B., Bataillon, G., Sazdovitch, V., Cazeneuve, C., Meininger, V., LeGuern, E., Salachas, F., Seilhean, D. and Millecamps, S. (2013) 'Mutations in SQSTM1 encoding p62 in amyotrophic lateral sclerosis: genetics and neuropathology', *Acta Neuropathol*, 125(4), pp. 511-22.

Thrower, J.S., Hoffman, L., Rechsteiner, M. and Pickart, C.M. (2000) 'Recognition of the polyubiquitin proteolytic signal', *EMBO J*, 19(1), pp. 94-102.

Thumm, M., Egner, R., Koch, B., Schlumpberger, M., Straub, M., Veenhuis, M. and Wolf, D.H. (1994) 'Isolation of autophagocytosis mutants of Saccharomyces cerevisiae', *FEBS Lett*, 349(2), pp. 275-80.

Tong, K.I., Katoh, Y., Kusunoki, H., Itoh, K., Tanaka, T. and Yamamoto, M. (2006) 'Keap1 recruits Neh2 through binding to ETGE and DLG motifs: characterization of the two-site molecular recognition model', *Mol Cell Biol*, 26(8), pp. 2887-900.

Tooze, S.A. and Yoshimori, T. (2010) 'The origin of the autophagosomal membrane', *Nat Cell Biol*, 12(9), pp. 831-5.

Tornatore, L., Thotakura, A.K., Bennett, J., Moretti, M. and Franzoso, G. (2012) 'The nuclear factor kappa B signaling pathway: integrating metabolism with inflammation', *Trends Cell Biol*, 22(11), pp. 557-66.

Trachootham, D., Lu, W., Ogasawara, M.A., Nilsa, R.D. and Huang, P. (2008) 'Redox regulation of cell survival', *Antioxid Redox Signal*, 10(8), pp. 1343-74.

Treusch, S., Cyr, D.M. and Lindquist, S. (2009) 'Amyloid deposits: protection against toxic protein species?', *Cell Cycle*, 8(11), pp. 1668-74.

Trumbly, R.J. and Bradley, G. (1983) 'Isolation and characterization of aminopeptidase mutants of Saccharomyces cerevisiae', *J Bacteriol*, 156(1), pp. 36-48.

Tsukada, M. and Ohsumi, Y. (1993) 'Isolation and characterization of autophagy-defective mutants of Saccharomyces cerevisiae', *FEBS Lett*, 333(1-2), pp. 169-74.

Umekawa, M. and Klionsky, D.J. (2012) 'The Cytoplasm-to-Vacuole Targeting Pathway: A Historical Perspective', *Int J Cell Biol*, 2012, p. 142634.

Uversky, V.N., Oldfield, C.J. and Dunker, A.K. (2005) 'Showing your ID: intrinsic disorder as an ID for recognition, regulation and cell signaling', *J Mol Recognit*, 18(5), pp. 343-84.

Vadlamudi, R.K., Joung, I., Strominger, J.L. and Shin, J. (1996) 'p62, a phosphotyrosine-independent ligand of the SH2 domain of p56lck, belongs to a new class of ubiquitin-binding proteins', *J Biol Chem*, 271(34), pp. 20235-7.

Valko, M., Leibfritz, D., Moncol, J., Cronin, M.T., Mazur, M. and Telser, J. (2007) 'Free radicals and antioxidants in normal physiological functions and human disease', *Int J Biochem Cell Biol*, 39(1), pp. 44-84.

van der Vaart, A., Mari, M. and Reggiori, F. (2008) 'A picky eater: exploring the mechanisms of selective autophagy in human pathologies', *Traffic*, 9(3), pp. 281-9.

van der Veen, A.G. and Ploegh, H.L. (2012) 'Ubiquitin-like proteins', *Annu Rev Biochem*, 81, pp. 323-57.

Van Remmen, H. and Richardson, A. (2001) 'Oxidative damage to mitochondria and aging', *Exp Gerontol*, 36(7), pp. 957-68.

Verma, R., Aravind, L., Oania, R., McDonald, W.H., Yates, J.R., 3rd, Koonin, E.V. and Deshaies, R.J. (2002) 'Role of Rpn11 metalloprotease in deubiquitination and degradation by the 26S proteasome', *Science*, 298(5593), pp. 611-5.

Vezina, C., Kudelski, A. and Sehgal, S.N. (1975) 'Rapamycin (AY-22,989), a new antifungal antibiotic. I. Taxonomy of the producing streptomycete and isolation of the active principle', *J Antibiot (Tokyo)*, 28(10), pp. 721-6.

Vidal, R.L., Matus, S., Bargsted, L. and Hetz, C. (2014) 'Targeting autophagy in neurodegenerative diseases', *Trends Pharmacol Sci*, 35(11), pp. 583-91.

Vives-Bauza, C., Zhou, C., Huang, Y., Cui, M., de Vries, R.L., Kim, J., May, J., Tocilescu, M.A., Liu, W., Ko, H.S., Magrane, J., Moore, D.J., Dawson, V.L., Grailhe, R., Dawson, T.M., Li, C., Tieu, K. and Przedborski, S. (2010) 'PINK1-dependent recruitment of Parkin to mitochondria in mitophagy', *Proc Natl Acad Sci U S A*, 107(1), pp. 378-83.

Vomhof-Dekrey, E.E. and Picklo, M.J., Sr. (2012) 'The Nrf2-antioxidant response element pathway: a target for regulating energy metabolism', *J Nutr Biochem*, 23(10), pp. 1201-6.

Vucetic, S., Brown, C.J., Dunker, A.K. and Obradovic, Z. (2003) 'Flavors of protein disorder', *Proteins*, 52(4), pp. 573-84.

Wagner, E., Luche, S., Penna, L., Chevallet, M., Van Dorsselaer, A., Leize-Wagner, E. and Rabilloud, T. (2002) 'A method for detection of overoxidation of cysteines: peroxiredoxins are oxidized in vivo at the active-site cysteine during oxidative stress', *Biochem J*, 366(Pt 3), pp. 777-85.

Walter, P. and Ron, D. (2011) 'The unfolded protein response: from stress pathway to homeostatic regulation', *Science*, 334(6059), pp. 1081-6.

Wang, S. and Kaufman, R.J. (2012) 'The impact of the unfolded protein response on human disease', *J Cell Biol*, 197(7), pp. 857-67.

Wang, X., Liu, J.Z., Hu, J.X., Wu, H., Li, Y.L., Chen, H.L., Bai, H. and Hai, C.X. (2011) 'ROS-activated p38 MAPK/ERK-Akt cascade plays a central role in palmitic acid-stimulated hepatocyte proliferation', *Free Radic Biol Med*, 51(2), pp. 539-51.

Wang, X. and Michaelis, E.K. (2010) 'Selective neuronal vulnerability to oxidative stress in the brain', *Front Aging Neurosci*, 2, p. 12.

Waris, G. and Ahsan, H. (2006) 'Reactive oxygen species: role in the development of cancer and various chronic conditions', *J Carcinog*, 5, p. 14.

Webb, J.L., Ravikumar, B., Atkins, J., Skepper, J.N. and Rubinsztein, D.C. (2003) 'Alpha-Synuclein is degraded by both autophagy and the proteasome', *J Biol Chem*, 278(27), pp. 25009-13.

Welchman, R.L., Gordon, C. and Mayer, R.J. (2005) 'Ubiquitin and ubiquitin-like proteins as multifunctional signals', *Nat Rev Mol Cell Biol*, 6(8), pp. 599-609.

Wesselborg, S. and Stork, B. (2015) 'Autophagy signal transduction by ATG proteins: from hierarchies to networks', *Cell Mol Life Sci*.

Wild, P., Farhan, H., McEwan, D.G., Wagner, S., Rogov, V.V., Brady, N.R., Richter, B., Korac, J., Waidmann, O., Choudhary, C., Dotsch, V., Bumann, D. and Dikic, I. (2011) 'Phosphorylation of the autophagy receptor optineurin restricts Salmonella growth', *Science*, 333(6039), pp. 228-33.

Wild, P., McEwan, D.G. and Dikic, I. (2014) 'The LC3 interactome at a glance', *J Cell Sci*, 127(Pt 1), pp. 3-9.

Wilkinson, K.D., Urban, M.K. and Haas, A.L. (1980) 'Ubiquitin is the ATP-dependent proteolysis factor I of rabbit reticulocytes', *J Biol Chem*, 255(16), pp. 7529-32.

Wilson, M.I., Gill, D.J., Perisic, O., Quinn, M.T. and Williams, R.L. (2003) 'PB1 domain-mediated heterodimerization in NADPH oxidase and signaling complexes of atypical protein kinase C with Par6 and p62', *Mol Cell*, 12(1), pp. 39-50.

Winklhofer, K.F., Tatzelt, J. and Haass, C. (2008) 'The two faces of protein misfolding: gain- and loss-of-function in neurodegenerative diseases', *EMBO J*, 27(2), pp. 336-49.

Winterbourn, C.C. and Metodiewa, D. (1999) 'Reactivity of biologically important thiol compounds with superoxide and hydrogen peroxide', *Free Radic Biol Med*, 27(3-4), pp. 322-8.

Wohlgemuth, S.E., Seo, A.Y., Marzetti, E., Lees, H.A. and Leeuwenburgh, C. (2010) 'Skeletal muscle autophagy and apoptosis during aging: effects of calorie restriction and life-long exercise', *Exp Gerontol*, 45(2), pp. 138-48.

Wong, E. and Cuervo, A.M. (2010) 'Integration of clearance mechanisms: the proteasome and autophagy', *Cold Spring Harb Perspect Biol*, 2(12), p. a006734.

Wong, P.M., Puente, C., Ganley, I.G. and Jiang, X. (2013) 'The ULK1 complex: sensing nutrient signals for autophagy activation', *Autophagy*, 9(2), pp. 124-37.

Wood, Z.A., Poole, L.B. and Karplus, P.A. (2003a) 'Peroxiredoxin evolution and the regulation of hydrogen peroxide signaling', *Science*, 300(5619), pp. 650-3.

Wood, Z.A., Schroder, E., Robin Harris, J. and Poole, L.B. (2003b) 'Structure, mechanism and regulation of peroxiredoxins', *Trends Biochem Sci*, 28(1), pp. 32-40.

Wooten, M.W., Seibenhener, M.L., Mamidipudi, V., Diaz-Meco, M.T., Barker, P.A. and Moscat, J. (2001) 'The atypical protein kinase C-interacting protein p62 is a scaffold for NF-kappaB activation by nerve growth factor', *J Biol Chem*, 276(11), pp. 7709-12.

Wurzer, B., Zaffagnini, G., Fracchiolla, D., Turco, E., Abert, C., Romanov, J. and Martens, S. (2015) 'Oligomerization of p62 allows for selection of ubiquitinated cargo and isolation membrane during selective autophagy', *Elife*, 4.

Yamamoto, A., Tagawa, Y., Yoshimori, T., Moriyama, Y., Masaki, R. and Tashiro, Y. (1998) 'Bafilomycin A1 prevents maturation of autophagic vacuoles by inhibiting fusion between autophagosomes and lysosomes in rat hepatoma cell line, H-4-II-E cells', *Cell Struct Funct*, 23(1), pp. 33-42.

Yamamoto, H., Kakuta, S., Watanabe, T.M., Kitamura, A., Sekito, T., Kondo-Kakuta, C., Ichikawa, R., Kinjo, M. and Ohsumi, Y. (2012) 'Atg9 vesicles are an important membrane source during early steps of autophagosome formation', *J Cell Biol*, 198(2), pp. 219-33.

Yang, D.S., Stavrides, P., Mohan, P.S., Kaushik, S., Kumar, A., Ohno, M., Schmidt, S.D., Wesson, D., Bandyopadhyay, U., Jiang, Y., Pawlik, M., et al. (2011) 'Reversal of autophagy dysfunction in the TgCRND8 mouse model of Alzheimer's disease ameliorates amyloid pathologies and memory deficits', *Brain*, 134(Pt 1), pp. 258-77.

Yang, K.S., Kang, S.W., Woo, H.A., Hwang, S.C., Chae, H.Z., Kim, K. and Rhee, S.G. (2002) 'Inactivation of human peroxiredoxin I during catalysis as the result of the oxidation of the catalytic site cysteine to cysteine-sulfinic acid', *J Biol Chem*, 277(41), pp. 38029-36.

Yang, Z. and Klionsky, D.J. (2010) 'Eaten alive: a history of macroautophagy', *Nat Cell Biol*, 12(9), pp. 814-22.

Yao, T. and Cohen, R.E. (2002) 'A cryptic protease couples deubiquitination and degradation by the proteasome', *Nature*, 419(6905), pp. 403-7.

Yao, T.P. (2010) 'The role of ubiquitin in autophagy-dependent protein aggregate processing', *Genes Cancer*, 1(7), pp. 779-786.

Yorimitsu, T. and Klionsky, D.J. (2005) 'Autophagy: molecular machinery for self-eating', *Cell Death Differ*, 12 Suppl 2, pp. 1542-52.

Yoshimori, T., Yamamoto, A., Moriyama, Y., Futai, M. and Tashiro, Y. (1991) 'Bafilomycin A1, a specific inhibitor of vacuolar-type H(+)-ATPase, inhibits acidification and protein degradation in lysosomes of cultured cells', *J Biol Chem*, 266(26), pp. 17707-12.

Yu, W.H., Cuervo, A.M., Kumar, A., Peterhoff, C.M., Schmidt, S.D., Lee, J.H., Mohan, P.S., Mercken, M., Farmery, M.R., Tjernberg, L.O., Jiang, Y., et al. (2005) 'Macroautophagy--a novel Beta-amyloid peptide-generating pathway activated in Alzheimer's disease', *J Cell Biol*, 171(1), pp. 87-98.

Yu, Z.Q., Ni, T., Hong, B., Wang, H.Y., Jiang, F.J., Zou, S., Chen, Y., Zheng, X.L., Klionsky, D.J., Liang, Y. and Xie, Z. (2012) 'Dual roles of Atg8-PE deconjugation by Atg4 in autophagy', *Autophagy*, 8(6), pp. 883-92.

Yue, Z. (2007) 'Regulation of neuronal autophagy in axon: implication of autophagy in axonal function and dysfunction/degeneration', *Autophagy*, 3(2), pp. 139-41.

Zaffagnini, G. and Martens, S. (2016) 'Mechanisms of Selective Autophagy', *J Mol Biol*, 428(9 Pt A), pp. 1714-24.

Zatloukal, K., Stumptner, C., Fuchsbichler, A., Heid, H., Schnoelzer, M., Kenner, L., Kleinert, R., Prinz, M., Aguzzi, A. and Denk, H. (2002) 'p62 Is a common component of cytoplasmic inclusions in protein aggregation diseases', *Am J Pathol*, 160(1), pp. 255-63.

Zhang, X.D., Gillespie, S.K. and Hersey, P. (2004) 'Staurosporine induces apoptosis of melanoma by both caspase-dependent and -independent apoptotic pathways', *Mol Cancer Ther*, 3(2), pp. 187-97.

Zhong, L., Arner, E.S., Ljung, J., Aslund, F. and Holmgren, A. (1998) 'Rat and calf thioredoxin reductase are homologous to glutathione reductase with a carboxyl-terminal elongation containing a conserved catalytically active penultimate selenocysteine residue', *J Biol Chem*, 273(15), pp. 8581-91.

Zhou, L., Wang, H.F., Ren, H.G., Chen, D., Gao, F., Hu, Q.S., Fu, C., Xu, R.J., Ying, Z. and Wang, G.H. (2013) 'Bcl-2-dependent upregulation of autophagy by sequestosome 1/p62 in vitro', *Acta Pharmacol Sin*, 34(5), pp. 651-6.

Zhou, P. (2004) 'Determining Protein Half-Lives', in Dickson, R. and Mendenhall, M. (eds.) *Signal Transduction Protocols*. Humana Press, pp. 67-77.

Zmijewski, J.W., Banerjee, S., Bae, H., Friggeri, A., Lazarowski, E.R. and Abraham, E. (2010) 'Exposure to hydrogen peroxide induces oxidation and activation of AMP-activated protein kinase', *J Biol Chem*, 285(43), pp. 33154-64.